EVALUATION OF THE MARGINAL OUTAGE COSTS IN ELECTRIC POWER SYSTEMS

A Thesis

Submitted to the College of Graduate Studies and Research
in Partial Fulfillment of the Requirements
for the Degree of

Doctor of Philosophy

in the

Department of Electrical Engineering
University of Saskatchewan

by

Raymond Fouad Ghajar

Saskatoon, Saskatchewan
June 1993

0-612-23917-9

COPYRIGHT

Dedicated to my parents

Fouad Ghajar & Yvonne Nakhoul

ACKNOWLEDGEMENTS

The author would like to express his sincere gratitude and appreciation to his supervisor, Dr. Roy Billinton, for his guidance and encouragement during the course of this research work.

The author also expresses his indebtedness to his parents, uncle George, relatives and friends for their constant encouragement and moral support.

This work was financed by the Natural Science and Engineering Research Council of Canada in the form of a Graduate Scholarship.

UNIVERSITY OF SASKATCHEWAN

Electrical Engineering Abstract 93 A380

EVALUATION OF THE MARGINAL OUTAGE COSTS IN ELECTRIC POWER SYSTEMS

Student: Raymond Fouad Ghajar Supervisor: Dr. Roy Billinton

Ph.D. Thesis Presented to the

College of Graduate Studies and Research

June 1993

ABSTRACT

Electricity spot pricing has been advocated in the past few years as a potential method for assigning incremental electricity costs to the time of delivery, and sending appropriate price signals to customers. Marginal outage costs constitute an important component of electricity spot prices. These costs are defined as the change in the expected customer outage costs that are incurred due to an incremental load change. The published literature indicates that the methods currently available for calculating the marginal outage costs utilize approximate economic models which do not take into consideration the stochastic nature of the power system and its effects on these costs. This thesis presents a method based on quantitative power system reliability concepts for calculating the marginal outage costs in electric power systems. This method is based on the premise that the marginal outage costs are expected quantities that depend upon two major factors: the customer economic costs that accompany various outage levels and the effects of load changes on the probabilities that these costs will

actually be incurred. The proposed method calculates the marginal outage cost as the product of the incremental expected unserved energy and the average cost of unserved energy. A method for calculating the incremental expected unserved energy in generating and composite generation and transmission systems is developed in this thesis. The average cost of unserved energy is represented by the interrupted energy assessment rate.

The proposed method is illustrated in this thesis by application to two reliability test systems in order to show the impact of system size on the robustness of the method and the accuracy of the approximations. In addition to the basic studies, a number of sensitivity analyses are conducted to show the impact of selected modelling assumptions and parameters on the marginal outage cost. The results from the sensitivity analyses are then used to provide recommendations for implementing the proposed method in practical systems.

TABLE OF CONTENTS

COPYRIGHT i
ACKNOWLEDGEMENTS ii
ABSTRACT iii
TABLE OF CONTENTS v
LIST OF FIGURES xi
LIST OF TABLES xvii
LIST OF ABBREVIATIONS xix

1. INTRODUCTION 1
   1.1. Background 1
   1.2. Spot Pricing of Electricity 2
   1.3. Power System Reliability in Perspective 5
      1.3.1. Adequacy evaluation at *HLI* 8
      1.3.2. Adequacy evaluation at *HLII* 9
      1.3.3. Adequacy evaluation at *HLIII* 10
   1.4. Scope and Objectives of the Thesis 10
      1.4.1. Research objectives for Phase 1 11
      1.4.2. Research objectives for Phase 2 11
      1.4.3. Research objectives for Phase 3 12
   1.5. Outline of the Thesis 13

2. MARGINAL OUTAGE COSTS IN ELECTRIC POWER SYSTEMS..... 16
   2.1. Introduction 16
   2.2. Components of Electricity Spot Prices 17
   2.3. Methodologies for Calculating the Marginal Outage Costs in Electric Power Systems 19

2.3.1. Annualized capital costs of installing new capacity 20
2.3.2. Reduction in consumer's surplus 21
2.3.3. Average customer economic costs resulting from power outages 22
2.4. Derivation of the Marginal Outage Costs Associated With Generating Systems 24
2.4.1. Derivation of the interrupted energy assessment rate in generating systems 26
2.4.2. Derivation of the incremental expected unserved energy in generating systems 28
2.5. Derivation of the Marginal Outage Costs Associated With Composite Power Systems 33
2.5.1. Derivation of the interrupted energy assessment rates in composite systems 37
2.5.2. Derivation of the incremental expected unserved energy in composite systems 39
2.6. Variation of the Marginal Outage Cost With the Lead Time 40
2.7. Summary 46

3. EVALUATION OF THE MARGINAL OUTAGE COSTS IN ISOLATED GENERATING SYSTEMS 48
3.1. Introduction 48
3.2. Reliability Test Systems 48
3.3. Evaluation of the Marginal Outage Costs Associated with the *RBTS* Generating System 50
3.3.1. Effect of the initial generating unit conditions 54
3.3.2. Effect of modelling derated states 56
3.3.3. Effect of load forecast uncertainty 59
3.3.4. Effect of removing generating units for maintenance 62
3.4. Evaluation of the Marginal Outage Costs Associated with the *IEEE-RTS* Generating System 64
3.4.1. Effect of the initial generating unit conditions 66
3.4.2. Effect of modelling derated states 71
3.4.3. Effect of load forecast uncertainty 72
3.4.4. Effect of removing generating units for maintenance 73
3.5. Summary 75

4. UTILIZATION OF APPROXIMATE TECHNIQUES TO CALCULATE THE MARGINAL OUTAGE COSTS IN ISOLATED GENERATING SYSTEMS 77

4.1. Introduction 77

4.2. Description of the Approximate Techniques 78

4.2.1. Discrete representation of capacity outages in generating systems 79

4.2.1.1. Rounding the capacity outage probability table 79

4.2.1.2. Fast Fourier Transform (*FFT*) algorithm 82

4.2.2. Continuous representation of capacity outages in generating systems 83

4.2.2.1. Normal probability distribution 84

4.2.2.2. Folded normal probability distribution 85

4.2.2.3. Modified distribution based on the Gram-Charlier series 85

4.2.2.4. Distribution fitting technique 86

4.2.2.5. Large deviation method 87

4.3. Utilization of Discrete Models to Calculate the Marginal Outage Cost of the *IEEE-RTS* Generating System 88

4.4. Utilization of Continuous Models to Calculate the Marginal Outage Cost of the *IEEE-RTS* Generating System 92

4.5. Comparison of the Accuracy and Computing Time Requirements of the Approximate Techniques 95

4.6. Summary 99

5. EVALUATION OF THE MARGINAL OUTAGE COSTS IN INTERCONNECTED GENERATING SYSTEMS 101

5.1. Introduction 101

5.2. Proposed Method for Calculating the Marginal Outage Costs in Interconnected Generating Systems 102

5.3. Application to Two Interconnected Generating Systems 103

5.4. Application to Two Areas Within a Single Generating System 106

5.5. Factors Affecting the Marginal Outage Cost in Interconnected Generating Systems 109

5.5.1. Effect of tie-line capacity 110

5.5.2. Effect of tie-line reliability 111

5.5.3. Effect of the number of tie-lines 112

5.5.4. Effect of tie capacity uncertainty 115
5.5.5. Effect of load forecast uncertainty 117
5.5.5.1. Load forecast uncertainty in the assisted system 117
5.5.5.2. Load forecast uncertainty in the assisting system 119
5.5.5.3. Load forecast uncertainty in both the assisted and the assisting systems 122
5.6. Application to More Than Two Interconnected Generating Systems 124
5.6.1. Three radial systems 125
5.6.2. More than three radial systems 127
5.6.3. Three generating systems interconnected in a ring fashion 129
5.7. Summary 139

6. EVALUATION OF THE MARGINAL OUTAGE COSTS IN COMPOSITE GENERATION AND TRANSMISSION SYSTEMS 141
6.1. Introduction 141
6.2. Description of the *COMREL* Program 142
6.2.1. System failure criteria 144
6.2.2. Contingency selection and evaluation 145
6.2.2.1. Predetermined contingency level 145
6.2.2.2. Ranking 146
6.2.2.3. Frequency cut-off 146
6.2.2.4. Sorting facility 146
6.2.3. Network analysis 147
6.2.3.1. Network flow method (Transportation model) 147
6.2.3.2. *DC* load flow method 148
6.2.3.3. *AC* load flow method 148
6.2.4. Remedial actions in the *COMREL* program 149
6.2.5. Implementation of load curtailment philosophy 150
6.3. Proposed Method for Calculating the Marginal Outage Costs at Bulk Customer Load points 150
6.4. Evaluation of the Marginal Outage Costs at the Bulk Customer Load Points of the *RBTS* 152

6.4.1. Comparison between the marginal outage costs of the *RBTS* calculated at *HLI* and *HLII* 157

6.5. Evaluation of the Marginal Outage Costs at the Bulk Customer Load Points of the *IEEE-RTS* 160

6.5.1. Comparison between the marginal outage costs of the *IEEE-RTS* calculated at *HLI* and *HLII* 164

6.6. Summary 166

7. SENSITIVITY OF THE MARGINAL OUTAGE COSTS IN COMPOSITE SYSTEMS TO SELECTED PERTINENT FACTORS 167

7.1. Introduction 167

7.2. Sensitivity Studies Using the *RBTS* 167

7.2.1. Effect of using aggregate system values 168

7.2.2. Effect of using the composite system *CCDF* 169

7.2.3. Effect of *IEAR* variations with the peak load 172

7.2.4. Effect of using the average interruption duration to calculate the *IEAR* 175

7.2.5. Effect of load flow solutions 177

7.2.6. Effect of load curtailment philosophy 178

7.2.7. Effect of removing components for maintenance 182

7.3. Sensitivity Studies Using the *IEEE-RTS* 184

7.3.1. Effect of using aggregate system values 184

7.3.2. Effect of using the composite system *CCDF* 186

7.3.3. Effect of *IEAR* variations with the peak load 187

7.3.4. Effect of using the average interruption duration to calculate the *IEAR* 189

7.3.5. Effect of load flow solutions 190

7.3.6. Effect of load curtailment philosophy 191

7.3.7. Effect of removing components for maintenance 192

7.4. Summary 194

8. PRACTICAL IMPLEMENTATION OF THE PROPOSED METHODS FOR CALCULATING MARGINAL OUTAGE COSTS 196

8.1. Introduction 196

8.2. Marginal Outage Costs in Isolated Generating Systems 197

8.3. Marginal Outage Costs in Interconnected Generating Systems 199

8.4. Marginal Outage Costs in Composite Generation and Transmission Systems 202
8.5. Summary 204

9. SUMMARY AND CONCLUSIONS 205

REFERENCES 210

A. DESCRIPTION OF THE ROY BILLINTON TEST SYSTEM 220

B. DESCRIPTION OF THE IEEE-RELIABILITY TEST SYSTEM 223

C. POWER INTERRUPTIONS COST DATA 228
C.1. Creating a Composite Customer Damage Function 230

D. REPRESENTATION OF CAPACITY OUTAGES IN GENERATING SYSTEMS USING NORMAL AND FOLDED NORMAL DISTRIBUTIONS 232
D.1. Calculation of the Probability of a Capacity Outage Using the Folded Normal Distribution 235

E. REPRESENTATION OF CAPACITY OUTAGES IN GENERATING SYSTEMS USING GRAM-CHARLIER SERIES 236
E.1. Calculation of the Probability of a Capacity Outage Using the Gram-Charlier Expansion of a distribution 240

F. CALCULATION OF THE PROBABILITY OF A CAPACITY OUTAGE USING THE LARGE DEVIATION METHOD 243
F.1. Modelling of Multi-State Generating Units 246
F.2. Formulation With Edgeworth Expansion for $v_m^*(x)$ 248
F.3. Modelling Adjustments for Negative Values of S_0 249

G. GENERATING A COMPOSITE CUSTOMER DAMAGE FUNCTION AND AN IEAR FOR EACH LOAD BUS IN THE *RBTS* 251
G.1. Development of the *IEAR* at Each Load Bus of the *RBTS* 255

H. GENERATING A COMPOSITE CUSTOMER DAMAGE FUNCTION AND AN IEAR FOR EACH LOAD BUS IN THE *IEEE-RTS* 259
H.1. Development of the *IEAR* at Each Load Bus of the *IEEE-RTS* 262

LIST OF FIGURES

Figure 1.1. Subdivision of system reliability........ 6

Figure 1.2. Basic functional zones of a power system........ 7

Figure 1.3. Hierarchical levels........ 7

Figure 1.4. Power system model for *HLI* studies........ 8

Figure 1.5. Model of interconnected generating systems in *HLI* studies........ 9

Figure 2.1. Concept of adequacy state assessment........ 20

Figure 2.2. Two-state reliability model of a component........ 25

Figure 2.3. Variation of the outage replacement rate with the lead time and the initial conditions of a component........ 27

Figure 2.4. Three-state reliability model of a component........ 29

Figure 2.5. Effect of the magnitude of Δt on the values of the state probabilities of a three-state model as a function of the lead time........ 29

Figure 3.1. Variation of the marginal outage cost of the *RBTS* as a function of the operating reserve for selected lead times........ 51

Figure 3.2. Variation of the marginal outage cost of the *RBTS* as a function of the lead time for selected operating reserves........ 52

Figure 3.3. Variation of the marginal outage cost of the *RBTS* as a function of the operating reserve and the lead time........ 53

Figure 3.4. Effect of generating unit initial conditions on the marginal outage cost of the *RBTS* for a lead time of 10 hours........ 55

Figure 3.5. Effect of generating unit initial conditions on the marginal outage cost of the *RBTS* for an operating reserve of 35 *MW*........ 55

Figure 3.6. Variation of the marginal outage cost of the *RBTS* as a function of the operating reserve and the lead time when the 40 *MW* hydro unit is assumed to be in the down state at $t = 0$........ 57

Figure 3.7. Effect of using a three-state model to represent the two 40 *MW* thermal units in the *RBTS* on the marginal outage cost as a function of the operating reserve. 58

Figure 3.8. Effect of using a three-state model to represent the two 40 *MW* thermal units in the *RBTS* on the marginal outage cost as a function of the lead time. 59

Figure 3.9. Seven-step approximation of the normal distribution. 61

Figure 3.10. Effect of load forecast uncertainty on the marginal outage cost profile of the *RBTS* as a function of the operating reserve 61

Figure 3.11. Effect of removing units for maintenance on the marginal outage cost profile of the *RBTS* as a function of the operating reserve. 63

Figure 3.12. Effect of removing units for maintenance on the marginal outage cost profile of the *RBTS* as a function of the lead time. 64

Figure 3.13. Variation of the marginal outage cost of the *IEEE-RTS* as a function the operating reserve for selected lead times 65

Figure 3.14. Variation of the marginal outage cost of the *IEEE-RTS* as a function of the lead time for selected operating reserves 66

Figure 3.15. Variation of the marginal outage cost of the *IEEE-RTS* with the operating reserve and the lead time 67

Figure 3.16. Effect of generating unit initial conditions on the marginal outage cost profile of the *IEEE-RTS* for a lead time of 10 hours 68

Figure 3.17. Effect of generating unit initial conditions on the marginal outage cost profile of the *IEEE-RTS* for an operating reserve of 500 *MW*. 69

Figure 3.18. Variation of the marginal outage cost of the *IEEE-RTS* as a function of the operating reserve and the lead time when a 400 *MW* unit is assumed to be in the down state at $t = 0$. 70

Figure 3.19. Effect of using a three-state model to represent the large units in the *IEEE-RTS* on the marginal outage cost as a function of the operating reserve. 72

Figure 3.20. Effect of load forecast uncertainty on the marginal outage cost profile of the *IEEE-RTS* as a function of the operating reserve 73

Figure 3.21. Effect of removing units for maintenance on the marginal outage cost profile of the *IEEE-RTS* as a function of the operating reserve. 74

Figure 4.1. Flowchart of the rounding algorithm implemented in the marginal outage costing program.... 81
Figure 4.2. Sharing process of an impulse.... 83
Figure 4.3. Effect of rounding the *COPT* on the marginal outage cost profile of the *IEEE-RTS* for a lead time of infinity.... 89
Figure 4.4. Effect of rounding the *COPT* on the marginal outage cost profile of the *IEEE-RTS* for a lead time of 10 hours.... 89
Figure 4.5. Comparison of the marginal outage cost profiles of the *IEEE-RTS* generated by the exact technique and the *FFT* algorithm for a lead time of infinity.... 90
Figure 4.6. Comparison of the marginal outage cost profiles of the *IEEE-RTS* generated by the exact technique and the *FFT* algorithm for a lead time of 10 hours.... 91
Figure 4.7. Comparison of the marginal outage cost profiles of the *IEEE-RTS* generated by the exact technique and the continuous models for a lead time of infinity.... 93
Figure 4.8. Comparison of the marginal outage cost profiles of the *IEEE-RTS* generated by the exact technique and the continuous models for a lead time of 10 hours.... 94
Figure 4.9. Comparison of the marginal outage cost profiles of the *IEEE-RTS* generated by the exact technique and the various large deviation methods for a lead time of 10 hours.... 95
Figure 4.10. Comparison of the errors produced by the various approximate techniques as a function of the operating reserve for a lead time of 10 hours.... 96
Figure 4.11. Load profile for a 24-hour forecast period.... 97
Figure 4.12. Comparison of the computing times required by each approximate technique to calculate the marginal outage cost for each hour in the forecast period.... 99
Figure 5.1. Two generating systems interconnected by a number of tie-lines.... 103
Figure 5.2. Effect of capacity assistance from System *B* on the marginal outage cost profile of System *A*.... 104
Figure 5.3. Effect of shifting the marginal outage cost profiles of the interconnected System *A* by amounts equal to the corresponding assistance levels available from System *B*.... 105
Figure 5.4. Variation of the marginal outage cost of the interconnected System *A* as a function of its operating reserve and the assistance available from System *B*.... 107
Figure 5.5. Two-area representation of the *IEEE-RTS*.... 108

Figure 5.6. Marginal outage cost profile of the *SOUTH* area in the *IEEE-RTS* as a function of its isolated operating reserve for selected assistance levels. 109

Figure 5.7. Effect of tie-line capacity on the marginal outage cost profile of System *A*. 111

Figure 5.8. Effect of the tie-line reliability on the marginal outage cost profile of System *A* 113

Figure 5.9. Effect of the number of tie-lines on the marginal outage cost profile of System *A* 115

Figure 5.10. Effect of tie capacity uncertainty on the marginal outage cost profile of System *A* 117

Figure 5.11. Effect of load forecast uncertainty in the assisted system on the marginal outage cost profile of System *A*. 118

Figure 5.12. Algorithm for incorporating the load forecast uncertainty of the assisting system in the calculation of the marginal outage cost. 120

Figure 5.13. Effect of load forecast uncertainty in the assisting system on the marginal outage cost profile of System *A* for a tie capacity of 30 *MW* 121

Figure 5.14. Effect of load forecast uncertainty in the assisting system on the marginal outage cost profile of the System *A* for an infinite tie capacity. 122

Figure 5.15. Effect of load forecast uncertainty in both the assisted and the assisting systems on the marginal outage cost profile of System *A*. 123

Figure 5.16. Three radially interconnected generating systems. 125

Figure 5.17. Marginal outage cost profiles of three radially interconnected *RBTS* systems. 127

Figure 5.18. Four radially interconnected generating systems. 128

Figure 5.19. Marginal outage cost profiles of four radially interconnected *RBTS* systems. 129

Figure 5.20. Three generating systems interconnected in a ring fashion 130

Figure 5.21. Effect tie-line reliability on the marginal outage cost of System *A* interconnected in a three-system ring fashion. 133

Figure 5.22. Improvements in the marginal outage cost of System *A* due to the existence of tie-line T_{BC} (Case 1) 133

Figure 5.23. Improvements in the marginal outage cost of System *A* due to the existence of tie-line T_{BC} (Case 2) 135

Figure 5.24. Equivalent model for Case 3 of the three systems interconnected in a ring type fashion. 136

Figure 5.25. Equivalent model for Case 4 of the three systems interconnected in a ring type fashion. 137

Figure 5.26. Effect of re-routing the assistance from System *B* via tie-line T_{BC} and System *C* on the marginal outage cost of System *A*. 138

Figure 6.1. Flowchart of the *COMREL* program. 143

Figure 6.2. Single line diagram of the *RBTS*. 153

Figure 6.3. Marginal outage cost profiles of each load bus in the *RBTS* 155

Figure 6.4. Contributions of the various buses to the marginal outage cost profiles at Bus 3 (a) and Bus 6 (b) of the *RBTS* 156

Figure 6.5. Comparison of the marginal outage cost profiles at Buses 3 and 6 of the *RBTS* to the generating system profile calculated at *HLI* 158

Figure 6.6. Contributions of the generation and transmission systems of the *RBTS* to the marginal outage costs at Bus 3 (a) and Bus 6 (b). 159

Figure 6.7. Single line diagram of the *IEEE-RTS*. 161

Figure 6.8. Marginal outage cost profiles of selected buses in the *IEEE-RTS*. 162

Figure 6.9. Contribution of selected buses in the various classes to the marginal outage cost of Bus 4 in the *IEEE-RTS*. 164

Figure 6.10. Comparison of the marginal outage cost profile calculated at *HLI* and that of Bus 4 calculated at *HLII* with the contributions of the generation and transmission systems of the *IEEE-RTS*. 165

Figure 7.1. Effect of using the aggregate system values on the marginal outage cost profiles of Bus 3 (a) and Bus 6 (b) of the *RBTS*. 170

Figure 7.2. Effect of using the composite system *CCDF* on the marginal outage cost profiles of Bus 3 (a) and Bus 6 (b) of the *RBTS*. 171

Figure 7.3. Variations of the *IEAR*'s at each load bus in the *RBTS* with the peak load 173

Figure 7.4. Effect of *IEAR* variations with the peak load on the marginal outage cost profiles of Bus 3 (a) and Bus 6 (b) of the *RBTS*. 174

Figure 7.5. Effect of using approximate *IEAR*'s on the marginal outage cost profiles of Bus 3 (a) and Bus 6 (b) of the *RBTS* 176

Figure 7.6. Effect of load flow solutions on the marginal outage cost profiles of Bus 3 (a) and Bus 6 (b) of the *RBTS*. 179

Figure 7.7. Effect of load curtailment philosophy on the marginal outage cost profiles of Bus 3 (a) and Bus 6 (b) of the *RBTS* 181

Figure 7.8. Effect of removing a few generating units for maintenance on the marginal outage cost profiles of Bus 3 (a) and Bus 6 (b) of the *RBTS*. 183

Figure 7.9. Effect of removing a few transmission lines for maintenance on the marginal outage cost profiles of Bus 3 (a) and Bus 6 (b) of the *RBTS*. 185

Figure 7.10. Effect of using the aggregate system values on the marginal outage cost profile of Bus 4 of the *IEEE-RTS*. 186

Figure 7.11. Effect of using the composite system *CCDF* on the marginal outage cost profile of Bus 4 of the *IEEE-RTS*. 187

Figure 7.12. Variations of the *IEAR*'s at selected buses in each class of the *IEEE-RTS* with the peak load. 188

Figure 7.13. Effect of *IEAR* variations with the peak load on the marginal outage cost profile of Bus 4 of the *IEEE-RTS*. 188

Figure 7.14. Effect of using approximate *IEAR*'s on the marginal outage cost profile of Bus 4 of the *IEEE-RTS*. 190

Figure 7.15. Effect of load flow solutions on the marginal outage cost profile of Bus 4 of the *IEEE-RTS*. 191

Figure 7.16. Effect of load curtailment philosophy on the marginal outage cost profile of Bus 4 of the *IEEE-RTS*. 192

Figure 7.17. Effect of removing a few generating units for maintenance on the marginal outage cost profile of Bus 4 of the *IEEE-RTS*. 193

Figure 7.18. Effect of removing a few transmission lines for maintenance on the marginal outage cost profile of Bus 4 of the *IEEE-RTS*. 194

Figure A.1. Single line diagram of the *RBTS*. 220

Figure B.1. Single line diagram of the *IEEE-RTS*. 224

Figure C.1. Composite customer damage function for the service area. 231

Figure D.1. Probability density function of capacity outages of a generating unit. 232

Figure E.1. Representation of *Area1* and *Area2* on the *pdf* of a standardized normal distribution. 241

LIST OF TABLES

Table 5.1. Basic reliability data of the tie-line. 112
Table 5.2. Equivalent models of two 15 *MW* and three 10 *MW* tie-lines... 114
Table 5.3. Scenarios of operating reserves for Systems *B* and *C*. 138
Table 6.1. *IEAR* values at each load bus of the *RBTS*.......................... 154
Table 6.2. *IEAR* values at each load bus of the *IEEE-RTS*. 163
Table A.1. Generating unit reliability data for the *RBTS*. 221
Table A.2. Three-state model for the two 40 *MW* thermal units in the *RBTS*... 221
Table A.3. Transmission line data for the *RBTS*................................. 222
Table A.4. Bus data for the *RBTS*.. 222
Table B.1. Generating unit reliability data for the *IEEE-RTS*................ 223
Table B.2. Generating unit locations for the *IEEE-RTS*......................... 225
Table B.3. Three-state model of the 350 and 400 *MW* units in the *IEEE-RTS*. 225
Table B.4. Transmission line data for the *IEEE-RTS*. 226
Table B.5. Bus data for the *IEEE-RTS*. 227
Table C.1. Sector interruption cost estimates (*CDF*'s) expressed as cost per *kW* of annual peak demand (*$/kW*)......................... 229
Table C.2. Load composition of the service area, based on annual peak demand and annual energy consumption. 230
Table C.3. Composite customer damage function for the service area. 231
Table G.1. Sector allocation at each load bus of the *RBTS*...................... 252
Table G.2. Sector peak load distribution at each load bus of the *RBTS*...... 252
Table G.3. Load factors of each user sector in the *RBTS*. 253
Table G.4. Sector average load at each load bus of the *RBTS*.................. 254
Table G.5. Sector energy distribution at each load bus of the *RBTS*. 254
Table G.6. *CCDF* for each bus of the *RBTS* (1987 *$/kW*)......................... 255

Table G.7. *IEAR* values for each load bus in the *RBTS*. 257

Table G.8. Effects of selected pertinent factors on the value of the *IEAR* in the *RBTS*. 258

Table H.1. Sector allocation at each load bus of the *IEEE-RTS*. 260

Table H.2. Sector peak load distribution at each load bus of the *IEEE-RTS*. 260

Table H.3. Sector average load at each load bus of the *IEEE-RTS*. 261

Table H.4. Sector energy distribution at each load bus of the *IEEE-RTS*. 261

Table H.5. *CCDF* for each bus of the *IEEE-RTS* (1987 $/kW). 262

Table H.6. *IEAR* values for each load bus in the *IEEE-RTS*. 263

Table H.7. Effects of selected pertinent factors on the value of the *IEAR* in the *IEEE-RTS*. 264

LIST OF ABBREVIATIONS

AC	Alternating Current
APM	*IEEE* sub-committee on the Application of Probability Methods
CCDF	Composite Customer Damage Function
CDF	Customer Damage Function
CEA	Canadian Electrical Association
CLT	Central Limit Theorem
COMREL	COMposite system RELiability evaluation
DAFOR	Derating-Adjusted Forced Outage Rate
DC	Direct Current
ΔEUE	Incremental Expected Unserved Energy
DPLVC	Daily Peak Load Variation Curve
DSM	Demand Side Management
EPRI	Electric Power Research Institute
EUE	Expected Unserved Energy
F&D	Frequency and Duration
FFT	Fast Fourier Transform
FOR	Forced Outage Rate
HLI	Hierarchical Level I
HLII	Hierarchical Level II

HLIII	Hierarchical Level III
i.i.d.	independent and identically distributed
IEAR	Interrupted Energy Assessment Rate
IEEE-RTS	*IEEE*-Reliability Test System
λ	failure rate of a component
L.F.	Load Factor
LDC	Load Duration Curve
LDM	Large Deviation Method
LFU	Load Forecast Uncertainty
LOLE	Loss Of Load Expectation
LRMC	Long Run Marginal Cost
μ	repair rate of a component
m.g.f.	moment generating function
M.O.C.	Marginal Outage Cost
MECORE	Monte-carlo simulation and Enumeration approach for COmposite system Reliability Evaluation
NSERC	Natural Sciences and Engineering Research Council
ORR	Outage Replacement Rate
pdf	probability density function
r.v.	random variable
RBTS	Roy Billinton Test System
s.d.	Standard Deviation
SIC	Standard Industrial Classification
SRMC	Short Run Marginal Cost
TOU	Time Of Use
WTP	Willingness To Pay

1. INTRODUCTION

1.1. Background

Electricity rate structures have been the subject of extensive studies in the past few decades. The economic and engineering literature contains many papers on the theoretical design and practical implementation of various rate structures [1-4]. A major Electric Power Research Institute (*EPRI*) rate study provides an extensive background [5]. The various rate structures proposed or implemented have sought improvements in a wide range of social objectives including the cost of electricity generation, the reliability of supply, utility profits and customer benefits. Another means of achieving improvements in these objectives which has recently received increasing attention is Demand Side Management (*DSM*). Generically, *DSM* is used to describe a variety of arrangements that are designed to modify the customers' pattern of electricity usage. Further background and a long list of references on demand side management can be found in [4,5].

Electric utilities are increasingly using rate incentives in order to achieve their *DSM* goals. In the United States, surveys of electric utilities by *EPRI* reveal substantial interest and implementation activity in introducing a wide variety of rate designs [6]. Most common among such "innovative rates" are interruptible tariffs, time-of-use (TOU) pricing, increasing block rates and industrial incentive/economic development rates. Other rate forms that have emerged include demand subscription service, coincident demand charges and special rates such as super off-peak pricing and spot pricing [7-11].

Many electric utilities see innovative rate structures as strategic options to improve their competitive position in the energy markets by offering electricity prices that more closely track actual costs at each point in time and space. The recent interest in such rate structures can be attributed to an emerging recognition in the industry that its traditional practice of providing all users with a uniform and very high level of service reliability at prices specified well in advance has major shortcomings. By introducing time- and space-differentiated pricing schemes, the utility can essentially unbundle the electric service and offer its customers a range of electric services at different prices. This tailoring of service is often referred to as spot pricing [12].

1.2. Spot Pricing of Electricity

The cost of providing electricity - generation and delivery - generally varies with time, location, supply voltage, weather conditions and other system and customer characteristics [12]. If this variation in cost is reflected in the price of electricity together with other costs that satisfy the demand side management objectives, the resulting spot price would maximize the overall social welfare of electricity. This maximization process is the product of customers reaching the socially optimal usage level as a result of their own efforts to maximize profits.

Traditional pricing of electricity for the vast majority of customers is based on the "average" cost of generation, transmission and distribution. It does not vary from season to season, day to day or hour to hour even though there are marked differences in instantaneous costs. Under this pricing regime, a utility sets the average price of electric energy in a way that covers the utility's costs and profits. The customers are therefore insensitive to the varying costs of electric energy and have no economic incentives to adjust their consumption to take advantage of low-cost periods or to avoid usage during high-cost periods. Spot prices, on the other hand, are capable of achieving significant gains in short-term efficiency. These gains can be to the benefit of both the utility and its customers and the incorporation of one or more real time elements into a tariff makes it more responsive to utility and customer needs [10-13].

Spot pricing of electricity is not a new concept. A modified version of it was first suggested by Vikery [14] and later developed by Schweppe et. al. [15]. Spot pricing has been referred to by several different names: Homeostatic control pricing, real time pricing, load adaptive pricing, flexible pricing, dynamic pricing and responsive pricing. There are slight semantical differences as to how these terms are used but, in general, the theme common to all is the time- and space-differentiated nature of the price of electricity. That is, the price of the commodity is dependent on the time that the consumption occurs and its location in the system, and therefore the price is varied to reflect the utility's cost of providing the energy at a given time and location.

The theory of spot pricing does away with concepts such as block rate, demand charges, back-up charges, capacity credits and so on. Instead, an energy marketplace for electric energy is established where the spot price for buying and selling electric energy is determined by the supply and demand conditions at that instant [16]. This theory does not distinguish between net consumers and net generators of electricity. Customers with self-generation or co-generation receive the spot price in effect at the time for each unit of electric energy when they are net generators and pay the spot price when they are net consumers. This encourages them to self dispatch efficiently [17,18].

The formal mathematical derivation of electricity spot pricing is beyond the scope of this thesis. Interested readers are referred to [12,17,18,19,20,21] for a complete derivation. The derived theory of spot pricing places constraints on energy balance and the behaviour of the transmission and distribution networks. However, there are no constraints on the revenues collected by the utility. Hence, a regulated utility using spot pricing is likely to have a rate of return on investment different than that allowed by regulators. This problem, which is often referred to as "Revenue Reconciliation", can be solved by refunding or surcharging customers at appropriate intervals. There is a well established theory on how to implement these options without altering customer behaviour away from the optimal level [2,12]. The uncertainties associated with the application of a revenue reconciliation strategy in practice are comparable for spot pricing and other approaches to electricity pricing which do not start out with optimal prices.

The components of a spot price can be grouped in two different categories: marginal operating costs and marginal outage costs. Marginal operating costs are generally defined as the additional fuel costs that are incurred in serving an incremental load, where these additional costs may partly arise from line losses and off-economic dispatch. Marginal outage costs - also called "shortage costs" or "curtailment costs" - are defined as the outage costs related to both capacity shortages and network capacity constraints that are incurred in serving an incremental load. In principle, the marginal operating costs needed for spot pricing can be estimated using economic dispatch models. Such models determine the output levels for all generating units in a system by minimizing the production costs subject to transmission constraints, system security and operating reliability constraints. A detailed exposition to the theory of economic dispatching and evaluation of marginal operating costs is beyond the scope of this thesis. Interested readers are directed to [12,22,23] for further detail. This thesis is concerned with the development of methodologies for evaluating the marginal outage costs in electric power systems using quantitative power system reliability concepts. These concepts are based on a hierarchical framework of analysis as described in the following section.

1.3. Power System Reliability in Perspective

A power system serves one function only and that is to supply customers, both large and small, with electric energy as economically as possible and with an acceptable degree of reliability and quality. The term "reliability" has a wide range of meaning and cannot be associated with a single specific definition such as that often used in a mission oriented sense [24,25]. It is therefore necessary to recognize the extreme generality of the word and to use it in a general rather than a specific sense to assess the ability of the system to perform its intended function. Power system reliability evaluation, both deterministic and probabilistic, can therefore be divided into two basic aspects: system adequacy and system security. The following discussion of the general area of reliability is depicted graphically in Figure 1.1.

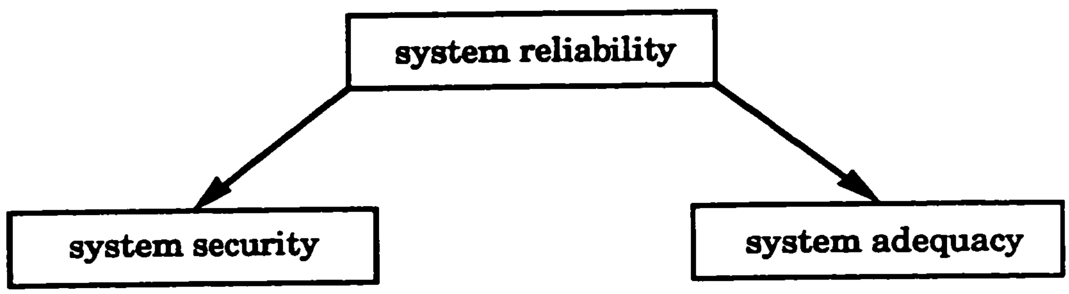

Figure 1.1. Subdivision of system reliability.

Adequacy relates to the existence of sufficient facilities within the system to satisfy the customer load demand. Adequacy is therefore associated with static conditions which do not include system disturbances. Security relates to the ability of the system to respond to disturbances arising within that system. Security is therefore associated with the response of the system to whatever perturbations it is subjected to. The reliability analyses described in this thesis are related to system adequacy and therefore the resulting marginal outage costs are associated with the existence of facilities within the system rather than the operational considerations which are covered by security evaluation.

The basic techniques for adequacy assessment can be categorized in terms of their application to segments of a complete system. These segments are shown in Figure 1.2 and are defined as the functional zones of generation, transmission and distribution. Adequacy studies can be, and are, conducted in each of these three functional zones.

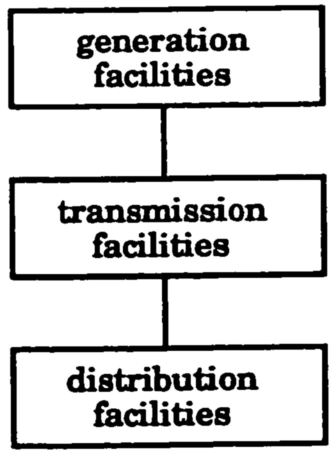

Figure 1.2. Basic functional zones of a power system.

The functional zones shown in Figure 1.2 can be combined to give the hierarchical levels shown in Figure 1.3. These hierarchical levels can also be used in adequacy assessment. Hierarchical Level I (*HLI*) is concerned only with the generation facilities, Hierarchical Level II (*HLII*) includes both generation and transmission facilities and *HLIII* includes all three functional zones in an assessment of customer load point adequacy.

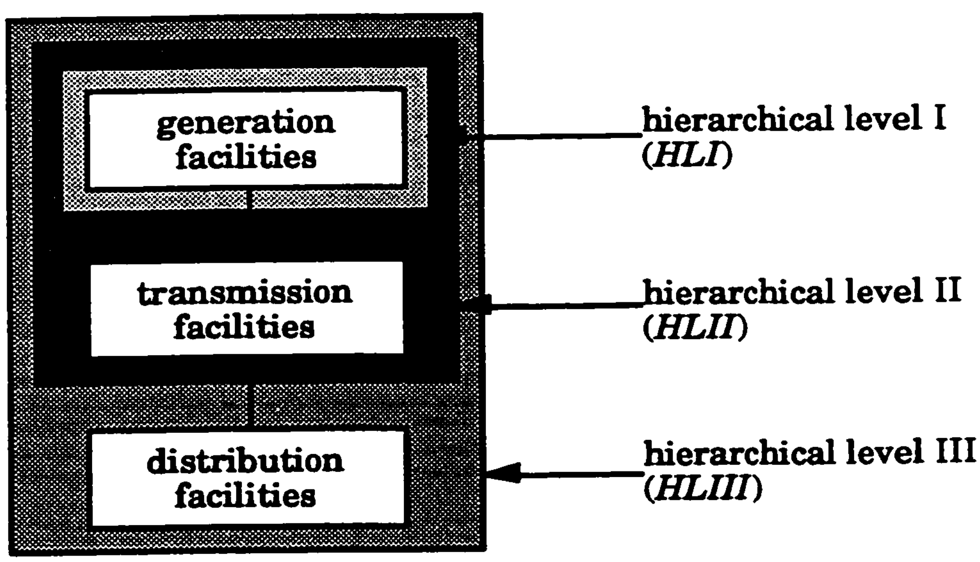

Figure 1.3. Hierarchical levels.

1.3.1. Adequacy evaluation at *HLI*

In *HLI* studies, the total system generation is examined to determine its ability to meet the total system load requirement. This activity is usually termed "generating capacity reliability evaluation". The system model at this level is shown in Figure 1.4. The transmission system and its ability to move the generated energy to the consumer load points is ignored in *HLI* evaluation. The basic concern is to estimate the generating capacity required to satisfy the system demand and to have sufficient generating capacity to perform corrective and preventive maintenance on the generating facilities. The historical technique used to determine this capacity requirement is the "percentage reserve" method [24,25]. Other criteria, such as one or more largest units, have also been used. These deterministic approaches have now been largely replaced by probabilistic methods which respond to and reflect the actual factors that influence the reliability of the system.

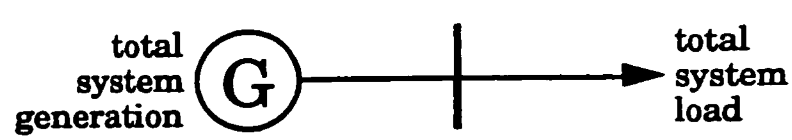

Figure 1.4. Power system model for *HLI* studies.

The most common reliability indices used by the electric utility industry are the Loss of Load Expectation (*LOLE*), the Expected Unserved Energy (*EUE*) and the Frequency and Duration (*F&D*). These indices can be calculated using direct analytical techniques or Monte Carlo simulation [25,26]. The *EUE* index is used in the *HLI* studies described in this thesis as it can most easily be linked with a cost factor in order to calculate the marginal outage costs in generating systems.

Although *HLI* studies are concerned with generation facilities only, limited consideration of transmission can be included in the form of interconnections to neighbouring systems as shown in Figure 1.5. In these cases, only the interconnections between adjacent systems are modelled; not the internal system connections. The capacity assistance available from the neighbouring system is modified by the reliability of the transmission link before it is added to the capacity model of the system under consideration.

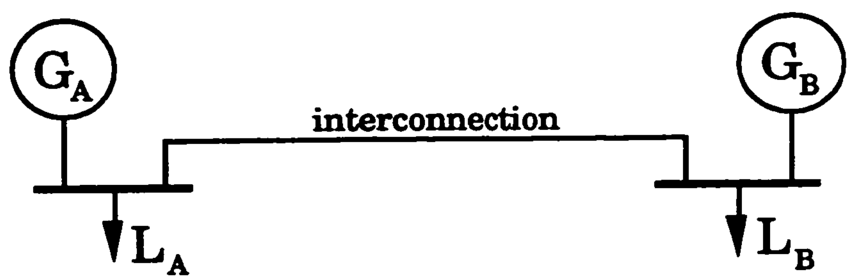

Figure 1.5. Model of interconnected generating systems in *HLI* studies.

1.3.2. Adequacy evaluation at *HLII*

In *HLII* studies, the simple generation-load model shown in Figure 1.4 is extended to include bulk transmission. Adequacy analysis at this level is concerned with the ability of the transmission system to move the generated energy to the bulk load points. This type of analysis is usually referred to as "composite system adequacy evaluation" as it involves the composite problem of both generation and transmission assessment. There is a wide range of indices which can be used to assess the adequacy of bulk load points and the overall system. These indices are described in detail in [25,26]. The expected unserved energy at each bulk load point can be linked with an appropriate average cost of unserved energy in order to estimate the expected customer outage costs and subsequently the marginal outage costs for that load point.

1.3.3. Adequacy evaluation at *HLIII*

The overall problem of *HLIII* evaluation can become very complex in most systems because this level involves all three functional zones, starting at the generating points and terminating at the individual customer load points. For this reason, the distribution functional zone is usually analyzed as a separate entity. However, the *HLIII* indices can be evaluated using the *HLII* bulk load point indices as the input values at the source of the distribution functional zone being analyzed. The analytical methods for evaluating these *HLIII* indices are highly developed and given in [26].

1.4. Scope and Objectives of the Thesis

Quantitative reliability assessment is an important aspect of power system planning and operation. The basic concepts utilized in reliability assessment of electric power systems at the generating capacity level are well known [27-31]. Research organizations and power utilities have also been working assiduously for the past two decades in reliability assessment of composite generation and transmission systems [27-32]. There is therefore a wide range of techniques and indices available for adequacy assessment at *HLI* and *HLII*. In the past, the majority of these techniques have been applied to power system operation and planning problems [25,26,33]. More recently, however, these techniques were used in cost/benefit assessments of electric power systems [34]. The objective of this thesis is to utilize these quantitative techniques to develop methodologies for calculating the marginal outage costs in electric power systems.

The Expected Unserved Energy (*EUE*) in the system or at a bulk load point is a basic adequacy index which represents the expected energy that cannot be supplied in a given period due to insufficient installed generating and/or transmission capacity. This index gives a measure of the severity of the deficiency and therefore bears a direct relationship to the interruption impacts on customers. The *EUE* index can therefore be directly integrated with the customer interruption costs to calculate the marginal outage costs in electric power systems.

The utilization of the *EUE* in marginal outage costing can be done using the same basic hierarchical framework outlined in Section 1.3. This type of analysis sub-divides the power system into hierarchical levels and performs reliability calculations in each level. A similar strategy is used in this thesis to develop methodologies for calculating the marginal outage costs at *HLI* and *HLII*. This strategy sub-divides the research activities in three phases that are summarized below.

1.4.1. Research objectives for Phase 1

The main objective of this phase was the utilization of quantitative power system reliability concepts to develop a methodology for calculating the marginal outage costs in isolated generating systems. A number of sensitivity analyses and approximate techniques were investigated to show the impact of selected modelling assumptions and approximations on the marginal outage cost profile. The results from these studies are used to draw some general conclusions about the applicability of the proposed method in practical system studies.

1.4.2. Research objectives for Phase 2

The objective of Phase 2 was to extend the methodology developed in

Phase 1 to interconnected generating systems. This new capability was used to calculate the marginal outage costs of a number of regions within the same system as well as the impact of capacity assistance from neighbouring systems on these costs. The effects on the marginal outage cost of selected interconnection topologies and modelling assumptions were investigated to show how simplified representations can be used to approximate the results obtained from more detailed reliability models.

1.4.3. Research objectives for Phase 3

Although the ultimate goal of any spot pricing scheme is to calculate and provide electricity prices at each individual customer load point in the system, it is impossible to accomplish this in a practical system. Instead, spot prices are estimated for groups of customers within defined geographic areas or at bulk load points. In the final phase of this research work, a methodology for calculating the marginal outage costs in composite generation and transmission systems was developed. This methodology is based on the principles used in composite system reliability evaluation. The cost values calculated in this phase provide a measure of the spatial variations in the marginal outage cost at bulk load points. Sensitivity analyses conducted in this phase quantify the effects of selected pertinent factors and customer outage cost models on the marginal outage cost profiles. The results from these studies show how a simplified model can be used to calculate the marginal outage costs in composite systems. Such a model has numerous practical applications because most electric utilities do not currently use composite system reliability models in their operating environment.

1.5. Outline of the Thesis

This thesis is divided into nine chapters. Following the introduction in Chapter 1, a review of the methodologies available for calculating the marginal outage costs in electric power systems is given in Chapter 2. Three methods are described in this chapter and detailed derivations of the proposed methodologies for calculating the marginal outage costs in generating and composite generation and transmission systems are presented.

The utilization of the proposed method for calculating the marginal outage costs in isolated generating systems is illustrated in Chapter 3 by application to two reliability test systems. The test systems are a small educational configuration designated as the Roy Billinton Test System (*RBTS*) [35] and a more practical system known as the *IEEE*-Reliability Test System (*IEEE-RTS*) [36]. Sensitivity studies are presented in Chapter 3 to show the effects of selected modelling assumptions and parameters on the marginal outage cost profiles of the two systems. The application of the proposed method to two test systems of different sizes is done in order to show the impact of system size on the robustness of the proposed method and the accuracy of the approximations.

Quantitative evaluation of the marginal outage costs associated with generating systems involves, among other things, the construction of a model of the system capacity outages. This model requires lengthy computations when applied to large power systems. Alternatively, approximate techniques can be used to model the generating system capacity model. These techniques can in some cases introduce inaccuracies in the results, which depend on the system under consideration. Chapter 4 presents a number of approximate techniques and discusses their potential applications for calculating the marginal outage costs in isolated generating systems. The results of the approximate techniques are illustrated in Chapter 4 by comparison with those produced using the exact technique described in Chapter 3 for the *RBTS* and the *IEEE-RTS*.

The proposed methodology for calculating the marginal outage costs in isolated generating systems is extended in Chapter 5 to interconnected generating systems. The newly extended method is used in this chapter to calculate the marginal outage costs on a regional basis within a single system and the impact of capacity assistance from neighbouring systems on these costs. This chapter illustrates the effect of selected interconnection topologies and modelling assumptions on the marginal outage costs in interconnected generating systems. The application of the derived methodology is illustrated using the *RBTS* and *IEEE-RTS*.

The utilization of the proposed methodology for calculating the marginal outage costs in composite generation and transmission systems is illustrated in Chapter 6. The proposed method is used in this chapter to calculate the marginal outage cost profiles of selected bulk load points in the *RBTS* and the *IEEE-RTS*. The contributions of the generation and transmission systems to the overall marginal outage cost are also calculated in this chapter.

The method used in Chapter 6 to calculate the marginal outage costs in composite systems is reasonably comprehensive and therefore it requires considerable computing time when applied to large power systems. In practical system studies, a number of approximations are normally made to the exact method in order to reduce the computer time requirements. These approximations are utilized due to a lack of computational tools, lack of data or in order to meet the stringent turnaround time constraints of the operating environment. Chapter 7 presents the results of a number of sensitivity analyses aimed at quantifying the effects of selected approximations on the marginal outage cost calculated at *HLII*.

Chapter 8 utilizes the findings from the sensitivity analyses conducted in Chapters 3, 4, 5, 6 and 7 to provide recommendations for implementing the proposed methods in practical systems. A summary of the research work done in this thesis and the conclusions are presented in Chapter 9.

There is a growing interest in the electric utility industry in quantitative assessment of power system reliability. This has led to intensive activity in the application of probabilistic techniques to power system planning and operation problems [25-33]. By contrast, there has been no effort spent in applying these techniques to marginal outage costing. The published literature indicates that the methods currently available for calculating the marginal outage costs in electric power systems utilize approximate economic models which do not take into consideration the stochastic nature of the power system and its effects on these costs [12,17,49,55]. This thesis presents a formal and practical approach for calculating the marginal outage costs using quantitative power system reliability concepts.

2. MARGINAL OUTAGE COSTS IN ELECTRIC POWER SYSTEMS

2.1. Introduction

The electric utility industry is undergoing rapid and irreversible changes. Volatile fuel prices, uncertain load growth, a more stringent regulatory environment and diminished technical progress are important examples of these changes. The need for growth in productivity and for increased flexibility to handle future uncertainties is, however, stronger and more challenging than ever. New directions for the utility industry are being actively sought by interested parties in government, the private sector and universities. One such direction has been the widespread interest in utility-customer cooperation through innovative rate structures characterized by broader options and better use of information on utility costs and customer needs [10,12].

A major utility concern is to find realistic and acceptable procedures for reducing demand at times of critical load conditions. These conditions may arise infrequently in emergency situations, but more regularly at peak load levels. Of equal concern are surplus periods where low cost energy is available but cannot be marketed because the price offered to customers does not reflect the abundance of the resource. Thus, both the utility and the customer fail to benefit from these time-varying conditions. Classical and time-of-use tariffs are pre-specified well in advance (one or more years) and thus do not provide utilities with an effective means for managing demand under changing conditions. Spot prices, on the other hand, are capable of achieving significant gains in short-term efficiency. These gains can be to the benefit of both the utility and its customers and the incorporation of one or more real time elements into a tariff makes it more responsive to utility and customer needs [10,12].

Marginal outage costs are an important component of electricity spot prices. This chapter describes a number of methodologies that can be used to calculate these costs and presents detailed derivations of the proposed methods for calculating the marginal outage costs in generating and composite generation and transmission systems. These methods are based on quantitative power system reliability concepts.

2.2. Components of Electricity Spot Prices

In general, spot prices are explicit functions of a number of random variables and therefore change over time as these random variables change [12]. Marginal, rather than embedded, costs are used in the calculation of electricity spot prices because, under optimal conditions, they: 1) satisfy the revenue requirements of the utility and 2) provide customers with information about the actual cost of electric service [37-41]. There are two types of marginal costs used in economic analyses of power systems. The Short-Run Marginal Cost (*SRMC*) is the cost of meeting additional electricity consumption with a fixed capacity, while the Long-Run Marginal Cost (*LRMC*) is the cost of providing an increase in consumption (sustained indefinitely into the future) in a situation where optimal capacity adjustments are possible [42,43]. When the system is optimally planned and operated, *SRMC* and *LRMC* coincide. However, if the system plan is sub-optimal, significant deviations between *SRMC* and *LRMC* will have to be resolved within the pricing policy framework (i.e. revenue reconciliation). Since most spot pricing schemes are applicable in the short term (i.e. next day or week), capacity adjustments are not possible and therefore *SRMC* estimates are used. Short-run marginal cost estimates developed for spot pricing purposes should ideally reflect cost differences over both time and space. Marginal costs vary over time due to changes in both the load level and the availability of system components. They also vary over space because the locations of loads relative to generators and the transmission system constraints significantly affect costs.

The components of a spot price can be grouped in two different categories: marginal operating costs and marginal outage costs. Marginal operating costs are generally defined as the additional fuel costs that are incurred in serving an incremental load, where these additional costs may partly arise from line losses and off-economic dispatch. Marginal outage costs are defined as the customer outage costs related to both capacity shortages and network capacity constraints that are incurred in serving an incremental load. The marginal operating costs needed for spot pricing can be estimated using economic dispatch models. Such models determine the output levels for all generating units in a system by minimizing the production costs subject to transmission constraints, system security and operating reliability constraints [12,22,23]. The marginal outage costs can be calculated using a number of methodologies as described in the following section.

2.3. Methodologies for Calculating the Marginal Outage Costs in Electric Power Systems

Marginal outage costs are included in electricity spot prices because rates should depend upon the extent to which the expected customer outage costs change as load changes. Although, the majority of outages are caused by factors that are unrelated to load levels, loads do affect the characteristics of outages (e.g. frequency, duration, unserved energy, etc.) and consequently their associated customer economic costs. The problem of estimating the economic costs incurred by customers due to power outages has been discussed quite extensively in the literature [44-52]. References 53 and 54 provide a comprehensive background on the evolution of the methodologies used to estimate the economic costs of power outages incurred by customers.

Marginal outage costs measure the change in the expected customer outage costs that accompanies an incremental load change. In order to implement hourly spot pricing, methodologies capable of forecasting these costs on an hourly basis must be developed. Three general techniques can typically be used to estimate the marginal outage costs. These techniques are:

1) annualized capital costs of installing additional capacity to avoid the incremental unit of shortfall,

2) price increase (i.e. reduction in consumer's surplus) needed to cause consumers to reduce their demands such that the incremental unit of unserved energy does not occur, and

3) average customer economic costs resulting from power outages.

The first methodology is related to the long-run marginal cost approach to pricing while the other two are related to the short-run marginal cost approach. A brief description of each methodology is given in the following sub-sections.

2.3.1. Annualized capital costs of installing new capacity

The justification for estimating the marginal outage cost from the cost of installing new capacity is that for an optimal system capacity, the investment cost to the utility for incrementally decreasing the unserved energy equals the cost to the customers for experiencing that amount of unserved energy [18,39]. If the capacity is not optimal, either because planners failed to correctly anticipate the future or because the investment is sporadic, then capacity costs will not accurately reflect the marginal outage costs. Furthermore, the capacity cost method pre-supposes the existence of outage cost estimates as the basis for the capacity plan. If such estimates are available, they should be used directly as shown in Sub-section 2.3.3 rather than inferred from the capacity expansion plan.

A slight variation to this method was proposed by Bental and Ravid [55] who used the annualized capital and variable costs spent by industrial customers on backup generators to estimate the marginal outage costs. The method takes into account the ability of firms to hedge against power outages by buying backup generators. The firms' behaviour in the generator market is used to compute the marginal outage costs. The basic conclusion presented in [55] states that the expected gain from the marginal self-generated energy is equal to the expected loss from the marginal energy which is not supplied by the utility. Therefore, the marginal cost of generating the power from a backup generator may serve as an estimate of the marginal outage cost. This method applies to those industrial customers that have outage costs large enough to justify the purchase of backup generators; but it excludes the remaining industrial customers and non-industrial customers that cannot justify the purchase of backup generators.

Since spot prices are forecast using relatively short lead times (e.g. a day, a weekend or a week), capacity adjustments to the power system are not possible in such timeframes and therefore the capital cost methodology cannot be used to estimate the marginal outage costs for the purposes of spot pricing. This method, however, is quite suitable for system planning studies.

2.3.2. Reduction in consumer's surplus

This method requires knowledge of customer demand response during hours of unserved energy in order to estimate the price increment that would cause demand to decrease by an amount equal to what would have otherwise been unserved energy [18]. All customers have a vague notion how they would alter their consumption in response to changes in unit price. That is, customers will reduce consumption as the rate increases or will increase consumption as the rate decreases. This implies that some uses of electricity must be worth more than others and certainly more than is presently paid for them. The difference between the amount paid for them and the worth to the user is called the "consumer's surplus". This surplus is lost to the consumer when the supply is interrupted. Generally, the surplus of a consumer is calculated by inferring the consumer's Willingness To Pay (*WTP*) to avoid outages from estimated demand curves for electricity. Such demand functions are derived from rate experiments or demonstrations [18,22,56].

The value of a consumer's surplus provides a measure of the outage cost of that consumer. The marginal outage cost of a consumer can be calculated as the change in that consumer's surplus that accompanies an incremental change in load. Although the consumer's surplus method provides adequate estimates of the customer outage costs, it cannot be used to estimate the outage costs of all types of customers. The customer survey method, on the other hand, is more suited for such purposes and is widely accepted by the electric utility industry. The application of the customer survey method to calculating the marginal outage costs in electric power systems is discussed in the following sub-section.

2.3.3. Average customer economic costs resulting from power outages

This method is based on the premise that the marginal outage costs are expected quantities that depend upon two major factors: 1) the customer economic costs that accompany various outage levels; and 2) the effects of load changes on the probabilities that these costs will actually be incurred. The customer economic costs resulting from power outages can be evaluated using a number of methodologies [53,54]. One method that is considered to yield acceptable results is the customer survey method where customers are surveyed to estimate their losses and to create Customer Damage Functions (*CDF*'s) which express the interruption cost as a function of the interruption duration for each customer group. The *CDF*'s developed using the survey method can be used to calculate an average cost of unserved energy for each customer group and for the entire service area. Such a cost factor was developed at the University of Saskatchewan for isolated generating systems [57] and composite generation and transmission systems [58]. The index is designated as the Interrupted Energy Assessment Rate (*IEAR*) expressed in $\$/kWh$.

The second component required to calculate the marginal outage cost incorporates the probabilities of capacity outages and the system load demand in the form of a quantitative risk index. The most suitable reliability index for calculating the marginal outage cost is the Expected Unserved Energy (EUE) expressed in $MWh/period$ where *"period"* refers to the length of the study period under consideration. Since most practical spot pricing schemes calculate the spot price on an hourly basis, the value of the study period is assumed to be 1 hour. The effect of load changes on EUE can be measured by taking the difference between two EUE values that are calculated at incrementally different load levels (e.g. a load increase of 1 MW). That is,

$$\Delta EUE = EUE_{(L+1)} - EUE_{(L)} \qquad (MWh/MW), \qquad (2.1)$$

where ΔEUE : incremental expected unserved energy resulting from an incremental change in load,

$EUE_{(L+1)}$: expected unserved energy for a load level of $(L+1)$ MW and

$EUE_{(L)}$: expected unserved energy for a load level of L MW.

Given the values of the $IEAR$ and ΔEUE, the hourly marginal outage cost ($M.O.C.$) can be calculated as follows:

$$M.O.C. = IEAR \times \Delta EUE \qquad (\$/kW). \qquad (2.2)$$

The two components in this expression can be calculated using established power system reliability evaluation techniques. The detailed derivations of these components for generating and composite generation and transmission systems are presented in Sections 2.4 and 2.5 respectively.

2.4. Derivation of the Marginal Outage Costs Associated With Generating Systems

The proposed method for calculating the hourly marginal outage costs in electric power systems is based on quantitative power system reliability concepts. The techniques used to assess the reliability of an electric power system are based on the hierarchical framework described in Section 1.3 of this thesis [24]. This section is concerned with the utilization of quantitative power system reliability techniques to calculate the marginal outage costs in generating systems (i.e. *HLI* evaluation).

The *HLI* model of a power system is basically a generation-load model that does not include the network configuration or topology required to move the energy from the generating stations to the bulk load centres. Generation system adequacy evaluation provides a measure of the ability of the generating system to meet the demand without considering the network constraints [26]. The techniques available for assessing the adequacy of a generating system can be broadly classified as analytical [25,26] or as Monte Carlo simulation [25,59,60]. Analytical techniques represent the system by a mathematical model and proceed to evaluate the reliability indices from this model using mathematical solutions. Monte Carlo simulation methods, however, estimate the reliability indices by simulating the actual process and random behaviour of the system. The method therefore treats the problem as a series of real experiments. Both techniques have merits and demerits, and can be very powerful when correctly applied. The main advantage of the analytical approach is its relative compactness which can be enhanced by making suitable approximations. Monte Carlo simulation, on the other hand, may be preferable if non-exponential distributions have to be modelled or the distributions associated with the output indices are required. In theory, Monte Carlo simulation can include any system effect or process which may have to be approximated in the analytical methods. It does, however, require large amounts of computer time and storage in order to obtain reasonable confidence in the results.

The most common probabilistic analytical methods used in generating capacity adequacy assessment are the loss of load method, the frequency and duration approach and the loss of energy method [26]. In all these methods, the generating system is represented by a mathematical model which is superimposed on the load model in order to calculate the reliability indices. The simplest form of the generating system model is represented by a Capacity Outage Probability Table (*COPT*) which gives the probability of having various quantities of capacity on forced outage. The system load model can be represented by the Daily Peak Load Variation Curve (*DPLVC*) or the Load Duration Curve (*LDC*) depending on the application.

A number of reliability indices can be calculated using either Monte Carlo simulation or the analytical techniques. The most widely used reliability index in generating capacity adequacy assessment is the Loss of Load Expectation (*LOLE*). This index measures the expected time in which the generation available will be insufficient to meet the demand. The *LOLE* index as normally calculated does not measure the severity of deficiencies. It is therefore difficult to relate this index directly to the interruption costs of electric customers. The Expected Unserved Energy (*EUE*) index specifies the expected energy that will not be supplied due to those occasions when the demand exceeds the available generating capacity. This index includes a measure of the severity of deficiencies rather than only the amount of time that a deficiency exists. Some utilities are commencing to utilize the *EUE* in generating capacity adequacy assessments. This index can also be used together with a customer cost function to obtain an estimate of the average cost of unserved energy in generating systems. Such a cost factor, designated as the Interrupted Energy Assessment Rate (*IEAR*), was developed at the University of Saskatchewan [57] using a basic Frequency and Duration (*F&D*) approach and Monte Carlo simulation. A description of the Monte Carlo simulation approach to establishing an *IEAR* for generating systems is presented in Sub-section 2.4.1. The variations in *EUE* resulting from an incremental load change (i.e. ΔEUE) can be calculated using the basic loss of energy method [26]. The utilization of this method to formulate a simple expression for calculating ΔEUE in generating systems has been recently published [61] and is described in Sub-section 2.4.2.

2.4.1. Derivation of the interrupted energy assessment rate in generating systems

The detailed description of the concepts involved in calculating an *IEAR* using a basic Frequency and Duration (*F&D*) approach or Monte Carlo simulation is presented in [57]. A brief description of the Monte Carlo simulation approach to establishing an *IEAR* at *HLI* is given here to illustrate the salient features.

In the simulation model, the generating system is modelled by specifying a set of "events" where an event is a random or deterministic occurrence that changes the "state" of the system [60]. The following events are recognized in the simulation model:

1) change in load,
2) change in reserve requirements,
3) failure of a generating unit,
4) completion of repair of a generating unit,
5) derating of a generating unit and
6) completion of a derating repair.

Each of the listed events produces a change in the state of the system. There are a number of ways in which the system state can be defined. The central measure used in this simulation model is the "available margin" which is defined as the difference between the available capacity (installed capacity less failed units and capacity loss due to derating) and load. Planned outages are not considered in this model. The simulation model examines the system life during a specified calendar year using repeated "yearly samples" each consisting of 8736 hours which are selected in their chronological succession (sequential approach). The advantage of using this approach is the output that it provides in the form of probability distributions. These distributions are particularly useful when the interruption costs have to be estimated from the distribution of interruption duration.

In order to calculate the *IEAR*, the simulation model is used to generate the duration r_i (hours), amount of load loss l_i (kW) and amount of energy loss e_i (kWh) for each load loss event (interruption) i. Using the interruption duration r_i, the cost associated with this load loss event, $C_i(r_i)$ ($\$/kW$), is obtained from the Composite Customer Damage Function (*CCDF*) of the entire system. This function represents the outage costs of all the customers in the service area as a function of the interruption duration. The *IEAR* is estimated by adding the costs from all the load loss events and normalizing the result by the total unserved energy as given by (2.3),

$$IEAR = \frac{\sum_{i=1}^{n} C_i(r_i) \times l_i}{\sum_{i=1}^{n} e_i} \qquad (\$/kWh), \qquad (2.3)$$

where n represents the total number of interruptions. Sensitivity studies conducted in [57] show that the $IEAR$ is quite stable and does not vary significantly with the load model and other pertinent operating considerations.

2.4.2. Derivation of the incremental expected unserved energy in generating systems

The second component required to calculate the marginal outage cost in generating systems is the Incremental Expected Unserved Energy (ΔEUE) which equals the difference between two EUE values that are evaluated at incrementally different load levels. The EUE is a basic reliability index that can be calculated using analytical techniques [26] or Monte Carlo simulation [59,60]. This sub-section is concerned with the utilization of the loss of energy technique to formulate a simple expression for calculating ΔEUE in generating systems [61].

The loss of energy technique is based on the convolution of a capacity model, usually in the form of a Capacity Outage Probability Table ($COPT$), and an hourly load model in the form of a load duration curve or a sequence of hourly data. The duration of the hourly load model can vary depending on the application. Since most practical spot pricing schemes calculate the spot price on an hourly basis, the duration of the load model is assumed to be 1 hour. The $COPT$ model can be generated using the well-known concept of recursive unit addition [26]. In its general form, this technique is used to calculate the cumulative probability of a particular capacity outage state after a generating unit is added to the capacity model using (2.4):

$$P(X) = \sum_{i=1}^{n} p_i \, P'(X - C_i), \tag{2.4}$$

where C_i : capacity on outage in State i of the unit being added (MW),
p_i : probability of residence in State i of the unit being added,
n : number of states in the generating unit model,
X : system capacity on outage (MW),
$P(X)$: cumulative probability of having X (MW) on outage after the generating unit is added to the *COPT*, and
$P'(X)$: cumulative probability of having X (MW) on outage before the generating unit is added to the *COPT*.

The expression given by (2.4) is initialized by setting $P(X) = 1$ for $X \leq 0$ and $P(X) = 0$ otherwise. When $n = 2$, (i.e. two-state model), the expression for $P(X)$ given by (2.4) reduces to that given by (2.5) where U_i denotes the unavailability or Forced Outage Rate (*FOR*) of the generating unit being added,

$$P(X) = (1 - U_i)\, P'(X) + (U_i)\, P'(X - C_i). \tag{2.5}$$

A *COPT* developed using the recursive technique consists of N discrete outage levels, $X(K)$, where $K = 1,2,3, \dots ,N$, which are arranged in strictly ascending order, $X(K+1) > X(K)$. Note that $X(1) = 0$ and $X(N) = C$, where C represents the installed capacity of the system. The *cumulative* probability $P(K)$ that a capacity outage greater than or equal to $X(K)$ occurs is given by (2.6) where the *individual* probability $p(K)$ refers to the probability that a capacity outage occurs which is exactly equal to $X(K)$,

$$P(K) = \sum_{\kappa=K}^{N} p(\kappa). \tag{2.6}$$

The expected unserved energy for a period of 1 hour and a load level of L MW, $EUE_{(L)}$, is calculated using (2.7) by taking into account all system outage states, $X(K)$, which cause capacity deficiency during that hour,

$$EUE_{(L)} = \sum_{\kappa=K}^{N} \left[L-(C-X(\kappa))\right]p(\kappa), \tag{2.7}$$

where K is defined such that $X(K)$ is the smallest capacity outage that causes capacity deficiency for a given load L. More precisely,

$$\begin{aligned} C-X(K) \quad &< L, \\ C-X(K-1) \quad &\geq L. \end{aligned} \tag{2.8}$$

Similarly, the expected unserved energy at a load level of $(L+1)$ MW (i.e. load increment of 1 MW), $EUE_{(L+1)}$, is given by (2.9),

$$EUE_{(L+1)} = \sum_{\kappa=K'}^{N} \left[L+1-(C-X(\kappa))\right]p(\kappa), \tag{2.9}$$

where K' is defined such that

$$\begin{aligned} C-X(K') \quad &< L+1, \\ C-X(K'-1) \quad &\geq L+1. \end{aligned} \tag{2.10}$$

By substituting (2.7) and (2.9) into (2.1), the following expression for ΔEUE can be developed:

$$\Delta EUE = \sum_{\kappa=K'}^{N} \left[L+1-(C-X(\kappa))\right]p(\kappa) - \sum_{\kappa=K}^{N} \left[L-(C-X(\kappa))\right]p(\kappa). \tag{2.11}$$

This expression can be simplified if a relationship between K and K' can be established. Due to the discrete nature of the $COPT$ and assuming that the load increment of 1 MW is smaller than the rated capacity of any generating unit in the system, there could only be two possible relationships between K and K':

1) the smallest capacity outage for load level L is the same as the smallest capacity outage for load level $(L+1)$. That is, $K' = K$, or

2) the smallest capacity outage for load level L is larger than the smallest capacity outage for load level $(L+1)$ by one discrete step. That is, $K' = K - 1$.

The assumption that the load increment of 1 MW is smaller than the rated capacity of any generating unit in the system is valid for most test and practical power systems. If, however, the power system is relatively small (i.e. total installed capacity of a few megawatts), the above relationships can still be applied by converting the capacities of all the generating units to kilowatts and assuming that the load increment is 1 kW instead of 1 MW.

<u>Case 1 : $K' = K$</u>

If K' equals K, the expression for ΔEUE can be written as:

$$\Delta EUE = \sum_{\kappa=K}^{N} \left[L+1-(C-X(\kappa))\right]p(\kappa) - \sum_{\kappa=K}^{N} \left[L-(C-X(\kappa))\right]p(\kappa). \qquad (2.12)$$

This expression can be simplified to (2.13) after cancelling the common terms in $EUE_{(L+1)}$ and $EUE_{(L)}$,

$$\Delta EUE = \sum_{\kappa=K}^{N} p(\kappa) = P(K). \qquad (2.13)$$

It can be seen from (2.13) that ΔEUE is simply a cumulative probability that is readily available from the $COPT$, and therefore the computation of the EUE reliability index is not required for the purposes of marginal outage costing.

<u>Case 2 : $K' = K - 1$</u>

In this case, the expression for ΔEUE is as follows:

$$\Delta EUE = \sum_{\kappa=K-1}^{N}\left[L+1-(C-X(\kappa))\right]p(\kappa) - \sum_{\kappa=K}^{N}\left[L-(C-X(\kappa))\right]p(\kappa). \quad (2.14)$$

By expanding the expression of $EUE_{(L+1)}$ and cancelling the common terms with $EUE_{(L)}$, ΔEUE can be rewritten as:

$$\Delta EUE = \left[L+1-(C-X(K-1))\right]p(K-1) + \sum_{\kappa=K}^{N} p(\kappa). \quad (2.15)$$

Rearranging the terms in (2.15) gives:

$$\Delta EUE = \left[L-(C-X(K-1))\right]p(K-1) + P(K-1). \quad (2.16)$$

Similarly to Case 1, the above expression does not require the calculation of the EUE reliability index in order to estimate ΔEUE. However, it requires the computation of the individual probability, $p(K\text{-}1)$, which is not readily available from the $COPT$ but can be calculated using (2.17),

$$p(K-1) = P(K-1) - P(K). \quad (2.17)$$

A close examination of (2.16) reveals that the first term of the equation represents the <u>exact</u> contribution to ΔEUE of the capacity deficiency caused by the difference between the load level L and the capacity outage level $X(K\text{-}1)$. The second term captures the <u>cumulative</u> contributions of all the capacity deficiencies starting with the capacity outage level $X(K\text{-}1)$. The contribution of the first term is only possible when the inequality $(L \neq C - X(K-1))$ is satisfied. But, if all the capacity outage states in the $COPT$ and the load levels are rounded off to the nearest MW; a condition that is normally satisfied by most test and practical power systems, the necessary condition for Case 2 (i.e. $K' = K\text{-}1$) will only occur if $L = C - X(K-1)$. This means that the first term in (2.16) is equal to zero and the expression for ΔEUE is reduced to:

$$\Delta EUE = P(K-1). \tag{2.18}$$

From the above two cases, a general expression for ΔEUE can be written as follows:

$$\Delta EUE = \begin{cases} P(K-1) & L = C - X(K-1), \\ P(K) & L > C - X(K), \end{cases} \tag{2.19}$$

where K is defined such that $X(K)$ satisfies the conditions outlined in (2.8). The expression for ΔEUE can be simplified further by defining a new variable K^* that satisfies the condition $L \geq C - X\left(K^*\right)$. Using this new variable, the expression for ΔEUE reduces to:

$$\Delta EUE = P\left(K^*\right) \qquad (MWh/MW). \tag{2.20}$$

This expression of the incremental expected unserved energy is used in the next chapter together with appropriate $IEAR$ values to calculate the marginal outage cost profiles of two reliability test systems.

2.5. Derivation of the Marginal Outage Costs Associated With Composite Power Systems

In addition to varying with the characteristics of generating units and the load level, the marginal outage cost also varies over space because the location of loads relative to generators and the transmission system constraints significantly affect costs [18]. The evaluation of the marginal outage cost at customer load centres requires a thorough investigation of the adequacy of the composite generation and transmission system. This can be done using composite system reliability methods [25-33]. This section provides a brief description of the techniques available for assessing the adequacy of composite systems and presents detailed derivations of the variables required for calculating the marginal outage costs associated with these systems.

A composite or bulk power system is a combined generation and transmission system. Composite system adequacy evaluation is a very complex problem that has been and still is under investigation by electric utilities, universities and research organizations [25-33]. An important factor in composite systems is the relationship between generation and transmission elements and how outages of these facilities affect the performance of the system.

The two main approaches used in composite system adequacy evaluation are based on analytical methods [62-66] and Monte Carlo simulation [59,67]. Both approaches assess the adequacy of a system state using the principle shown in Figure 2.1 [68]. That is, both approaches use a load flow to identify the system deficiencies and to assess the effect of remedial actions. This aspect, therefore, determines the severity of a system state deficiency. The load flow method varies widely from transportation models [69] and *DC* load flow [70] to *AC* load flow [71,72]. The latter is rarely used in the simulation approach because of excessive computing time. This is a practical limitation however, not a theoretical one. If reactive power violation or voltage deficiencies are being assessed, then an *AC* load flow is required.

There has been considerable debate regarding the relative merits of the analytical and Monte Carlo techniques. Reference 73 attempts to address this problem by presenting the results for the *IEEE*-Reliability Test System [36] using computer programs based on the two approaches. This comparison indicates the conceptual differences in modelling and problem perception and allows better understanding of the merits and demerits of each approach.

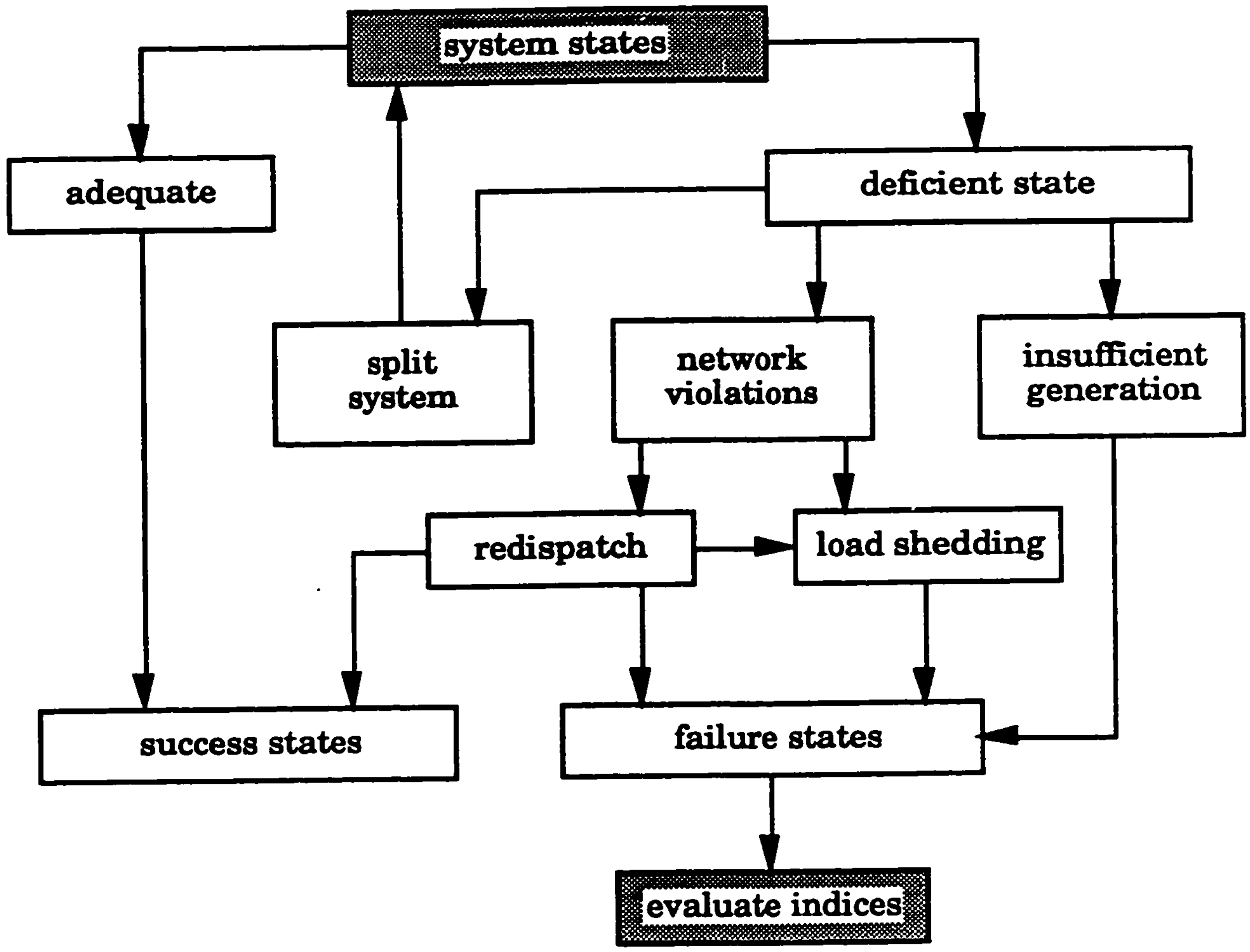

Figure 2.1. Concept of adequacy state assessment.

The major difference between the two approaches is in the process of selecting states and the way the likelihood and other adequacy indices are evaluated. The analytical approach generally selects states in an increasing order of the contingency level (i.e. zero outages, first order outages, second order outages, etc.). The process is usually stopped at a particular contingency level or when the state probability becomes less than a specified value. A state is therefore assessed only once and the indices are calculated from the statistical data defining each state such as probability, frequency, duration, etc. The number of states examined can be reduced using ranking techniques or selection procedures [74].

The simulation approach selects states randomly using the concept of gaming theory and random numbers [67,75]. States having a greater probability of occurrence are more likely to be simulated several times. The process is stopped either after a fixed number of simulations or on the basis of statistical stopping rules [67,75]. The expected values of the indices are determined by averaging the indices obtained during each simulation. Other statistical indices such as standard deviation and complete probability distributions can be found similarly from the individual simulation results.

A substantial amount of research work in the area of composite system adequacy evaluation has been done at the University of Saskatchewan. This research has resulted in the development of two computer programs, *COMREL* (COMposite system RELiability evaluation) and *MECORE* (Monte-carlo simulation and Enumeration approach for COmposite system Reliability Evaluation). The *COMREL* program is based on the contingency enumeration technique [76-78] whilst the *MECORE* program utilizes the random sampling approach typical of Monte Carlo methods [79,80]. The utilization of the *COMREL* program for calculating the marginal outage costs at bulk load points in composite systems is presented in this section.

The marginal outage cost at a customer load point, k, is defined as the change in the system's expected outage costs resulting from an incremental change in load at that point [12,22]. That is, if a load increment at Bus k causes the expected outage costs to increase at other locations, it should be the responsibility of the customers at Bus k to cover the additional costs. The same concept can also be used if the consumption at Bus k is reduced and a reduction in the marginal outage cost is needed. This concept is formulated in (2.21) by adding the incremental expected outage costs caused by a load increase at Bus k of all the load buses in the system.

$$M.O.C._k = \sum_{i=1}^{nbus} IEAR_i \times \Delta EUE_{ki}, \qquad (2.21)$$

where $M.O.C._k$: marginal outage cost at load Bus k,
$IEAR_i$: interrupted energy assessment rate at load Bus i,
ΔEUE_{ki} : incremental expected unserved energy at load Bus i caused by a load increment at Bus k and
$nbus$: total number of load buses in the system.

The expression for calculating the marginal outage cost at Bus k given in (2.21) requires a cost model (*IEAR*) and a reliability index (*EUE*) for each load bus in the system. A simpler method of estimating the marginal outage cost at Bus k can be obtained by multiplying the aggregate system *IEAR* and the total incremental expected unserved energy caused by a load increase at Bus k, $\Delta EUE_k(system)$. That is,

$$M.O.C._k = IEAR(aggregate) \times \Delta EUE_k(system) \qquad (\$/kW), \qquad (2.22)$$

where $\Delta EUE_k(system) = \sum_{i=1}^{nbus} \Delta EUE_{ki}$. The derivations of the various variables in (2.21) and (2.22) from the basic results of *COMREL* are described in the following sub-sections.

2.5.1. Derivation of the interrupted energy assessment rates in composite systems

The *IEAR* in generating systems is an expected value of the cost of unserved energy resulting from the inadequacy of the generating system.

This idea of utilizing expected values has also been used to evaluate practical *IEAR* estimates for the individual load buses and the overall system in a composite generation and transmission system adequacy assessment [34,58]. This work can be done using the *COMREL* program which uses a contingency enumeration approach to select the outages of components up to a prescribed level. For each outage contingency, the system state is scrutinized and if necessary, appropriate corrective actions are taken. A system failure is recorded when corrective actions, short of curtailing customer loads, are unable to eliminate the system problem. The severity of a failure is evaluated by calculating the frequency, duration, magnitude and location of load curtailment. For each Contingency j that leads to load curtailment at a load Bus i, the variables generated by *COMREL* are the magnitude L_{ij} (MW) of load curtailment, the frequency f_j (occ/yr) and the duration d_j $(hours)$ of the Contingency j. The EUE at Bus i due to all the contingencies that lead to load curtailment, EUE_i, is given by:

$$EUE_i = \sum_{j=1}^{NC} L_{ij} f_j d_j \qquad (MWh/yr), \qquad (2.23)$$

where NC is the total number of contingencies that lead to power interruptions at Bus i. The interruption cost to customers at Bus i of an outage of duration d_j, $C_j(d_j)$, can be obtained from the composite customer damage function of that bus, $(CCDF_i)$. This function represents the interruption costs of all the customers at Bus i as a function of the interruption duration [34]. The expected cost of power interruptions to customers at Bus i for all contingencies, $ECOST_i$, is given by (2.24). The *IEAR* at Bus i, $IEAR_i$, is calculated using (2.25) and the aggregate system *IEAR*, $IEAR(aggregate)$, is calculated using (2.26),

$$ECOST_i = \sum_{j=1}^{NC} L_{ij}\, f_j\, c_j(d_j) \qquad (MW \times occ/yr \times \$/kW), \qquad (2.24)$$

$$IEAR_i = \frac{\sum_{j=1}^{NC} L_{ij}\, f_j\, c_j(d_j)}{\sum_{j=1}^{NC} L_{ij}\, f_j\, d_j} \qquad (\$/kWh) \text{ and} \qquad (2.25)$$

$$IEAR(aggregate) = \sum_{i=1}^{nbus} IEAR_i \times q_i \qquad (\$/kWh). \qquad (2.26)$$

where q_i is the fraction of system load utilized by the customers at Bus i. Sensitivity studies conducted in [34] show that the $IEAR$'s in composite systems are relatively stable and do not vary significantly with the load model, load flow solution or load curtailment policy employed.

2.5.2. Derivation of the incremental expected unserved energy in composite systems

The second component required for calculating the marginal outage cost is the incremental expected unserved energy at load Bus i resulting from a load increment at Bus k (ΔEUE_{ki}). This variable can be calculated by taking the difference between two EUE values that are evaluated at incrementally different load levels. The expected unserved energy at Bus i, EUE_i, can be calculated using (2.23). If the load at Bus k is increased by 1 MW, the expression given by (2.27) can be used to calculate the new expected unserved energy at Bus i, EUE_i'.

$$EUE_i' = \sum_{j=1}^{NC'} L_{ij}'\, f_j'\, d_j' \qquad (MWh/yr), \qquad (2.27)$$

where the variables L_{ij}', f_j', d_j' and NC' have the same definitions as those given in (2.23). Given the values of EUE_i and EUE_i', the incremental expected unserved energy at Bus i caused by a load increment at Bus k can be calculated using (2.28). The factor of 1/8760 is employed to express the results on an hourly rather than annualized basis.

$$\Delta EUE_{ki} = \frac{1}{8760}\left\{ \sum_{j=1}^{NC'} L'_{ij} f'_j d'_j - \sum_{j=1}^{NC} L_{ij} f_j d_j \right\} \qquad (MWh/MW). \qquad (2.28)$$

The proposed method for calculating the marginal outage costs in composite systems is illustrated in Chapter 6 of this thesis by application to two reliability test systems. Sensitivity analyses are conducted in Chapter 7 to show the effects of system size, location of load increment and other pertinent considerations on the calculated marginal outage costs.

2.6. Variation of the Marginal Outage Cost With the Lead Time

The relationships between the marginal outage cost and the characteristics of generating units and transmission lines have been discussed in Sections 2.4 and 2.5 respectively. A basic parameter used to describe the unavailability of a component (generating unit or transmission line) is the Forced Outage Rate (*FOR*). This parameter provides an estimate of the probability of the component being forced out of service at some distant time in the future. Consider the two-state model of a component shown in Figure 2.2. The *FOR* of this model is given by the following equation:

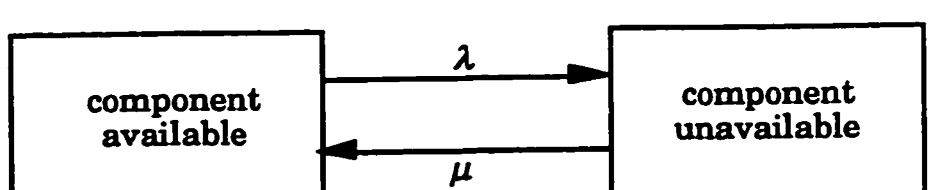

Figure 2.2. Two-state reliability model of a component.

$$FOR = \frac{\lambda}{\lambda+\mu}, \tag{2.29}$$

where λ : failure rate of the component (failures/hour) and
μ : repair rate of the component (repairs/hour).

The *FOR* as defined by (2.29), cannot be used to calculate ΔEUE in the short term as it describes the unavailability of the component in the steady state. A parameter capable of doing this is the time dependent unavailability which is also referred to as the Outage Replacement Rate (*ORR*). This statistic is a function of the lead time t into the future. The lead time is defined as the length of time between the forecast hour and the time the forecast is made. The equation for $ORR(t)$ for a two-state model as derived in [81] is as follows:

$$ORR(t) = \frac{\lambda}{\lambda+\mu} + \frac{e^{-(\lambda+\mu)t}}{\lambda+\mu}[\mu U(0) - \lambda A(0)], \tag{2.30}$$

where t : lead time in hours,
$A(0)$: availability of the component at time $t = 0$ and
$U(0)$: unavailability of the component at time $t = 0$.

It can be seen from (2.30) that the steady state value ($t \to \infty$) of $ORR(t)$ is $(\lambda/\lambda+\mu)$ which is the component forced outage rate. The lead time required for $ORR(t)$ to reach the steady state depends on the status of the component at $t = 0$ and the values of the parameters λ and μ. If the status of the unit at $t = 0$ is known, $A(0)$ and $U(0)$ should be set such that one of them is equal to 1 and the other is equal to 0. If, on the other hand, the initial status is not known, $A(0)$ and $U(0)$ should be set to values that reflect the likelihood of finding the component in one state or the other.

In order to illustrate the impact of the initial conditions on the outage replacement rate of a component, the variation of $ORR(t)$ with the lead time for a component having a forced outage rate of 0.12, a failure rate of 7.96 (failures/year) and a repair rate of 58.4 (repairs/year) was calculated and is shown in Figure 2.3. It can be seen from this figure that the initial conditions have a large impact on the value of the outage replacement rate for short lead times. As the lead time increases, however, the outage replacement rate profiles converge to the same steady state value which is equal to the forced outage rate of the component.

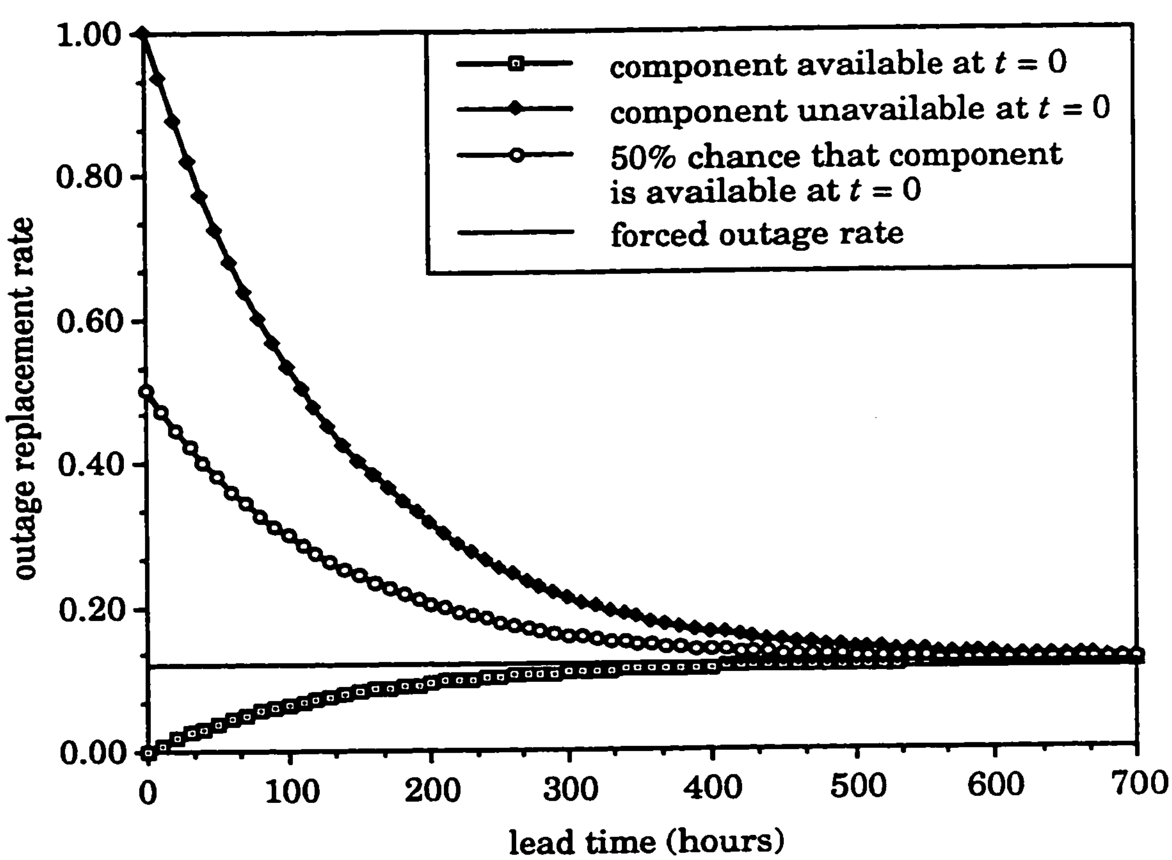

Figure 2.3. Variation of the outage replacement rate with the lead time and the initial conditions of a component.

The evaluation of $ORR(t)$ for a two-state model is relatively simple because the time dependent probabilities can be easily derived. As the number of states increases, however, it becomes increasingly more difficult to derive the time dependent probabilities. In these cases, the probabilities can be calculated using the matrix multiplication method [81] which is normally used to evaluate the probabilities of a discrete Markov chain after n equal intervals of time. The basic concept used in the matrix multiplication method is given by:

$$P(n) = P(0) \times P^n, \qquad (2.31)$$

Where P^n : stochastic transitional probability matrix,
$P(n)$: vector of the time dependent probabilities,
$P(0)$: vector of the initial values of the state probabilities and
n : number of time intervals at which the state probabilities are to be evaluated.

The stochastic transitional probability matrix represents, in a matrix form, the transitional probabilities of the stochastic process. In a continuous Markov model, these probabilities equal the transition rates between states multiplied by a small time interval Δt. The value of Δt must be chosen so that the probability of two or more transitions occurring in this interval of time is negligible. This requires a thorough knowledge of the system being analyzed.

In order to study the accuracy of the matrix multiplication method in calculating the state probabilities of a three-state model of a component, a study was conducted using the three-state model shown in Figure 2.4. The variations of the state probabilities with the lead time was calculated using selected values of Δt and the results are shown in Figure 2.5.

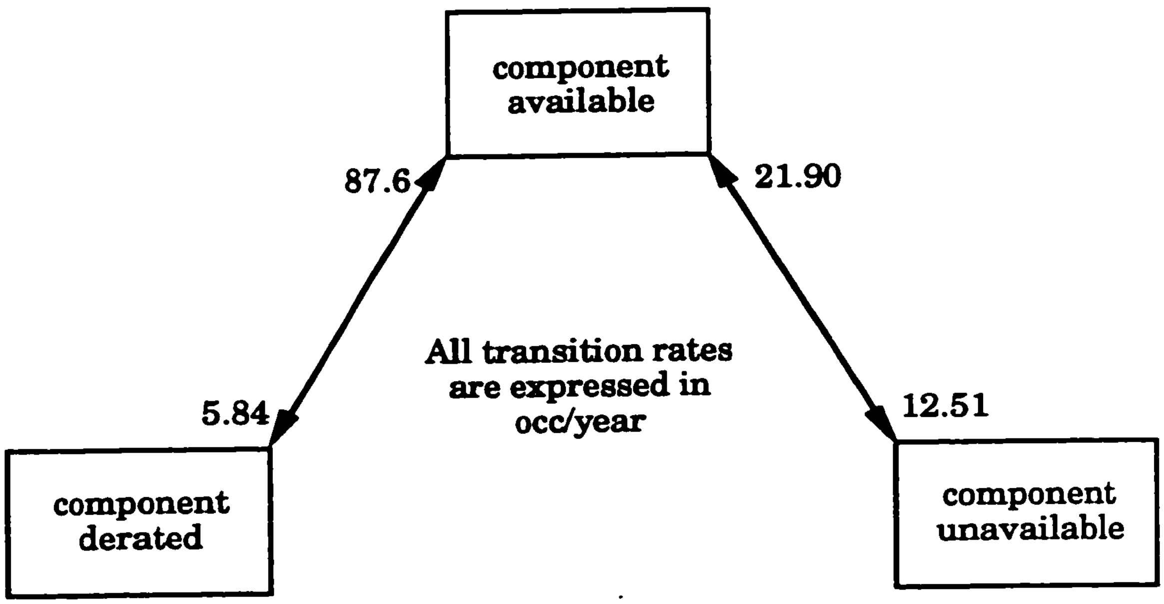

Figure 2.4. Three-state reliability model of a component.

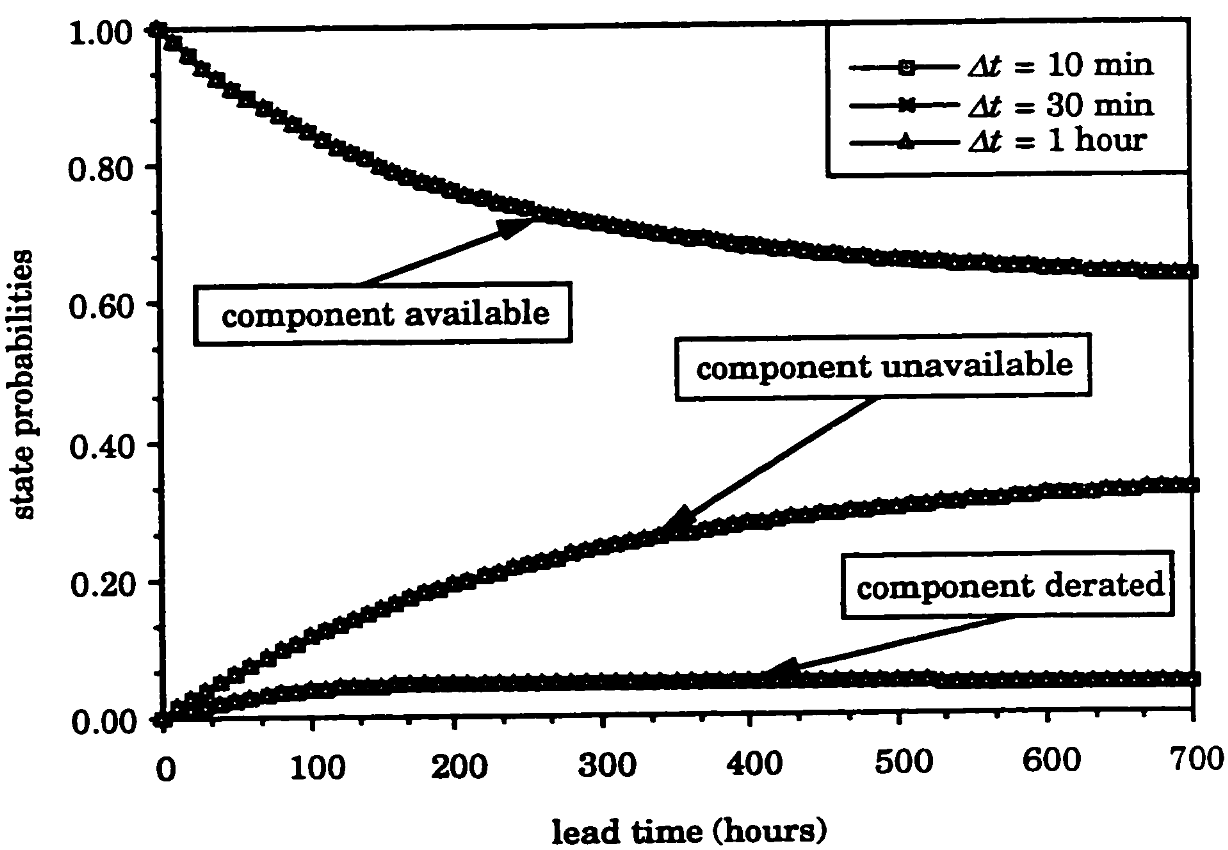

Figure 2.5. Effect of the magnitude of Δt on the values of the state probabilities of a three-state model as a function of the lead time.

It can be seen from Figure 2.5 that the variation of each state probability profile with the lead time is not affected by the value of Δt. Since most spot pricing schemes calculate the spot price (marginal operating and marginal outage cost) on an hourly basis, a value of 1 hour will be used for Δt. This value corresponds to the lowest computing time required to calculate the marginal outage cost.

The variations of the marginal outage cost with the lead time and the customer location within the system allows the utility to calculate the spot prices at each point in the system as a function of the supply and demand conditions at that instant. Under a realistic implementation of spot pricing, however, not all participants will receive real-time updates of the spot price. Some customers will get price updates only daily, monthly or even yearly. This will keep metering and communications costs reasonable. In this case, the price at time t does not reflect the actual costs at that time, but instead the expected values of these costs calculated based on the information available at the time the prices are set. Such prices are termed "predetermined" prices recognizing that they are only predetermined until the next update [17,18].

The update frequency and valid horizon for spot prices can be determined by three factors: 1) the utility's short-run marginal cost structure, 2) electricity usage characteristics of the customers being served, especially regarding the potential of being able to respond to variations in the spot price and 3) the costs and benefits of additional metering, communication control and billing required to support the new pricing scheme. For example, a utility whose generating mix is predominantly thermal and whose cost structure exhibits substantial variation by time-of-day and season may offer 24 hourly spot prices that are updated every 24 hours. On the other hand, hydro-dominant systems that are more likely to be energy constrained might find that a monthly or quarterly update horizon is sufficient to adequately reflect variations in their cost structure which is linked to the underlying hydrology.

Spinning and other types of reserves can be included in the evaluation of the marginal outage cost using shorter lead times and more appropriate reliability models [26]. Such an undertaking makes the calculated marginal outage costs more applicable to real-time rather than predetermined spot pricing schemes. This, however, may require the implementation of a number of approximations when applied to practical power systems in order to satisfy the short turnaround time of the operating environment [82]. The methods and the studies presented in this thesis are applicable to predetermined spot prices. It is believed that such prices are more practical than real-time spot prices because they provide the customers with an opportunity to adjust their consumption patterns to take advantage of low cost periods and avoid high cost periods.

2.7. Summary

This chapter provides a general description of three methodologies that can be used to calculate the marginal outage costs in a electric power systems. The proposed methodology which is based on quantitative power system reliability concepts calculates the marginal outage cost at a given load level by multiplying the incremental expected unserved energy of the system at that load level by an average cost of unserved energy. Methods are proposed for calculating the incremental expected unserved energy in generating and composite generation and transmission systems using established reliability techniques. The average cost of unserved energy is represented by the interrupted energy assessment rate of the system. The next chapter illustrates the proposed method of calculating the marginal outage costs in isolated generating systems by application to two reliability test systems. Sensitivity analyses of these costs to selected modelling assumptions and parameters are also presented.

3. EVALUATION OF THE MARGINAL OUTAGE COSTS IN ISOLATED GENERATING SYSTEMS

3.1. Introduction

This chapter illustrates the proposed method for calculating the marginal outage costs in an isolated generating system by application to two reliability test systems. The variations of the marginal outage cost profiles of these systems with the operating reserve and the lead time are presented. A number of sensitivity analyses are conducted to show the effects on the marginal outage cost of the initial generating unit conditions, modelling of derated states, load forecast uncertainty and the removal of generating units for maintenance. The application of the proposed method to two test systems of different sizes is done to show the impact of system size on the robustness of the method and the accuracy of the approximations.

3.2. Reliability Test Systems

The experience of one electric utility with its system may be different from that of another and therefore the characteristic features and modelling assumptions of different methods will differ according to the intent behind the development and utilization. The establishment of acceptable reliability test systems is therefore extremely important as they provide reference networks for testing the proposed methods.

Two reliability test systems will be used to test the methodologies that are developed in this thesis. The Roy Billinton Test System (*RBTS*) [35] is a small reliability test system which was developed at the University of Saskatchewan for educational purposes. The main objective of the *RBTS* is to provide a test system which is sufficiently small to permit the user to conduct a large number of reliability studies with reasonable solution time, but sufficiently detailed to reflect the actual complexities involved in a practical reliability analysis. The *IEEE*-Reliability Test System (*IEEE-RTS*) was developed by the *IEEE* Sub-committee on the Application of Probability Methods (*APM*) in 1979 [36]. The nature of the *IEEE-RTS* reflects the essential characteristics of a practical power system. This system is larger than the *RBTS* and therefore it can be used to study the applicability of proposed techniques and modelling assumptions to practical system studies. The detailed descriptions of the *RBTS* and *IEEE-RTS* are given in [35] and [36] and summarized in Appendices A and B respectively.

In addition to the generating system reliability data presented in Appendices A and B, cost of interruption data are required in order to calculate the *IEAR*'s of the *RBTS* and the *IEEE-RTS*. The most commonly used method to gather this data is the customer survey method where customers are surveyed to estimate their economic losses and to create customer damage functions for each customer group and for the entire service area. These functions represent the customer outage costs as a function of interruption durations. The Power Systems Research Group at the University of Saskatchewan has been involved with postal surveys of electric customers for the last decade [46,50,52]. A summary of the results from these surveys and the derivation of the composite customer damage function for a selected service area are presented in Appendix C.

The Composite Customer Damage Function (*CCDF*) derived in Appendix C was used together with the generating system reliability data of the *RBTS* and *IEEE-RTS* to calculate their respective interrupted energy assessment rates [34]. The results from these studies show that the value of the *IEAR* is relatively stable and does not vary significantly with the load model or the modelling assumptions used. Therefore, the following *IEAR* values will be used in the following sections to calculate the marginal outage costs associated with the generating systems of the *RBTS* and the *IEEE-RTS* :

IEAR for the *RBTS* = 3.60 ($\$/kWh$) and
IEAR for the *IEEE-RTS* = 3.13 ($\$/kWh$).

The utilization of a constant *IEAR* to calculate the marginal outage cost is not a limitation of the proposed method. The values of 3.60 and 3.13 are used to illustrate the procedure. Given sufficient cost of interruption data, the *IEAR* value is tailored to the system under consideration and could even be time dependent given the supporting data.

3.3. Evaluation of the Marginal Outage Costs Associated with the *RBTS* Generating System

The object of this section is to calculate the marginal outage cost profile associated with the *RBTS* generating system and to study the sensitivity of this profile to changes in selected modelling assumptions and parameters. In order to produce the profile, the marginal outage costs are calculated at different load levels and plotted versus the operating reserves corresponding to these load levels. The complete generation system data for the *RBTS* are given in [35] and summarized in Table A.1. The *IEAR* value used in all the studies reported in this section is 3.60 $\$/kWh$.

The marginal outage cost profile for the *RBTS* is shown in Figure 3.1 for three different lead times and the steady state condition (i.e. lead time is infinity). It can be seen from this figure that the marginal outage cost is equal to the *IEAR* when the system is deficient or has no operating reserves and it decreases as the operating reserves become more plentiful. The steps in the profiles are due to the discrete nature of the capacity outage probability table and the size of the *RBTS*. The *COPT* of a larger system such as the *IEEE-RTS* has smaller steps and therefore the marginal outage cost profiles for that system will be smoother than those shown in Figure 3.1. The evaluation of the marginal outage costs associated with the generating system of the *IEEE-RTS* is discussed in Section 3.4.

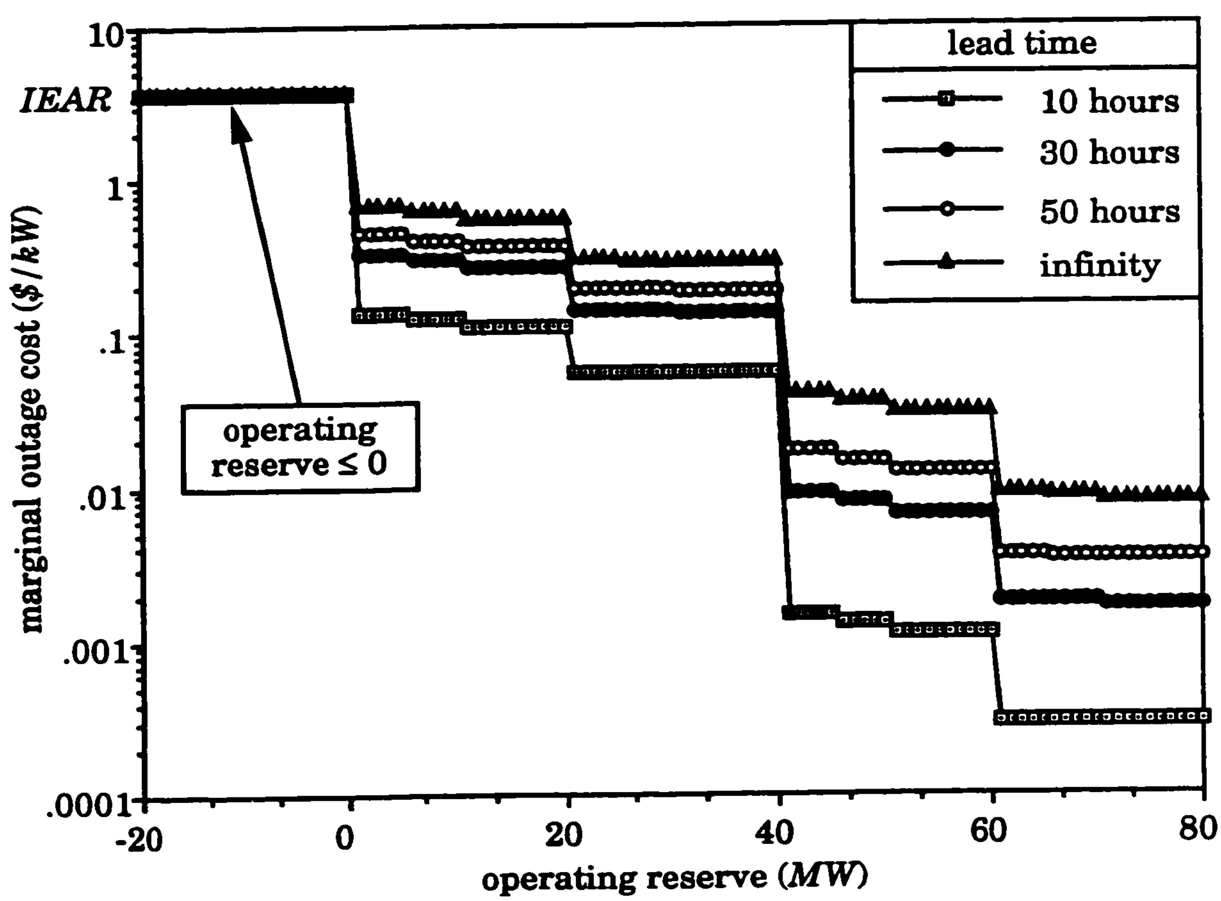

Figure 3.1. Variation of the marginal outage cost of the *RBTS* as a function of the operating reserve for selected lead times.

In addition to varying with the operating reserve, the marginal outage cost also varies with the lead time which is equal to the duration of time between the hour being forecast and the time the forecast is made. A number of marginal outage cost profiles corresponding to different lead times are presented in Figure 3.1. A better way of representing the variation of the marginal outage cost with the lead time is shown in Figure 3.2 where the marginal outage cost is plotted against the lead time for three different operating reserve levels. It can be seen from this figure that each profile tends towards its respective steady state value as the lead time increases.

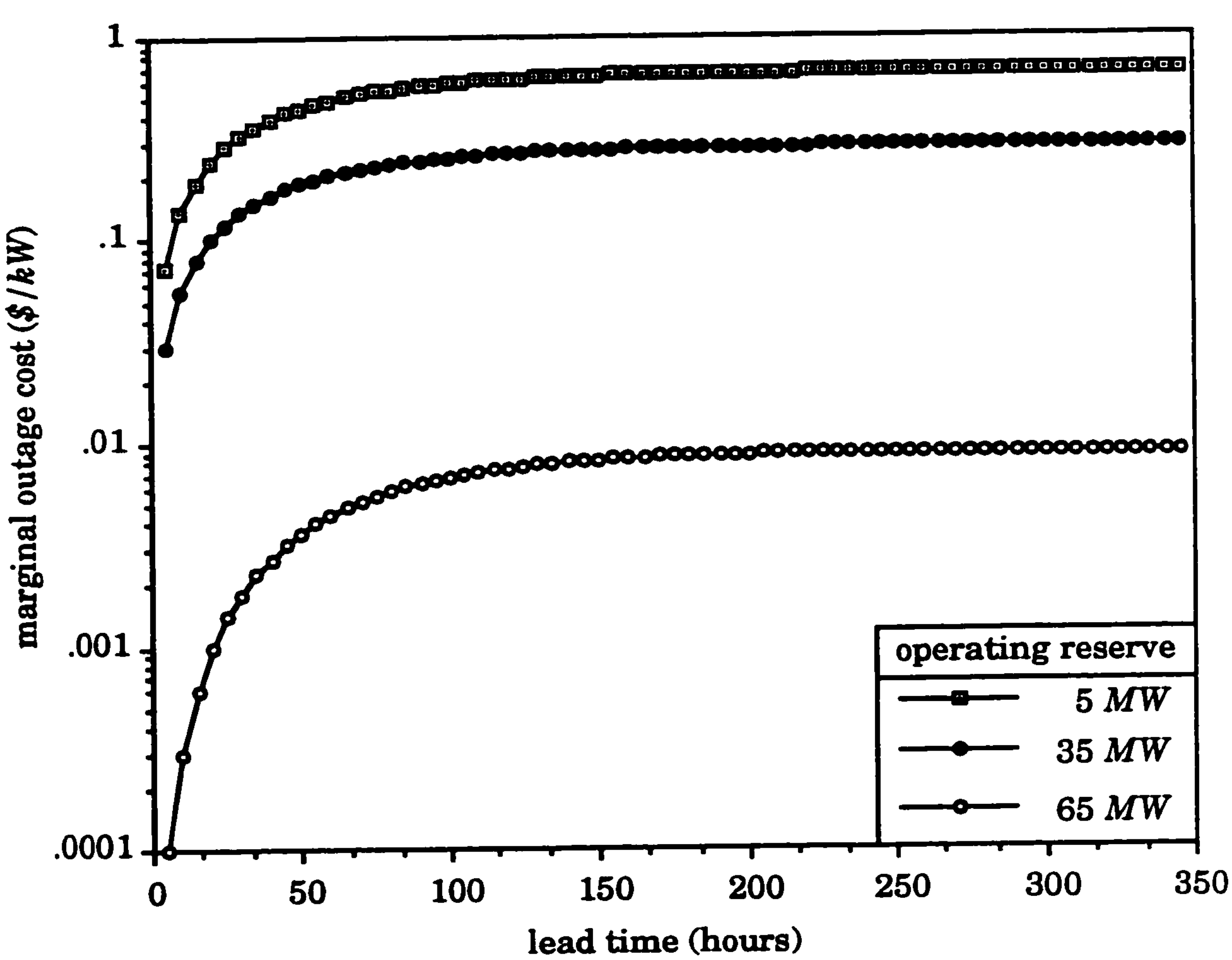

Figure 3.2. Variation of the marginal outage cost of the *RBTS* as a function of the lead time for selected operating reserves.

It is clear from Figures 3.1 and 3.2 that the marginal outage cost varies with both the operating reserve level and the lead time. These variations can be combined into a single three dimensional (*3D*) surface plot that describes the relationship between the marginal outage cost and both the operating reserve and the lead time, Such a plot is shown in Figure 3.3 for the *RBTS*.

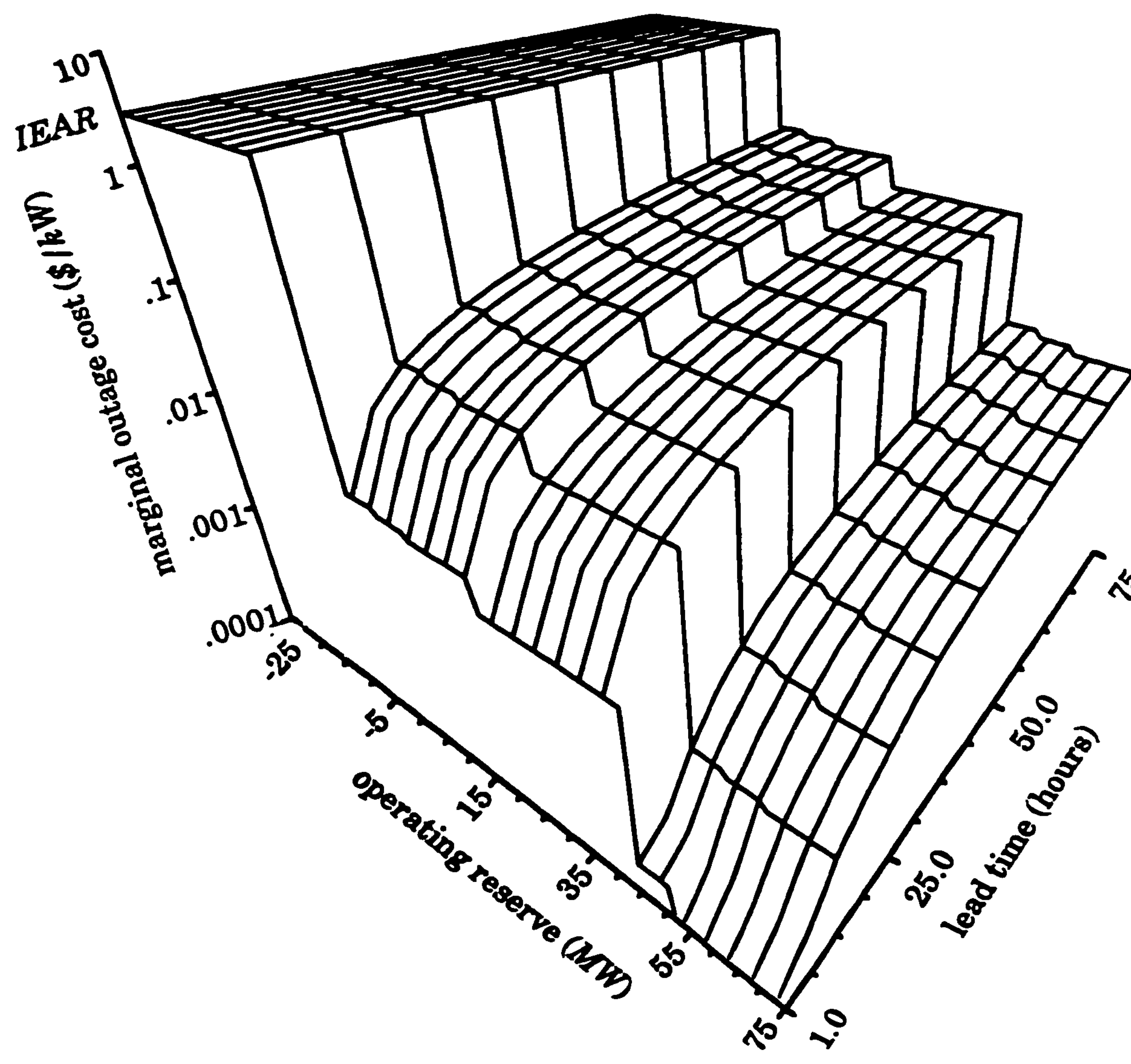

Figure 3.3. Variation of the marginal outage cost of the *RBTS* as a function of the operating reserve and the lead time.

3.3.1. Effect of the initial generating unit conditions

In calculating the marginal outage costs presented in Section 3.3, all the generating units were assumed to be available at time $t = 0$. If this assumption is not valid for some generating units, the resulting marginal outage costs could be significantly different. The degree of variation in the marginal outage cost depends on the number and characteristics of generating units that are in the down state. The direction of the variation is such that, for the same operating reserve and lead time, the marginal outage cost will increase as more and/or larger units are in the down state at $t = 0$.

Two studies are conducted in this sub-section in order to show the effects on the marginal outage cost profile of the *RBTS* of the initial generating unit conditions. The first study shows the impact of having the 20 *MW* thermal unit or the 40 *MW* hydro unit in the down state at time $t = 0$ for a lead time of 10 hours. The results from this study are shown in Figure 3.4. It can be seen from this figure that, for <u>any</u> operating reserve point, the marginal outage cost generally increases as the capacity of the generating unit in the down state at $t = 0$ increases.

The second study is done to show that the impact on the calculated marginal outage cost of the initial generating unit conditions diminishes as the lead time increases. That is, for a given operating reserve level, the marginal outage cost converges to the same steady state value regardless of the initial generating unit conditions. The study was done for an operating reserve of 35 *MW* and assuming that either the 20 *MW* thermal unit or the 40 *MW* hydro unit is in the down state at $t = 0$. The results shown in Figure 3.5 reveal that the initial generating unit conditions can have a significant

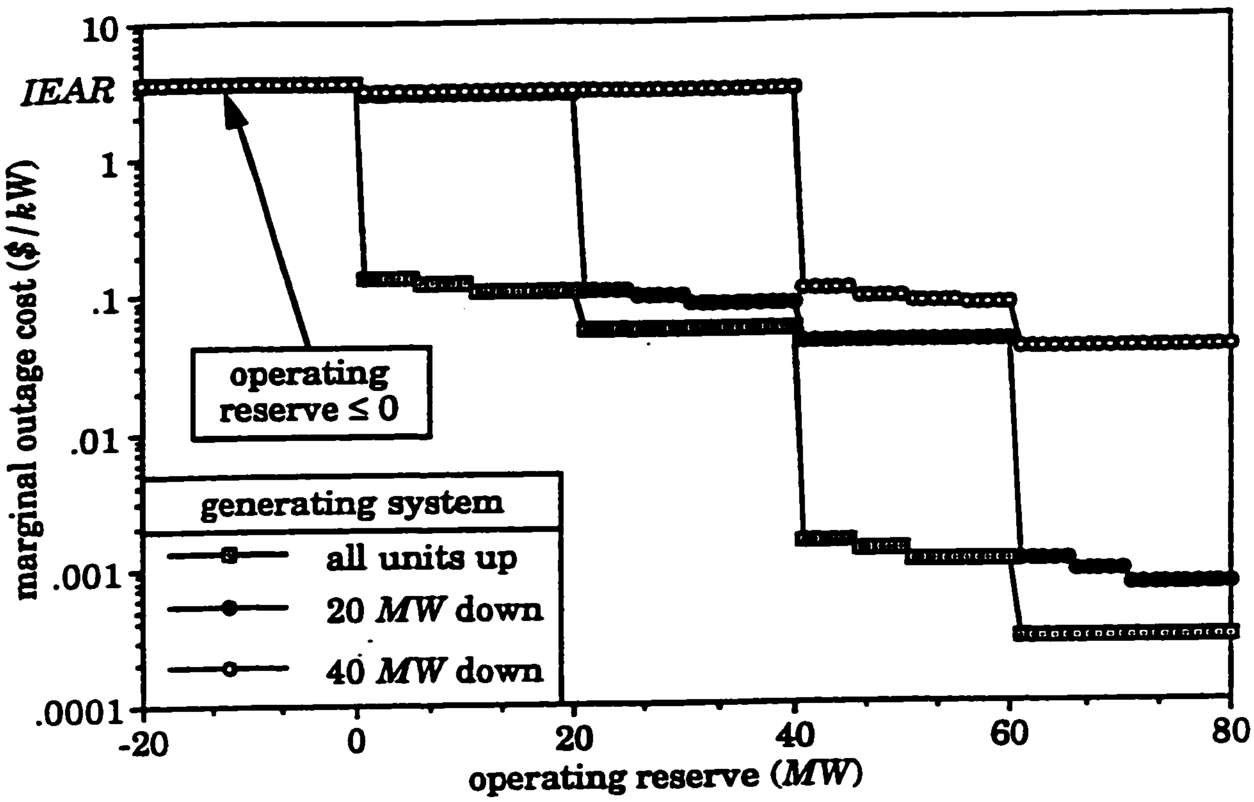

Figure 3.4. Effect of generating unit initial conditions on the marginal outage cost of the *RBTS* for a lead time of 10 hours.

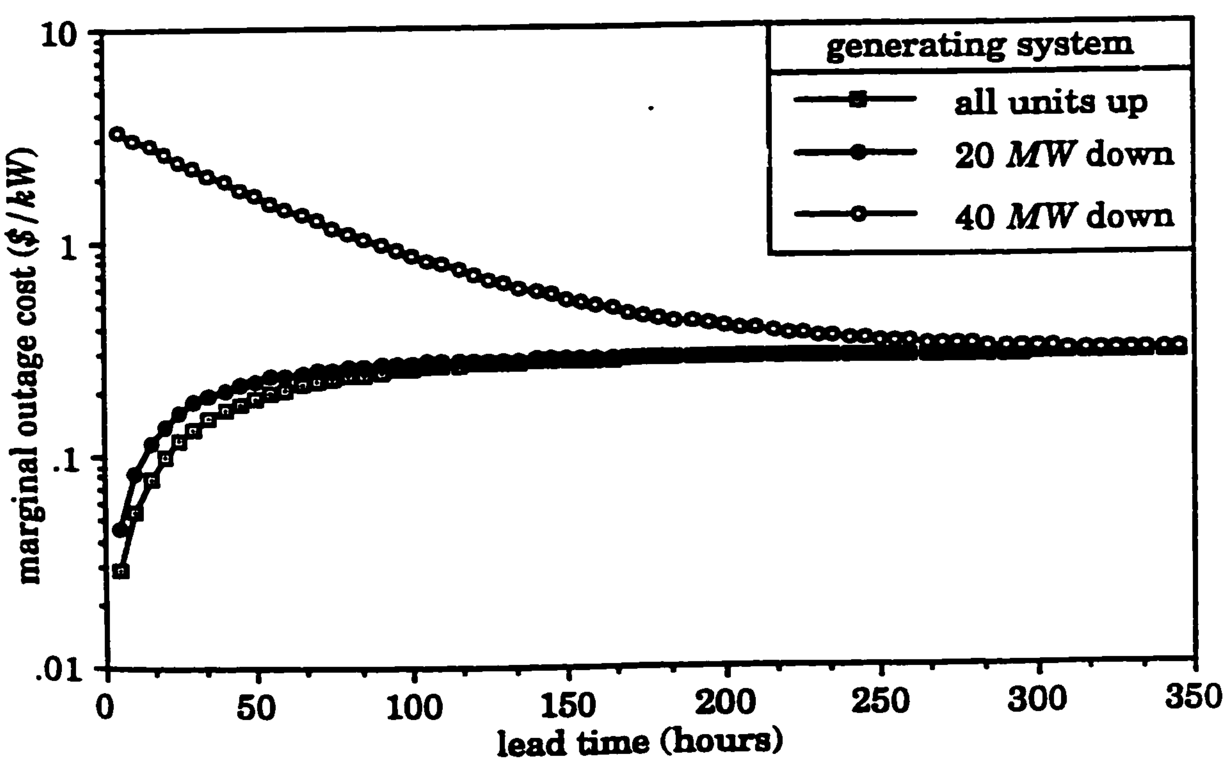

Figure 3.5. Effect of generating unit initial conditions on the marginal outage cost of the *RBTS* for an operating reserve of 35 *MW*.

impact on the marginal outage cost for short lead times. As the lead time increases, however, this impact becomes negligible and the marginal outage cost profiles calculated using the various initial conditions converge to the same steady state value.

The studies reported in this sub-section indicate that the initial generating unit conditions can have a very significant impact on the value of the marginal outage cost for those lead times that are normally used in spot pricing (i.e. 10 to 130 hours). Therefore, it is important to include the correct initial conditions in the calculation of the marginal outage cost. This recommendation is clearly supported by the surface plot shown in Figure 3.6 which is a combination of both Figures 3.4 and 3.5. A comparison between this surface plot and that shown in Figure 3.3 shows the significance of the initial generating unit conditions on the value marginal outage cost.

3.3.2. Effect of modelling derated states

The utilization of multi-state models to represent large generating units in reliability studies results in a more accurate representation of the power system [25,26], which in turn, will result in better estimates of the system's marginal outage costs. In order to show how multi-state modelling can affect the marginal outage costs of a generating system, the two 40 *MW* thermal units of the *RBTS* were assigned a 50% derated state as given in Table A.2 [35]. The state probabilities and transition rates of the derated model are such that the Derating-Adjusted Forced Outage Rate (*DAFOR*) of the generating unit is identical to the Forced Outage Rate (*FOR*) of the two-state model. This ensures that any difference in the resulting marginal outage cost profile can be attributed to the change in the generating unit models used.

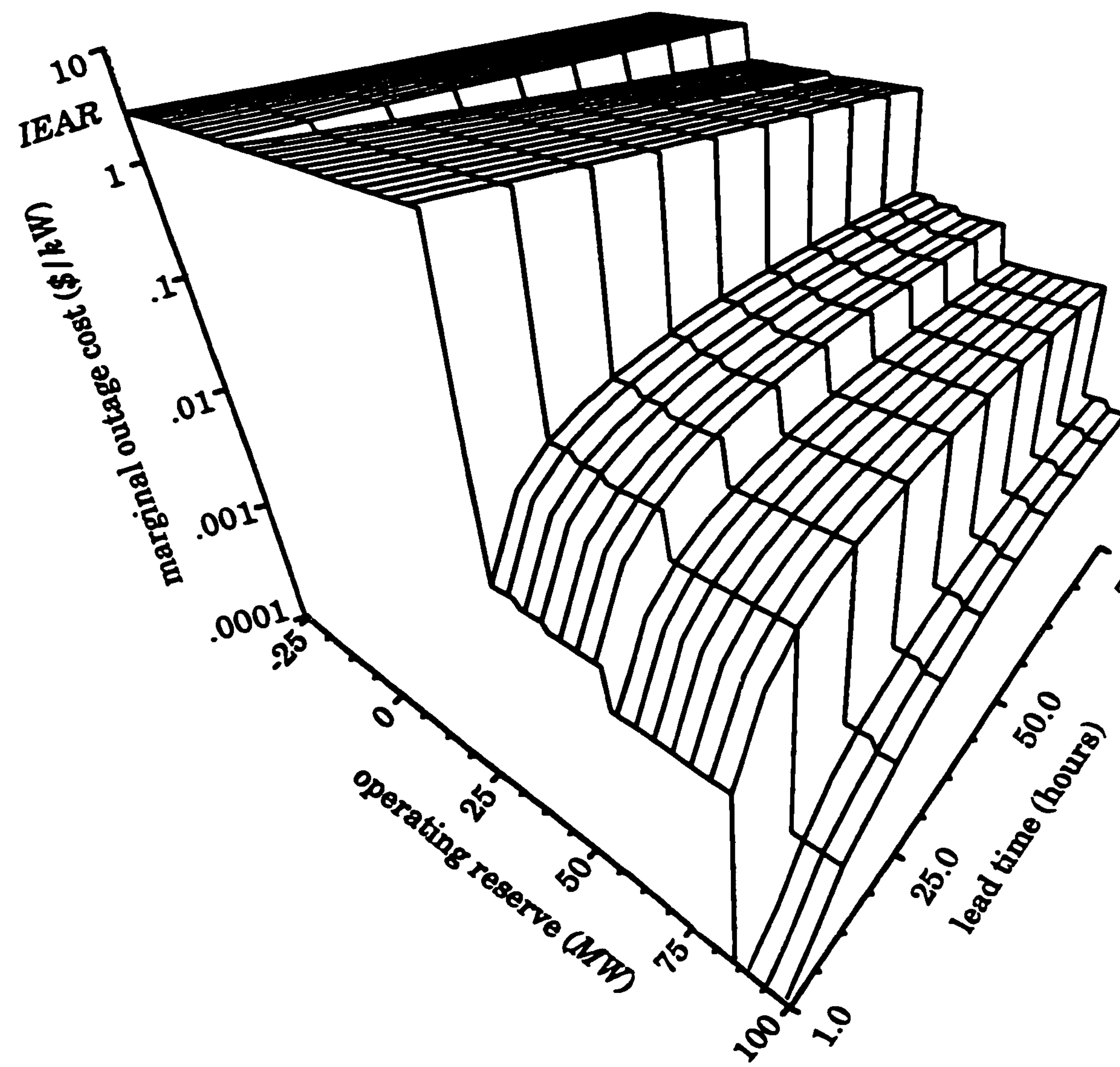

Figure 3.6. Variation of the marginal outage cost of the *RBTS* as a function of the operating reserve and the lead time when the 40 *MW* hydro unit is assumed to be in the down state at $t = 0$.

The results from this study are compared to the base case (i.e. two-state model) for two different lead times, 10 hours and infinity, in Figure 3.7. It can be seen from this figure that the marginal outage costs calculated using the three-state models are slightly higher than or equal to those calculated in the base case for low operating reserves and lower otherwise. The difference between each pair of marginal outage cost profiles is relatively small, but it tends to increase as the operating reserve increases. This difference will be insignificant in a practical system because the magnitude of the marginal outage cost at high operating reserves is very small. However, if a large number of generating units are represented using multi-state models, it is expected that the impact of multi-state modelling will be more significant.

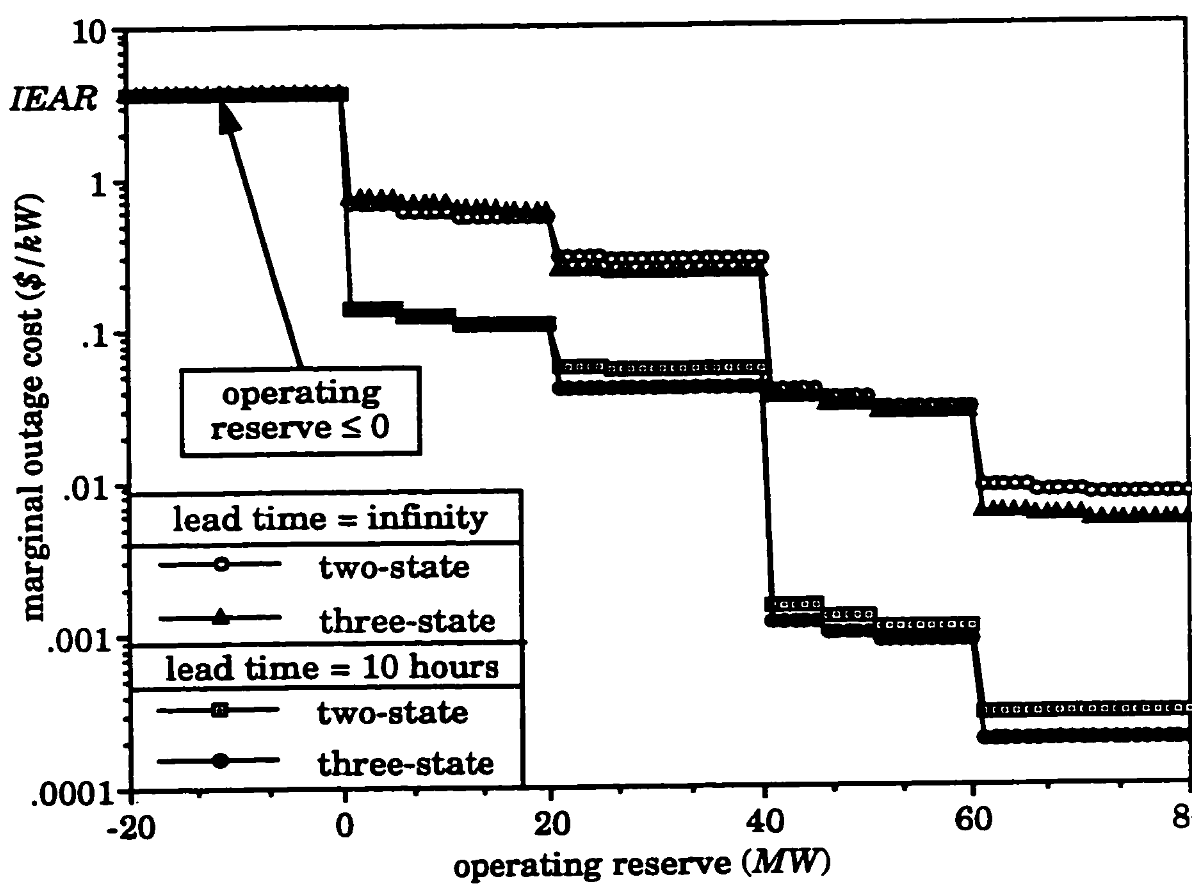

Figure 3.7. Effect of using a three-state model to represent the two 40 MW thermal units in the $RBTS$ on the marginal outage cost as a function of the operating reserve.

Since the marginal outage costs also vary with the lead time, it was decided to investigate the impact of multi-state modelling on these costs as a function of the lead time. The results from this study are shown in Figure 3.8 for an operating reserve of 35 *MW*. It can be seen from this figure that the impact on the marginal outage cost of using multi-state generating unit models is not affected greatly by the variation in the lead time because the profiles shown in Figure 3.8 remain parallel for all lead time values.

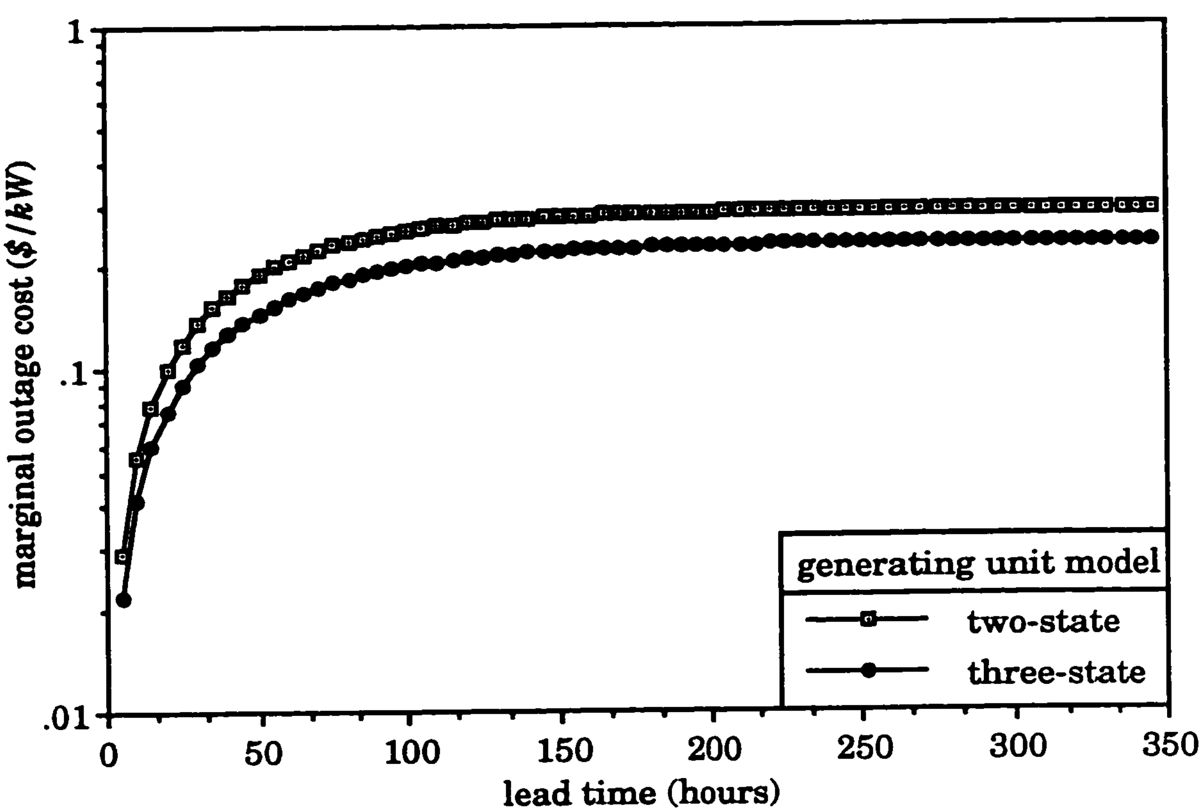

Figure 3.8. Effect of using a three-state model to represent the two 40 *MW* thermal units in the *RBTS* on the marginal outage cost as a function of the lead time.

3.3.3. Effect of load forecast uncertainty

In the previous studies reported in this section, it has been assumed that the load level is known with a probability of 1.0. This is extremely unlikely in actual practice as the forecast is normally predicted based on past experience. If it is realized that some uncertainty can exist, it can be described by a probability distribution whose parameters can be determined from past experience, future load modelling and possible subjective evaluation [26].

The uncertainty in load forecasting can be included in the calculation of the marginal outage cost by dividing the load forecast probability distribution into class intervals, the number of which depends upon the accuracy desired. The area of each class interval represents the probability and the load is the class interval's mid-value. The marginal outage cost is computed for each load represented by the class interval and multiplied by the probability of existence of that load level. The expected marginal outage cost for the forecast mean of the distribution is calculated by adding the weighted products.

It is extremely difficult to obtain sufficient historical data to determine the distribution describing the load forecast uncertainty. Published data, however, have suggested that the uncertainty can be reasonably described by a normal distribution whose mean is the forecast load level [26]. The distribution can be divided into a discrete number of class intervals. The load representing the class interval mid-point is assigned the designated probability for that class interval. This is shown in Figure 3.9 where the distribution is divided into seven steps. A similar approach can be used to represent an unsymmetrical distribution if required.

The impact of load forecast uncertainty on the marginal outage cost of the *RBTS*, is calculated using the seven-step approximation of the normal distribution and a number of standard deviations. The results for the 3% and 5% standard deviations are compared to the base case (i.e. standard deviation of 0%) in Figure 3.10 for a lead time of 10 hours.

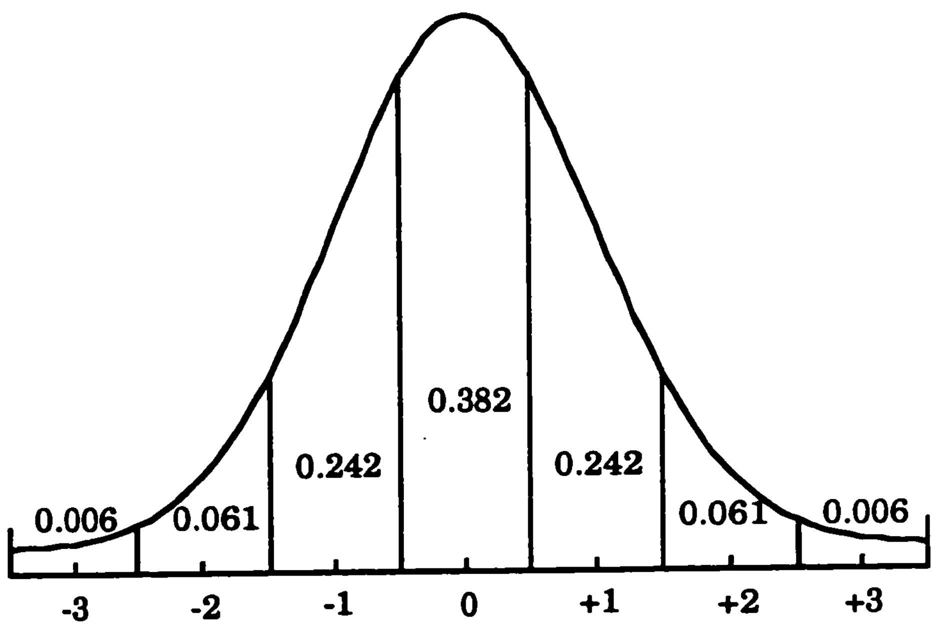

Figure 3.9. Seven-step approximation of the normal distribution.

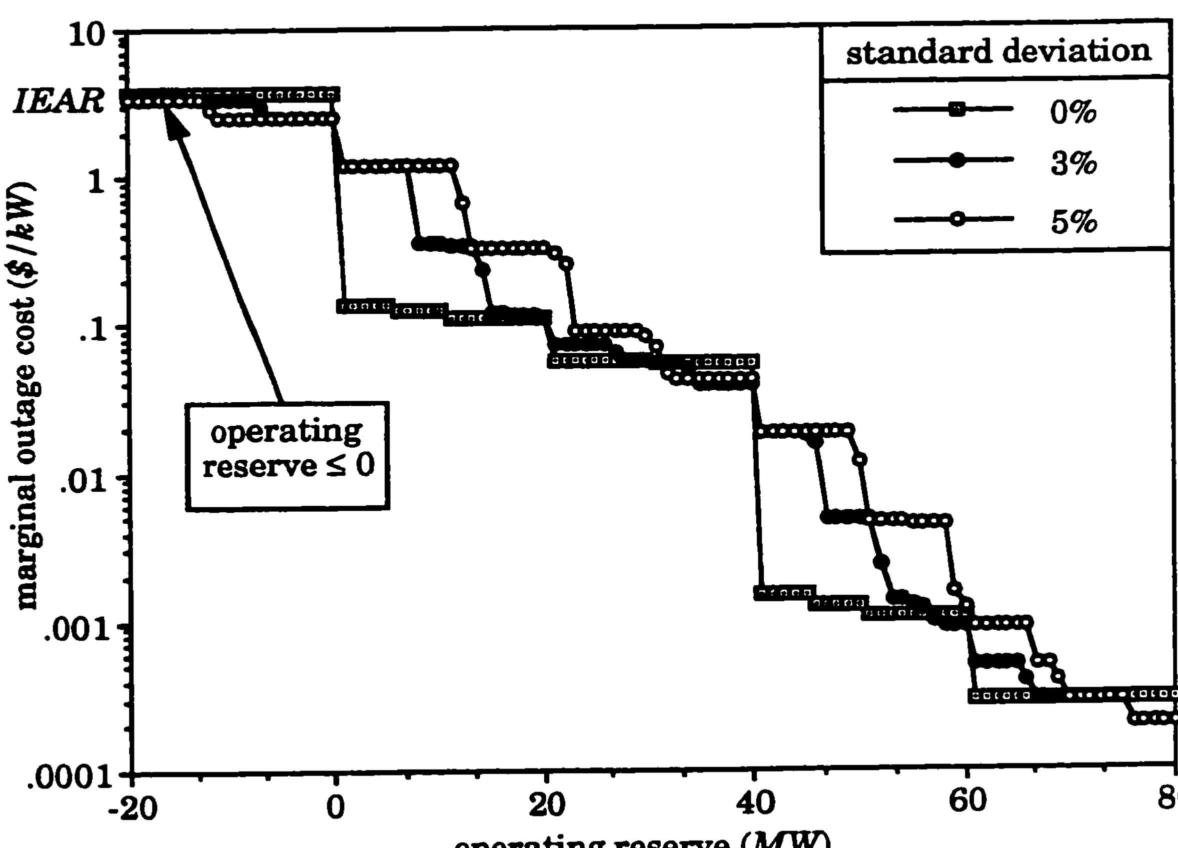

Figure 3.10. Effect of load forecast uncertainty on the marginal outage cost profile of the *RBTS* as a function of the operating reserve.

It can be seen from Figure 3.10 that the marginal outage cost generally increases as the standard deviation increases. In addition, the load forecast uncertainty has a smoothing effect on the profile because the resulting marginal outage costs are expected values that are calculated using seven different load levels.

3.3.4. Effect of removing generating units for maintenance

The marginal outage cost for a particular operating reserve and lead time is calculated by constructing the capacity outage probability table at that lead time and extracting the appropriate cumulative probability from it to multiply by the *IEAR*. The construction of the *COPT* for every hour in the forecast period of spot prices (typically 24 to 120 hours) is very time consuming. Therefore, if it can be shown that the marginal outage costs are not affected greatly by removing a few units for maintenance, then a number of pre-calculated marginal outage cost profiles can be used for any day-type regardless of which units are on maintenance that day.

In order to study the impact on the marginal outage cost profile of the *RBTS* of removing generating units for maintenance, two studies were conducted where units of different sizes were removed for maintenance and the marginal outage costs calculated using the rest of the units in the system. The object of the first study is to show the impact on the marginal outage cost as a function of the operating reserve of removing 20 and 60 MW for maintenance. The results from this study are compared to the base case (i.e. no units removed for maintenance) in Figure 3.11 for a lead time of 10 hours. It can be seen from this figure that the marginal outage cost profile is not significantly affected by the removal of the 20 MW unit for maintenance. As the capacity of generating units removed for maintenance increases, however, the marginal outage cost becomes lower than the base case for most operating reserve levels. The operating reserve for each case is calculated by subtracting the load from the available capacity which is equal to the installed capacity minus the capacity of units on maintenance.

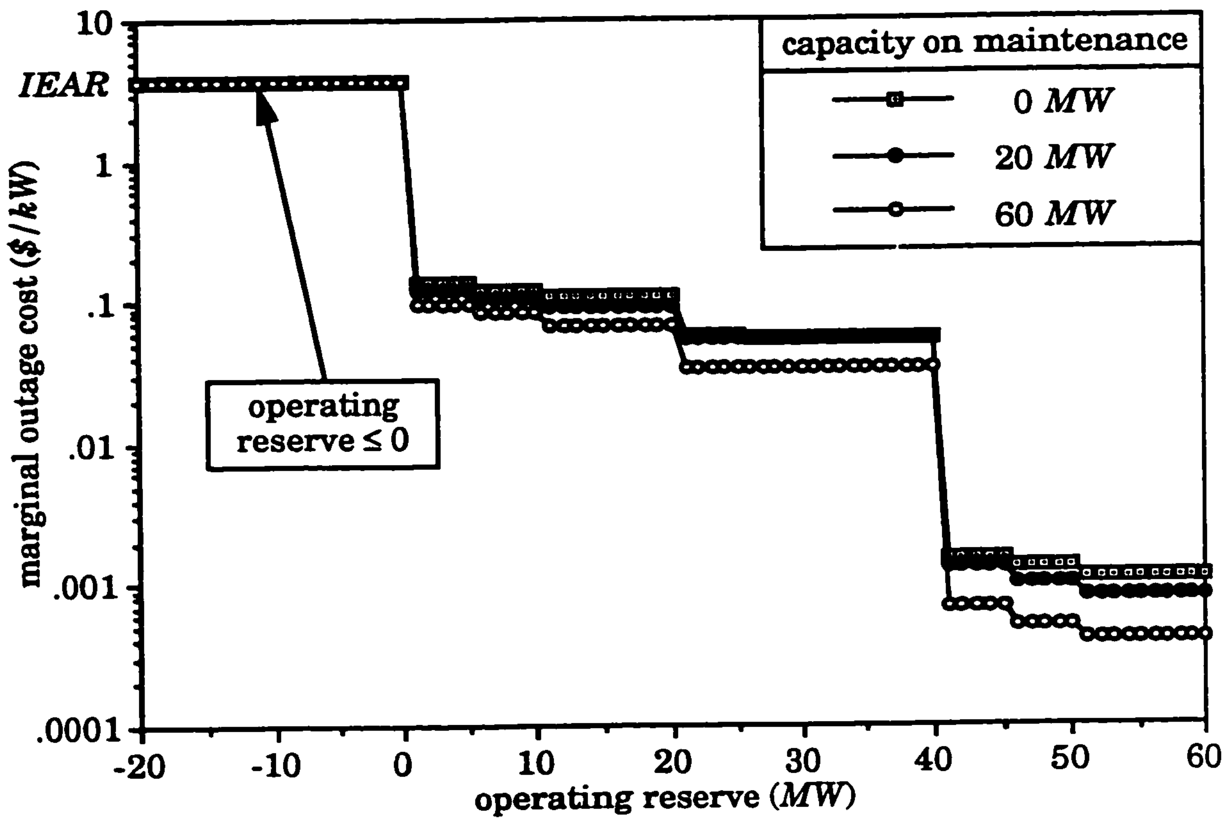

Figure 3.11. Effect of removing units for maintenance on the marginal outage cost profile of the *RBTS* as a function of the operating reserve.

The second study illustrates the effect of removing generating units for maintenance on the marginal outage cost of the *RBTS* as a function of the lead time for an operating reserve of 35 *MW*. The results from this study are shown in Figure 3.12. It can be seen from this figure that the effect on the marginal outage cost profile of the *RBTS* of removing units for maintenance is consistent for all values of the lead time.

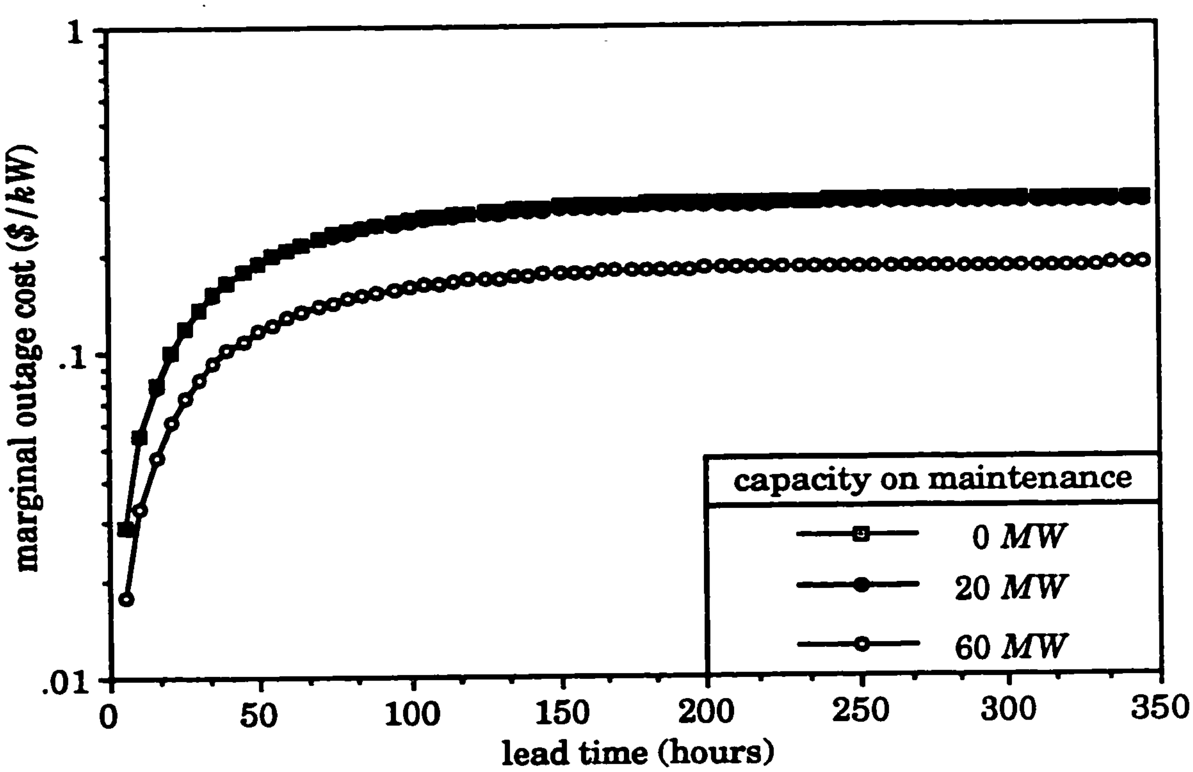

Figure 3.12. Effect of removing units for maintenance on the marginal outage cost profile of the *RBTS* as a function of the lead time.

3.4. Evaluation of the Marginal Outage Costs Associated with the *IEEE-RTS* Generating System

The object of this section is to illustrate the proposed method for calculating the marginal outage cost by application to the *IEEE-RTS* generating system. This system is larger than the *RBTS* and therefore it will be used to test the robustness of the proposed method to the size of the system. The marginal outage cost of the *IEEE-RTS* can be calculated using the same procedure that was used in the *RBTS* study. The detailed generation system data for the *IEEE-RTS* are given in [36] and summarized in Table B.1. The *IEAR* value used in all the studies reported in this section is 3.13 $\$/kWh$. The marginal outage cost profile of the *IEEE-RTS* is shown in Figure 3.13 for three different lead times and the steady state condition (i.e. lead time is infinity). It can be seen from this figure that the marginal outage cost is equal to the *IEAR* for operating reserves that are less than or equal to zero and decreases as the operating reserves increases. A comparison between the marginal outage cost profiles of the *IEEE-RTS* shown in Figure 3.13 and those of the *RBTS* shown in Figure 3.1 reveals that they have the same shape. The profiles of the *IEEE-RTS* are smoother however due to the number of generating units of this system and their characteristics.

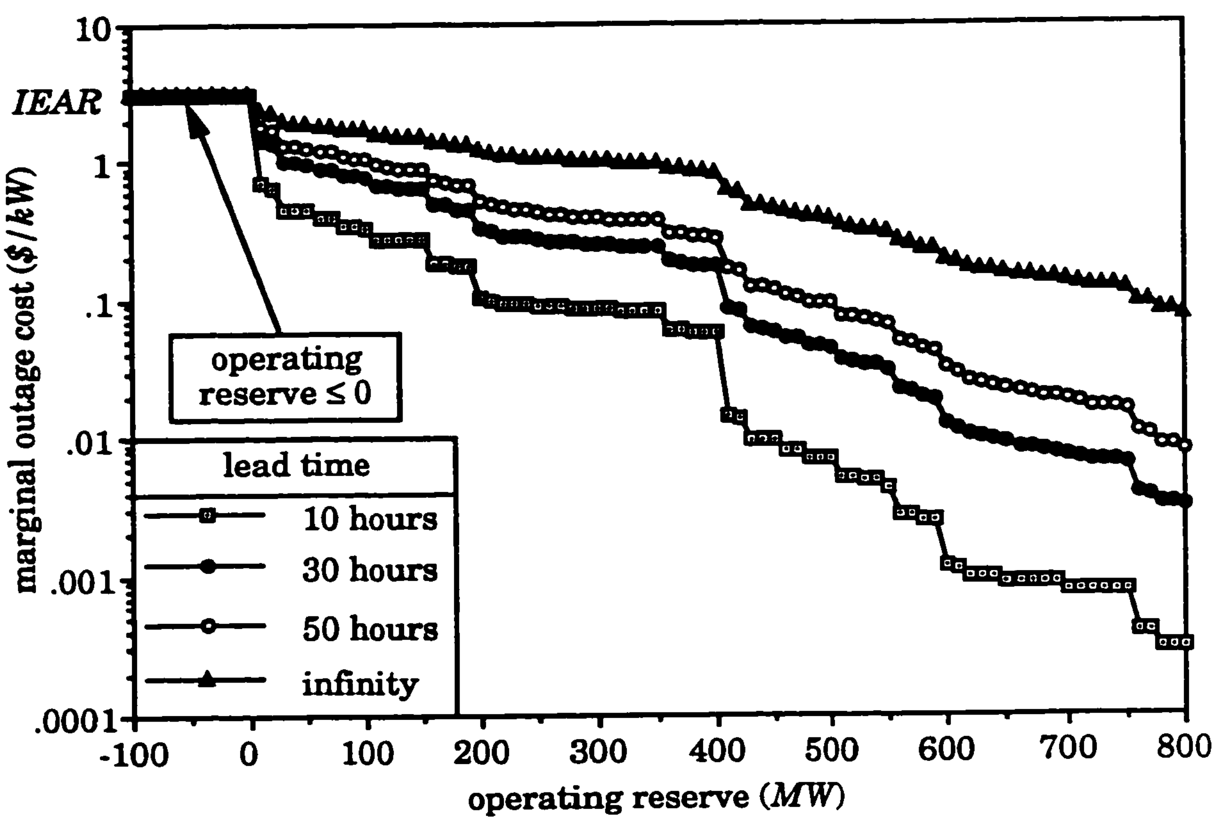

Figure 3.13. Variation of the marginal outage cost of the *IEEE-RTS* as a function the operating reserve for selected lead times.

The variation of the marginal outage cost of the *IEEE-RTS* with the lead time is shown in Figure 3.14 for selected operating reserve levels. It can be seen from this figure that, as in the case of the *RBTS*, the marginal outage cost profiles converge towards their respective steady state values as the lead time increases.

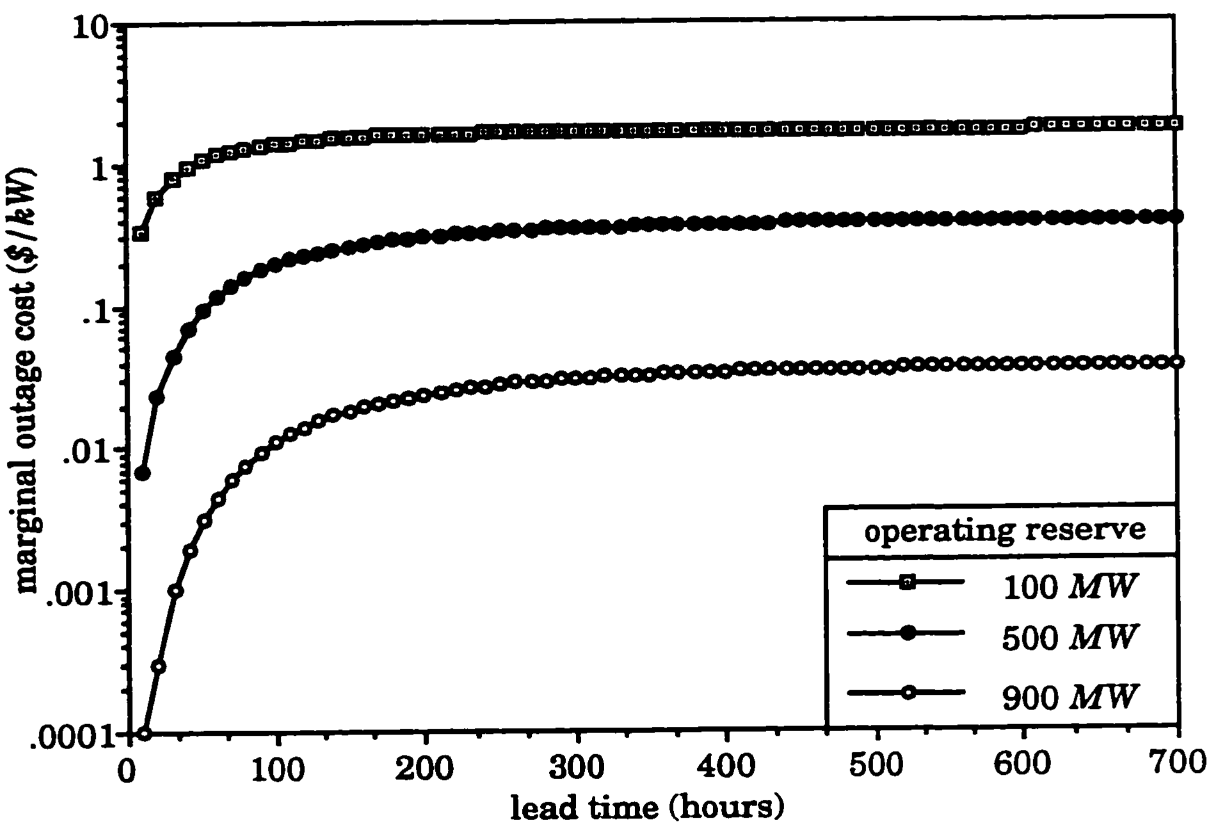

Figure 3.14. Variation of the marginal outage cost of the *IEEE-RTS* as a function of the lead time for selected operating reserves.

The variations of the marginal outage cost of the *IEEE-RTS* generating system with both the operating reserve and the lead time can be combined into a single *3D* surface plot as shown in Figure 3.15. The discrete steps shown in this figure are smaller than those of the *RBTS* shown in Figure 3.3 due to the size of the *IEEE-RTS* generating system.

3.4.1. Effect of the initial generating unit conditions

It was reported in Sub-section 3.3.1 that the initial conditions of generating units can have a very significant impact on the value of the marginal outage cost. The object of this sub-section is to illustrate the impact of these conditions on the marginal outage cost of a more practical system such as the *IEEE-RTS*. Two studies were conducted, the first of

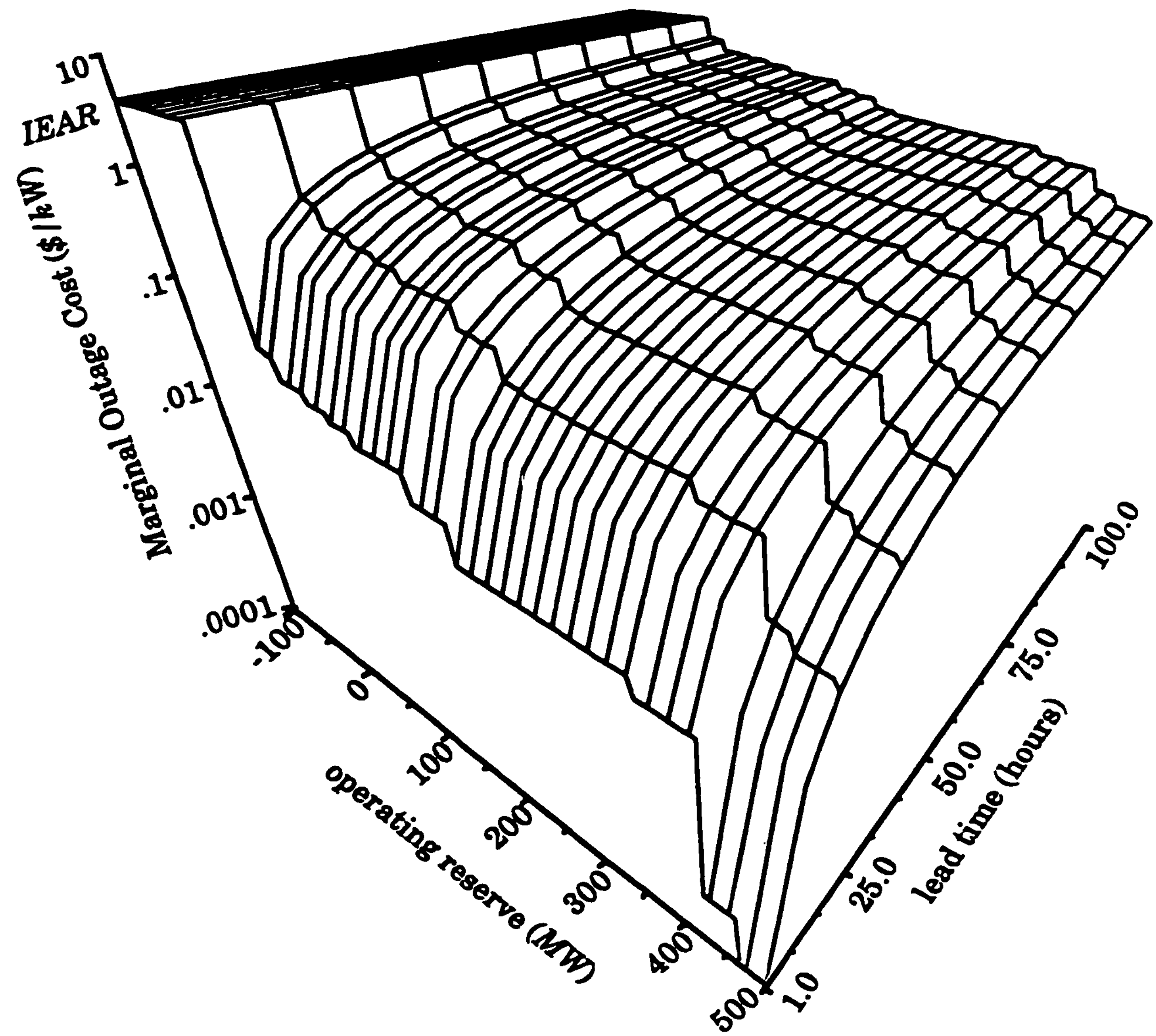

Figure 3.15. Variation of the marginal outage cost of the *IEEE-RTS* with the operating reserve and the lead time.

which shows the impact of having 12 *MW*, 155 *MW* or 400 *MW* in the down state at time $t = 0$ for a lead time of 10 hours. The results from this study are shown in Figure 3.16. It can be seen from this figure that the marginal outage cost of the *IEEE-RTS* is not affected greatly by the initial conditions of the 12 *MW* unit. However, as the capacity of the generating unit in the down state at $t = 0$ increases, the marginal outage cost increases.

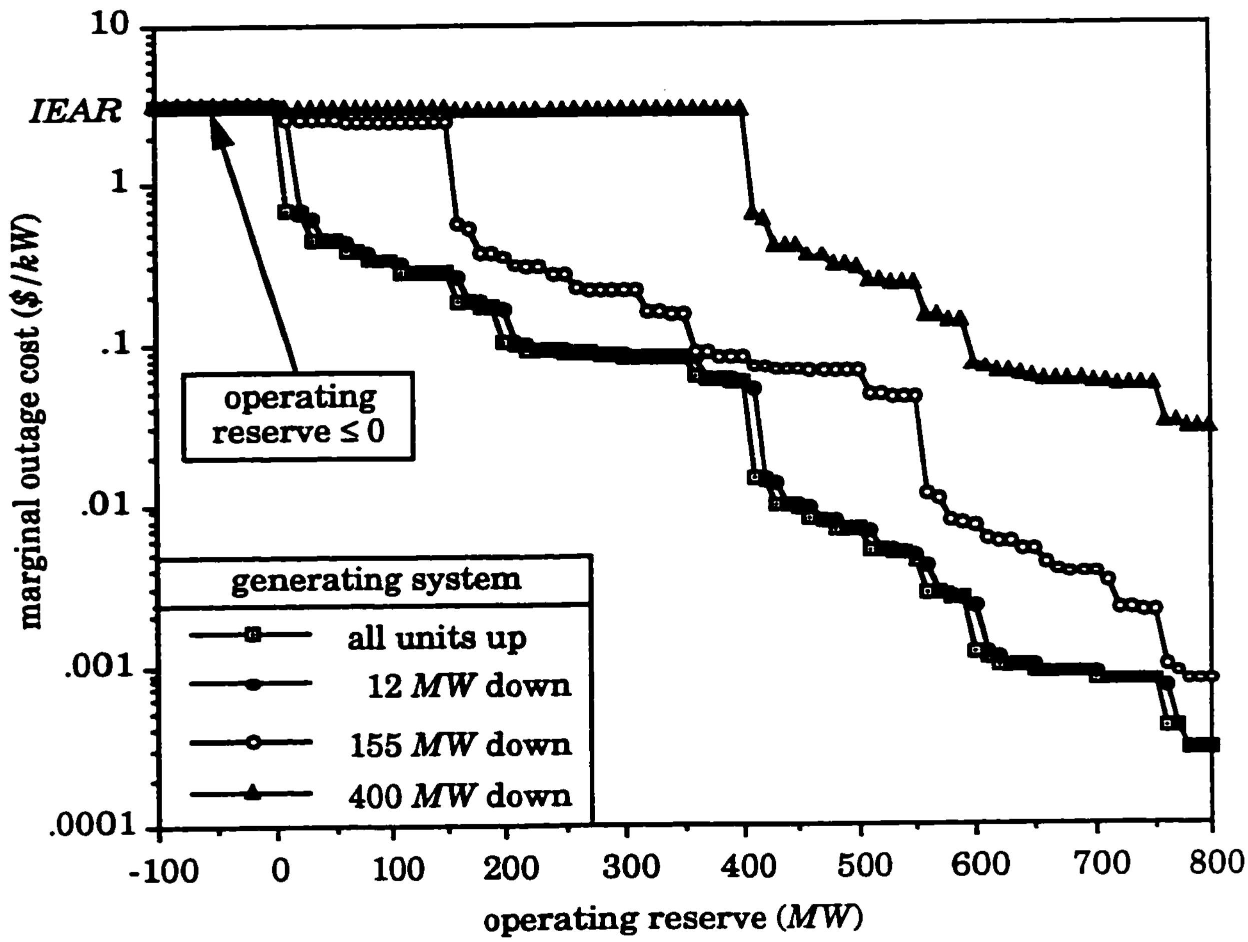

Figure 3.16. Effect of generating unit initial conditions on the marginal outage cost profile of the *IEEE-RTS* for a lead time of 10 hours.

As in the case of the *RBTS*, a second study was done to show the impact of the initial generating unit conditions on the calculated marginal outage cost as a function of the lead time. The study was done for an operating reserve of 500 *MW* and the results are shown in Figure 3.17. It can be seen from this figure that the effect of the initial conditions diminishes as the lead time increases. A comparison between the results of the *IEEE-RTS* shown in Figure 3.17 and those of the *RBTS* shown in Figure 3.5 clearly shows that the times required to reach the steady state values of the marginal outage costs for these two systems are different. This is the result of system size and the number and characteristics of the generating units that start off in the down state. For example, if three or more units of average size are assumed to be in the down state at time $t = 0$, the times required for convergence of the *IEEE-RTS* profiles will be different than those shown in Figure 3.17.

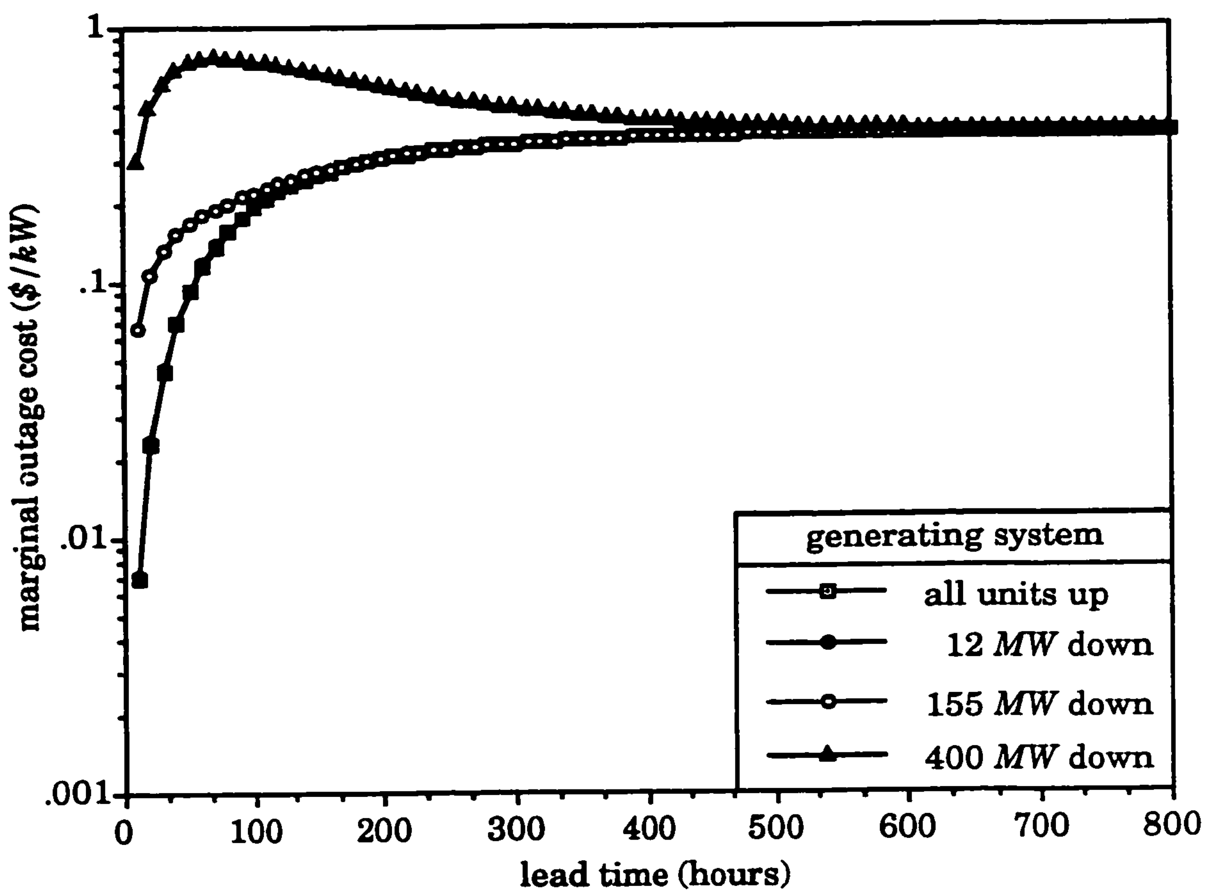

Figure 3.17. Effect of generating unit initial conditions on the marginal outage cost profile of the *IEEE-RTS* for an operating reserve of 500 *MW*.

The studies reported in this sub-section indicate that the initial generating unit conditions can have a very significant impact on the marginal outage cost values for those lead times that are normally used in spot pricing (i.e. 10 to 130 hours). This conclusion is clearly supported by the surface plot shown in Figure 3.18 which is a combination of both Figures 3.16 and 3.17.

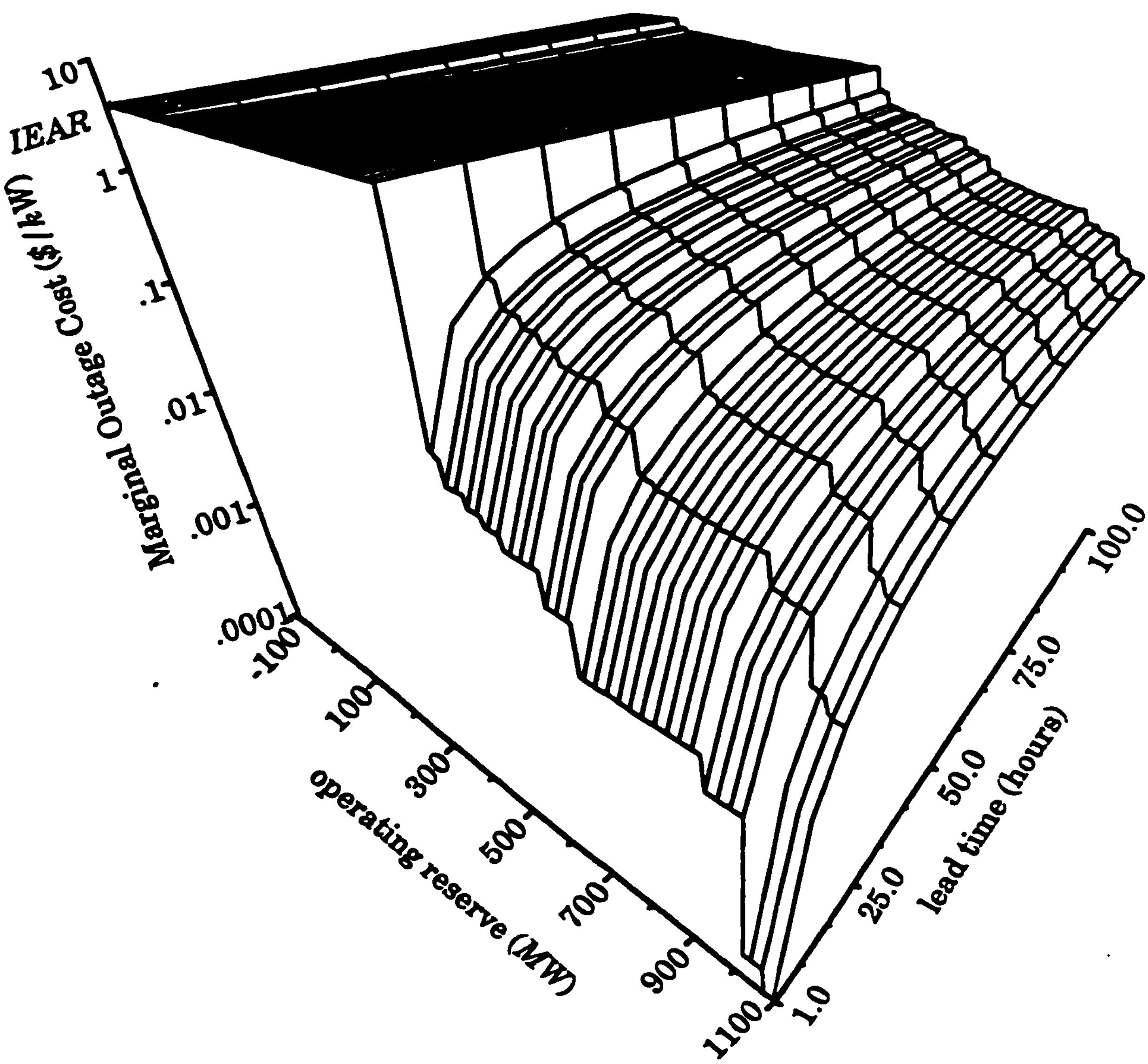

Figure 3.18. Variation of the marginal outage cost of the *IEEE-RTS* as a function of the operating reserve and the lead time when a 400 *MW* unit is assumed to be in the down state at $t = 0$.

The large variations in the marginal outage cost resulting from the initial generating unit conditions have a very important practical significance. It can be argued that if a unit is forecast to be available at a certain time T in the not too distant future (e.g., $T \leq 12$ hours), its availability at that time should not depend on its current condition. This argument is not always valid because, given that the unit is not available at time $t = 0$, there is a high probability that it will not be available at time $t = T$ even though it was scheduled to be available at that time. In other words, the availability of the unit at time T will be lower if the unit was not available at $t = 0$. Therefore, the capability of modelling the initial generating unit allows the user to select the most suitable initial condition for each unit in the system. It should be left up to the scheduler to decide, based on the most current information available, how much confidence can be placed on the availability of a particular unit and therefore select the most appropriate initial condition for that unit.

3.4.2. Effect of modelling derated states

In order to represent partial outages in the evaluation of the marginal outage costs, the 350 *MW* and the 400 *MW* units of the *IEEE-RTS* were assigned a 50% derated state as given in [84] and summarized in Table B.2. The state probabilities and transition rates of the derated model are such that the *DAFOR* is identical to the forced outage rate of the two-state model. The effect of using multi-state models on the marginal outage cost of the *IEEE-RTS* is shown in Figure 3.19 for two different lead times, 10 hours and infinity. It can be seen from this figure that the marginal outage costs calculated using the three-state models are higher than or equal to those calculated in the base case for low operating reserve levels and lower otherwise. These observations are not greatly affected by the magnitude of the lead time because a change in the lead time does not necessarily affect the number of states in the capacity outage probability table. It does, however, have an impact on the values of the state probabilities. Therefore, a change in the lead time should only have an impact on the magnitude of the increase or decrease in the marginal outage cost. Other changes can be attributed to the truncation of small probabilities in the capacity outage probability table.

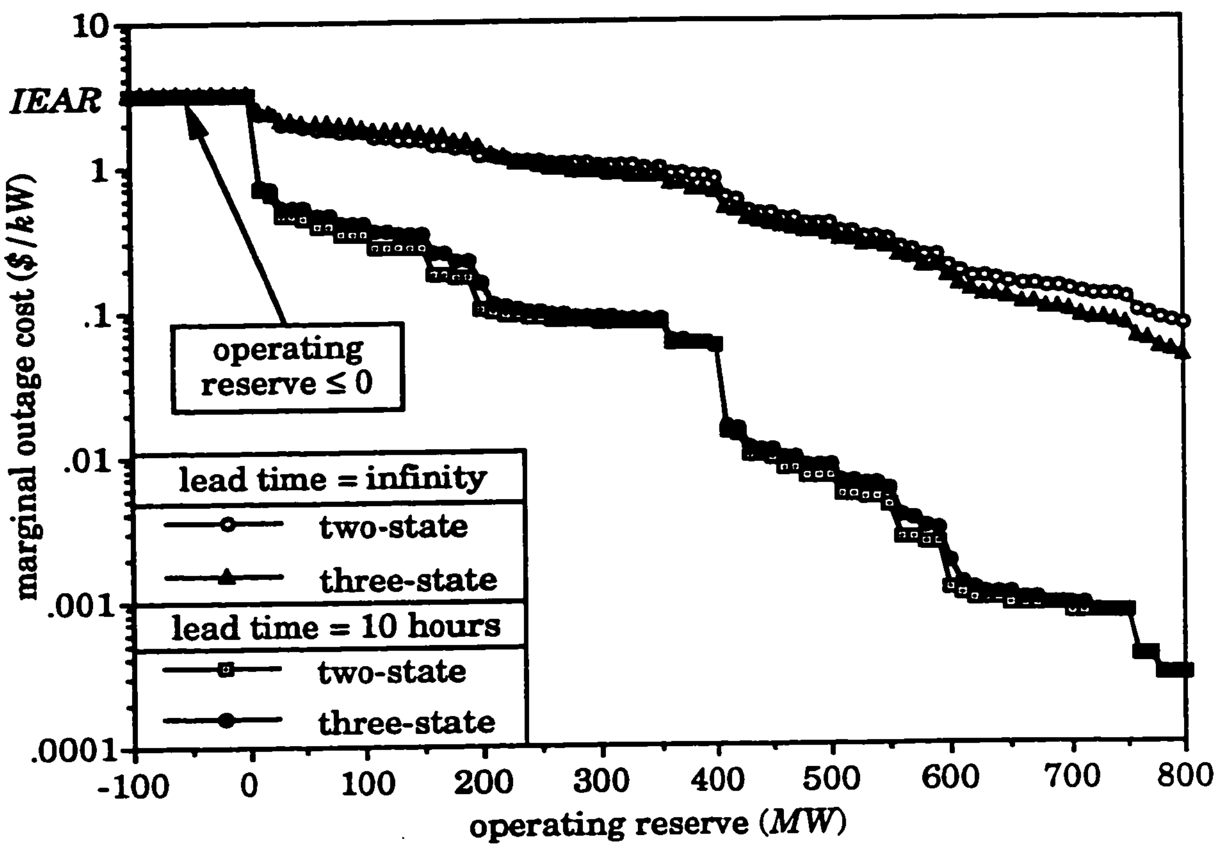

Figure 3.19. Effect of using a three-state model to represent the large units in the *IEEE-RTS* on the marginal outage cost as a function of the operating reserve.

3.4.3. Effect of load forecast uncertainty

In order to show the impact of the load forecast uncertainty on the marginal outage cost profile of the *IEEE-RTS*, a number of studies were conducted using the seven-step approximation of the normal distribution shown in Figure 3.9 and selected standard deviations. The results for the 3% and 5% standard deviations are compared to the base case (i.e. standard deviation of 0%) in Figure 3.20 for a lead time of 10 hours. It can be seen from this figure that the marginal outage cost generally increases as the standard deviation increases. As in the case of the *RBTS*, the load forecast uncertainty has a smoothing effect on the profiles and the values of the marginal outage cost for operating reserves that are less than or equal to zero are not necessarily equal to the *IEAR*.

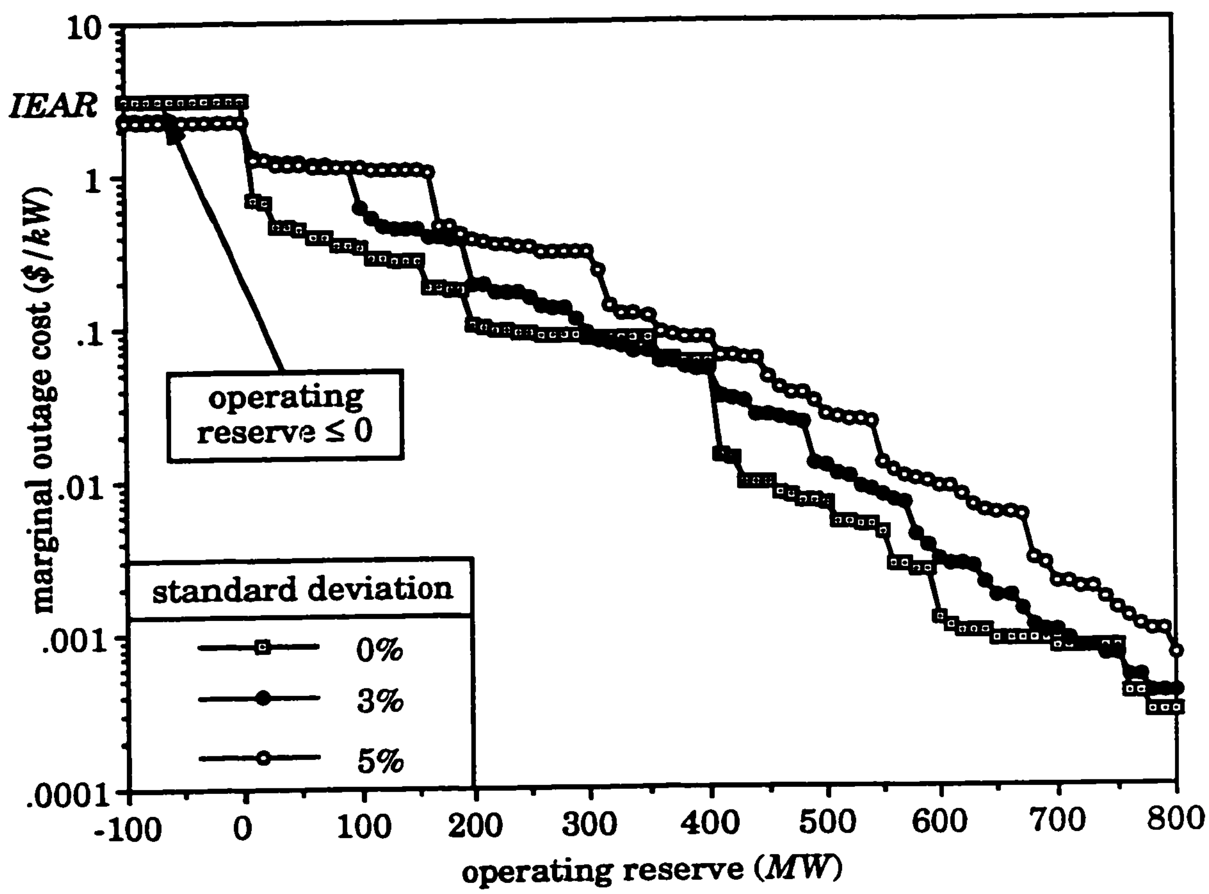

Figure 3.20. Effect of load forecast uncertainty on the marginal outage cost profile of the *IEEE-RTS* as a function of the operating reserve.

3.4.4. Effect of removing generating units for maintenance

In order to show the impact on the marginal outage cost profile of the *IEEE-RTS* of removing units for maintenance, a study was done where units of different sizes were removed for maintenance and the marginal outage costs calculated using the rest of the units in the system. The results from this study are compared to the base case (no units removed for maintenance) in Figure 3.21 for a lead time of 10 hours. It can be seen from this figure that the marginal outage cost profile is not significantly affected by the removal of the 100 *MW* and 200 *MW* units. However, when the 400 *MW* unit (11.7% of installed capacity) is removed for maintenance, the marginal outage cost becomes lower than the base case for most operating reserve levels. Therefore, it can be concluded from this study that a number of marginal outage cost profiles pre-calculated using selected combinations of generating units can be used to approximate the marginal outage costs in a practical system for the purposes of spot spicing.

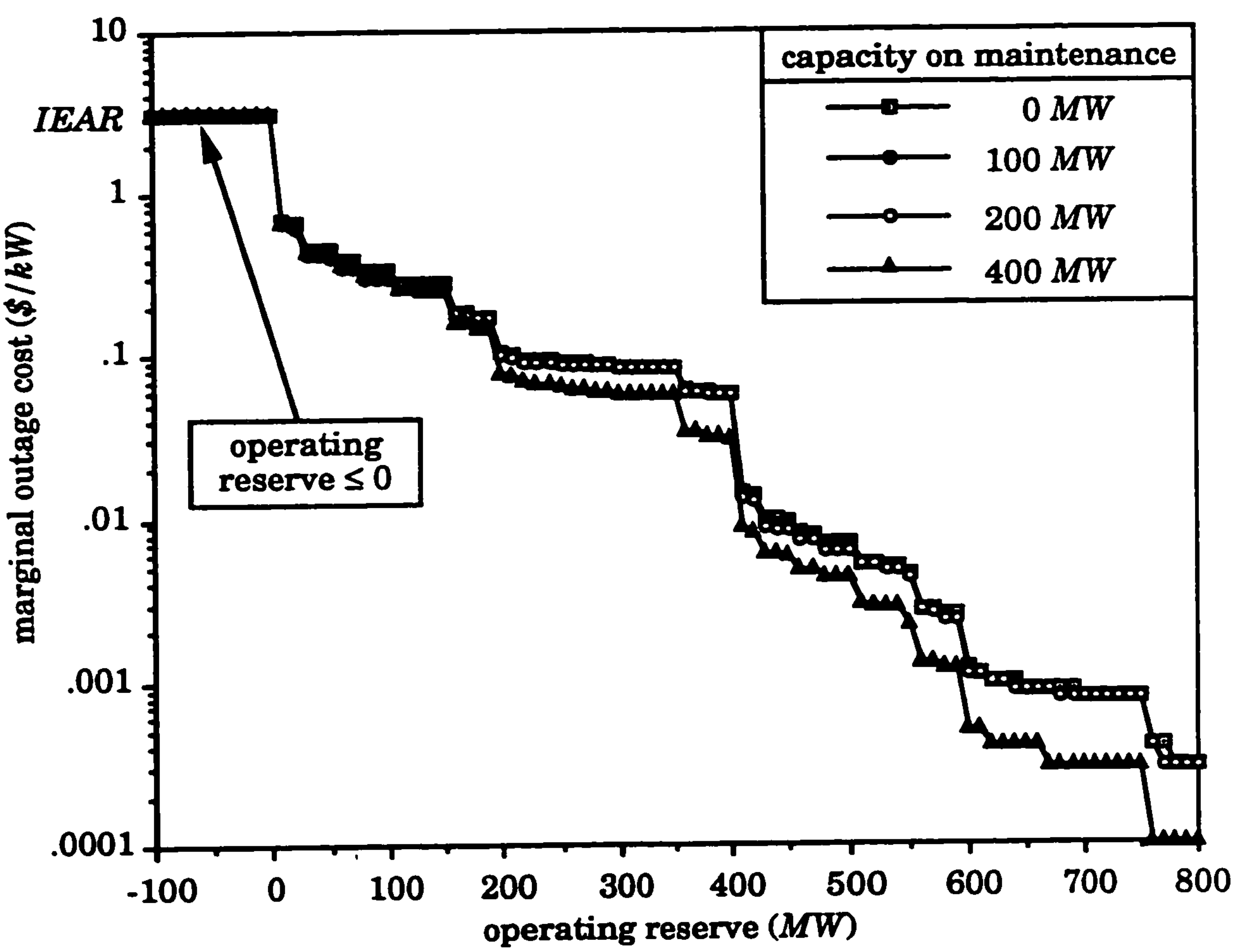

Figure 3.21. Effect of removing units for maintenance on the marginal outage cost profile of the *IEEE-RTS* as a function of the operating reserve.

3.5. Summary

This chapter illustrates the proposed method for calculating the marginal outage costs in isolated generating systems by application to the *RBTS* and the *IEEE-RTS*. The application of the proposed method to two test systems of different sizes is done to show the effect of modelling assumptions and parameters on the marginal outage cost and to draw some general conclusions regarding the applicability of the proposed method to large practical systems.

The marginal outage cost profiles of both test systems were calculated as a function of the operating reserve level and the lead time. The marginal outage cost is equal to the *IEAR* when the system has no operating reserves or when it is reserve deficient. As the reserves become more plentiful, the marginal outage cost decreases. The variation of the marginal outage cost with the lead time shows that the initial generating unit conditions have a large impact on the marginal outage cost profile especially at very short lead times. As the lead time increases, however, the impact of the initial conditions diminishes.

A number of sensitivity analyses were conducted to show the effect of selected modelling assumptions on the marginal outage cost profiles. It was found that the inclusion of generating unit derated states does not have a large impact on the marginal outage cost profile. However, if a large number of units are represented using multi-state models, it is expected that the marginal outage cost profile will be significantly different. It was also found that the marginal outage cost is generally higher when load forecast uncertainty is included in the model. The magnitude of the increase depends on the standard deviation of the load forecast uncertainty distribution. Finally, a number of studies were conducted in order to show the sensitivity of the marginal outage cost profile to the number of units on line. The purpose of these studies was to see if a number of pre-calculated marginal outage cost profiles can be used regardless of which units are unavailable due to scheduled maintenance on a particular day. The results from these studies show that the marginal outage cost profiles are affected by the number of units removed for maintenance particularly when the capacity of these units is large relative to the installed capacity of the system. In practical system studies, such variations will be minimal if the installed capacity of the system is large and the capacities of most generating units are relatively small compared to the installed capacity of the system. The conclusions drawn in this chapter are made with respect to the *RBTS* and the *IEEE-RTS*. It is believed that they are reasonably representative of the results which will be obtained for a wide range of practical systems. They will however have to be tested in each case prior to being considered for use in an actual system.

4. UTILIZATION OF APPROXIMATE TECHNIQUES TO CALCULATE THE MARGINAL OUTAGE COSTS IN ISOLATED GENERATING SYSTEMS

4.1. Introduction

Quantitative evaluation of the marginal outage costs associated with generating systems involves, among other things, the construction of a model of the system capacity outages. This model is inherently discrete and application of the well-known and basic recursive technique requires lengthy computations when applied to large power systems such as the *IEEE*-Reliability Test System. Alternatively, rounding of the capacity outage probability table, Fast Fourier transforms and continuous distributions can be used to approximate the generating system capacity model. The main advantage of the approximate techniques is the reduction in the computing time requirements. These techniques can in some cases introduce inaccuracies in the results, which depend on the system under consideration. Several authors have used these approximate techniques in the calculation of capacity outage probabilities, the study of parameter uncertainty in generating capacity reliability evaluation, the calculation of the expected energy production costs and the maintenance scheduling of generating facilities. This chapter discusses the potential application of the approximate techniques to calculating the marginal outage costs in large generating systems. The results of the approximate techniques are illustrated by comparison with those produced by the exact recursive technique for the *IEEE*-Reliability Test System [36].

4.2. Description of the Approximate Techniques

The marginal outage costs associated with electric generating systems can be calculated by multiplying the *IEAR* of the system by the incremental expected unserved energy [61]. A simple expression for calculating ΔEUE in generating systems was derived in Sub-section 2.4.2 and is given by:

$$\Delta EUE = P\left(K^{*}\right), \tag{4.1}$$

where K^{*} is the system capacity outage state number that satisfies the following inequality,

$$L \geq C - X\left(K^{*}\right). \tag{4.2}$$

The random variable X describes the probability density function of capacity outages in the generating system, C is the installed capacity of the system and L is the load level.

The conventional method of calculating the cumulative probability, $P(K^{*})$, in large generating systems involves the construction of a capacity outage probability table (*COPT*) to model the generating system capacity outages [26]. This process requires lengthy computations when applied to large power systems. Alternatively, the discrete distribution of the system capacity outages can be rounded using an appropriate rounding increment [26], approximated by continuous distributions [86,87] if the system is very large or a Fast Fourier Transform (*FFT*) algorithm [88] can be used to perform the convolution process by multiplying the Fourier transforms of the density functions of generating units in the frequency domain.

This section provides a brief description of the approximate techniques that can be used to calculate the marginal outage costs in an isolated generating system. A comparison between the results of the approximate techniques and those produced by the exact recursive technique has been published [82] and is detailed in the remaining sections of this chapter.

4.2.1. Discrete representation of capacity outages in generating systems

In a practical system the probability of having a large quantity of capacity forced out of service is usually quite small, as this condition requires the outage of several units. Theoretically, the capacity outage probability table incorporates all system capacity. The table can be truncated by omitting all capacity outages for which the cumulative probability is less than a specified amount (e.g. 10^{-8}). This results in a considerable saving in computer time as the table is truncated progressively with each unit addition. Since the cumulative probabilities are calculated directly using the recursive approach, no error results from the truncation process. The computing time requirements can also be reduced by rounding the capacity outage probability table [26] or by utilizing a Fast Fourier transform [88] to perform the convolution process. These techniques are briefly described in the following sub-sections.

4.2.1.1. Rounding the capacity outage probability table

The capacity outage probability table of a practical power system containing a large number of generating units of different capacities will contain several hundred possible discrete capacity outage levels. This number can be reduced by grouping the units into identical capacity groups prior to combining or by rounding the table to discrete levels after combining. Unit grouping prior to building the table introduces unnecessary approximations which can be avoided by the table rounding approach. The capacity rounding increment used depends upon the accuracy desired. The final rounded table will contain capacity outage magnitudes that are multiples of the rounding increment. The number of capacity levels decreases as the rounding increment increases, with a corresponding decreases in accuracy. The general expression for rounding a *COPT* as defined in [26] is given by (4.3) for all states i falling between the required rounding states j and k,

$$p(C_j)=\sum_i \frac{C_k-C_i}{C_k-C_j}\,p(C_i) \text{ and}$$

$$p(C_k)=\sum_i \frac{C_i-C_j}{C_k-C_j}\,p(C_i). \tag{4.3}$$

The flowchart of the rounding algorithm implemented in the program that was developed for calculating the marginal outage costs in generating systems is shown in Figure 4.1. This algorithm is performed as the capacity outage probability table is being built to minimize the computing time required to generate that table for every hour in the forecast period of spot prices (typically 24 to 120 hours). Rounding the table after it has been fully constructed is of little value because building the capacity outage probability table is the most time consuming task of the whole process. The proposed rounding algorithm may introduce some errors and is affected by the order in which the generating units are added to the table. However, as will be shown later in this chapter, the marginal outage costs

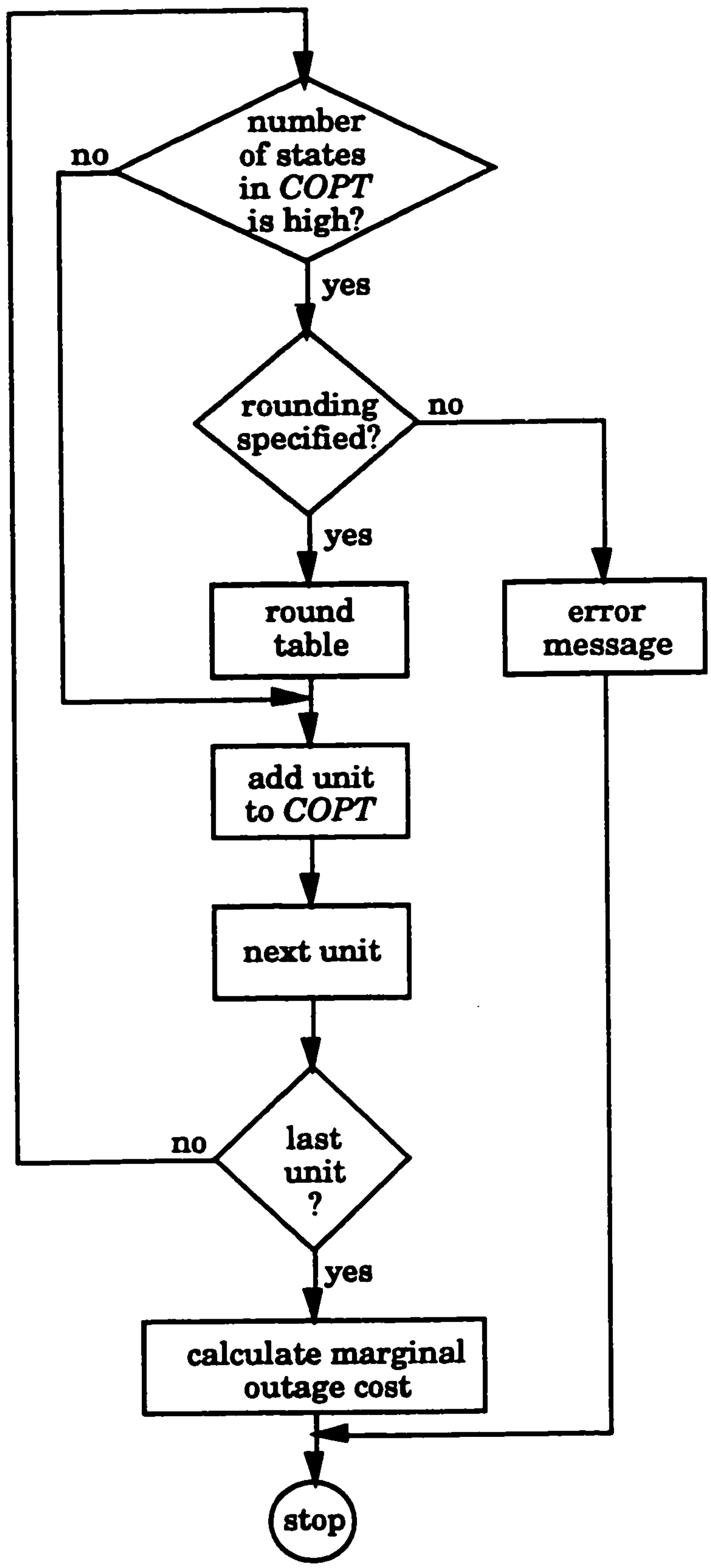

Figure 4.1. Flowchart of the rounding algorithm implemented in the marginal outage costing program.

calculated using the proposed algorithm are in close agreement with the exact values calculated using the basic recursive technique.

4.2.1.2. Fast Fourier Transform (*FFT*) algorithm

The process used to build the capacity outage model of a generating system involves the convolution of discrete functions in the form of probability density functions of generating units. There are a number of ways in which this convolution can be performed but most are based on manipulating the convolution integral. Another method, proposed by R.N. Allan et. al. [88] performs the convolution process using Fast Fourier transforms by multiplying the Fourier transforms of the density functions in the frequency domain. The main advantage of this technique is its execution time which increases linearly with the number of discrete points that have to be convolved instead of quadratically as in the case of the recursive technique. However, it is important to note that the accuracy of the *FFT* algorithm and the execution time decrease as the number of points used in the *FFT* algorithm decreases.

The *FFT* algorithm takes advantage of some properties of exponential functions to give fast and precise representation of the random variable that describes the capacity on outage in the frequency domain. The details of *FFT* techniques are well documented in [89]. The utilization of these algorithms simplifies the convolution problem. Consider the two functions $f_i(x)$ and $f_j(x)$ in a form ready to be convolved. Using an *FFT* algorithm, these functions can be transformed into the frequency domain as $S_i(n)$ and $S_j(n)$ respectively. In the frequency domain, the convolution process is simply one of point-by-point multiplication. The two transforms are therefore multiplied point-by-point to give the final function $S_{ij}(n)$ in the frequency domain. Finally, an inverse *FFT* algorithm is used to re-transform $S_{ij}(n)$ into $f_{ij}(x)$, thus completing the convolution process.

The interval T_{ij} in which the function $f_{ij}(x)$ will exist is equal to the sum of the capacities of the units i and j. This interval is usually divided into N_{ij} points which, for the most common *FFT* algorithms, must satisfy the relation $N_{ij}=2^{M_{ij}}$ where M_{ij} is an integer. When a convolved impulse falls between two pre-determined points, it is shared between them using a weighted averaging method depending on the distance of the convolved impulse from the two fixed points as shown in Figure 4.2. The *FFT* algorithm described in this sub-section is used later in this chapter to calculate the marginal outage costs associated with the generating system of the *IEEE-RTS*.

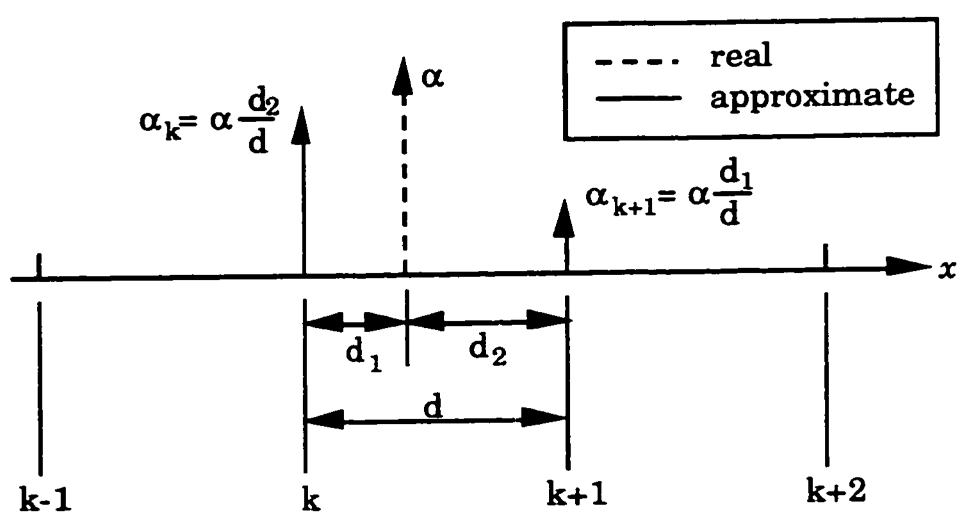

Figure 4.2. Sharing process of an impulse.

4.2.2. Continuous representation of capacity outages in generating systems

In addition to the discrete representations of the generating system capacity model described in Sub-section 4.2.1., it is found under certain conditions that if the system is very large, the discrete distribution of the system capacity outages can be approximated by a continuous distribution

[86,87]. These continuous models may introduce some inaccuracy in the results which depends on the system under consideration. Some continuous models have been reported in the literature and are briefly described in the following sub-sections.

4.2.2.1. Normal probability distribution

The distribution of the capacity available in large generating systems is positively skewed [86]. According to the Central Limit Theorem (*CLT*) [90], this distribution may be approximated by a normal distribution as the system size increases, or alternatively, as unit sizes relative to system size become small. Similarly, since the capacity on outage equals the installed capacity minus the available capacity, the distribution of the capacity on outage will also approach a normal distribution under the same conditions. The derivation of the parameters of the normal distribution from the outage statistics of generating units is discussed in [86,87] and summarized in Appendix D.

The normal distribution model has been used to develop the capacity outage probability tables for large power systems [86,87]. Although the continuous model is simpler and requires less computational effort than the discrete one, caution is necessary when applying it to very small systems. This could include systems with low unit forced outage rates and systems to which a unit much larger than those already present is added [93]. It has been found that the normally distributed generation model gives reasonable results when [87]:

1) the number of units in the system is large,
2) the forced outage rates of the units are large and
3) the system has a large number of small units relative to system size.

4.2.2.2. Folded normal probability distribution

It is perhaps reasonable to approximate the capacity model of a generating system by a normal distribution when the number of units in the system is large. However, the existence of several large units and otherwise mostly small units in a typical generation mix violates the spirit of the central limit theorem. The assumption of normality may not necessarily cause problems if one is computing probabilities in the central part of the distribution, but the tail probabilities may well be estimated inaccurately.

One approach to the problem of near normality proposed by Rau and Schenk [91] uses the summation of two normally distributed random variables to describe the distribution of capacity outages in the generating system. The resulting distribution is referred to as the folded normal distribution. The detailed derivation of this distribution can be found in [91] and only a brief summary of the calculation of the probability of a capacity outage is given in Appendix D.

The accuracy of the folded normal distribution as an approximation to the discrete model of capacity outages in generating systems was tested in [91]. It was found that the cumulative probabilities obtained for large capacity outages were not sufficiently accurate.

4.2.2.3. Modified distribution based on the Gram-Charlier series

Another approach to the problem of near normality is to make small corrections to the normal or the folded normal distribution approximations using asymptotic expansions (Edgeworth or Gram-Charlier) based on the central limit theorem [90]. The expansions of the Edgeworth type have been used in a variety of applications including the evaluation of capacity outage probabilities [91,94,95], the study of parameter uncertainty in generating capacity reliability evaluation [96,97], the calculation of the expected energy production costs [98,99] and the maintenance scheduling of generating facilities [100]. This chapter extends the scope of application of the Edgeworth type expansions to the evaluation of the marginal outage costs in large generating systems.

The general form of representing the capacity outages in generating systems using Edgeworth type expansions is derived in Appendix E. The Gram-Charlier expansion can be derived from this general form by considering all the terms up to the fourth order.

The accuracy of the Edgeworth type expansions in calculating the probability of capacity outages in large generating systems has been thoroughly examined [91,93,96]. It was found that the accuracy of these expansions generally improves with increasing system size, average forced outage rate and number of generators. Levy and Khan [93], and Hamoud and Billinton [96] found that the Gram-Charlier approximation gives better results when the higher order terms are included. The inclusion of the higher order terms, however, may create difficulties regarding convergence and behaviour of the series. The conditions under which the series converges when the higher order terms are included have not been mathematically established. The sum of a finite number of terms of the Gram-Charlier series may give in certain systems negative values for the cumulative probabilities associated with some capacity outages.

4.2.2.4. Distribution fitting technique

This approach consists of fitting a suitable (non-normal) distribution that adequately describes the data on system capacity outages and estimating the probabilities from the fitted distribution. This technique has been used by Mazumdar and Gaver [101,102] to fit a distribution to the capacity outages in generating systems. It was found that the Pearson Type I family (Beta distribution) provides the best approximation to the distribution of the generating system capacity outages. Although the distribution fitting technique is explored as a potential solution, it was found that it does not provide very accurate estimates of the tail probabilities [101,102].

4.2.2.5. Large deviation method

The basic shortcoming of all the continuous models discussed in this section lies in their inability to provide very accurate estimates of the tail probabilities and their tendency to exhibit peculiar behaviours when the high-order Edgeworth terms are included. The large deviation method is proposed as an enhancement to these continuous models. The detailed derivations of this method can be found in [101-103] and are summarized in Appendix F.

The idea behind the large deviation method is to displace the distribution of capacity outages in generating systems toward a value of interest y which is situated on the tail of the distribution. That is, to induce the displaced distribution to center at y. The probability determination (i.e. the evaluation of the area under the probability density curve) is now being made on the central part of the shifted distribution where the normal distribution (with, perhaps, an added Edgeworth correction term) should give good estimates [101-103]. The final step consists of compensating for the artificial displacement. This method is used extensively for risk computations in the insurance industry [104].

4.3. Utilization of Discrete Models to Calculate the Marginal Outage Cost of the *IEEE-RTS* Generating System

This section illustrates the discrete models (i.e. rounding and *FFT* algorithms) for calculating the marginal outage costs in large generating systems [82]. The *IEEE-RTS* is a relatively large test system with an exact capacity outage probability table containing 1872 states when the cumulative probability of a capacity outage is truncated at 10^{-8}. The computing time required to generate this table for every hour in a typical forecast period of spot prices (24 to 120 hours) is lengthy. The exact recursive technique cannot therefore be used in an operating environment where the turnaround time of the program should be in the order of few minutes. The table rounding technique may offer a solution to this problem if it can be shown that the marginal outage cost profile of the *IEEE-RTS* is not greatly affected by the rounding of the *COPT*.

The accuracy of the rounding algorithm is examined by calculating the marginal outage costs of the *IEEE-RTS* using a number of rounding increments and lead times. The results for selected rounding increments are compared to the no rounding case in Figures 4.3 and 4.4 for the lead times of infinity and 10 hours respectively. It can be seen from these figures that the accuracy of the rounding increment is not affected by the value of the lead time. Rounding the *COPT* using a 40 *MW* increment has no detectable impact on the marginal outage cost whereas the 100 *MW* rounding increment tends to discretize the profile. The relatively small loss in accuracy resulting from the rounding process is compensated for by the large reduction in the computing time. It was found from the studies conducted in this section that the rounding process reduces the computing time on a *VAX* 6340 by factors of 50 and 220 corresponding to the rounding increments of 40 *MW* and 100 *MW* respectively.

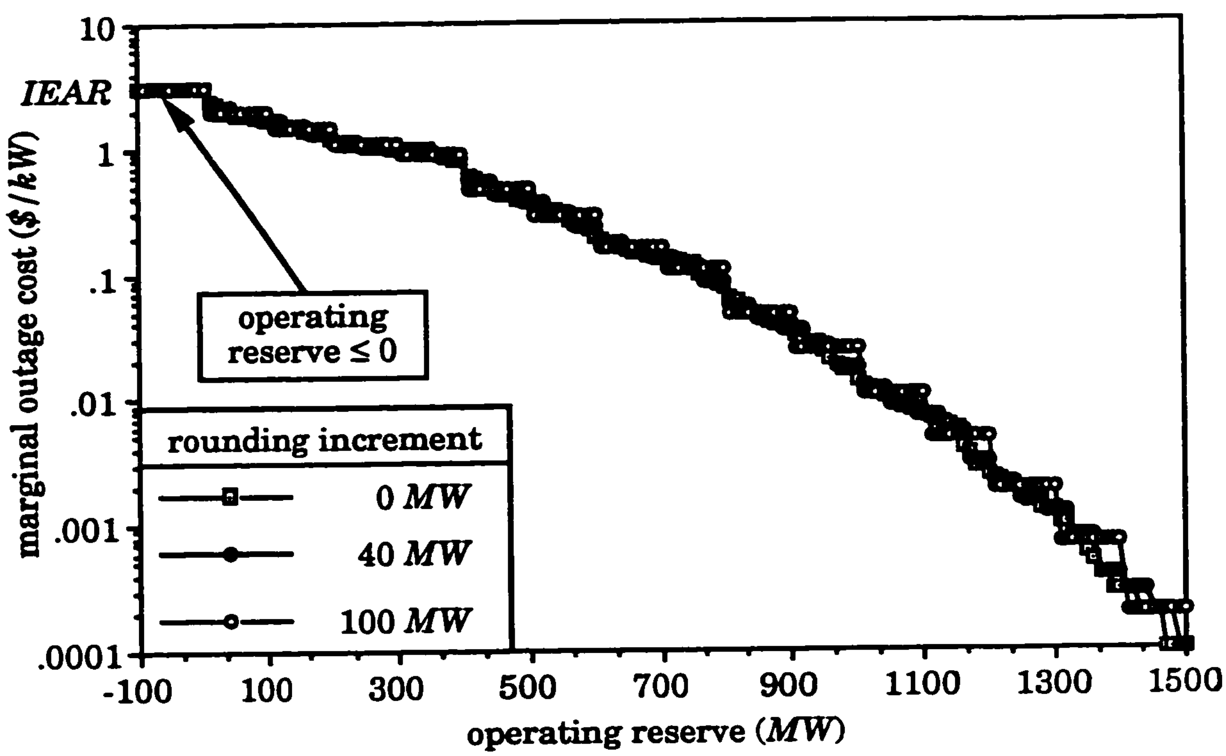

Figure 4.3. Effect of rounding the *COPT* on the marginal outage cost profile of the *IEEE-RTS* for a lead time of infinity.

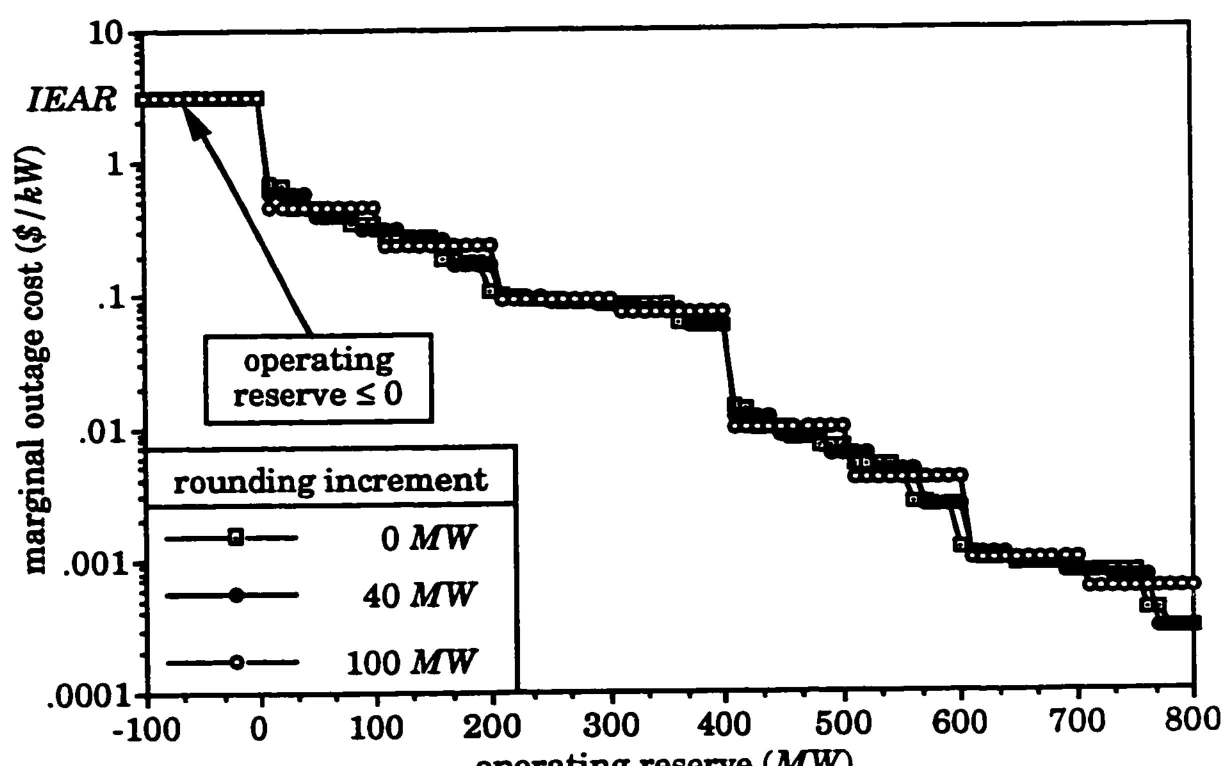

Figure 4.4. Effect of rounding the *COPT* on the marginal outage cost profile of the *IEEE-RTS* for a lead time of 10 hours.

The marginal outage cost profile of the *IEEE-RTS* was also calculated using the *FFT* algorithm with different number of points and the results are compared to the exact values in Figure 4.5 for a lead time of infinity. It can be seen from this figure that the accuracy of the *FFT* algorithm is largely dependent on the number of points considered. In the case of the *IEEE-RTS*, the minimum number of points required to achieve reasonable accuracy is 512 points. Increasing the number of points beyond this value does not improve the accuracy of the *FFT* algorithm significantly; but adds a considerable amount to the computing time.

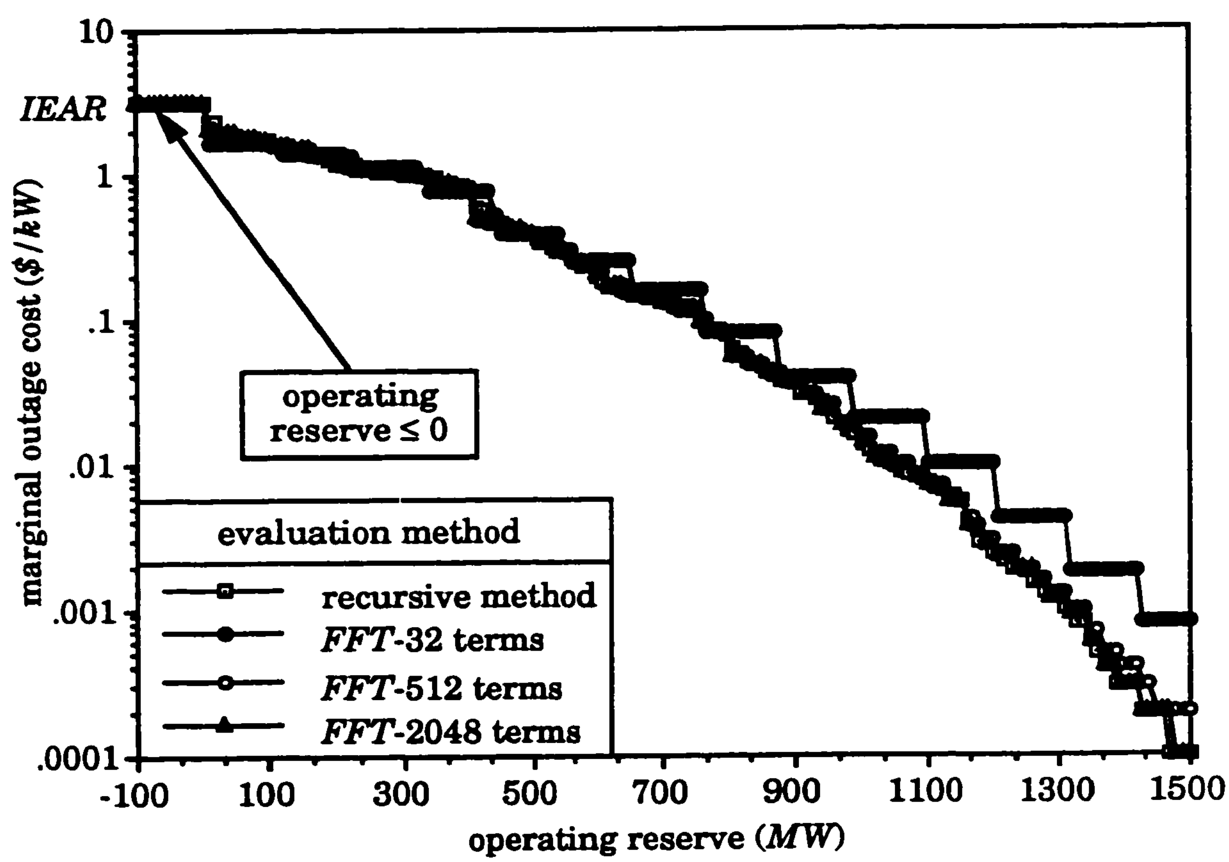

Figure 4.5. Comparison of the marginal outage cost profiles of the *IEEE-RTS* generated by the exact technique and the *FFT* algorithm for a lead time of infinity.

The impact of changing the lead time on the accuracy of the marginal outage costs produced by the *FFT* algorithm was also investigated. The lead time was decreased from infinity to 10 hours and the results plotted in Figure 4.6. It can be seen from this figure that the change in lead time has a slight impact on the accuracy of the *FFT* algorithm especially when the number of points is small. However, as the number of points increases, the marginal outage costs produced by the *FFT* algorithm converge towards the exact values.

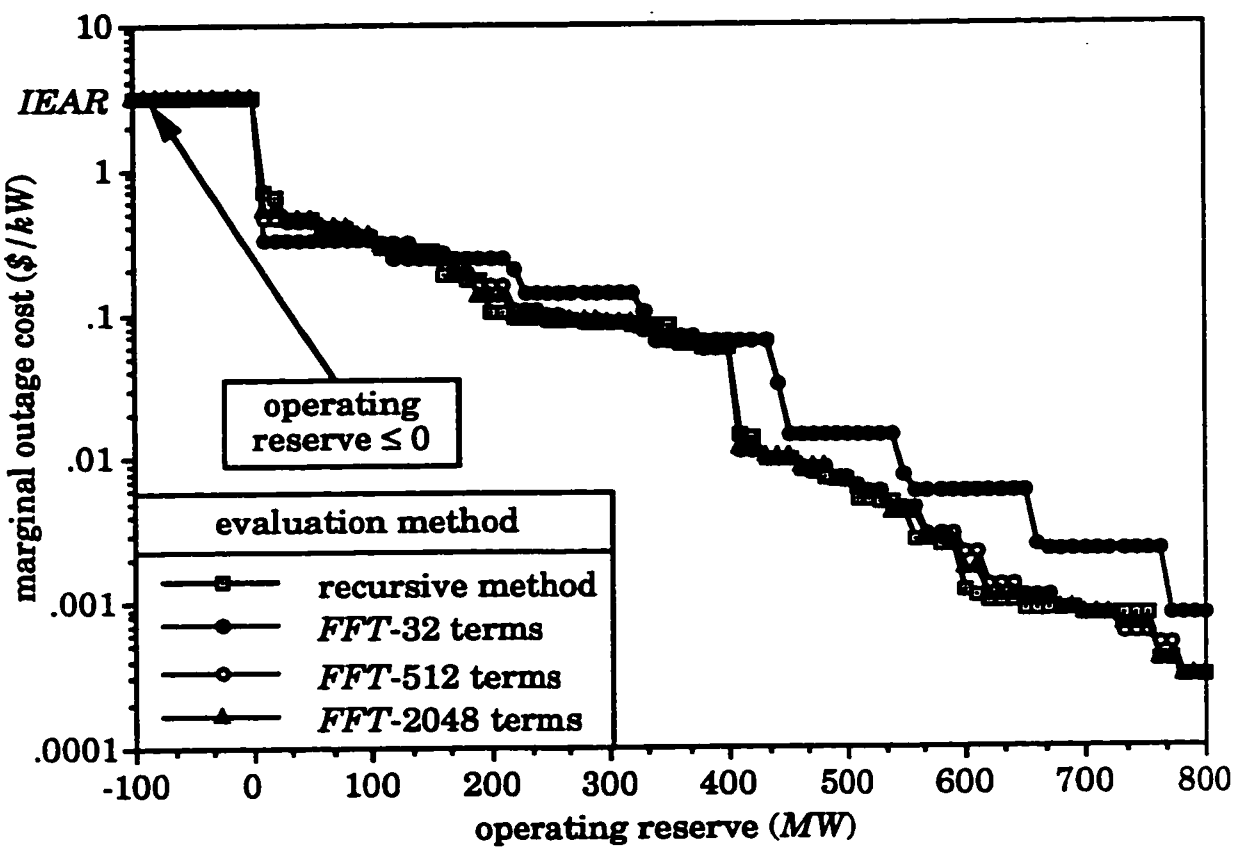

Figure 4.6. Comparison of the marginal outage cost profiles of the *IEEE-RTS* generated by the exact technique and the *FFT* algorithm for a lead time of 10 hours.

It can be concluded from the above studies that the rounding and the *FFT* algorithms provide practical methods for evaluating the marginal outage costs in generating systems. The usefulness of these algorithms will be more evident in large practical system studies where the computing times of the exact recursive technique are prohibitive.

4.4. Utilization of Continuous Models to Calculate the Marginal Outage Cost of the *IEEE-RTS* Generating System

Marginal outage cost evaluation of the *IEEE-RTS* using the recursive technique is time consuming because of the computing time required to build the *COPT*. It was shown in Section 4.3 that the computational effort required to calculate the marginal outage costs in generating systems can be decreased by applying the rounding or the *FFT* algorithms without significant impact on the results. This section is concerned with the utilization of continuous models to calculate the marginal outage cost of the *IEEE-RTS* [82] generating system. A number of studies are conducted using the continuous models and the results are compared to the exact values obtained using the recursive technique. It has already been reported by several authors that the normal, folded normal and distribution fitting techniques do not provide very accurate estimates of tail probabilities, and therefore only the Gram-Charlier expansion, the high-order Edgeworth expansion and the large deviation method are used in the following comparisons.

The first study compares the marginal outage costs calculated using the Gram-Charlier expansion, the high-order Edgeworth expansion and the large deviation method to those calculated using the recursive technique (exact method) for a lead time of infinity. The results shown in Figure 4.7 reveal that both the Gram-Charlier series and the large deviation method provide good results for all operating reserve levels. However, the large deviation method is clearly more accurate at high operating reserves. The high-order Edgeworth expansion, on the other hand, is almost equivalent to the Gram-Charlier expansion for operating reserve levels smaller than 950 *MW*; but it deteriorates very quickly as the operating reserve level increases (estimation of tail probabilities).

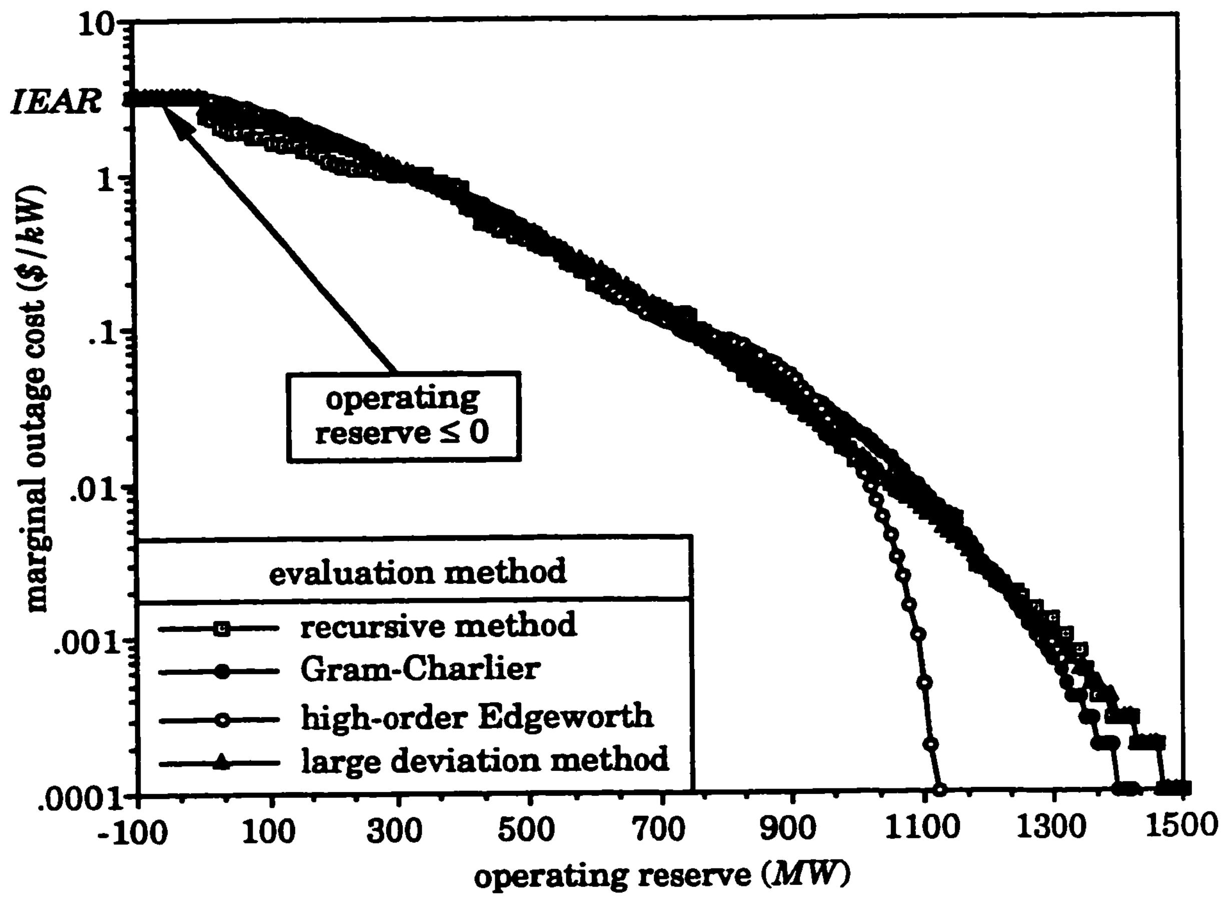

Figure 4.7. Comparison of the marginal outage cost profiles of the *IEEE-RTS* generated by the exact technique and the continuous models for a lead time of infinity.

In the second study, the lead time was decreased from infinity to 10 hours to show the impact of short lead times on the accuracy of the continuous models. The results from this study are shown in Figure 4.8. It can be seen from this figure that the decrease in lead time causes some peculiar behaviour in the results produced by the Gram-Charlier expansion and the high-order Edgeworth expansion. The accuracy of the large deviation method, however, remains very high. The discontinuity in the marginal outage cost profile generated by the high-order Edgeworth expansion is due to negative probability values which are physically impossible.

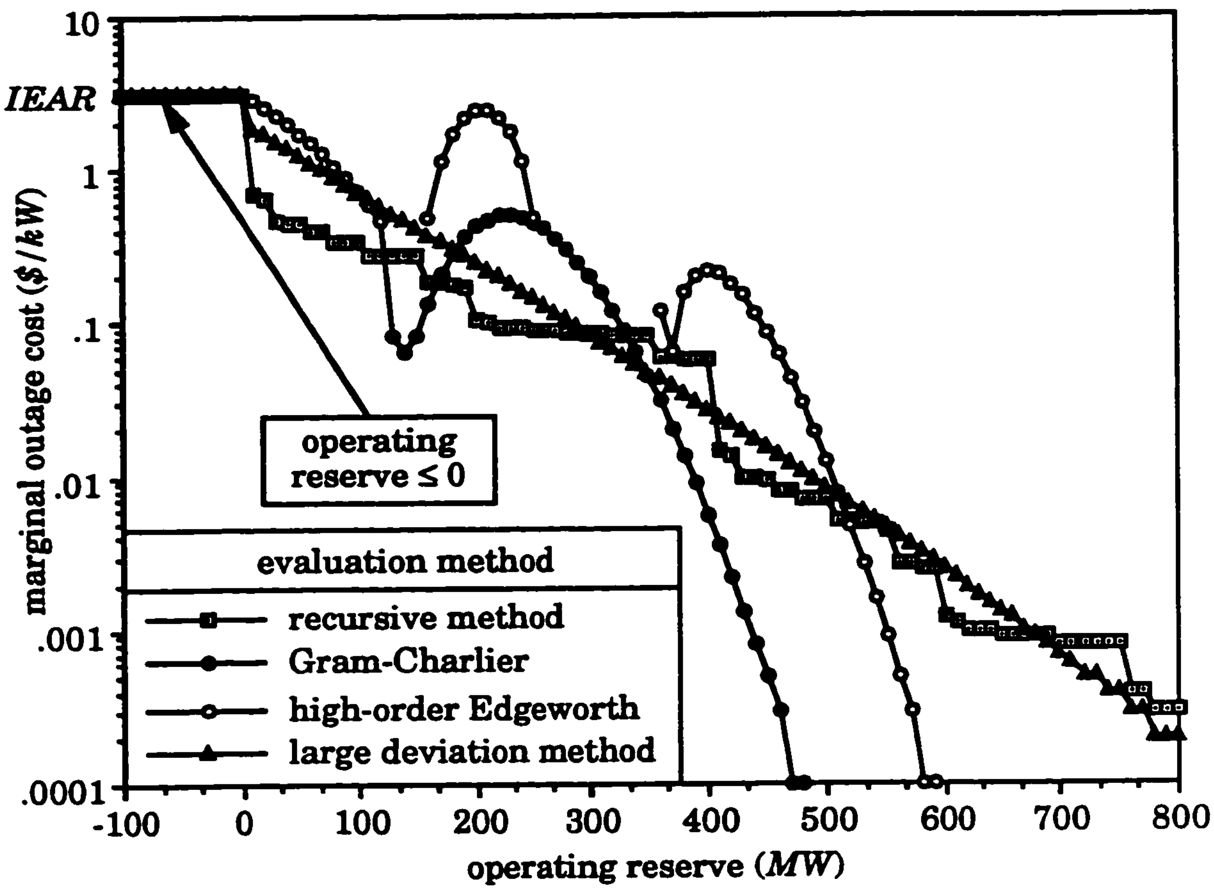

Figure 4.8. Comparison of the marginal outage cost profiles of the *IEEE-RTS* generated by the exact technique and the continuous models for a lead time of 10 hours.

At short lead times, the assumption that the distribution of system capacity outages is normal is no longer valid. In order to improve the accuracy of the large deviation method, it was decided to study the impact of adding the first and second order Edgeworth terms to the normal distribution used in the large deviation method. The results from this study are compared to the exact values and those produced by the simple large deviation method in Figure 4.9 for a lead time of 10 hours. It is clear from this figure that the addition of the first and second order Edgeworth terms generally improves the accuracy of the large deviation method. The magnitude of the improvement is higher at low operating reserve levels.

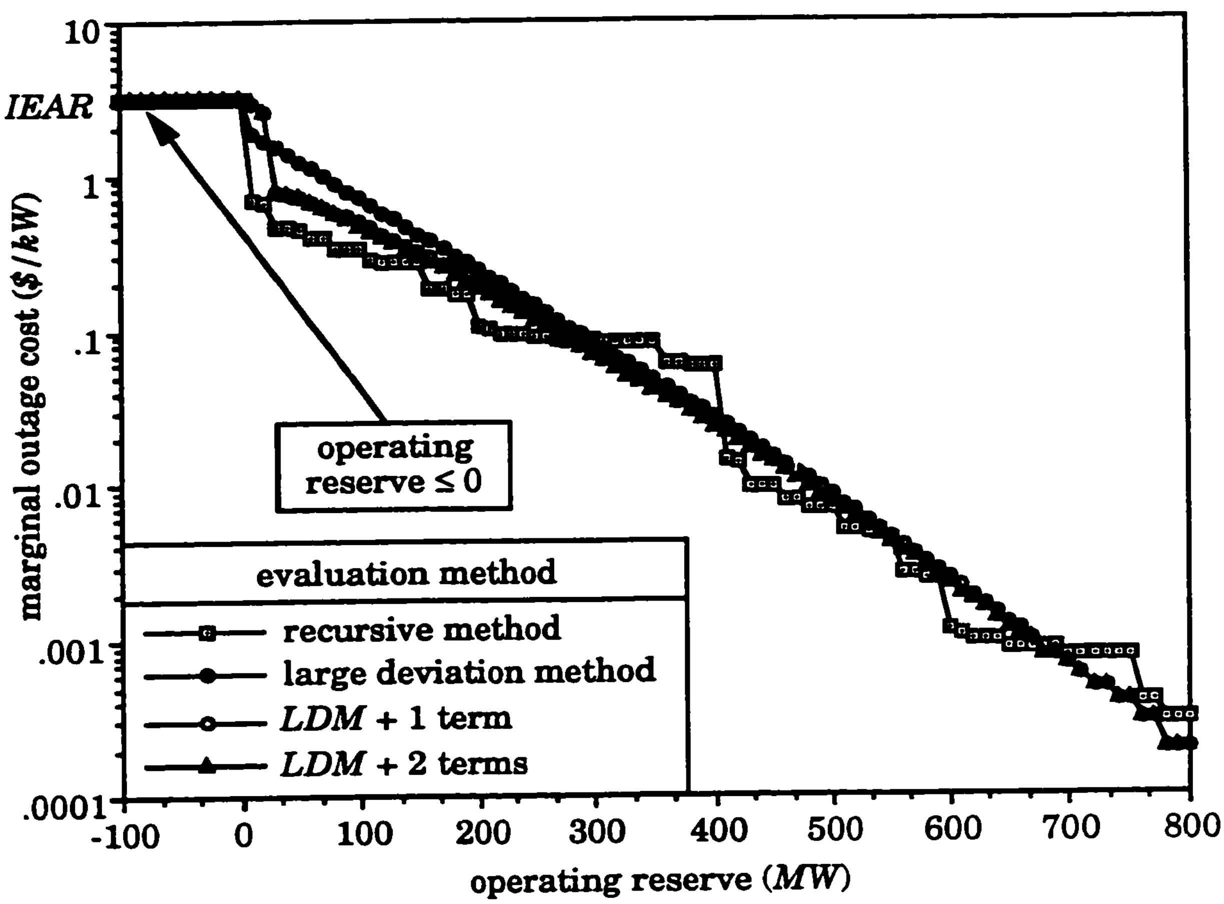

Figure 4.9. Comparison of the marginal outage cost profiles of the *IEEE-RTS* generated by the exact technique and the various large deviation methods for a lead time of 10 hours.

4.5. Comparison of the Accuracy and Computing Time Requirements of the Approximate Techniques

It is shown in Sections 4.3 and 4.4 of this chapter that the rounding algorithm with an increment of 40 *MW*, the *FFT* method with 512 terms and the large deviation method with an Edgeworth correction term provide the best marginal outage cost estimates for the *IEEE-RTS*. In order to quantify the accuracy of these methods, the errors produced by each method are compared in Figure 4.10 for a lead time of 10 hours. These errors are calculated as the difference between the exact values and the values calculated by the approximate techniques.

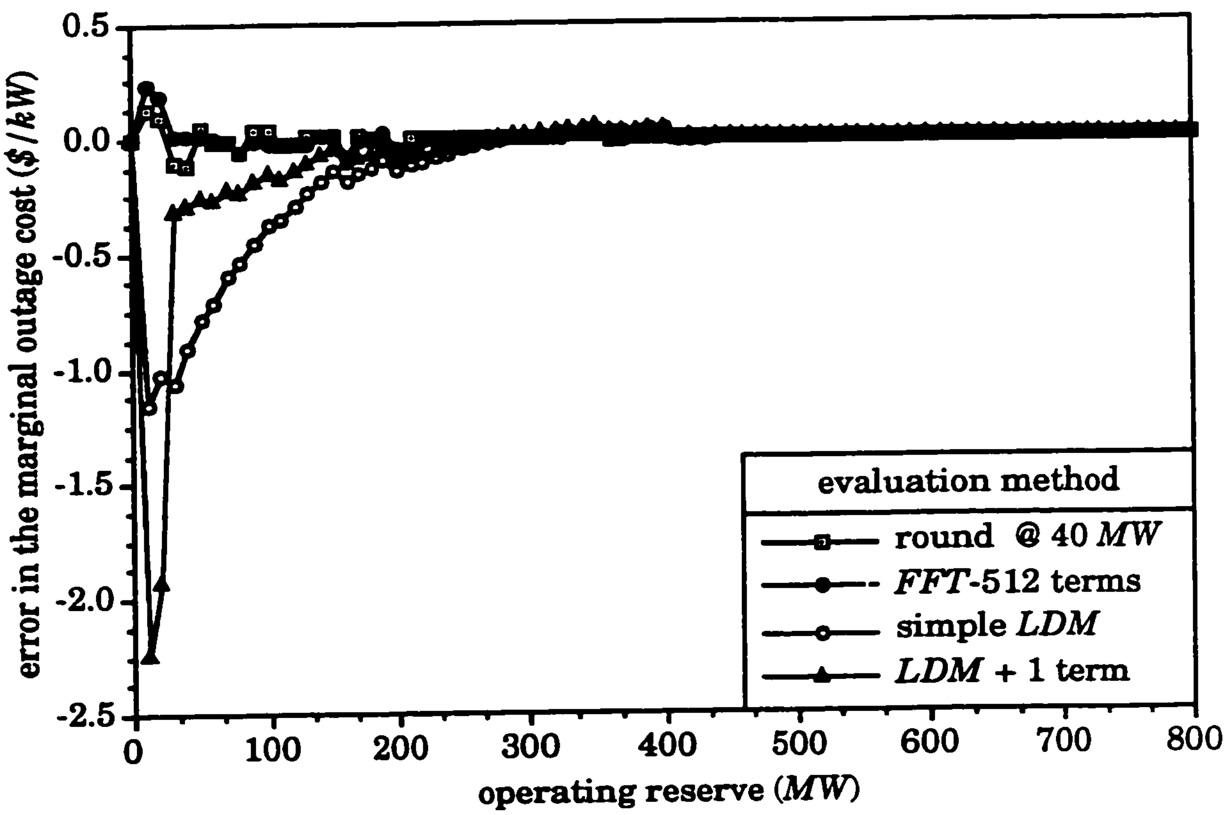

Figure 4.10. Comparison of the errors produced by the various approximate techniques as a function of the operating reserve for a lead time of 10 hours.

It can be clearly seen from Figure 4.10 that the error in the marginal outage cost values estimated using the rounding and the *FFT* algorithms are negligible. However, the error resulting from the application of the large deviation method is significant at low operating reserves and negligible at high operating reserves. This result was expected because the strength of the large deviation method lies in its ability to estimate the tail probabilities of a distribution (i.e. probabilities corresponding to high operating reserves) accurately. As the evaluation moves towards the centre of the distribution, the accuracy of the large deviation method decreases.

In addition to the accuracy, the computing time requirements of an approximate technique play a major role in the selection of suitable techniques for evaluating the marginal outage costs in generating systems. These costs are generally evaluated on a day-ahead basis for every hour in the forecast period. It was decided, therefore, to compare the computing times required by each approximate technique to calculate the hourly marginal outage cost for the 24-hour forecast period shown in Figure 4.11. The calculations were performed on a *VAX* 6340 assuming that the lead time to the first hour in the forecast period is 10 hours. The results of this comparison are shown in Figure 4.12.

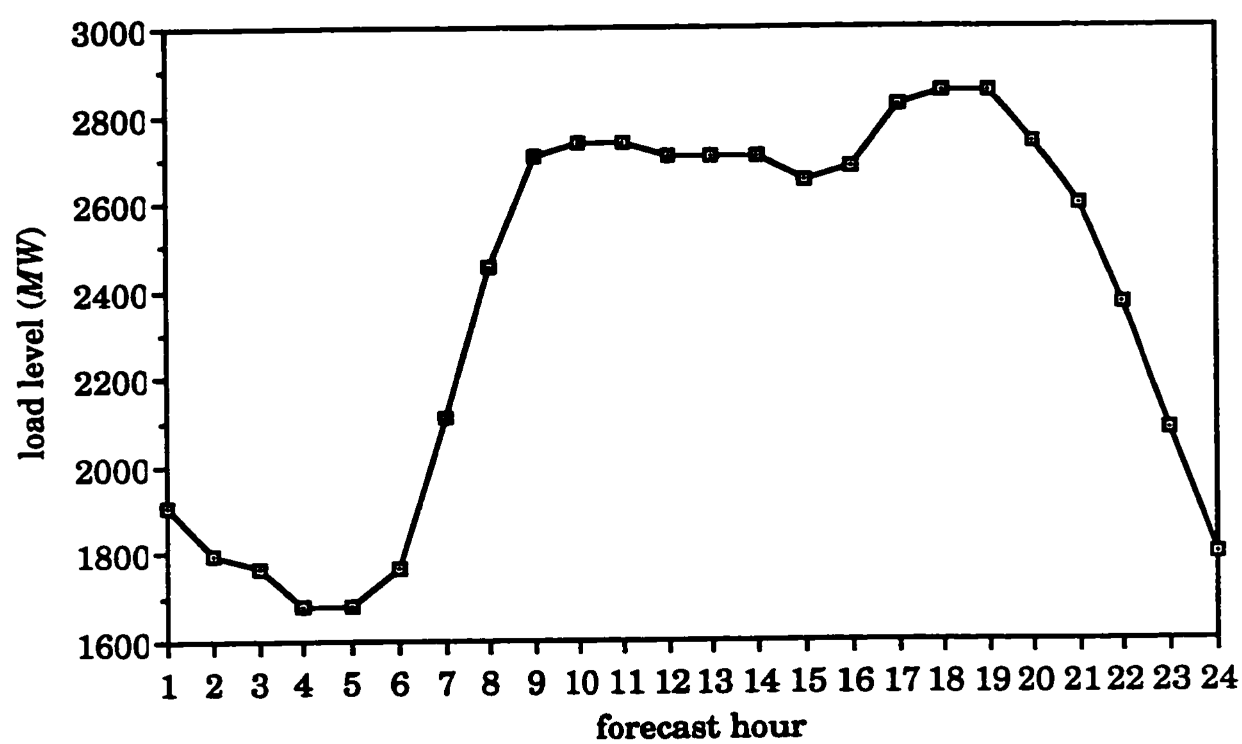

Figure 4.11. Load profile for a 24-hour forecast period.

It can be seen from Figure 4.12 that the computing times required by the rounding and the *FFT* algorithms are not affected by the load level or the lead time to the hour being forecast. The computing times required by these techniques to calculate the marginal outage cost for any one hour vary between 0.55 and 0.85 seconds on the *VAX* 6340. The computing time required by the large deviation method "*simple LDM*" is significantly higher than that required by the other approximate techniques and is definitely dependent upon the load level and the lead time to the hour being forecast as shown in Figure 4.12. A comparison between Figures 4.11 and 4.12 shows that the computing time profile of the large deviation method has a similar shape as the inverted load level profile and it tends to decrease as the load level increases and vice versa. In addition to varying with the load level, the computing time of the large deviation method also varies with the lead time such that, for any given operating reserve, the computing time decreases as the lead time increases.

The large magnitude of the computing time required by the large deviation method is due to the number of iterations required to find the amount of distribution displacement using the Newton-Raphson technique. This number of iterations is, in turn, a function of the initial condition used by the program. In order to improve the speed of the large deviation method, the solution from the Newton-Raphson iteration process for one hour is used as the initial condition for the next hour. The results from this study are also shown in Figure 4.12 using the label "*improved LDM*". It is clear from this figure that the computing time required to calculate the marginal outage cost for the first hour in the forecast period remains unchanged. It becomes negligible (0.03 seconds), however, for the remaining hours in the forecast period. Therefore, the improved large deviation method should be used if its accuracy is acceptable for the given application. The comparisons performed in this section also show that the rounding and the *FFT* algorithms provide the best overall results in a reasonable amount of computing time. The selection of a suitable rounding increment or number of terms for the *FFT* algorithm should depend on the system under study.

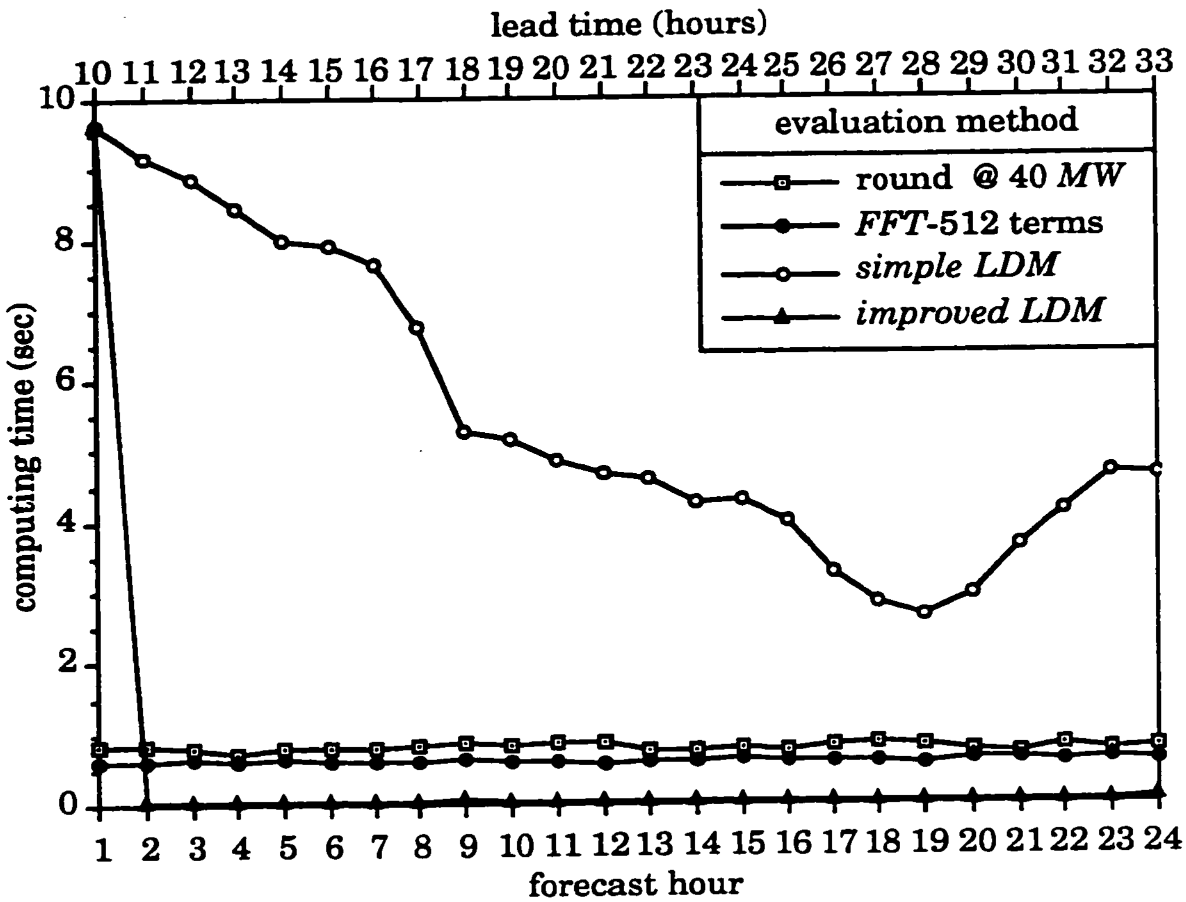

Figure 4.12. Comparison of the computing times required by each approximate technique to calculate the marginal outage cost for each hour in the forecast period using a 10-hour lead time.

4.6. Summary

Evaluation of the marginal outage costs associated with large generating systems can be very time consuming if exact recursive techniques are used to model the system capacity outages. One way of decreasing the computing time requirements involves the utilization of approximate techniques to create a generating system capacity outage model. This chapter illustrates the use of such techniques in the evaluation of the marginal outage costs in generating systems. The approximate techniques investigated in this chapter include the rounding algorithm, the Fast Fourier Transform algorithm, the Gram-Charlier expansion, the high-order Edgeworth expansion and the large deviation method. These techniques were used to calculate the marginal outage cost profile for the *IEEE*-Reliability Test System as a function of the operating reserve level for selected lead times. The results from the approximate technique are compared to the exact values calculated using the recursive techniques for very high and very low lead time values. These comparisons show that the rounding and the *FFT* algorithms provide the best accuracy for all operating reserves in a reasonable amount of computing time. The implementation of the rounding algorithm is much simpler however since it is based on the general and widely used recursive technique [26]. The accuracy of the large deviation method falls closely behind the first two techniques. The computing time required by this method, however, is much smaller than that required by the previous techniques if the proper initial conditions are used in the Newton-Raphson iteration process. The accuracy of the Gram-Charlier and the high-order Edgeworth expansions is a function of the lead time considered. When the lead time is very short, these techniques exhibit peculiar behaviours that produce negative probabilities under certain conditions. The conclusions reached in this chapter are made with respect to the *IEEE-RTS*. It is expected that the accuracy of some of these techniques will improve as the size of the system increases and/or the characteristics of its generating units are different.

5. EVALUATION OF THE MARGINAL OUTAGE COSTS IN INTERCONNECTED GENERATING SYSTEMS

5.1. Introduction

The evaluation of the marginal outage costs associated with isolated generating systems using quantitative power system reliability techniques has been demonstrated in Chapters 3 and 4. The proposed method calculates the marginal outage cost as the product of the Interrupted Energy Assessment Rate (*IEAR*) and the Incremental Expected Unserved Energy (ΔEUE) of the generating system. The method was illustrated in Chapter 3 using the *RBTS* [35] and the *IEEE-RTS* [36].

Evaluation of the marginal outage cost associated with large generating systems can be very time consuming if exact recursive techniques are used to model the system capacity outages. One way of decreasing the computing time requirements involves the utilization of approximate techniques to create a capacity outage model for the generating system. The application of a number of approximate techniques to marginal outage costing is illustrated in Chapter 4.

There is considerable interest in applying marginal outage cost evaluation in actual utility systems. The techniques illustrated in Chapters 3 and 4 have been implemented in a spot pricing procedure utilized by a large electric power utility [106]. The basic recursive technique illustrated in Chapter 3 is extended to interconnected generating systems in this chapter. The newly extended method is used to calculate the marginal outage costs on a regional basis within a single system and the impact of assistance from neighbouring systems on these costs. The chapter also illustrates the effect of selected interconnection topologies and modelling assumptions on the marginal outage costs in interconnected generating systems. The application of the derived methodology is illustrated using the *RBTS* [35] and the *IEEE-RTS* [36].

5.2. Proposed Method for Calculating the Marginal Outage Costs in Interconnected Generating Systems

In order to calculate the marginal outage cost in interconnected generating systems, methods capable of calculating the *IEAR* and ΔEUE in these systems must be developed. This requires a detailed assessment of the reliability of the interconnected generating systems using exact analytical techniques [107-112] or Monte Carlo simulation [113]. In addition, a number of the approximate techniques discussed in Chapter 4 can and have been used to assess the reliability of interconnected generating systems [114-118]. Alternatively, the assistance from one system can be modelled as a multi-state equivalent unit which describes the potential ability of one system to accommodate capacity deficiencies in the other [26,108]. The assistance level for a particular outage state in the assisting system is given by the minimum of the tie capacity and available system reserve at that outage state. All assistance levels greater than or equal to the tie capacity are replaced by one assistance level which is equal to the tie capacity. The resulting assistance table can be converted into a capacity model of an equivalent multi-state unit which is added to the existing capacity model of the assisted system. The marginal outage cost of the assisted system is then calculated as if it is a single area system. This approach to assessing the reliability of interconnected generating systems is referred to as the "equivalent assisting unit method" [26].

The utilization of the equivalent assisting unit method to represent the capacity assistance in radially interconnected generating systems is relatively simple [26,108]. This method can also be used to represent the capacity assistance in multi-area looped systems. A procedure which helps in breaking up complicated interconnected system configurations depending upon the operating conditions can be used [112]. Such a procedure is illustrated in this chapter using a three-area looped system.

5.3. Application to Two Interconnected Generating Systems

The application of the proposed methodology for calculating the marginal outage costs in interconnected generating systems is presented in this section by considering the two systems shown in Figure 5.1. System A is designated as the assisted system and System B as the assisting system. In addition, it has been assumed that any negative capacity margin in the assisting system does not affect the assisted system. Positive capacity margins in either system do, however, increase the operating reserve of the other system.

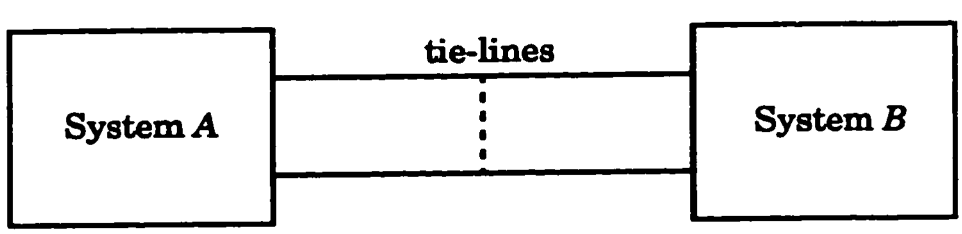

Figure 5.1. Two generating systems interconnected by a number of tie-lines.

In order to illustrate the two system interconnection case, two *RBTS* test systems are assumed to be interconnected by a perfect tie-line with infinite capacity. The generation models of both systems are identical and defined in [35] and Appendix A. The value of the *IEAR* is assumed to be 3.6 $\$/kWh$. A range of studies were performed using selected assistance levels for a lead time of 10 hours which is typical in forecasting day-ahead marginal outage costs for spot pricing purposes. The object of the study is to show the effect of the assistance available from System *B* (assisting system) on the marginal outage cost profile of System *A* (assisted system). The study was carried out by varying the assistance level available from System *B* and calculating the corresponding marginal outage cost profile of System *A*. The resulting profiles are expressed as a function of the operating reserve of the isolated System *A* in Figure 5.2. This representation highlights the shift in the marginal outage cost profile of System *A* caused by the assistance from System *B*.

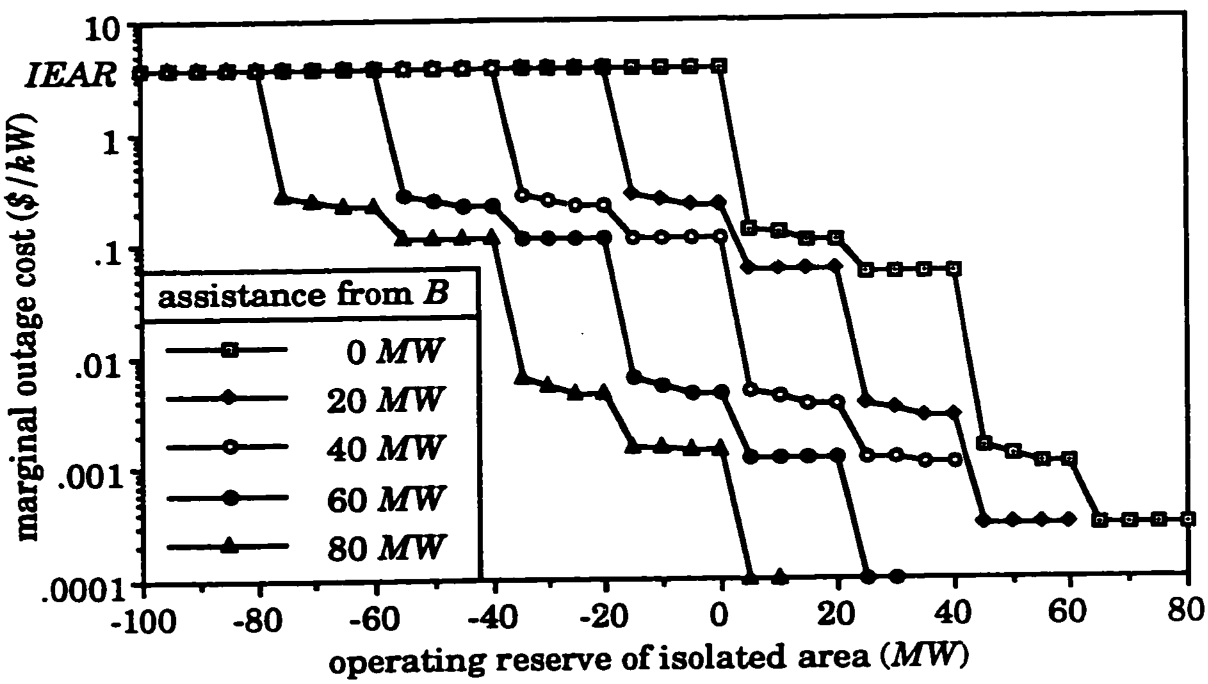

Figure 5.2. Effect of capacity assistance from System *B* on the marginal outage cost profile of System *A*.

It can be seen from Figure 5.2 that the marginal outage cost of the isolated System *A* (i.e. no assistance) is equal to the *IEAR* when the system has no operating reserves or when it is reserve deficient and it decreases as the operating reserve increases. As the assistance available from System *B* increases, the value of the marginal outage cost for any given operating reserve level decreases. The amount of the reduction is a function of the generation and load models in both systems and the reserve sharing policy employed. A close examination of Figure 5.2 shows that the marginal outage cost profiles of the interconnected system *A* have the same general shape as the isolated system profile. Therefore, it was decided to see if these profiles can be directly estimated from the isolated system profile. To do this, the marginal outage cost profiles of the interconnected System *A* were shifted by amounts that correspond to the assistance level available from System *B* and the results are plotted in Figure 5.3.

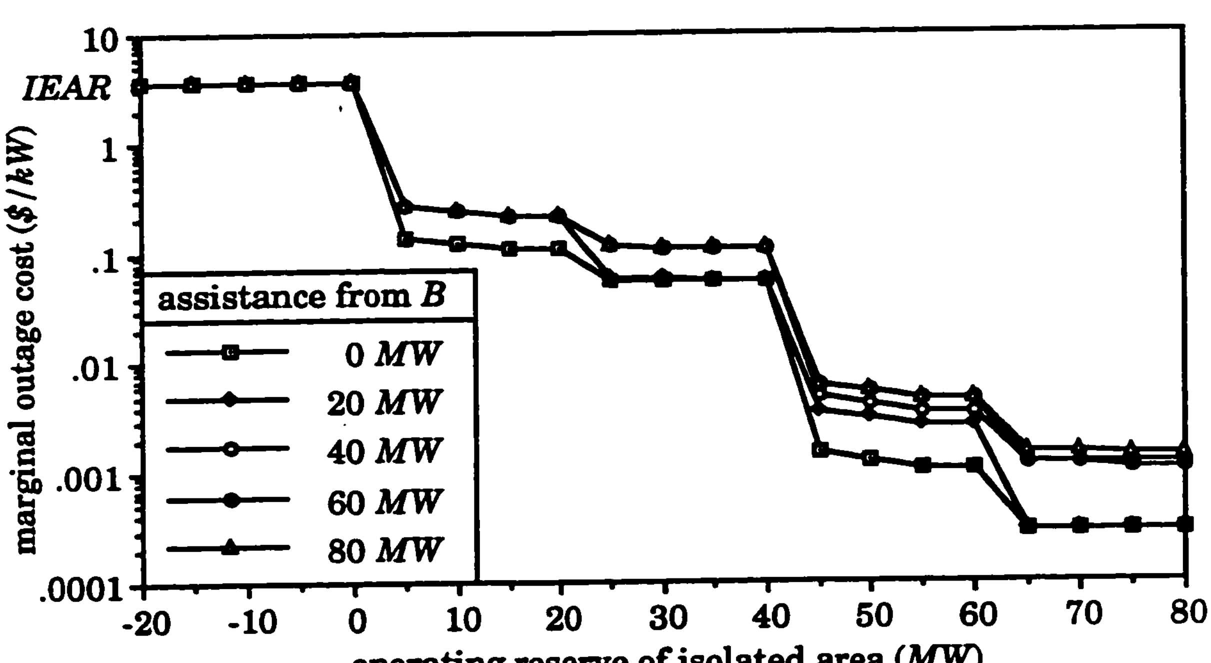

Figure 5.3. Effect of shifting the marginal outage cost profiles of the interconnected System *A* by amounts equal to the corresponding assistance levels available from System *B*.

It can be clearly seen from Figure 5.3 that there are considerable differences in the shapes of the shifted profiles and therefore it is not recommended to use this approximate method to derive accurate estimates of the marginal outage costs in interconnected generating systems. However, this procedure provides a quick means of approximating these costs without performing any interconnected generating system reliability studies.

The variations of the marginal outage cost of the interconnected System *A* with both the operating reserve and the assistance available from System *B* can be highlighted using a three-dimensional surface plot as shown in Figure 5.4. It can be seen from this figure that the marginal outage cost of System *A* is equal to the *IEAR* when the sum of its isolated operating reserve and the assistance available from System *B* is less than or equal to zero and decreases as the operating reserve, the assistance from System *B* or both increase.

5.4. Application to Two Areas Within a Single Generating System

The main objective of electricity spot pricing is to offer customers prices that vary over time and space [12]. Variation of the spot price over time can be calculated using suitable lead times [61]. Variation over space, however, requires the evaluation of spot prices at customer load points. This analysis is generally time consuming and requires the application of composite system reliability concepts as will be discussed in Chapter 6 of this thesis. Some form of variation over space can be achieved at *HLI* by calculating the spot prices in geographical areas within the same system.

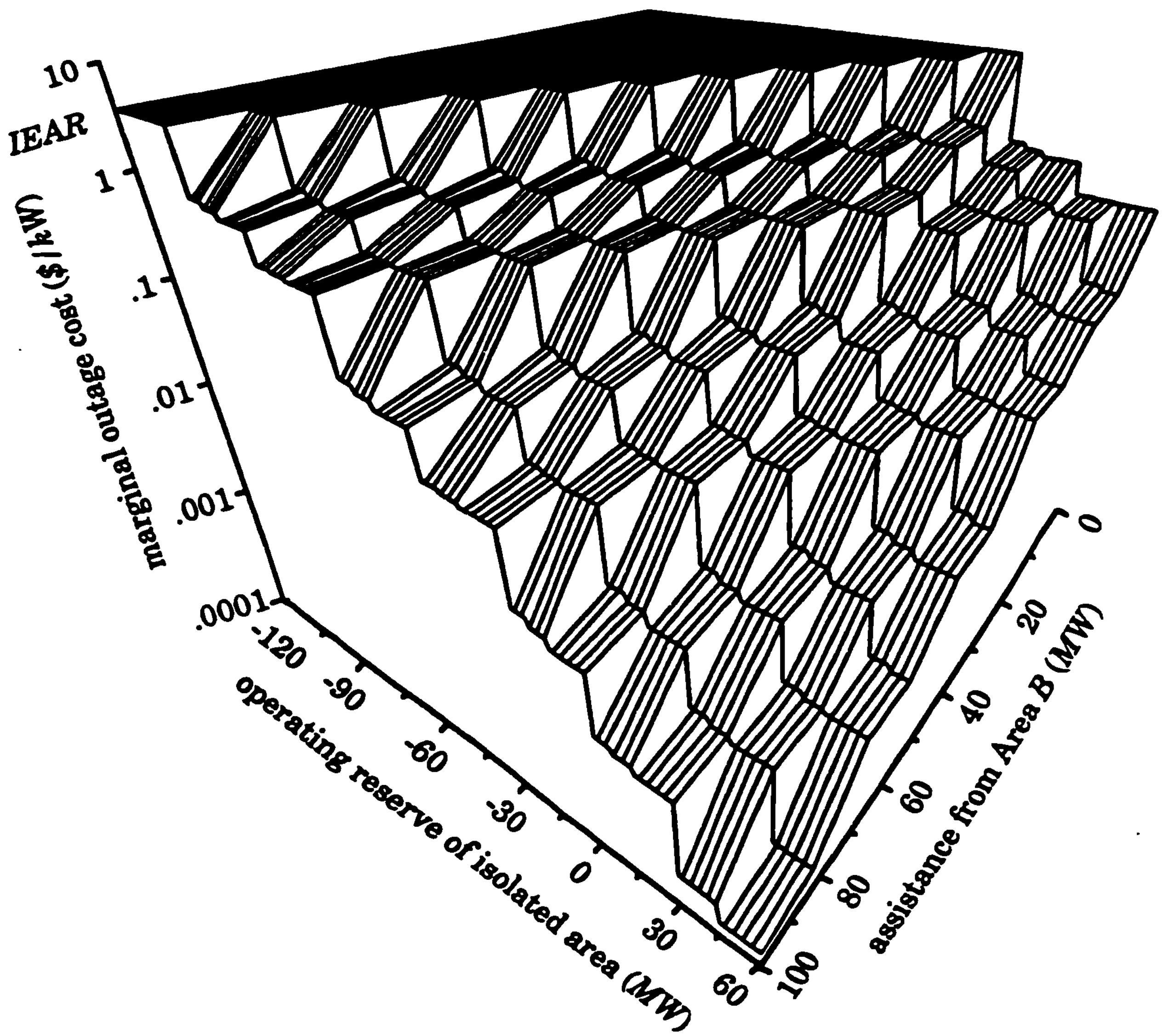

Figure 5.4. Variation of the marginal outage cost of the interconnected System A as a function of its operating reserve and the assistance available from System B.

The purpose of this section is to show that the method developed for interconnected generating systems can also be used to calculate the marginal outage costs of two areas within the same system. In order to show this, the *IEEE-RTS* is used because it can be easily divided into two distinct areas that correspond to the voltage levels and the geographic locations of generation and transmission facilities [36]. These areas are designated as the *NORTH (230 kV)* and *SOUTH (138 kV)* areas respectively. The total generation in the *NORTH* area is 2721 *MW* with a peak load of 1519 *MW* resulting in a surplus of 1202 *MW*. The *SOUTH* area, on the other hand, has a total generation of 684 *MW* and a peak load of 1331 *MW* resulting in a deficiency of 647 *MW*. The two areas are interconnected by a number of transmission lines of sufficient transfer capability to allow assistance to be transferred from the *NORTH* to the *SOUTH* area. A schematic representation of the two areas is shown in Figure 5.5.

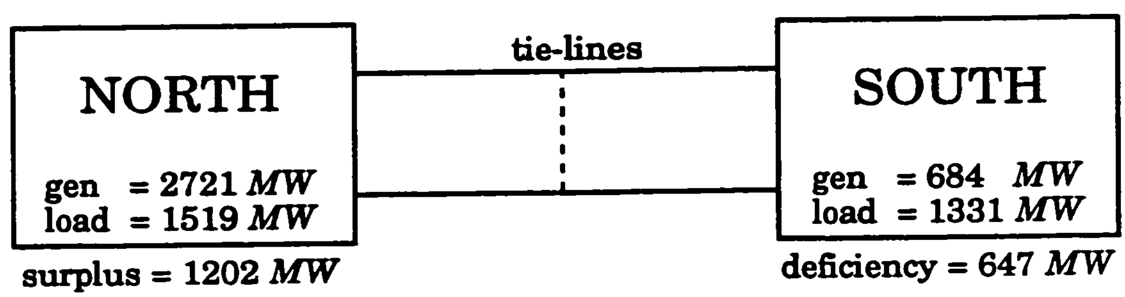

Figure 5.5. Two-area representation of the *IEEE-RTS*.

Since the *SOUTH* area is reserve deficient on an isolated basis, the marginal outage cost at the peak load is equal to the *IEAR* of the area. For the purposes of this study, the *IEAR* of the *SOUTH* area is assumed to be 3.13 $\$/kWh$ and the lead time is set at 10 hours. The object of this study is to show the impact of the assistance from the *NORTH* area on the marginal outage cost profile of the *SOUTH* area assuming a perfect tie-line with infinite carrying capability. The results from this study are shown in Figure 5.6. As in the case of the two interconnected *RBTS* systems, it can be observed from this figure that as the assistance available from the *NORTH* area increases, the marginal outage cost profile of the interconnected *SOUTH* area shifts to the left by a corresponding amount. The assistance levels of 300 and 600 *MW* are not large enough to reduce the marginal outage cost of the *SOUTH* area at the peak load below the *IEAR* value. However, when the assistance is equal to 900 *MW*, the marginal outage cost at the peak load decreases to a value well below the *IEAR* value. In fact, any assistance level larger than 647 *MW* will reduce the marginal outage cost of the *SOUTH* area at the peak load point below the *IEAR* value.

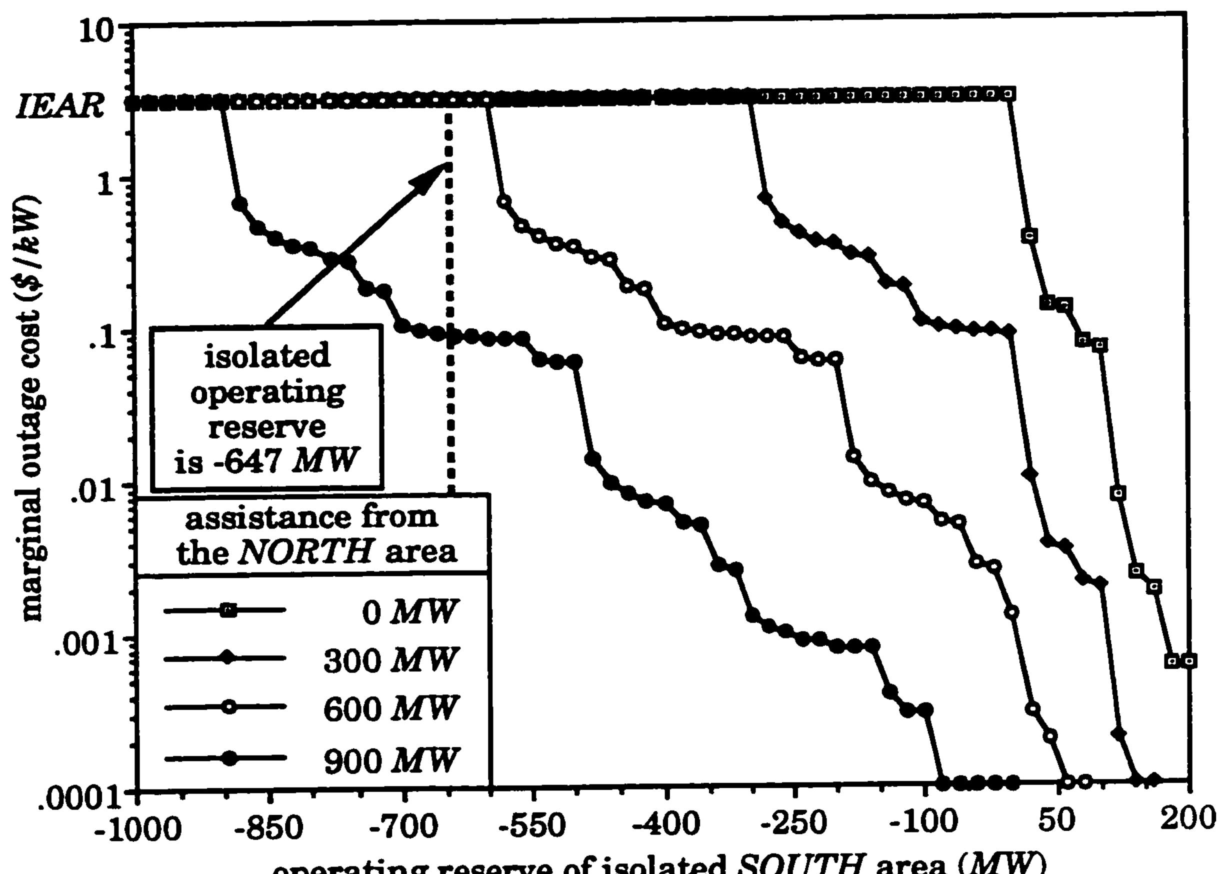

Figure 5.6. Marginal outage cost profile of the *SOUTH* area in the *IEEE-RTS* as a function of its isolated operating reserve for selected assistance levels.

5.5. Factors Affecting the Marginal Outage Cost in Interconnected Generating Systems

The two generating systems examined in Section 5.3 were assumed to be interconnected by a single perfect tie-line with infinite capacity. This section examines the effects on the marginal outage cost of the assisted system of selected modifications to these assumptions. The individual impact of each modelling assumption is illustrated using two interconnected *RBTS* systems as shown in Figure 5.1. The lead time used in all the studies reported in this section is 10 hours. The purpose of the studies conducted in this section is to compare the results from detailed reliability models to those reported in Section 5.3 of this chapter.

5.5.1. Effect of tie-line capacity

There are two basic factors determining the extent of the interconnection assistance from one system to the other. They are the operating reserve in the assisting system and the tie-line transfer capability. In addition, the reserve sharing policy between the two systems is essential in determining the extent of the assistance available from each system. The operating reserve in the assisting system determines the assistance available. The effect of varying this assistance was studied in Section 5.3. This section is concerned with the impact of tie-line capacity on the marginal outage cost profile of the assisted system.

The effect of tie-line capacity on the marginal outage cost of System *A* is illustrated by varying the capacity from 0 to 80 *MW* in steps of 20 *MW*. The assistance available from System *B* is assumed to be 55 *MW*, the tie-lines are assumed to be fully reliable and the results are shown in Figure 5.7. It can be seen from this figure that the marginal outage cost profile of System *A* decreases as the capacity of the tie-line increases. The marginal outage cost profile of System *A* converges to a limiting value which represents the minimum profile that System *A* can attain under these conditions. The marginal outage cost profile at this point is designated as the "infinite tie capacity profile" as there will be no further decrease in the marginal outage cost with the addition of further tie capacity. The infinite tie capacity value is directly related to the assistance level available from System *B*. This is easily seen in this example since any tie capacity greater than 55 *MW* does not contribute significantly to the reduction of the marginal outage costs in System *A*.

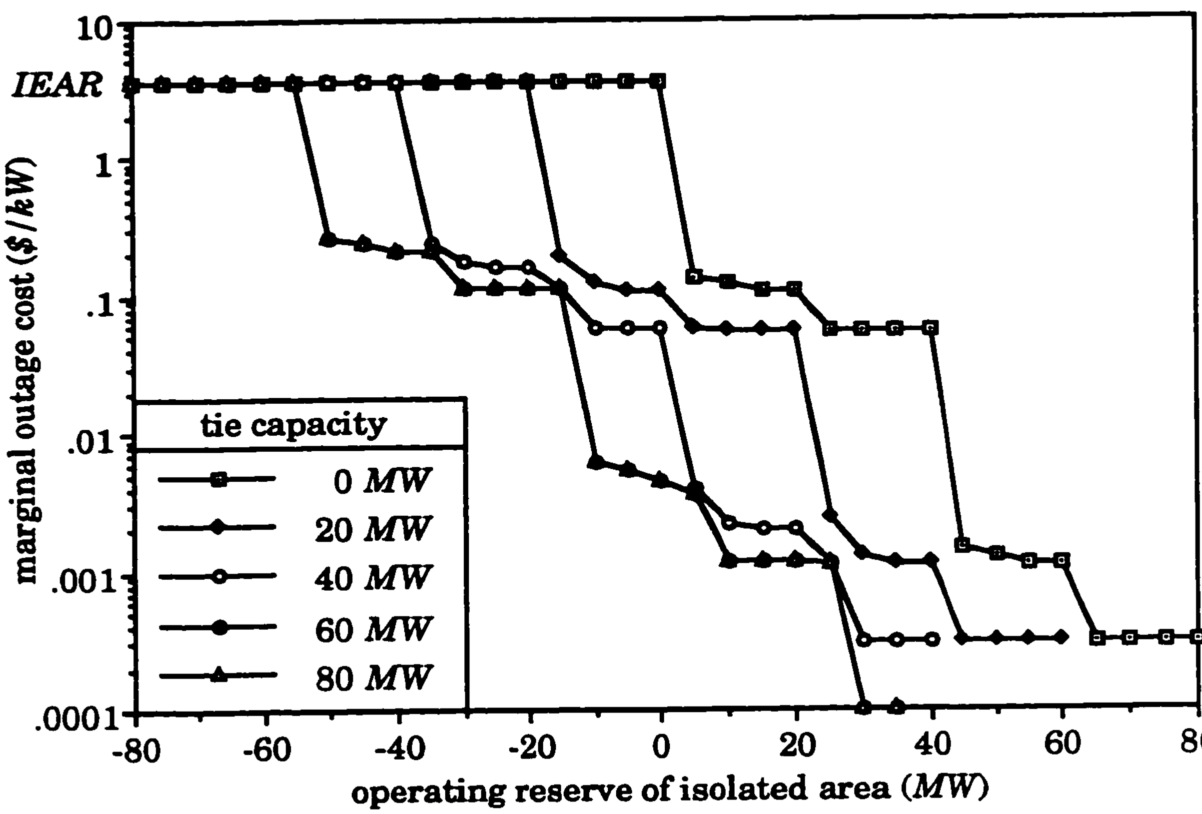

Figure 5.7. Effect of tie-line capacity on the marginal outage cost profile of System *A*.

5.5.2. Effect of tie-line reliability

Systems may be interconnected by several tie-lines, each of which has an availability that is less than unity [26,119]. The various tie-line capacity states impose capacity limits on the assistance available through the interconnections. This effect can be evaluated by convolving the capacity states of the tie-lines with those of the equivalent assisting unit obtained from the assisting system. The output model of the combination will effectively represent a tie-line constrained multi-state generating unit of the assisting system. This equivalent unit can then be added to the existing capacity model of the assisted system.

Consider the case in which there is only one tie-line interconnecting Systems A and B and having the basic reliability data given in Table 5.1. These data are used together with an assistance level from System B of 55 MW to show the impact of tie-line reliability on the marginal outage cost profile of System A. The results from this study are compared to those obtained using a perfect tie-line (i.e. FOR = 0.0) in Figure 5.8. It can be clearly seen from this figure that the reliability of the tie-line has a negligible effect on the marginal outage cost for most operating reserve levels. This is due to the fact that, in general, tie-lines and transmission lines have smaller forced outage rates than generating units [119].

Table 5.1. Basic reliability data of the tie-line.

tie-line capacity (MW)	forced outage rate (FOR)	failure rate $\lambda\,(f/yr)$	repair rate $\mu\,(r/yr)$
30	0.001	1	999
30	0.005	5	995
30	0.010	10	990

5.5.3. Effect of the number of tie-lines

The assumption that interconnected generating systems are linked with only one tie-line may not be valid in large practical systems. If the systems are interconnected by more than one tie-line and the tie-lines are perfectly reliable, then they may be considered equivalent to one tie-line with a capacity equal to the sum of the capacities of all the tie-lines. If the tie-lines are not perfectly reliable, however, the approach must be modified.

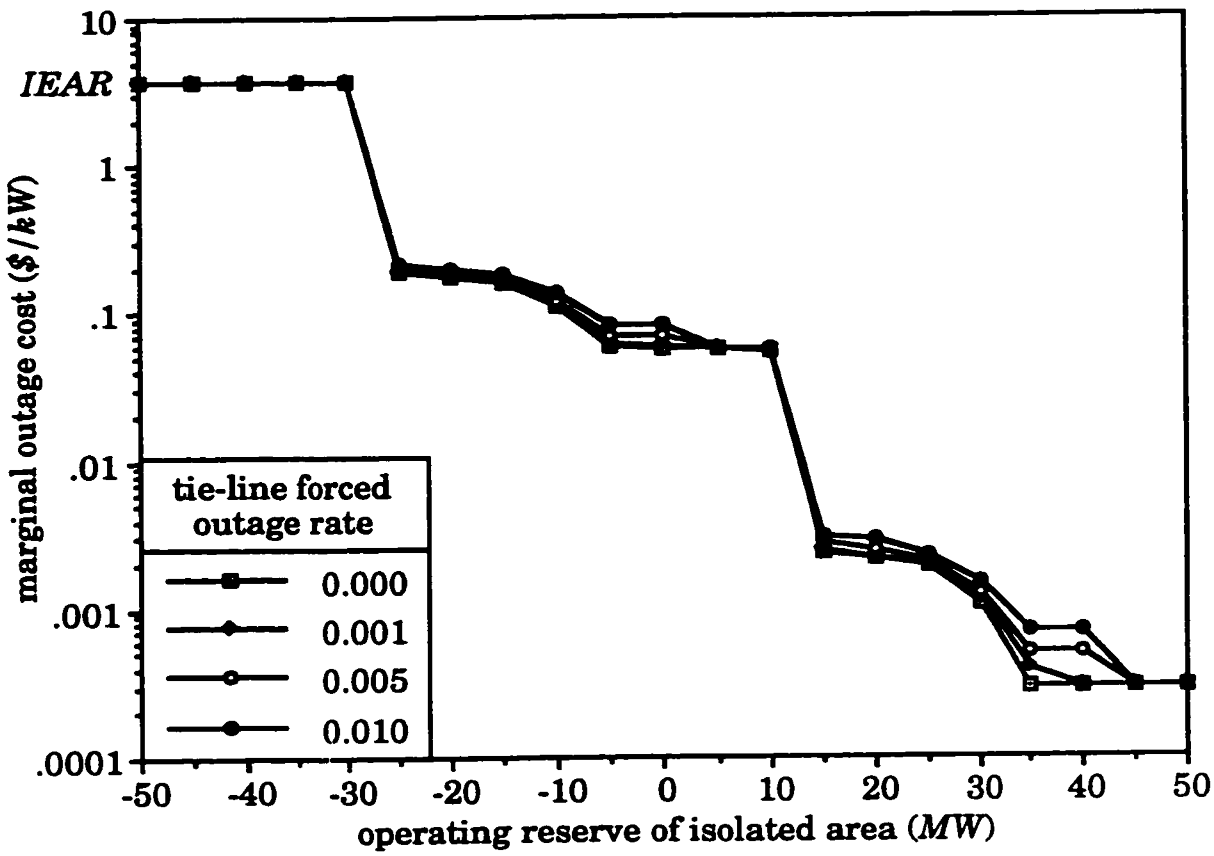

Figure 5.8. Effect of the tie-line reliability on the marginal outage cost profile of System *A*.

Consider the case in which the interconnection between Systems *A* and *B* consists of two or three identical tie-lines having a total carrying capability of 30 *MW* (i.e. two 15 *MW* or three 10 *MW* tie-lines). The failure and repair rates of each tie-line are assumed to be 5 (f/yr) and 995 (r/yr) respectively. In order to estimate the marginal outage cost at short lead times, the transition rates associated with the equivalent model of transmission facilities must be calculated. This can be accomplished using a basic Frequency and Duration (*F&D*) technique [26]. The equivalent models of the two 15 *MW* tie-lines and the three 10 *MW* tie-lines are given in Table 5.2. The upward and downward departure rates represent the transition rates to lower outage and higher outage states respectively.

Table 5.2. Equivalent models of two 15 *MW* and three 10 *MW* tie-lines.

state	capacity outage (*MW*)	state probability	upward departure rate	downward departure rate
equivalent model of two 15 *MW* tie-lines				
1	0	0.990025	0	10
2	15	0.009950	995	5
3	30	0.000025	1990	0
equivalent model of three 10 *MW* tie-lines				
1	0	0.98507488	0	15
2	10	0.01485037	995	10
3	20	0.00007463	1990	5
4	30	0.00000012	2985	0

The effect of tie-line constraints can be included in the calculation of the marginal outage cost by combining the capacity outage states of both the equivalent assisting unit and the equivalent multi-state tie-line models given in Table 5.2. The resulting tie-line constrained model of capacity assistance is used in this section to study the effect of the number of tie-lines on the marginal outage cost profile of System A using an assistance level of 55 *MW* from System *B*. The results from this study are compared to the single tie-line *(1*30 MW)* scenario in Figure 5.9. It is clear from this figure that the number of tie-lines has a very negligible effect on the marginal outage cost of System *A*.

The studies conducted in the previous sub-sections show that the marginal outage costs associated with two interconnected generating systems are only slightly affected by the number of tie-lines connecting the two systems and their reliabilities. Therefore, it can be concluded that, for the purposes of calculating the marginal outage cost in two interconnected generating systems, tie-lines can be represented by their transfer capability. The slight variations associated with small marginal outage cost values can be neglected as they do not contribute significantly to the overall spot price of electricity. This conclusion is based on studies conducted using the *RBTS* which is a small reliability test system designed for educational purposes. Additional studies conducted using the *IEEE-RTS* which is a more practical test system have resulted in the same conclusions. The validity of these conclusions will have to be tested however using practical systems before actual use.

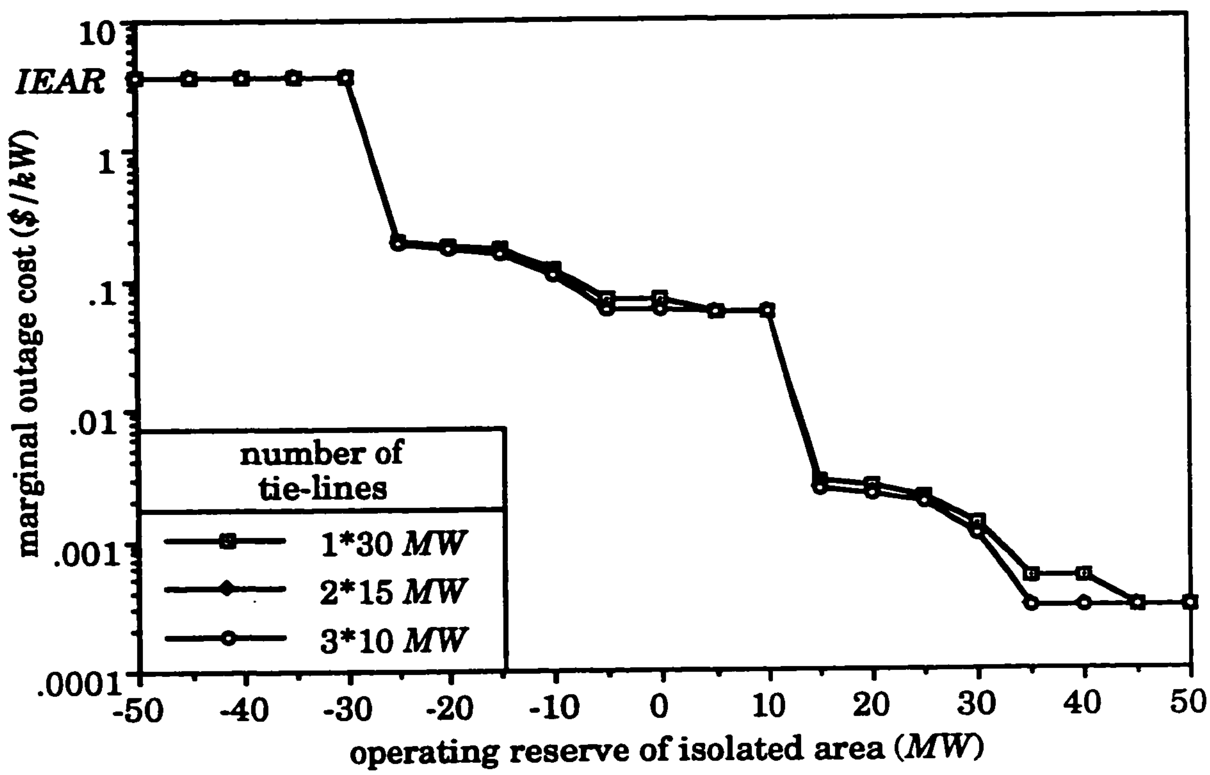

Figure 5.9. Effect of the number of tie-lines on the marginal outage cost profile of System *A*.

5.5.4. Effect of tie capacity uncertainty

In the previous sub-sections, it was assumed that the capacity of the tie-line is fixed. This may not be the case in practice due to changing transmission and other conditions in the two interconnected systems. The random variation in tie capacity can be represented by a discrete or continuous probability distribution. The conditional probability rule [26] used to incorporate load forecast uncertainty in the analysis of single generating systems can also be utilized in this case. The concepts involved in applying the conditional probability rule are outlined in Sub-section 3.3.3 of this thesis.

Consider the case in which the tie-line linking Systems A and B is fully reliable and has a capacity that can be described by a normal distribution with a mean of 30 MW and a standard deviation of 3%, 5% or 7%. This distribution can be approximated by seven discrete steps each corresponding to a different tie capacity as described in Sub-section 3.3.3. The marginal outage cost is computed for each tie capacity and multiplied by the probability of existence of that tie capacity. The sum of these weighted products represents the expected marginal outage cost for the forecast tie capacity. The results from these computations are compared to the base case (i.e. no tie capacity uncertainty) in Figure 5.10 for an assistance level of 55 MW from System B. It can be seen from this figure that the marginal outage cost is largely unaffected by the tie capacity uncertainty. This is due to the small size of the tie-line as compared to the installed capacity of the system (e.g. when the standard deviation is 7%, the maximum deviation of the tie capacity is 6.3 MW). It is expected, however, that the effect of the tie capacity uncertainty will be more significant for larger systems with bigger tie-lines. The inclusion of the tie capacity uncertainty in the calculation of the marginal outage cost also has a smoothing effect on the profile. This is very evident at the largest discrete steps of the original (i.e. standard deviation of 0%) profile.

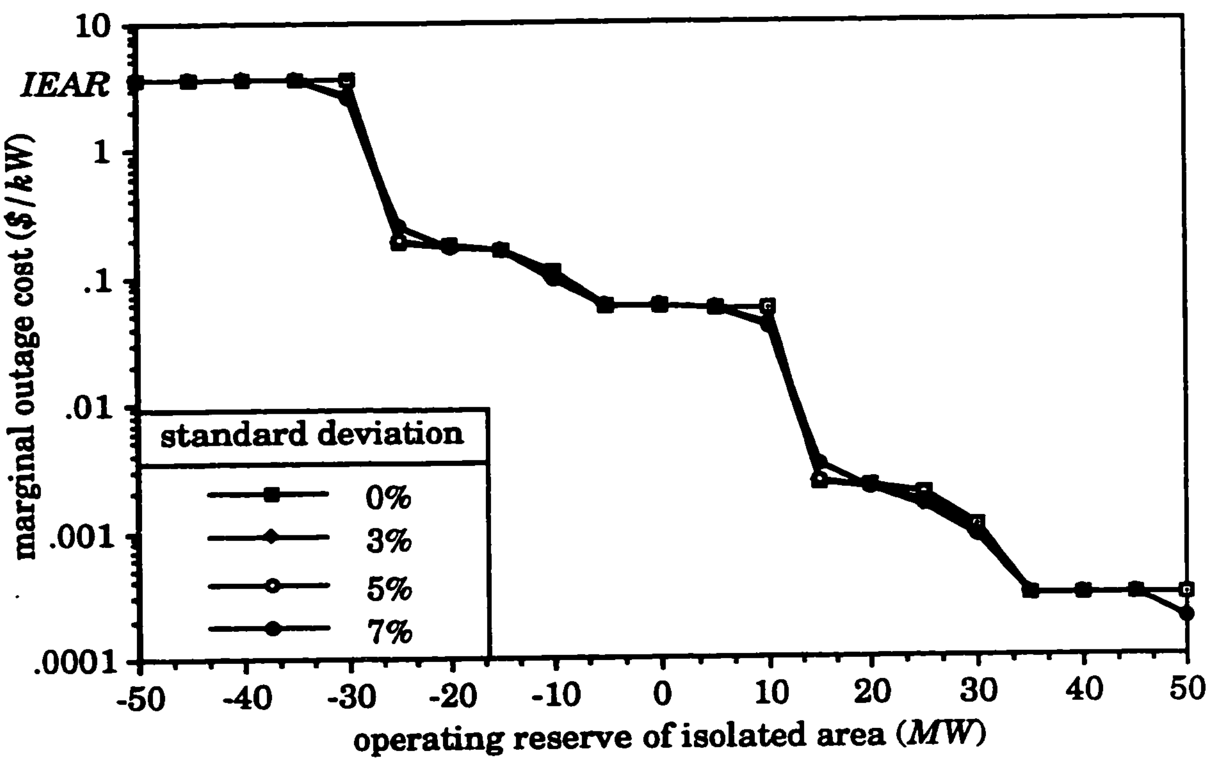

Figure 5.10. Effect of tie capacity uncertainty on the marginal outage cost profile of System A.

5.5.5. Effect of load forecast uncertainty

The Load Forecast Uncertainty (LFU) can be included in the calculation of the marginal outage costs in interconnected generating systems using a procedure similar to that employed in single generating systems [26]. The impact of the load forecast uncertainty on the marginal outage costs in interconnected generating systems depends on its existence in the assisted system, the assisting system or both. The following sub-sections present the results of three separate studies that measure the impact of load forecast uncertainty on the marginal outage costs.

5.5.5.1. Load forecast uncertainty in the assisted system

When load forecast uncertainty is present in the assisted system, the marginal outage cost is calculated using the same concept of conditional probability discussed in Sub-section 3.3.3. This concept is illustrated in this sub-section by examining the effect of load forecast uncertainty in the assisted system (System *A*) on its marginal outage cost profile. The distribution of load forecast uncertainty is approximated by a seven-step normal distribution with a standard deviation of 3%, 5% or 7%, The assistance available from System *B* is assumed to be 55 *MW* and the tie-line is assumed to be fully reliable with a capacity of 30 *MW*. The results from this study are compared to the base case (i.e. *s.d.* = 0%) in Figure 5.11. It is clear from this figure that, as in the case of single generating systems, the marginal outage cost generally increases as the standard deviation increases. Therefore, it is important to incorporate load forecast uncertainty in practical system studies.

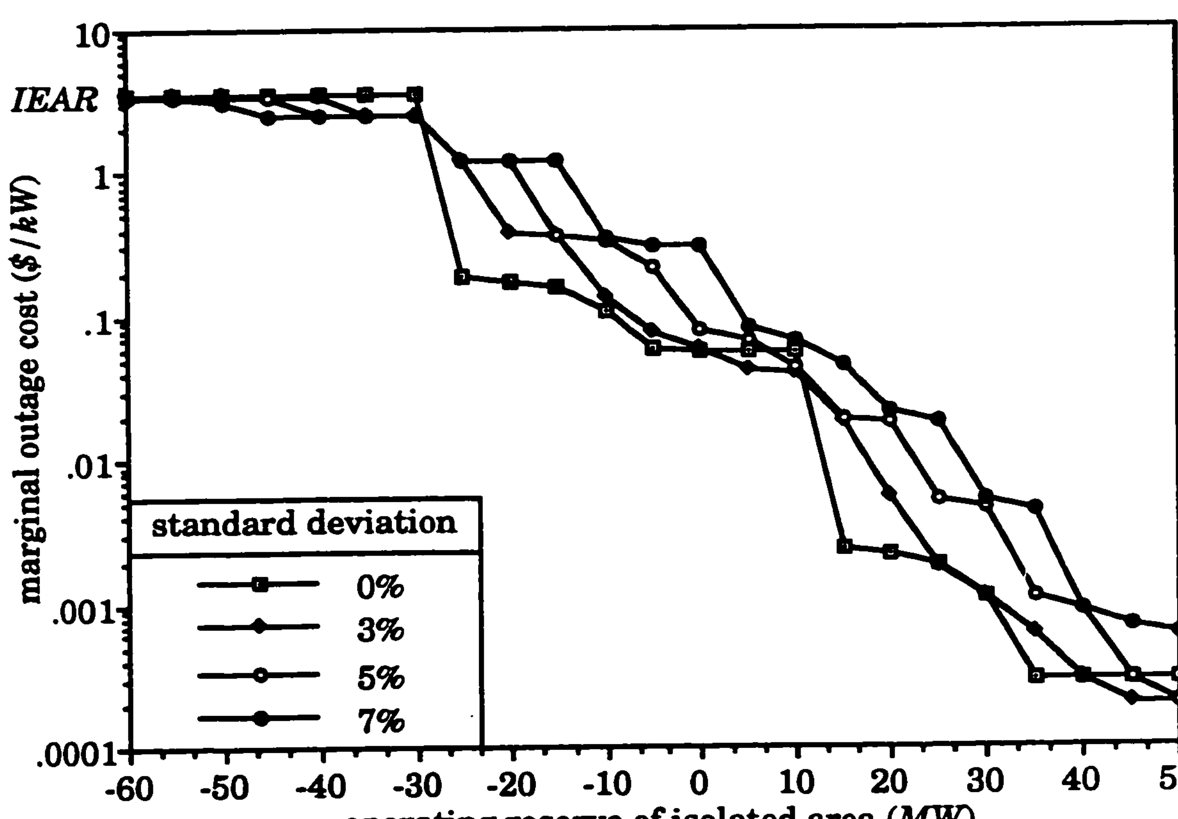

Figure 5.11. Effect of load forecast uncertainty in the assisted system on the marginal outage cost profile of System *A*.

5.5.5.2. Load forecast uncertainty in the assisting system

The inclusion of load forecast uncertainty in the assisting system affects the assistance available to the assisted system. A flowchart of the algorithm used to incorporate load forecast uncertainty of the assisting system in the analysis is shown in Figure 5.12. The process begins by choosing a load level for the assisting system from the distribution of load forecast uncertainty. This load level is used to determine the assistance available and calculate the equivalent assisting unit to be added to the capacity model of the assisted system. The new capacity model of the assisted system is used to calculate the marginal outage cost that corresponds to the calculated assistance level and the process is repeated for each load level in the distribution. The expected marginal outage cost is the sum of the weighted products of the marginal outage cost at each assistance level and the probability of existence of that assistance level.

Using the algorithm shown in Figure 5.12, the marginal outage cost profile of System A was calculated assuming that the assisting system (System B) has a load forecast uncertainty with a mean of 185 MW (assistance of 55 MW) and a standard deviation of 3%, 5% or 7%. The tie-line was assumed to be fully reliable with a capacity of 30 MW. The results are compared to the base case in Figure 5.13. It can be seen from this figure that the effect of load forecast uncertainty in the assisting system is negligible mainly because the large variations in the assistance level are trapped by the relatively small capacity of the tie-line.

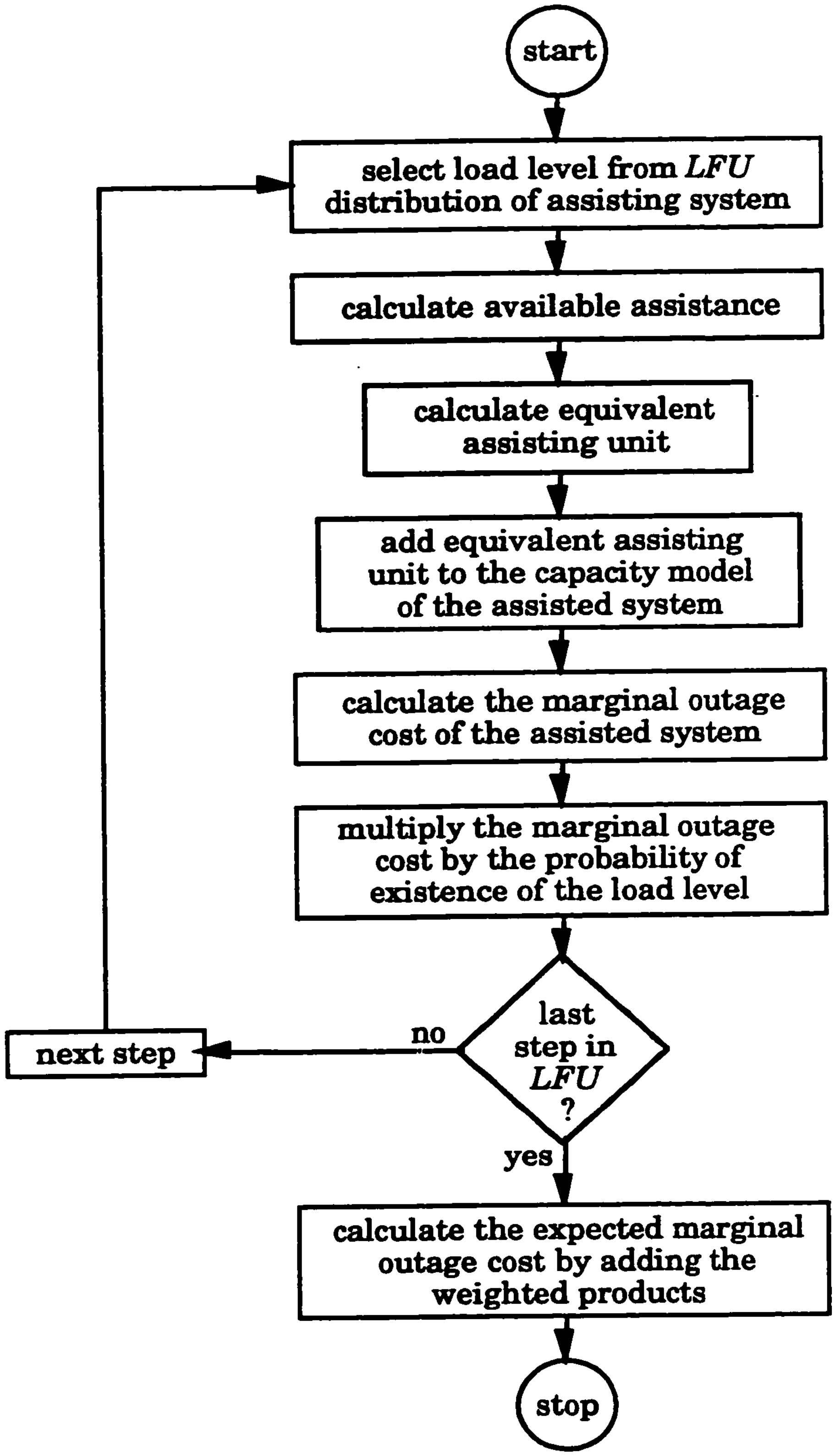

Figure 5.12. Algorithm for incorporating the load forecast uncertainty of the assisting system in the calculation of the marginal outage cost.

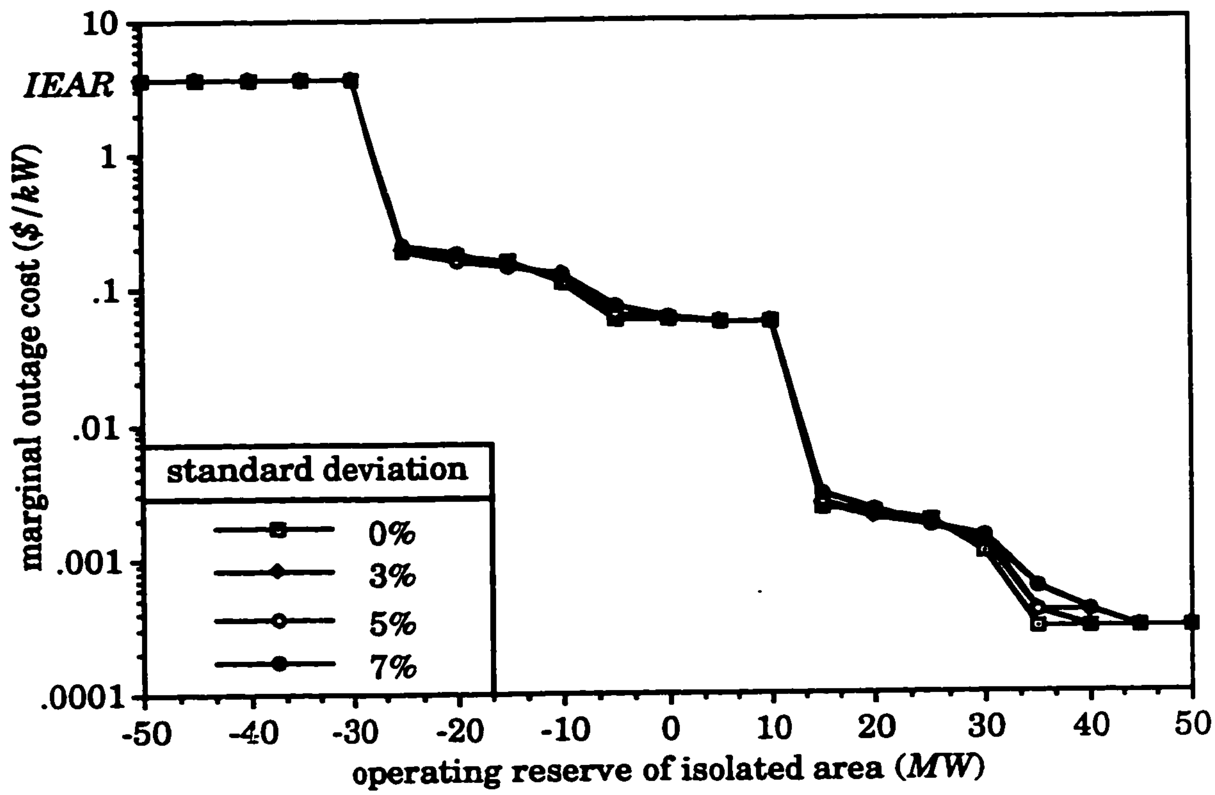

Figure 5.13. Effect of load forecast uncertainty in the assisting system on the marginal outage cost profile of System *A* for a tie capacity of 30 *MW*.

The effect on the marginal outage cost in the assisted system of load forecast uncertainty in the assisting system may become more prominent if the capacity of the tie-line is increased. This scenario was tested by increasing the capacity of the tie-line to a very large value and calculating the marginal outage costs in the assisted system using the same basic assumptions as above. The results from this study which are shown in Figure 5.14 indicate that the effect of load forecast uncertainty of the assisting system is quite significant when the capacity of the tie-line is large. Therefore, it can be concluded from these two studies that the effect of load forecast uncertainty in the assisting system depends not only on the standard deviation of the distribution but also on the capacity of the tie-line linking the two systems.

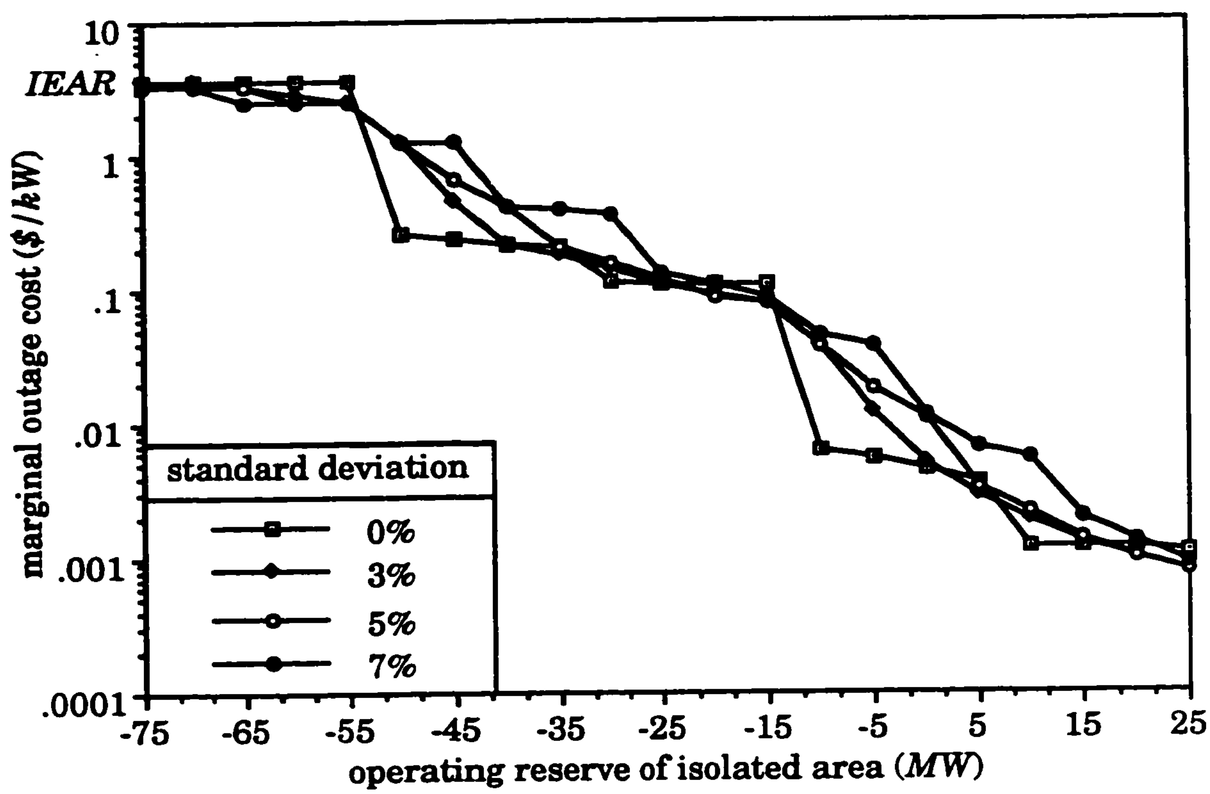

Figure 5.14. Effect of load forecast uncertainty in the assisting system on the marginal outage cost profile of the System *A* for an infinite tie capacity.

5.5.5.3. Load forecast uncertainty in both the assisted and the assisting systems

The impact of having load forecast uncertainty in both the assisted and the assisting systems can be incorporated in the marginal outage cost analysis using the two methods described in the previous sub-sections. The resulting marginal outage cost will vary with the characteristics of the load forecast uncertainty distributions and the capacity of the tie-line linking the two systems. In order to show these variations, a study was done using the two interconnected *RBTS* systems. The mean value of the assistance from System *B* was set at 55 *MW* and the tie-line was assumed to be fully reliable with a capacity of 30 *MW*. The results from this study are shown in Figure 5.15. It can be seen from this figure that the marginal outage cost profiles are similar to those shown in Figure 5.11 because the contribution of the load forecast uncertainty in the assisting system is blocked by the finite capability of the tie-line. As stated in Sub-section 5.5.5.2, a higher tie capacity will make the contribution of load forecast uncertainty in the assisting system more significant.

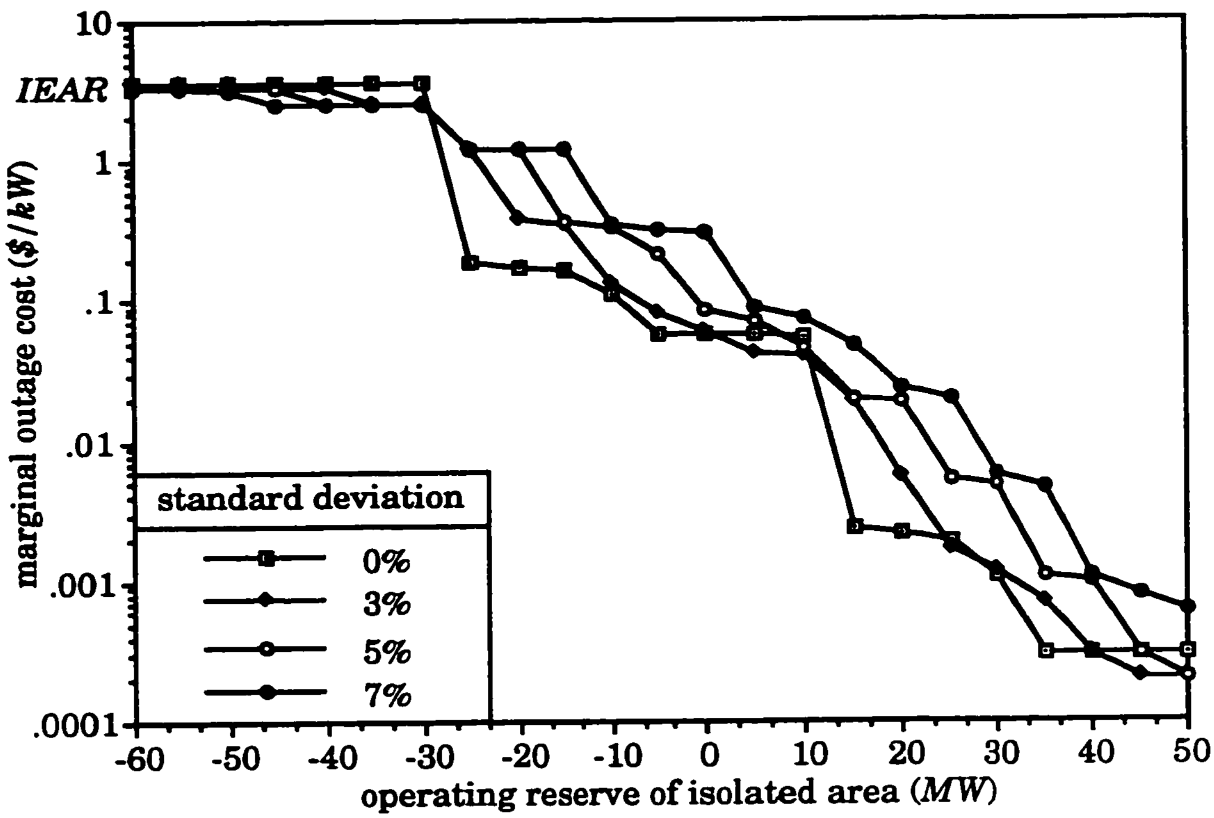

Figure 5.15. Effect of load forecast uncertainty in both the assisted and the assisting systems on the marginal outage cost profile of System *A*.

The interconnected system studies conducted in Sub-sections 5.5.4 and 5.5.5 show that tie capacity uncertainty and load forecast uncertainty in either or both systems have significant impacts on the marginal outage costs associated with two interconnected generating systems. Therefore, it is important to include these modelling considerations in the analysis given the supporting data.

5.6. Application to More Than Two Interconnected Generating Systems

The evaluation of the marginal outage cost involving any type of agreement can be performed for two systems. In many cases, individual probabilities of various events will have to be considered and the computations may increase considerably. The computations will become very involved for multi-system configurations [26,109]. For more than two systems, the assumption is made that if one system is interconnected with several other systems, it can be assisted to the maximum extent by all the systems. In the case of simultaneous outages in several systems, if alternate paths of routing the assistance are available, only the system under consideration will be helped. The actual interconnection agreements dictate the priority conditions in practical systems.

The method used to determine the equivalent assisting units of a number of interconnected generating systems and their impacts on the marginal outage costs of the systems are presented in the following sub-sections. The procedure used to calculate the equivalent assisting unit model for each generating system will be described using the following notation [112]:

S_e = equivalent generation model of System S after incorporation of assistance from other systems,

S_a = equivalent assisting unit of System S,

T_e = $S_a \rightarrow T = S_a + T$,
= equivalent generation model of System T after assistance from System S has been incorporated into it,

$(S_a \rightarrow T)_a$ = $(S_a + T)_a$,
= equivalent assisting unit of System T after assistance from System S has been incorporated into it, and

R_e $= S_a + T_a + R,$
= equivalent assisting units from systems S and T are added to System R.

5.6.1. Three radial systems

Consider three systems A, B and C interconnected by two tie-lines as shown in Figure 5.16. The calculation of the assistance for System B is performed in a slightly different manner than for Systems A and C.

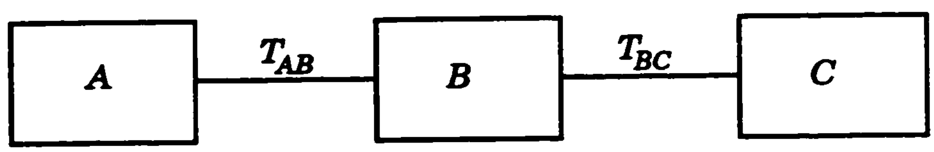

Figure 5.16. Three radially interconnected generating systems.

In the case of System B, both Systems A and C can assist independently and limited only by their respective tie-line capacities or operating reserves. The first step involves adding the equivalent assisting unit of System C as influenced by the availability of T_{BC} to the generation model of System B. The equivalent assisting unit of System A can then be added to this equivalent model after pushing it through T_{AB}. The resulting model is not dependent upon the order of adding the equivalent assisting unit models for Systems A and C if no rounding is employed [26]. In case of rounding, the accuracy of the results will depend on the size of the system, the characteristics of the generating units and the rounding increment employed. In practical system studies, the rounding increment should be chosen in such a way that minimizes the computing time without significantly affecting the accuracy of the results.

In the case of Systems A and C, System B can directly assist them. In order that one of them may assist the other, however, the assistance will have to be routed through System B. Therefore, the assistance from System A to System C or vice versa will be influenced by the reserve margins in System B. The required results can be obtained by adding the equivalent assisting unit model of System C or A to the generation system model of System B. This equivalent generation model is then used to form an equivalent assisting unit of System B which is added to the generation system model of System A or System C. In summary, the procedure used for calculating the equivalent generation model of each area in the system can be expressed by the following equations,

$$\begin{aligned} A_e &= (C_a \rightarrow B)_a + A, \\ B_e &= C_a + A_a + B \text{ and} \\ C_e &= (A_a \rightarrow B)_a + C. \end{aligned} \tag{5.1}$$

The application of the proposed methodology for calculating the marginal outage costs in radially interconnected generating systems is illustrated in this section by considering the three systems shown in Figure 5.16. The purpose of this study is to show the impact of interconnection topology on the marginal outage cost of each system. The generation models of all three systems are assumed to be equal to that of the $RBTS$. The capacities of tie-lines T_{AB} and T_{BC} are assumed to be 30 MW and 70 MW respectively. The assistance available from Systems A, B and C are 55 MW, 40 MW and 20 MW respectively. The marginal outage cost profile of each system in the network was calculated as a function of its isolated operating reserve and the results are compared in Figure 5.17. It can be seen from this figure that the marginal outage cost profile of System C benefits the most from the available interconnections. System A, on the other hand, does not benefit greatly from this interconnection configuration because the assistance levels available from Systems C and B are constrained by the finite capacity of T_{AB}.

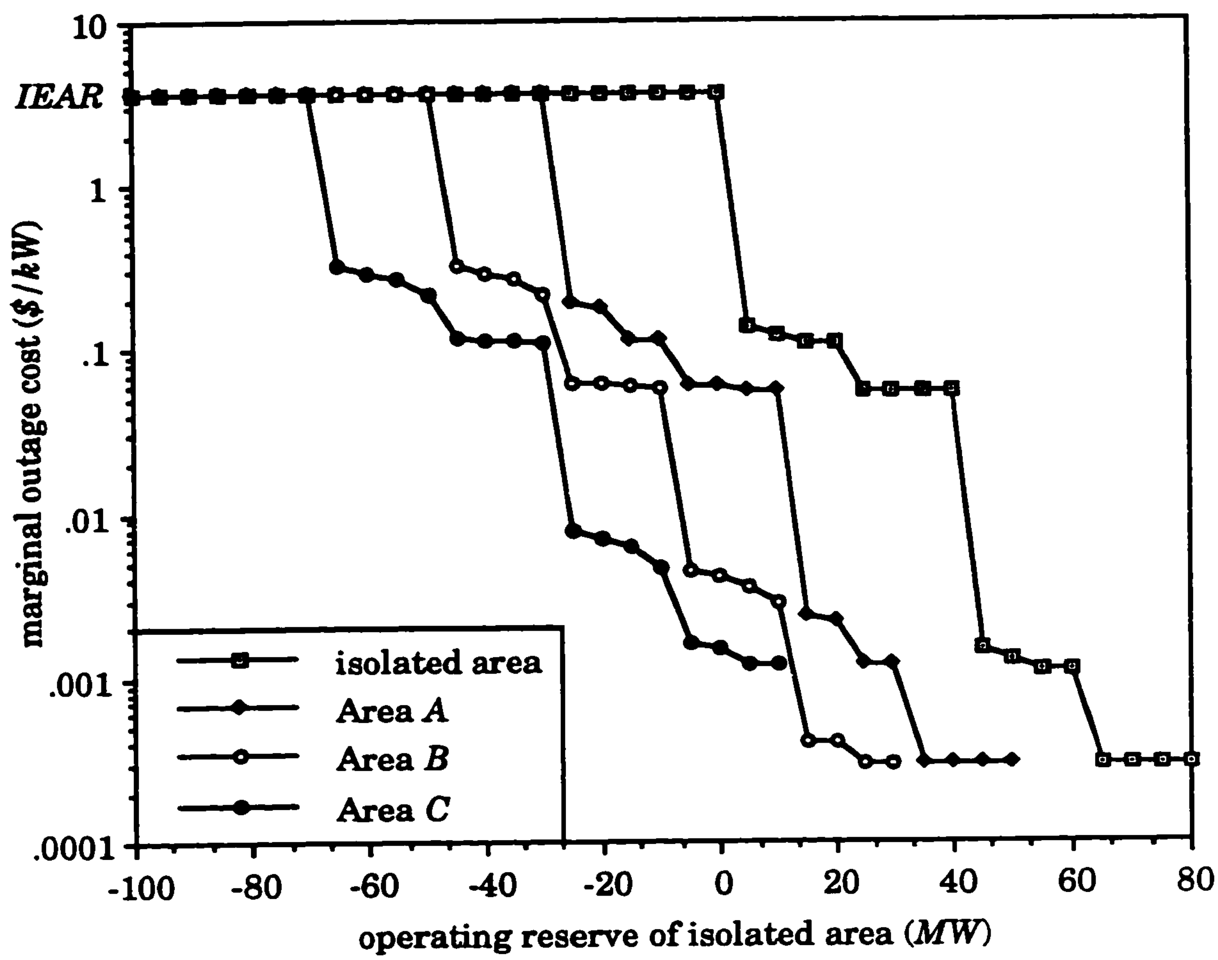

Figure 5.17. Marginal outage cost profiles of three radially interconnected *RBTS* systems.

5.6.2. More than three radial systems

The approach outlined in the previous section can be readily applied to any number of radially interconnected generating systems. Consider the four systems interconnected in a tree-type configuration and shown in Figure 5.18.

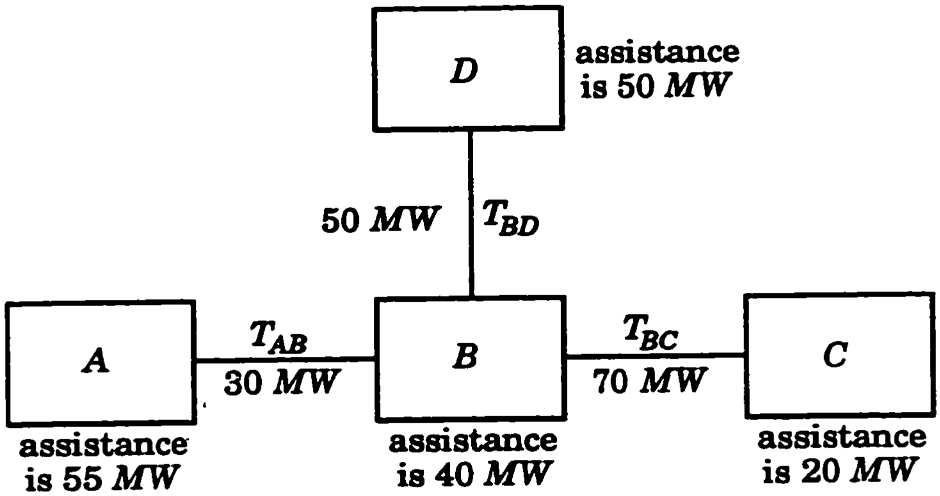

Figure 5.18. Four radially interconnected generating systems.

The equivalent generation model of each area in the system can be expressed by (5.2) using the notation outlined earlier,

$$\begin{aligned} A_e &= (C_a + D_a + B)_a + A, \\ B_e &= A_a + D_a + C_a + B, \\ C_e &= (A_a + D_a + B)_a + C \text{ and} \\ D_e &= (A_a + C_a + B)_a + D. \end{aligned} \tag{5.2}$$

Assuming that the generating models of the systems shown in Figure 5.18 are identical to that of the *RBTS*, the marginal outage cost profile of each system was calculated and is compared to the isolated system profile in Figure 5.19. It can be seen from this figure that System *B* has the lowest marginal outage cost because it receives the largest assistance (System *B* is assisted by the other three systems individually for a total assistance of 100 *MW*). The other systems, on the other hand, receive their assistance from a modified System *B* after it has been assisted itself by two systems. Therefore, it is very likely that the assistance available from the modified System *B* will be bottlenecked by the finite capacity of the tie-line.

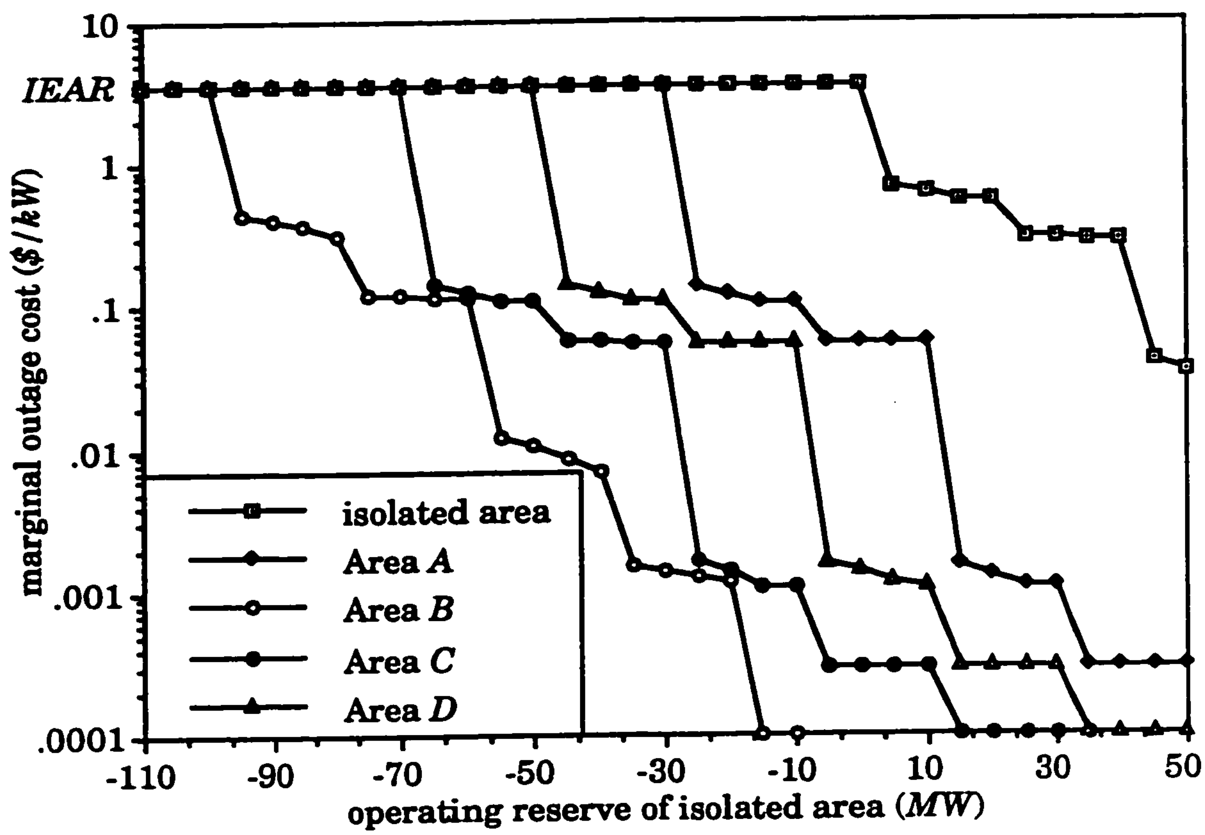

Figure 5.19. Marginal outage cost profiles of four radially interconnected *RBTS* systems.

5.6.3. Three generating systems interconnected in a ring fashion

The approach outlined in the previous section can be applied to any number of radially interconnected generating systems. The problems associated with systems which are interconnected in a mesh or non-radial configuration are quite complicated. The most obvious solution to the problem is a complete enumeration of all capacity outage and interconnection assistance levels. This approach is applicable to small simple systems but is not practical when applied to several large realistic systems. A better approach to use in such cases involves extending the methods developed for radially interconnected systems to find the marginal outage cost in meshed systems [112].

The basic configuration in multiple interconnected systems is a ring type one involving three systems as shown in Figure 5.20. Each system in this figure has two possible assistance paths. The effect of the second path is to release some capacity assistance otherwise locked in due to transmission inadequacy. When the directly connected tie-line can carry the entire available assistance, the other tie-line may not contribute significantly to the decrease in the marginal outage cost of the assisted system. This can be seen by considering the case in which System A is being assisted by System B. If the operating reserve in System B is less than T_{AB}, the entire assistance can be directed over the tie-line T_{AB}. The alternate path T_{BC} is also available but the assistance is dependent upon the availability of two series lines and modified by the limitations of lines T_{BC} and T_{CA}.

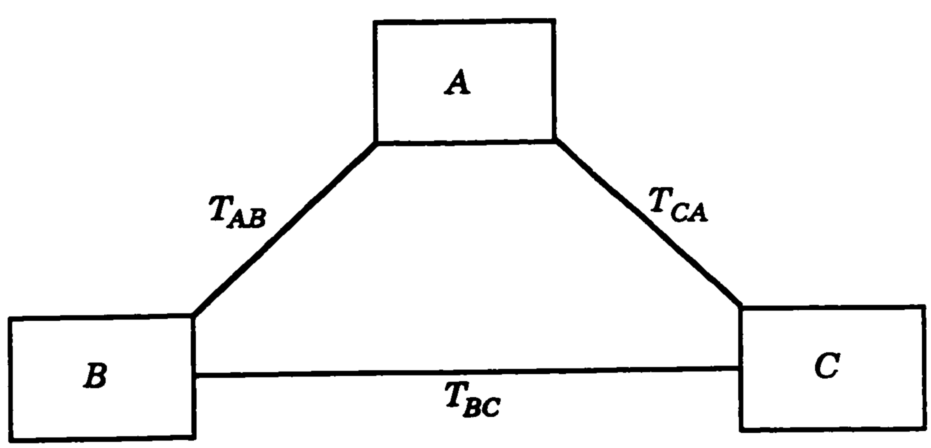

Figure 5.20. Three generating systems interconnected in a ring fashion.

This approach leads to a relatively simple algorithm which can be utilized to solve the ring type configuration of three interconnected systems assuming a given interconnection agreement. The following agreement is used in the studies reported in this sub-section:

1) all members assist with their positive margins only. That is, they assist if they have surplus generation,

2) members with positive margins assist other members with negative margins to the maximum extent,

3) assistance from a member with a positive margin to a member with a negative margin cannot be wheeled through a member which itself has a negative margin. That is, the assistance can be wheeled through a member only after that member's deficiency is satisfied, and

4) the assisting systems take a direct route in helping the assisted system.

The possible conditions existing in the three systems shown in Figure 5.20 can be represented by four cases which are detailed in [112]. In all four cases, System A is considered to be assisted by Systems B and C. The effect of wheeling on the marginal outage cost of a system can also be incorporated in the analysis using the proposed method. However, such an undertaking is beyond the scope of this thesis. Nevertheless, it is important to recognize that the marginal outage cost constitutes an important component of wheeling rates that are based on marginal-cost theory [120-123].

__*Case 1*__ *Operating reserves in both systems are less than their respective connecting tie-lines.*

If the operating reserve margins in Systems B and C are denoted by $OR_{(b)}$ and $OR_{(c)}$, the conditions for this case can be expressed by the following inequalities,

$$\begin{aligned} &OR_{(b)} \leq T_{AB} \text{ and} \\ &OR_{(c)} \leq T_{CA}. \end{aligned} \tag{5.3}$$

The effective assistance to System A from each of the two assisting systems is comprised of two parts. When the directly connected tie-line is available, it will be used for dispatching the assistance. When this line is unavailable, some assistance can be routed over the path T_{BC}. The negative reserves in the other assisting system affect the reliability of the assistance when it is routed over T_{BC}. The extent of the increase in assistance (i.e. decrease in marginal outage cost) due to the presence of tie-line T_{BC} depends upon the reliability of the tie-line and the operating reserves in Systems B and C.

Three $RBTS$ systems A, B and C interconnected in a loop were used for these studies. The assistance available from Systems B and C is 30 MW and 50 MW respectively. The transfer capabilities of T_{AB}, T_{BC} and T_{CA} are considered to be 40 MW, 40 MW and 50 MW respectively. The impact of the additional link T_{BC} on the marginal outage cost of the assisted system was studied first and the results are shown in Figure 5.21. System A was considered to be assisted by both Systems B and C. When the tie-lines are perfect (i.e. FOR = 0.0) there is no improvement in the marginal outage cost of System A caused by tie-line T_{BC} because all the assistance can be routed by the directly connected lines. As the forced outage rates of the tie-lines increase, however, the marginal outage cost profile of System A increases. The magnitude of the increase is negligible due to the relatively small values of the forced outage rates.

The effect on the marginal outage cost of the existence of T_{BC} is shown in Figure 5.22 for two different forced outage rate values. It can be observed from this figure that there is an improvement in the marginal outage cost of System A due to the presence of tie-line T_{BC}. The magnitude of the improvement is not very large because, in this case, all the assistance available from Systems B and C can be routed through the directly connected tie-lines. The degree of improvement depends on the forced outage rates of the tie-lines. The higher the forced outage rate, the greater is the improvement due to tie-line T_{BC}.

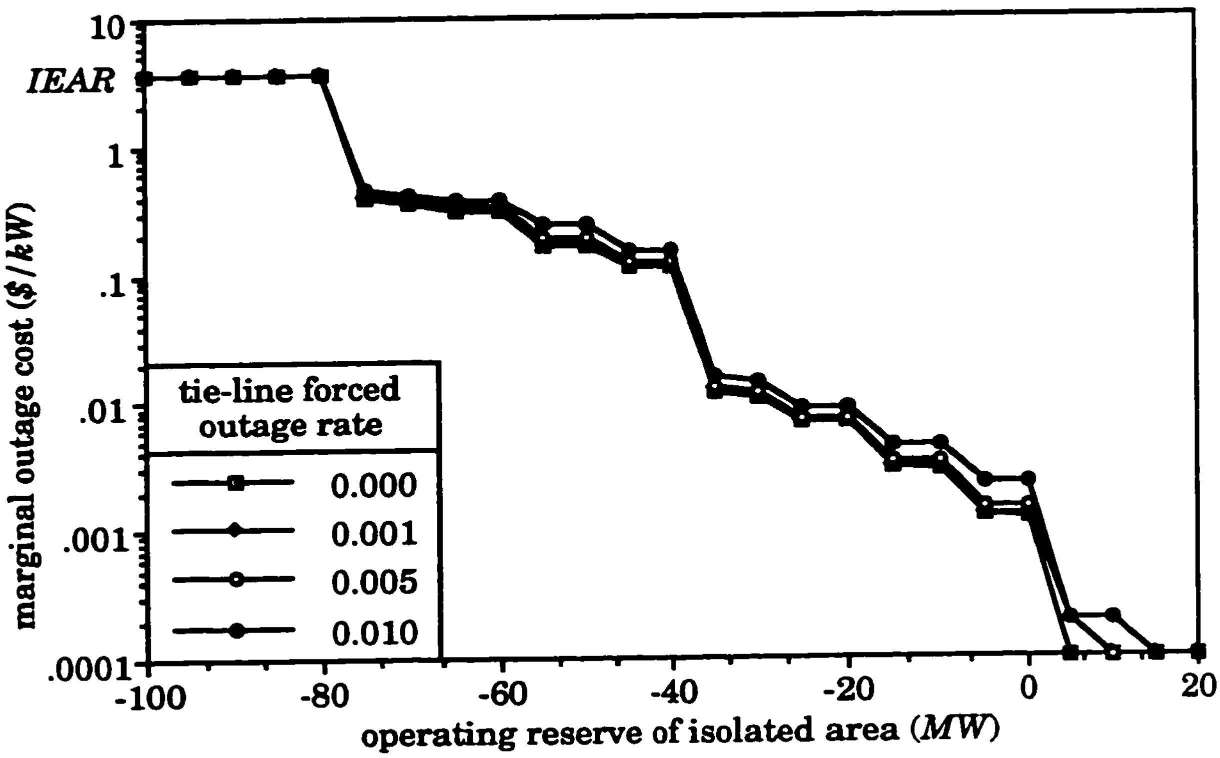

Figure 5.21. Effect tie-line reliability on the marginal outage cost of System A interconnected in a three-system ring fashion.

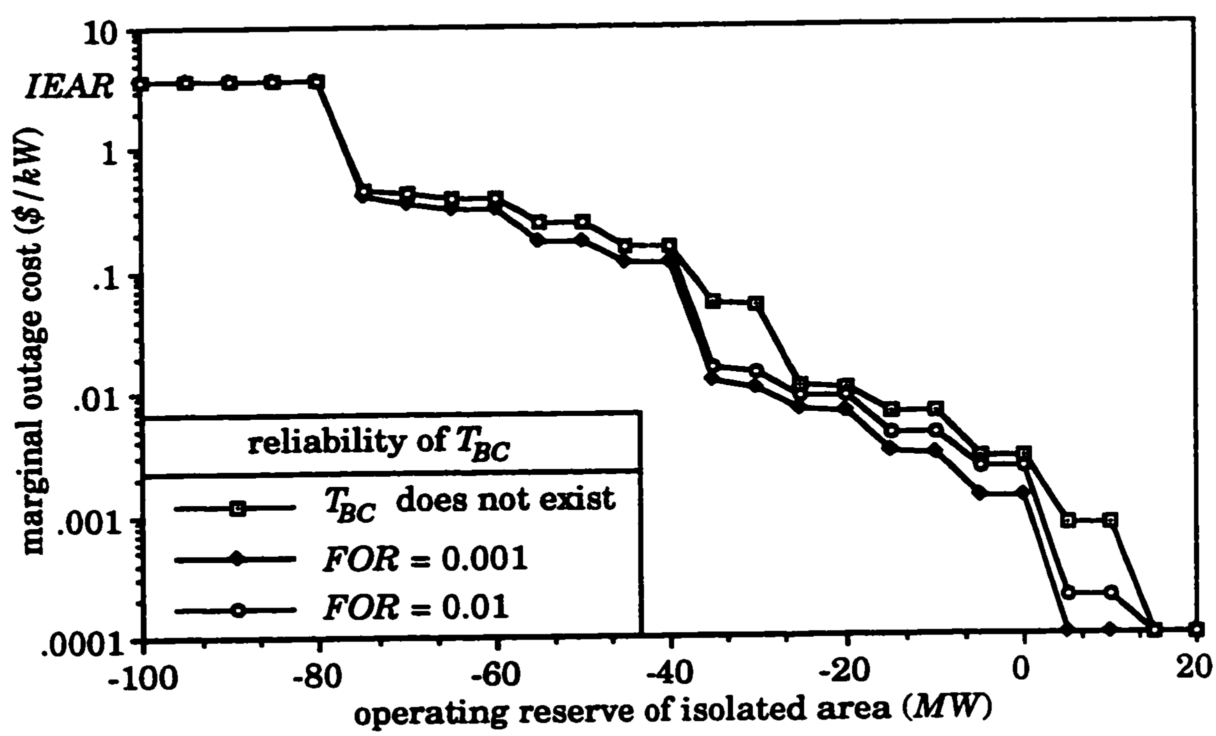

Figure 5.22. Improvements in the marginal outage cost of System A due to the existence of tie-line T_{BC} (Case 1).

Case 2 *Operating reserves in both assisting systems exceed the respective carrying capabilities of the connecting tie-lines.*

In this case, both assisting systems have more operating reserves than the transfer capabilities of the directly connected tie-lines. The conditions for this case can be expressed by the following inequalities,

$$OR_{(b)} > T_{AB} \text{ and}$$
$$OR_{(c)} > T_{CA}. \tag{5.4}$$

When tie-line T_{BC} is unavailable, the system is reduced to three radially interconnected areas as shown in Figure 5.16. In this case, the assistance from Systems B and C is represented by equivalent assisting units of sizes T_{AB} and T_{CA} respectively. When tie-line T_{BC} is available, however, Systems B and C can interact among themselves to increase the assistance beyond the directly connected tie-line capabilities. The procedure used to calculate the effect of this interaction amongst the assisting systems is presented in [112].

In order to illustrate this case, the operating reserves in Systems B and C were assumed to be 60 MW and 90 MW respectively and the results are shown in Figure 5.23. The forced outage rates of all tie-lines are assumed to be 0.005. The improvement in the marginal outage cost of System A due to the existence of tie-line T_{BC} is consistent for most operating reserve levels. The difference in the two curves will increase as the reliability of the tie-line decreases. The magnitude of the improvement in such cases will be significant because T_{BC} will be needed to wheel the excess capacity assistance from Systems B and C to System A.

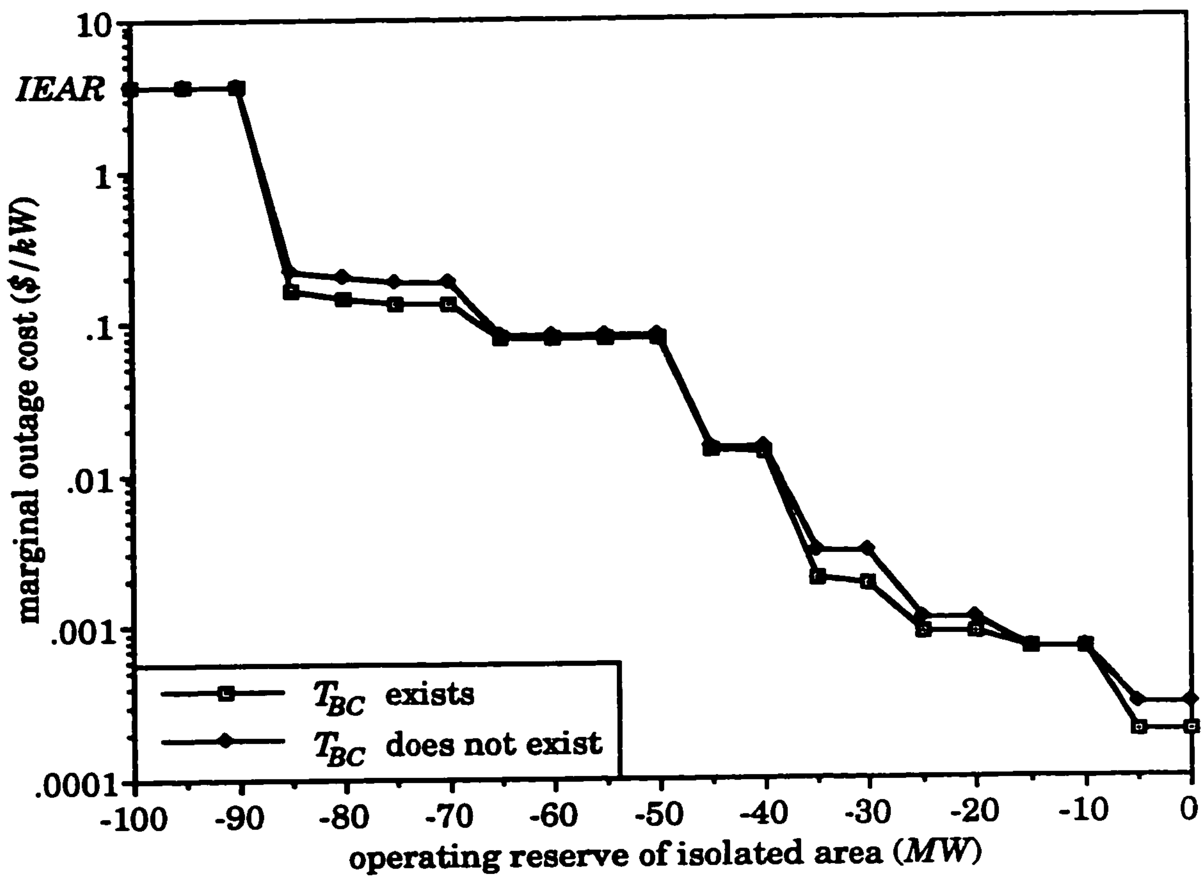

Figure 5.23. Improvements in the marginal outage cost of System A due to the existence of tie-line T_{BC} (Case 2)

__Case 3__ *Operating reserve in one assisting system is positive while the generation margin in the other assisting system is negative and greater than either the intermediate tie-line T_{BC} or the operating reserves in the assisting system.*

The conditions for this case can be expressed by the following inequalities,

$$OR_{(b)} \text{ is positive,}$$
$$OR_{(c)} \text{ is negative and}$$
$$\left|OR_{(c)}\right| > \min\left\{T_{BC}\, ,\, OR_{(b)}\right\}. \tag{5.5}$$

If the operating reserve in System B is greater than the transfer capability of tie-line T_{AB} and it wants to route the excess assistance via tie-line T_{BC} and System C, all the assistance will be absorbed by System C. Therefore, under the indicated reserve sharing policy, no assistance will be routed through T_{BC}. The system will then be reduced to that of Figure 5.24 and analyzed using the method developed for radially interconnected systems.

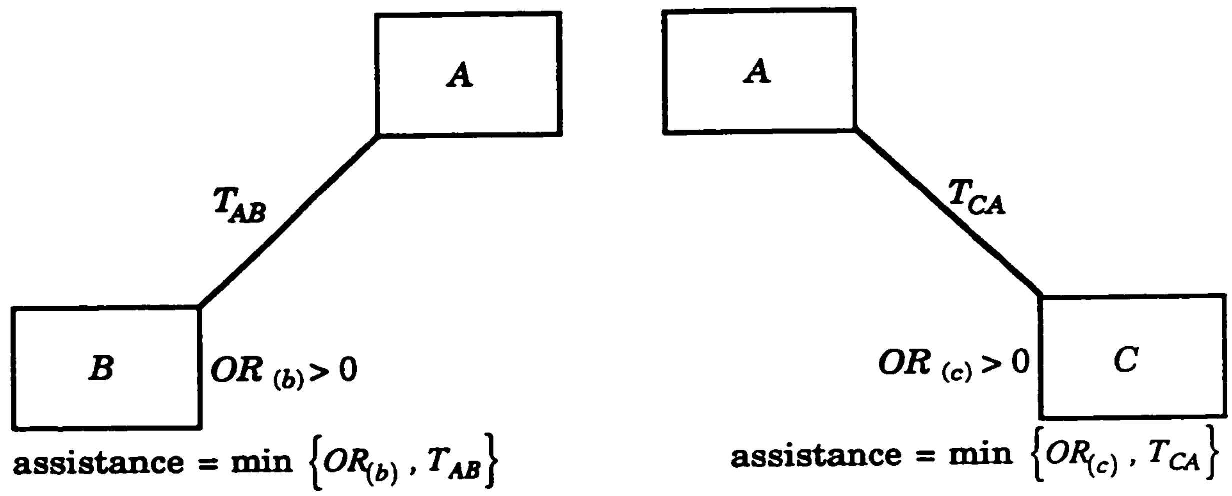

Figure 5.24. Equivalent model for Case 3 of the three systems interconnected in a ring type fashion.

__Case 4__ *The operating reserve in one assisting system is positive and greater than the connecting tie-line while the operating reserve in the other assisting system is either slightly negative but less than the intermediate link or positive but less than the connecting link of the other system.*

The conditions for this case can be expressed by the following inequalities,

$$OR_{(b)} > T_{AB} \text{ while either}$$

$$\left\{\begin{matrix} OR_{(c)} \textit{ is negative}; \text{ and} \\ \left|OR_{(c)}\right| < \min\left\{T_{BC}; \left(OR_{(b)} - T_{AB}\right)\right\} \end{matrix}\right\} \text{ or}$$

$$\left\{\begin{matrix} OR_{(c)} \textit{ is positive}; \text{ and} \\ OR_{(c)} < T_{CA} \end{matrix}\right\}. \tag{5.6}$$

In Cases 1 and 2, the alternate path of routing the assistance was used to improve the assistance to System A. In this case, the alternate path plays a more important role. System B will use T_{BC} as a normal route as shown in Figure 5.25. Determination of various amounts of assistance to be routed via different paths can be performed using the algorithm presented in [112].

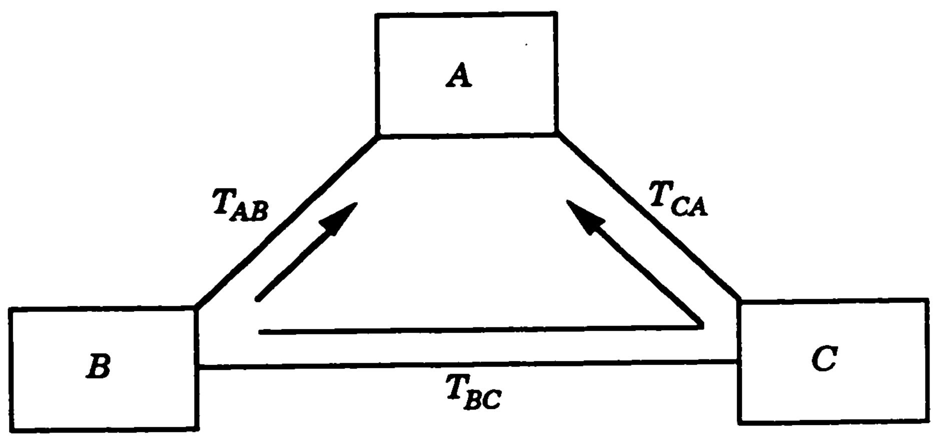

Figure 5.25. Equivalent model for Case 4 of the three systems interconnected in a ring type fashion.

This case is more important than the other three since some capacity from one assisted system uses the other system as a normal route. System B was assumed to have more assistance available (*40 MW*) than the transfer capability of the directly connected tie-line T_{AB} and System C was assumed to have less assistance (*50 MW*) available than T_{CA}. The total operating reserve in both systems was maintained at 90 MW. The operating reserve in System B was increased and the operating reserve in System C was decreased in steps of 20 MW as shown in Table 5.3 and the results are given in Figure 5.26. The forced outage rates of all the tie-lines were set at 0.005. It can be seen from this figure that the marginal outage cost is not affected greatly by the amount of power that has to be re-routed through System C. The total assistance received by System A remains constant at 90 MW. As in the other cases, it is expected that the effect of routing the excess capacity through T_{BC} will be more significant if the forced outage rates of the tie-lines are much higher.

Table 5.3. Scenarios of operating reserves for Systems B and C.

Scenario	$OR_{(b)}$ (MW)	$OR_{(c)}$ (MW)
A	40	50
B	60	30
C	80	10

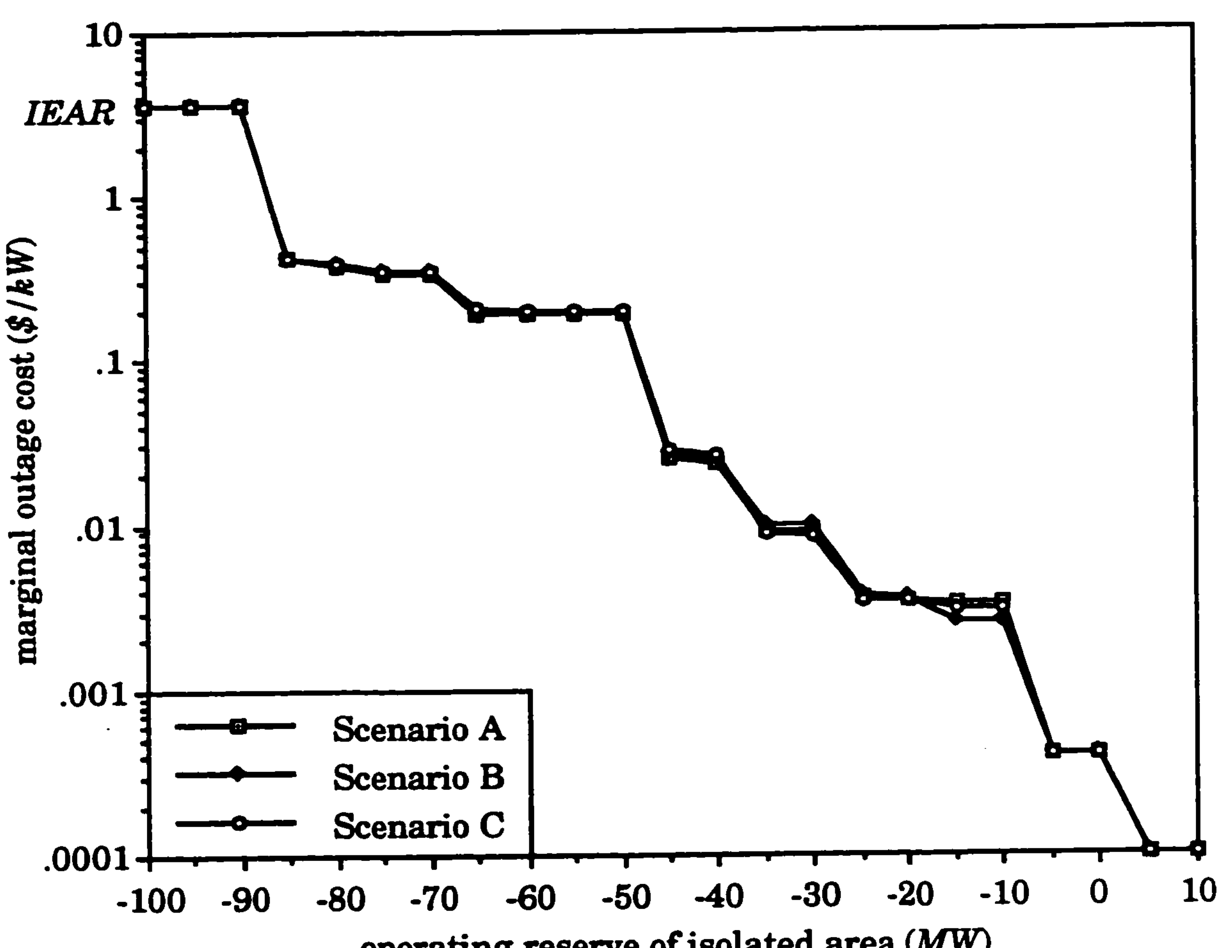

Figure 5.26. Effect of re-routing the assistance from System B via tie-line T_{BC} and System C on the marginal outage cost of System A.

5.7. Summary

This chapter describes a methodology based on quantitative reliability evaluation techniques for the calculation of the marginal outage costs in interconnected generating systems. The proposed method is illustrated in this chapter by calculating the marginal outage costs on a regional basis within a system and the impact of assistance from neighbouring systems on these costs.

The proposed method has been applied to radially interconnected and looped systems. It is found from these studies that, for all interconnection topologies, the marginal outage cost is mostly affected by the total transfer capability of all the tie-lines. The number of tie-lines and their reliabilities have an insignificant impact on the marginal outage cost. Additional studies also show that the interconnection topology has an insignificant impact on the marginal outage cost. Therefore, it can be concluded from these studies that, for the purposes of marginal outage costing, tie-lines may be represented by their total transfer capability. This conclusion is based on studies of the *RBTS*, which is a small test system designed for educational purposes. Further research and testing is required to see if the conclusion remains valid when applied to large and meshed generating systems.

The incorporation of tie capacity uncertainty and load forecast uncertainty in the calculation of the marginal outage costs associated with two interconnected generating systems shows that such modelling considerations have a significant impact on these costs. Therefore, it is important to include these uncertainties in the analysis given the supporting data.

Finally, it is shown in this chapter that the assistance available from one system to another has a significant impact on the shape of the marginal outage cost profile of the assisted system. Therefore, it is not generally recommended to simply shift the marginal outage cost profile of an isolated system by the available assistance in order to calculate its interconnected profile. However, such an approximation provides a quick means of estimating the marginal outage cost of an interconnected generating system without performing any detailed interconnected system reliability studies.

6. EVALUATION OF THE MARGINAL OUTAGE COSTS IN COMPOSITE GENERATION AND TRANSMISSION SYSTEMS

6.1. Introduction

The evaluation of the marginal outage costs in generating systems (*HLI* evaluation) using quantitative power system reliability techniques is discussed in Chapters 3, 4 and 5. It is reported in these chapters that the marginal outage cost varies with the lead time, operating reserve and the capacity assistance available from neighbouring systems. This chapter is concerned with the variation of the marginal outage cost over space because the location of loads with respect to the overall system topology containing both generation and transmission facilities has an impact on these costs. This involves the calculation of the marginal outage costs at bulk customer load points in the composite generation and transmission system (*HLII* evaluation).

Quantitative reliability assessment in composite systems is a very complex problem that has been and is still under investigation by electric utilities, universities and research organizations [25-33]. A substantial amount of research work in the area of composite system reliability evaluation has been done at the University of Saskatchewan [76-78] and a computer program called *COMREL* (COMposite system RELiability

Evaluation) has been developed. This chapter provides a brief description of this program and illustrates its utilization in calculating the marginal outage costs at bulk customer load points by application to the *RBTS* [35] and the *IEEE-RTS* [36].

6.2. Description of the *COMREL* Program

The development of the *COMREL* program was initiated at the University of Saskatchewan by Billinton in the 1960's. Extensive work done in this area in subsequent years by Billinton and Bhavaraju [63,64], Medicherla [76,77], Kumar [78] and Khan [74] has resulted in a refined digital software package which is now one of the innovative tools in the state of the art of composite system adequacy evaluation.

The *COMREL* program is based on the analytical concepts of reliability evaluation and employs the contingency enumeration technique for the assessment of composite systems. The program can handle independent outages as well as common mode events and station-originated outages when required. However, only independent outages are considered in the analyses reported in this thesis. The *COMREL* program is equipped with three network solution techniques (i.e. the transportation model [69], the *DC* load flow algorithm [70] and the *AC* load flow algorithm [71,72]) for analyzing system contingencies. Any one of the solution techniques can be selected for evaluating the system performance depending on the prescribed set of system failure criteria. The basic structure of the contingency enumeration algorithm used in *COMREL* is illustrated by the flowchart in Figure 6.1. Additional features of the *COMREL* program are discussed in the following sub-sections.

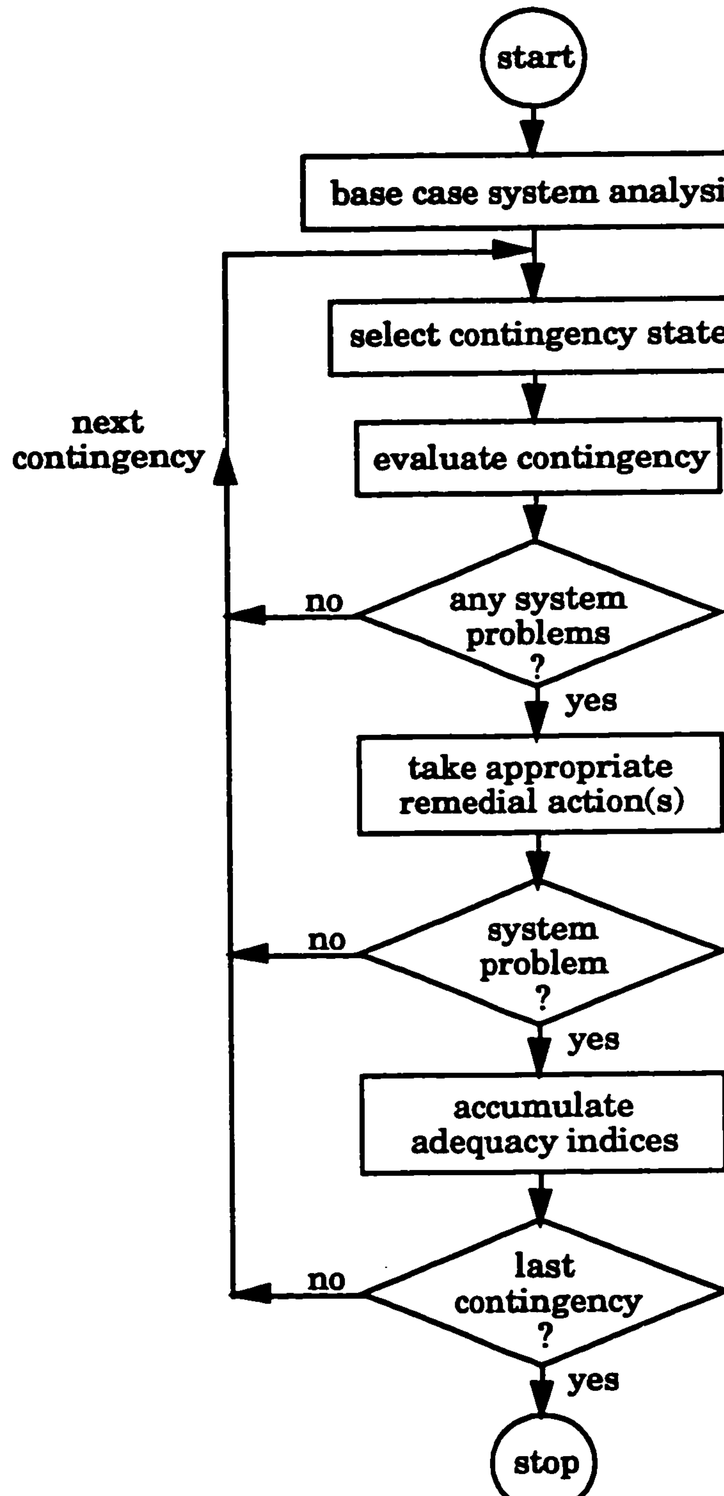

Figure 6.1. Flowchart of the *COMREL* program.

In the contingency enumeration approach shown in Figure 6.1, a contingency is selected and tested to ascertain whether it causes any immediate system problem such as a circuit overload or bus voltage out of limits. If it does not, a new contingency is selected and tested. The occurrence of a system problem may by itself be entered as a failure. In some cases, however, it is possible to adjust generation or phase shifters to relieve overloads and to adjust transformer taps to bring bus voltages back within the acceptable range. A system failure is therefore recorded when the remedial actions, short of curtailing customer loads, are insufficient to eliminate the system problems. The severity of such system problems are assessed by calculating the amount and location of load curtailment necessary to eliminate the problem. In this way, it is possible to compute area or bus reliability indices that measure the frequency, duration and amount of expected load curtailment.

6.2.1. System failure criteria

Quantitative adequacy analysis in a composite system is performed based on a prescribed set of criteria by which the system must be judged as being in the success or failed state. Generally, a bulk power system is considered to be failed if the service at the load buses is interrupted or its quality becomes unacceptable. Such a condition arises if any of the following events occur:

1. lack of sufficient generation in the system to meet load demand,
2. interruption of continuity of power supply to a load point,
3. overload of transmission facilities,
4. violation of bus voltage tolerances,
5. generating unit *MVAr* limit violations or
6. ill-conditioned network violations.

Failure by any of these criteria does not necessarily mean the collapse of the entire system, although this could be recorded as a failure event. While it is possible for an overload condition to develop into a cascading sequence of events finally leading to the collapse of the system, it is more likely that such a catastrophe would be averted by taking appropriate corrective measures. It should therefore be appreciated that the system failure criteria are only a set of undesirable events which form a basis for the calculation of the reliability indices.

6.2.2. Contingency selection and evaluation

The large number of system contingency states that need to be evaluated has been emphasized as the major handicap of the state enumeration approach. In order to handle these problems, the *COMREL* program has been equipped with the following features most of which seek to truncate the state space in order to reduce the computational requirements.

6.2.2.1. Predetermined contingency level

This feature provides for the truncation of the state space by selecting and specifying the order of overlapping outages to be considered. The *COMREL* program can consider simultaneous independent outages of generating units up to the 4th level, of transmission facilities up to the 3rd level and up to the 3rd level for generating units together with transmission facilities combined. The user is offered the flexibility of specifying as input data the appropriate levels within this range to suit the system requirements. It is therefore possible and convenient to study the incremental effect of higher order overlapping outages on system adequacy in order to determine the optimum cut-off point for the particular system.

6.2.2.2. Ranking

In a recent update of the program [74], a contingency ranking facility was provided to further the truncation process by considering in the analysis, only those contingencies having a significant impact on the system.

6.2.2.3. Frequency cut-off

In order to enhance the computational speed still further, the program employs a frequency cut-off criterion which automatically neglects those contingencies with a frequency of occurrence less than a pre-specified value [78].

6.2.2.4. Sorting facility

The sorting facility is a computational speed enhancement feature that avoids unnecessary repetitive evaluations of identical outage events. With this facility, the reliability indices are calculated based on the outcome of system analysis for only one of the identical contingency states. The contribution of other identical contingencies is computed by multiplying the indices obtained using the first calculation by the number of identical contingencies. This means that the repetition of load flow analysis for contingency states that would have ultimately produced identical effects is avoided, thus resulting in significant savings in computing time. In the analysis, identical generating units are considered to be those units with the same capacity rating, equal failure and repair rates and are located at the same generating bus.

6.2.3. Network analysis

The adequacy analysis of a bulk power system generally involves the solution of the network configuration under selected outage conditions. Since the analysis normally involves many repetitive calculations for the various system contingency states to be examined, the efficiency and speed of the evaluation process depends appreciably on the load flow algorithm employed in the network analysis. Depending on the prescribed set of failure criteria which in turn depend on the intent behind the studies, various solution techniques are available, each producing a unique set of results. The three network solution techniques implemented in *COMREL* are listed below and the following sub-sections provide a brief description of each method.

1. The network flow method (or the transportation model),
2. the *DC* load flow method and
3. the *AC* load flow method.

6.2.3.1. Network flow method (Transportation model)

The network flow method is basically concerned with the continuity of power supply from the generating stations to the major load centres in order to satisfy the customer load demand. The failure constraints addressed in the linear network flow model are limited to the availability of power at the generating stations to satisfy the system load requirements and the continuity of power flow to the major load centres.

In the transportation model, capacity levels are assigned to every system component together with a probability corresponding to each capacity level. The network is solved using max-flow min-cut concepts [69], ensuring that the line flows do not exceed the prescribed capacities. The reliability indices obtained using this method are of a low level of accuracy, but may be acceptable in some applications.

6.2.3.2. *DC* load flow method

Approximate linear power flow techniques such as the *DC* load flow algorithm can be used to enhance the computation speed in composite system adequacy assessment. In addition to recognizing generation unavailability and lack of supply continuity as system constraints, the *DC* load flow solution technique also provides information regarding line overload conditions in the composite system and considers them to be system failure conditions when estimating the adequacy indices. This technique, like the transportation model, does not provide any estimate of the bus voltages and the reactive power limits of generating units.

6.2.3.3. *AC* load flow method

AC load flow techniques are required when the continuity and the quality of power supply (i.e. proper bus voltage levels and correct *MVAr* limits of the generating units) are important concerns in the adequacy assessment of composite systems. The *AC* load flow is capable of recognizing all the system failure criteria listed in Section 6.2.1 and produces indices that reflect the impact on adequacy of the operational characteristics of the power system. The conventional *AC* load flow techniques such as Gauss-Seidel, Newton Raphson and more accurate second order load flow methods are, however, rarely used for adequacy studies due to their large computing time and storage requirements. Several approximate versions of these algorithms, which are faster and require less storage have been developed and are more frequently used to produce results with an acceptable degree of accuracy [71,72].

The selection of an appropriate network solution technique, therefore, is of prime importance and is basically an engineering decision. The selected technique, however, should be capable of satisfying the intent behind the studies with reasonable accuracy and within the time constraints.

6.2.4. Remedial actions in the *COMREL* program

It is important to determine whether it is possible to eliminate a system problem by employing a remedial action (or corrective measure). The *COMREL* program is equipped with the following broad range of remedial actions based on the system failure criteria:

1. generation rescheduling in the case of capacity deficiency in the system,
2. handling of bus isolation and system splitting problems arising from transmission line(s) and transformer(s) outages,
3. line overload alleviation,
4. correction of a bus voltage problem,
5. correction of generating unit *MVAr* limit violations,
6. solution of ill-conditioned network situations, and
7. load curtailment in the event of unavoidable system problems.

The selection of a corrective measure is dependent on the situation that causes an outage in the system. If a generating unit outage at a generation bus results in a capacity shortfall at that bus, then the generation at other generation buses with reserve capacity will be increased proportionately to make up the deficiency. However, if the system remains deficient even after supplying all the available reserve, load is curtailed at the relevant buses as dictated by the load curtailment philosophy.

6.2.5. Implementation of load curtailment philosophy

In the *COMREL* program, a deterministic load curtailment policy is implemented. Load at each system load bus is classified into two categories: *firm load* and *curtailable load*. The proportion of curtailable load at each bus is pre-specified as a percentage of the total bus load and this information is made available to the program as input data. When there is a system problem, such as a deficiency in system generation capacity, that has to be alleviated by a load curtailment action, curtailable load is interrupted first followed by the interruption of firm load, if necessary.

The flexibility of either confining the load curtailment to the neighbourhood of the outage problem or distributing it over a wider area is implemented by defining three load curtailment passes, one of which must be selected by the analyst to indicate the preferred choice of confinement. The passes define sequential levels, each spreading the required curtailment over a wider area. This feature considerably enhances the flexibility of the *COMREL* program and makes it adaptable for use in a wide range of power system operational studies such as marginal outage costing.

6.3. Proposed Method for Calculating the Marginal Outage Costs at Bulk Customer Load points

In practical implementations of spot pricing, the marginal outage cost charged to customers at a given location for an incremental increase in load at that location includes the contributions from all the load buses in the system. That is, if a load increment at Bus k causes the expected outage costs to increase at other locations, it should be the responsibility of the

the customers at Bus k to cover the additional costs. The same concept can also be used if the consumption at Bus k is reduced and a reduction in the spot price is needed. Therefore, the marginal outage cost at a customer load point, k, can be defined as the change in the system's expected outage costs resulting from an incremental load change at that load point [12,22]. This is equivalent to the sum of the incremental expected outage costs of all the load buses in the system caused by a load increase at Bus k, That is,

$$M.O.C._k = \sum_{i=1}^{nbus} IEAR_i \times \Delta EUE_{ki}, \tag{6.1}$$

where $M.O.C._k$: marginal outage cost at load Bus k,
$IEAR_i$: interrupted energy assessment rate at load Bus i,
ΔEUE_{ki} : incremental expected unserved energy at Bus i caused by a load increment at Bus k and
$nbus$: total number of load buses in the system.

The idea of utilizing *COMREL* to calculate practical estimates of the *IEAR* and ΔEUE at individual load buses was discussed in Section 2.5 of this thesis. The formulas developed for calculating these variables at a load Bus i for a load increase at Bus k are as follows:

$$IEAR_i = \frac{\sum_{j=1}^{NC} L_{ij} f_j C_j(d_j)}{\sum_{j=1}^{NC} L_{ij} f_j d_j} \quad (\$/kWh) \text{ and} \tag{6.2}$$

$$\Delta EUE_{kj} = \frac{1}{8760}\left\{\sum_{j=1}^{NC'} L'_{ij} f'_j d'_j - \sum_{j=1}^{NC} L_{ij} f_j d_j\right\} \quad (MWh/MW), \tag{6.3}$$

where L_{ij} : magnitude of load curtailment at Bus i (MW) due to contingency j,
f_j : frequency of contingency j (occ/yr),
d_j : duration of contingency j ($hours$),

$C_{ij}(d_j)$: interruption cost to customers at Bus i caused by a contingency of duration d_j ($\$/kW$), and

NC : total number of contingencies that lead to power interruptions at Bus i.

L'_{ij}, f'_j, d'_j and NC' have the same definitions as above but are calculated when the load is increased at Bus k by 1 MW. The factor of 1/8760 is used to express the results on an hourly rather than annualized basis.

Most of the variables in (6.2) and (6.3) can be estimated directly from the output of the *COMREL* program. The interruption cost to customers at Bus i resulting from Contingency j, $C_{ij}(d_j)$, can be obtained from the composite customer damage function of Bus i ($CCDF_i$). This function represents the interruption costs of all the customers at Bus i as a function of the interruption duration. The derivations of such functions for every load bus in the *RBTS* and the *IEEE-RTS* are given in Appendices G and H respectively. The utilization of the proposed method of calculating the marginal outage costs at the load buses of the *RBTS* and the *IEEE-RTS* is illustrated in the following sections of this chapter.

6.4. Evaluation of the Marginal Outage Costs at the Bulk Customer Load Points of the *RBTS*

The single line diagram of the *RBTS* is given in Figure 6.2. This system has 6 buses, 5 of which are load buses. The generation and transmission systems data for the *RBTS* are given in Appendix A and the *CCDF* for each load bus are derived in Appendix G. This section presents the results from a number of studies aimed at calculating and comparing the marginal outage cost profiles of every load bus in the *RBTS*.

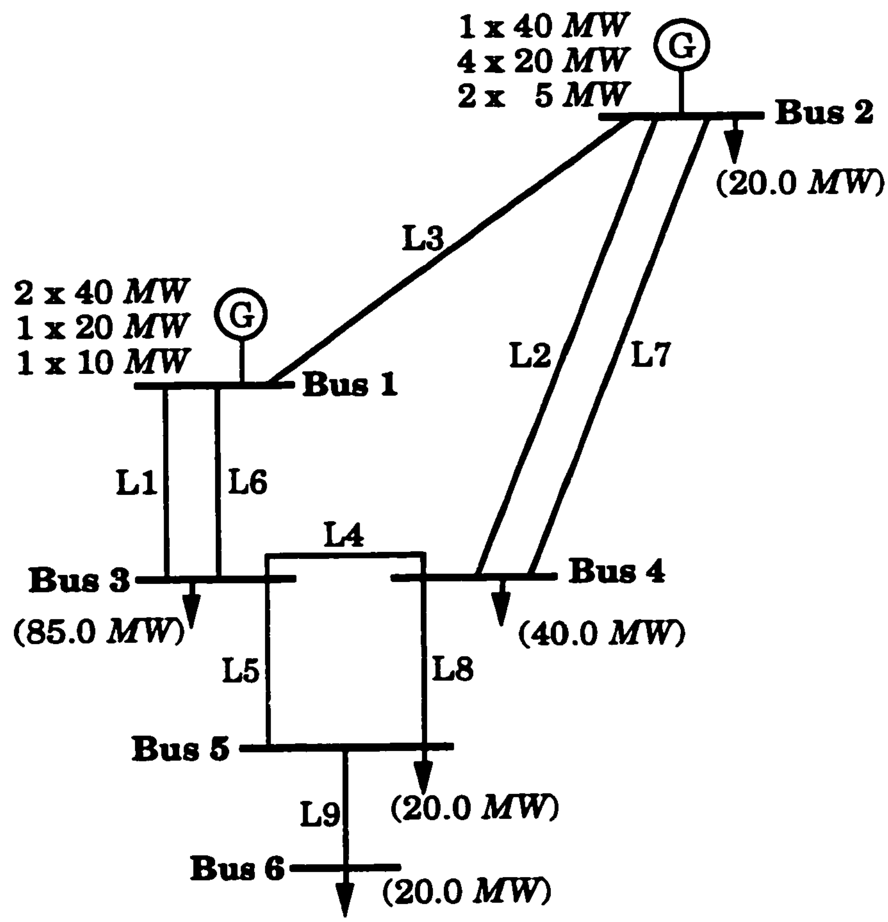

Figure 6.2. Single line diagram of the *RBTS*.

Before calculating the marginal outage costs, the *IEAR* value at each load bus of the *RBTS* was calculated as shown in Appendix G using the following modelling assumptions and parameters. The results from these calculations are reproduced in Table 6.1.

1) The peak load of the *RBTS* was set at 185 *MW*.
2) A single step load model is used in the analysis. The effect of multi-step load model can be included in composite system reliability studies in order to produce more representative annual *IEAR* values at the expense of computational time.
3) All load buses were assumed to have 20% curtailable load.
4) *Pass1* load curtailment philosophy was used.

5) The *AC* load flow technique was used.

6) Contingency enumeration of up to the following contingencies was used:

   i) four or less generating units were examined,

   ii) three or less transmission lines were examined and

   iii) up to two generating units and one line and one generating unit and two lines were considered.

7) The effects of station originated outages were not considered.

8) The effects of common-mode outages were not considered.

Table 6.1. *IEAR* values at each load bus of the *RBTS*.

load bus	*IEAR* ($\$/kWh$)
Bus 2	7.41
Bus 3	2.69
Bus 4	6.78
Bus 5	4.82
Bus 6	3.63

The marginal outage cost profiles of each load bus in the *RBTS* were calculated using (6.1) and plotted as a function of the system operating reserve in Figure 6.3. It can be seen from this figure that there are two distinct shapes to the marginal outage cost profile. Buses 2, 3, 4 and 5 appear to have similar profiles while Bus 6 has a different profile of its own. This is due to the topology of Bus 6 which is fed radially by a single transmission line and therefore most of the unserved energy at that bus is caused by the isolation of the bus. Hence, even when the system is lightly loaded (i.e. high operating reserve), the marginal outage cost at Bus 6 remains high while the marginal outage costs at the other buses experience a substantial decrease.

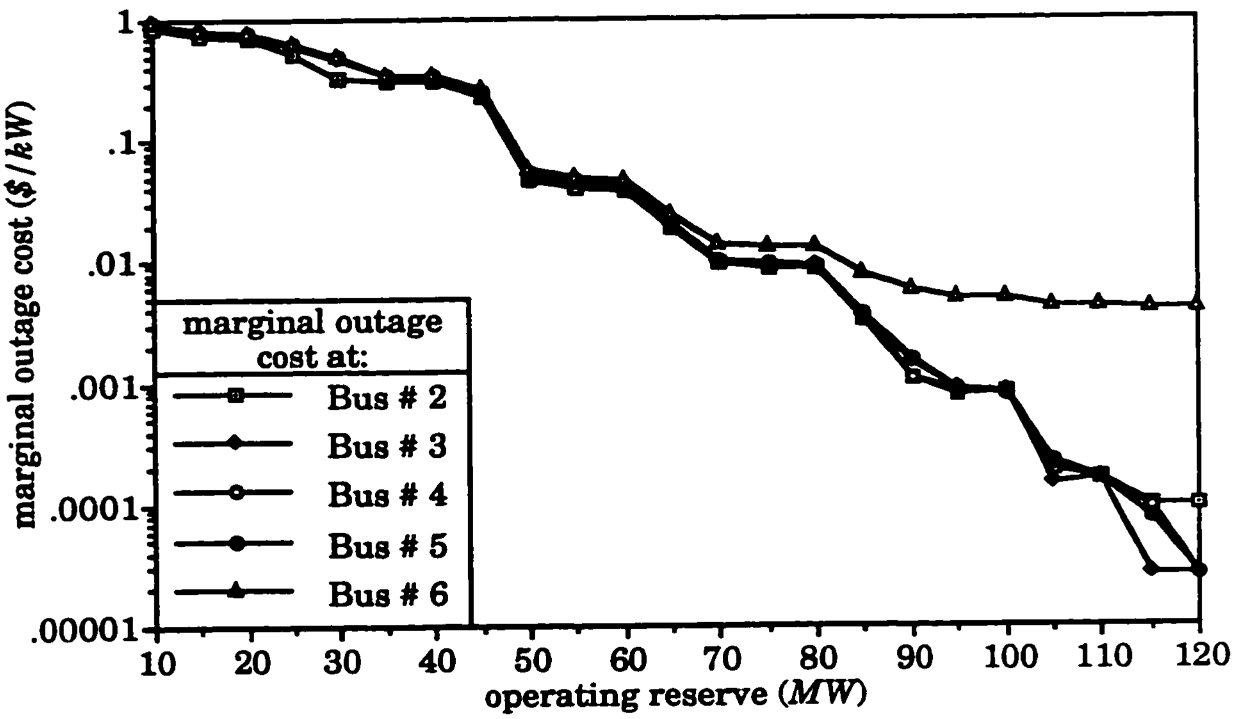

Figure 6.3. Marginal outage cost profiles of each load bus in the *RBTS*.

It can be observed from this study that the marginal outage cost does not appear to be affected by the location of the load bus in the system unless the bus is fed by one or more radial lines. This is a very significant observation because a number of pre-calculated marginal outage cost profiles can then be calculated and used to represent the marginal outage cost at selected buses instead of performing detailed reliability analysis for each bus individually. The validity of this observation is tested in Section 6.5 using the *IEEE-RTS*, which is a more practical system.

The magnitude of the marginal outage cost at a given load bus largely depends on the contributions from the individual load buses. The contribution of each bus is a function of the sensitivity of the bus to load increases in the system and its *IEAR*. In the case of the *RBTS*, the contribution of each bus to the marginal outage cost of Buses 3 and 6 was calculated and is plotted in Figure 6.4.

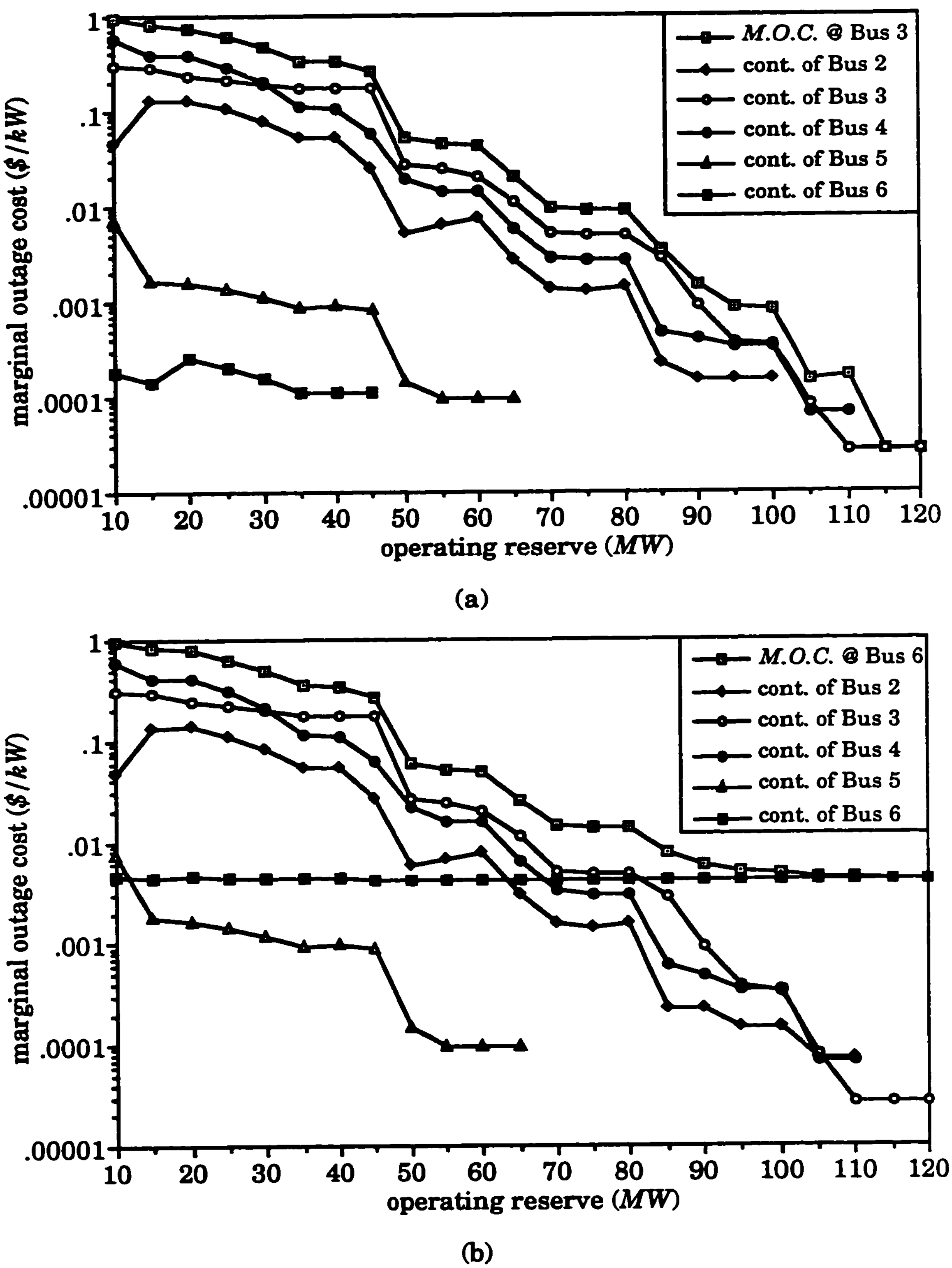

Figure 6.4. Contributions of the various buses to the marginal outage cost profiles at Bus 3 (a) and Bus 6 (b) of the *RBTS*.

It can be seen from Figure 6.4 (a) that Bus 3 has the largest overall contribution even though the *IEAR* value at that bus is the smallest. This is due in part to the unreliability of the bus which is reflected in its high expected unserved energy as compared to the other buses in the system. When the load is increased at Bus 6 (Figure 6.4 (b)), however, the contribution of Bus 3 remains higher than the other buses but the contribution of Bus 6 maintains the same value for all operating reserves. Hence, the shape of the marginal outage cost profile at Bus 6 is largely affected by the contribution of Bus 6.

6.4.1. Comparison between the marginal outage costs of the *RBTS* calculated at *HLI* and *HLII*

It is clear from the studies conducted in Section 6.4 that there are two types of marginal outage cost profiles for the *RBTS*; one for radially fed buses and another for all other buses. This sub-section compares the results from the *HLII* studies discussed in Section 6.4 with those obtained using *HLI* analysis. The comparison is performed using the marginal outage cost profiles of Buses 3 and 6 as shown in Figure 6.5. It can be seen from this figure that the marginal outage cost of Bus 3 is slightly higher than that of the generating system (*HLI* evaluation). When the load is increased at Bus 6, the difference between the *HLI* and *HLII* profiles increases. Since the generating system reliability data and the basic customer outage cost data used in the *HLI* and *HLII* studies are essentially unchanged, the difference between the profiles can be attributed to the method used in the analysis (i.e. *HLI* versus *HLII* adequacy evaluation).

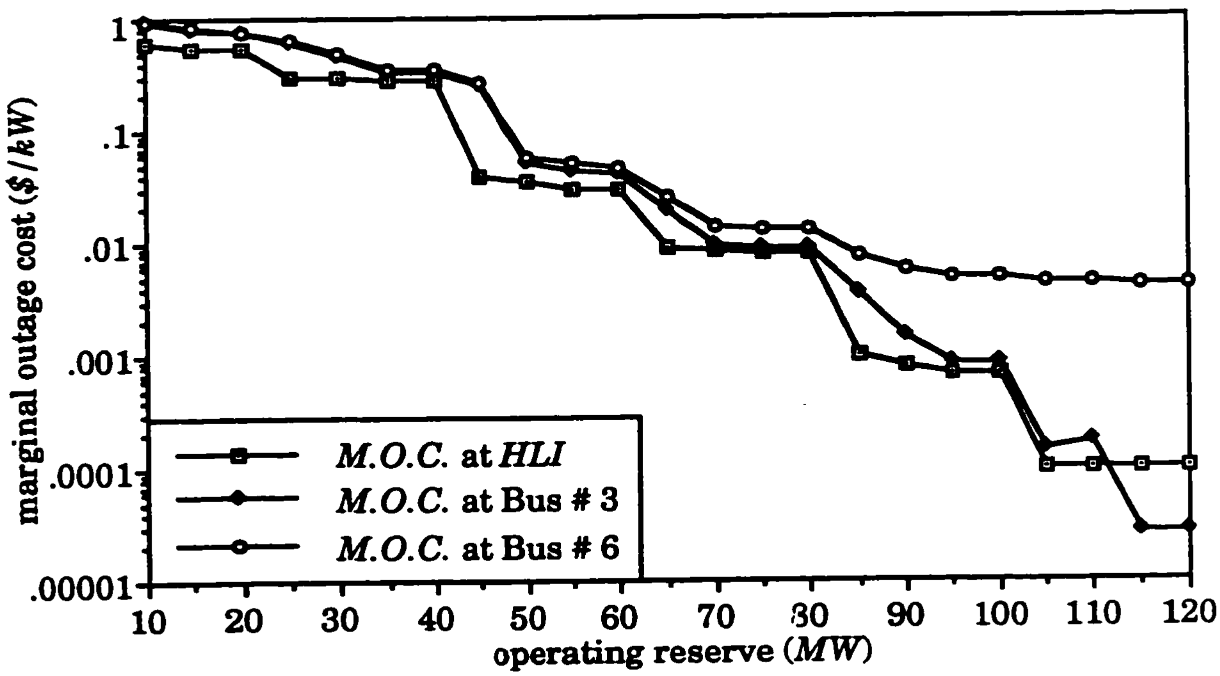

Figure 6.5. Comparison of the marginal outage cost profiles at Buses 3 and 6 of the *RBTS* to the generating system profile calculated at *HLI*.

In an effort to identify the contributions of the generation and transmission systems to the marginal outage cost at a given load bus, the marginal outage costs calculated at *HLII* were re-calculated using a fully reliable generation system (transmission contribution) and a fully reliable transmission system (generation contribution). The results from these studies are compared to the marginal outage cost profiles of Buses 3 and 6 and that of the generating system in Figure 6.6. It can be clearly seen from this figure that the contribution of the generation system is much larger than that of the transmission system. The transmission system contribution becomes more prominent at high operating reserves for the marginal outage cost of Bus 6. It is also clear from this figure that the contribution of the generation system at *HLII* and the marginal outage cost profile calculated at *HLI* are in reasonable agreement for all operating reserve levels. The small differences between these two profiles are due to the limitations placed on the generation model used in *HLII* studies (i.e. only up to 4 overlapping independent outages of generating units).

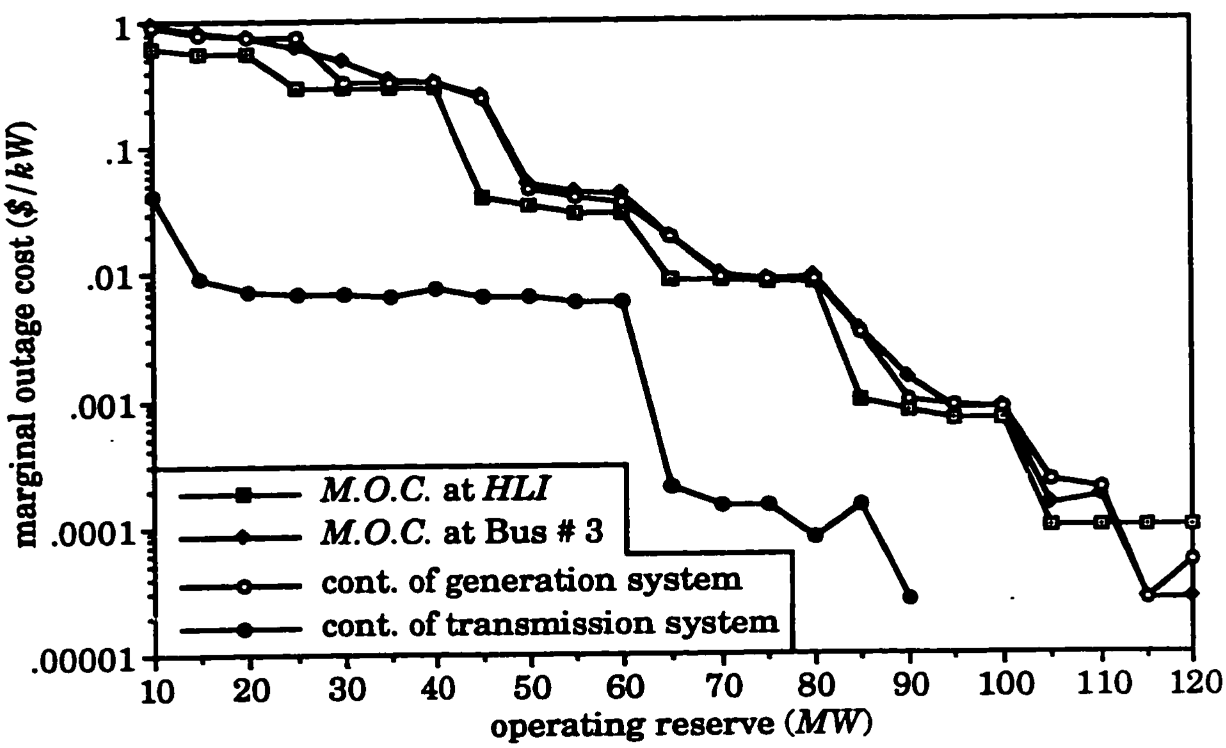

(a)

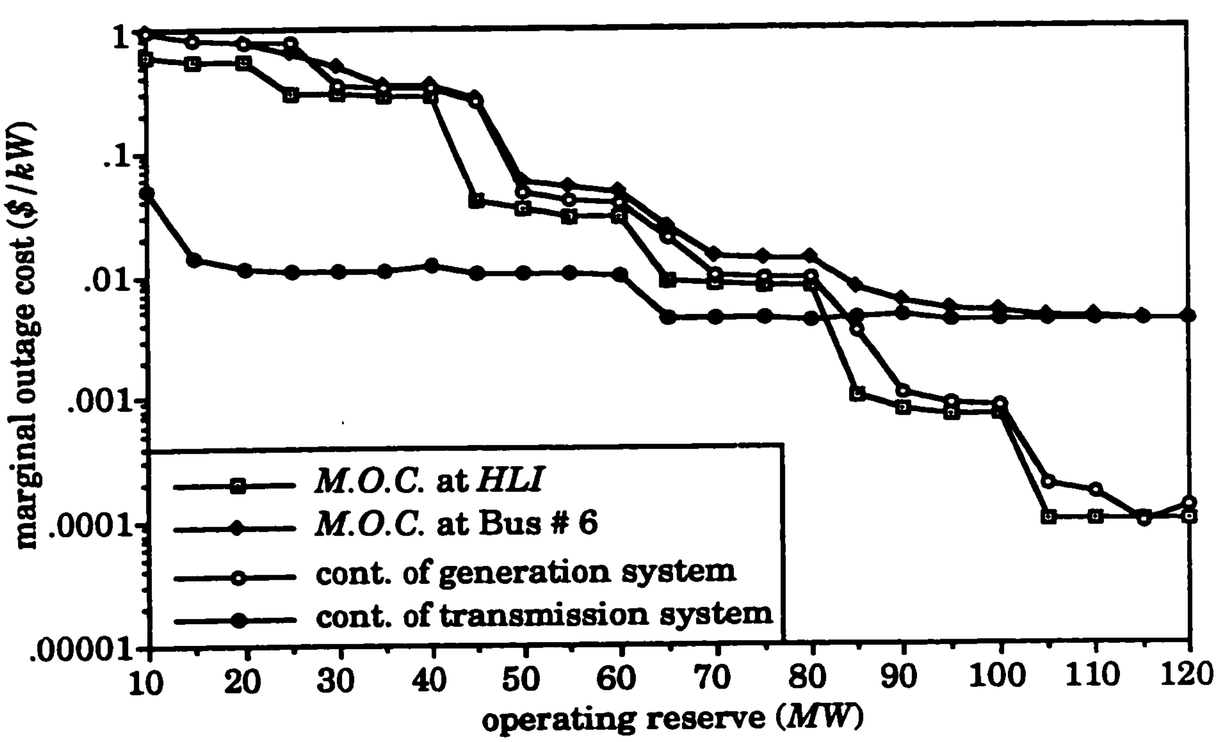

(b)

Figure 6.6. Contributions of the generation and transmission systems of the *RBTS* to the marginal outage costs at Bus 3 (a) and Bus 6 (b).

6.5. Evaluation of the Marginal Outage Costs at the Bulk Customer Load Points of the *IEEE-RTS*

The single line diagram of the *IEEE-RTS* is given in Figure 6.7. This system has 17 buses which have loads connected to them. The remaining buses are either free buses or generator buses without connected load. The generation and transmission systems data for the *IEEE-RTS* are given in Appendix B and the *CCDF*'s of each load bus are derived in Appendix H.

This section is concerned with the evaluation of the marginal outage costs at the various load buses of the *IEEE-RTS*. In order to facilitate the comparison between the marginal outage cost profiles at these buses, six categories of load buses have been chosen according to their type, voltage level, and location relative to a generating station. This classification helps in comparing the marginal outage cost profiles of buses falling into one class with those of buses falling into other classes. The buses in the six categories are as follows:

(a) <u>138 *kV* buses (South region)</u>

Class 1: buses having local generation (Buses 1, 2 and 7),

Class 2: buses that are one line away from generating stations and connected with two lines (Buses 4, 5 and 6),

Class 3: buses that are one line away from generating stations and terminated with three or more with lines (Buses 3 and 8) and

Class 4: buses that are two lines away from generating stations (Buses 9 and 10).

(b) <u>230 *kV* buses (North region)</u>

Class 5: buses having local generation (Buses 13, 15, 16 and 18) and

Class 6: buses with no local generation (Buses 14, 19 and 20).

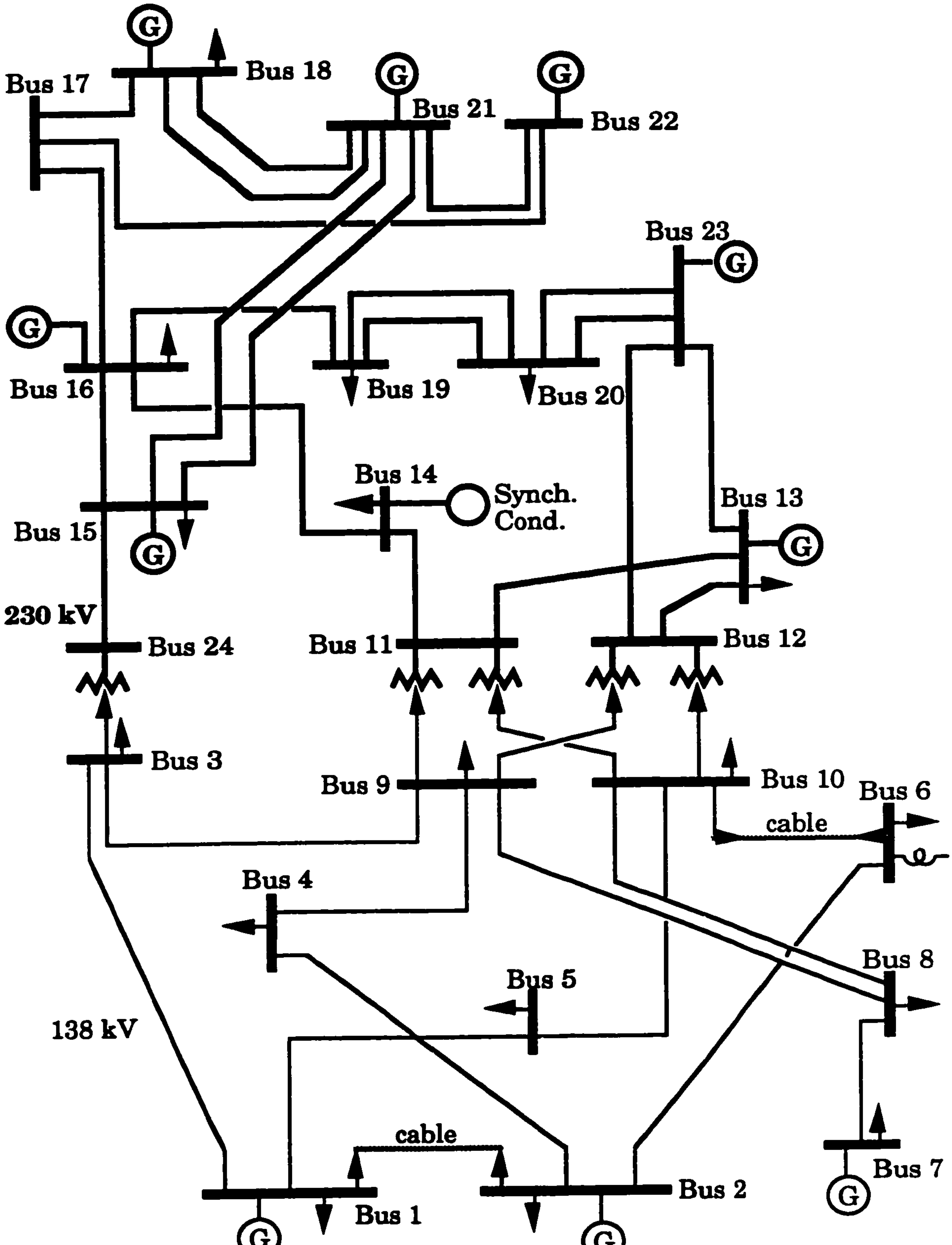

Figure 6.7. Single line diagram of the *IEEE-RTS*.

On the basis of the above classification, the marginal outage cost for one bus in each class is calculated and plotted as a function of the system operating reserve in Figure 6.8. The *IEAR* values used in the analysis are calculated in Appendix H using the same modelling assumptions employed in the *RBTS* study except that the peak load was set at 2850 *MW*. A summary of the results is given in Table 6.2. It can be seen from this figure that there are no significant differences between the marginal outage cost profiles of buses in all six classes. Therefore, it can be concluded that the marginal outage cost profile of the *IEEE-RTS* at *HLII* does not appear to depend on the load increment location within the system.

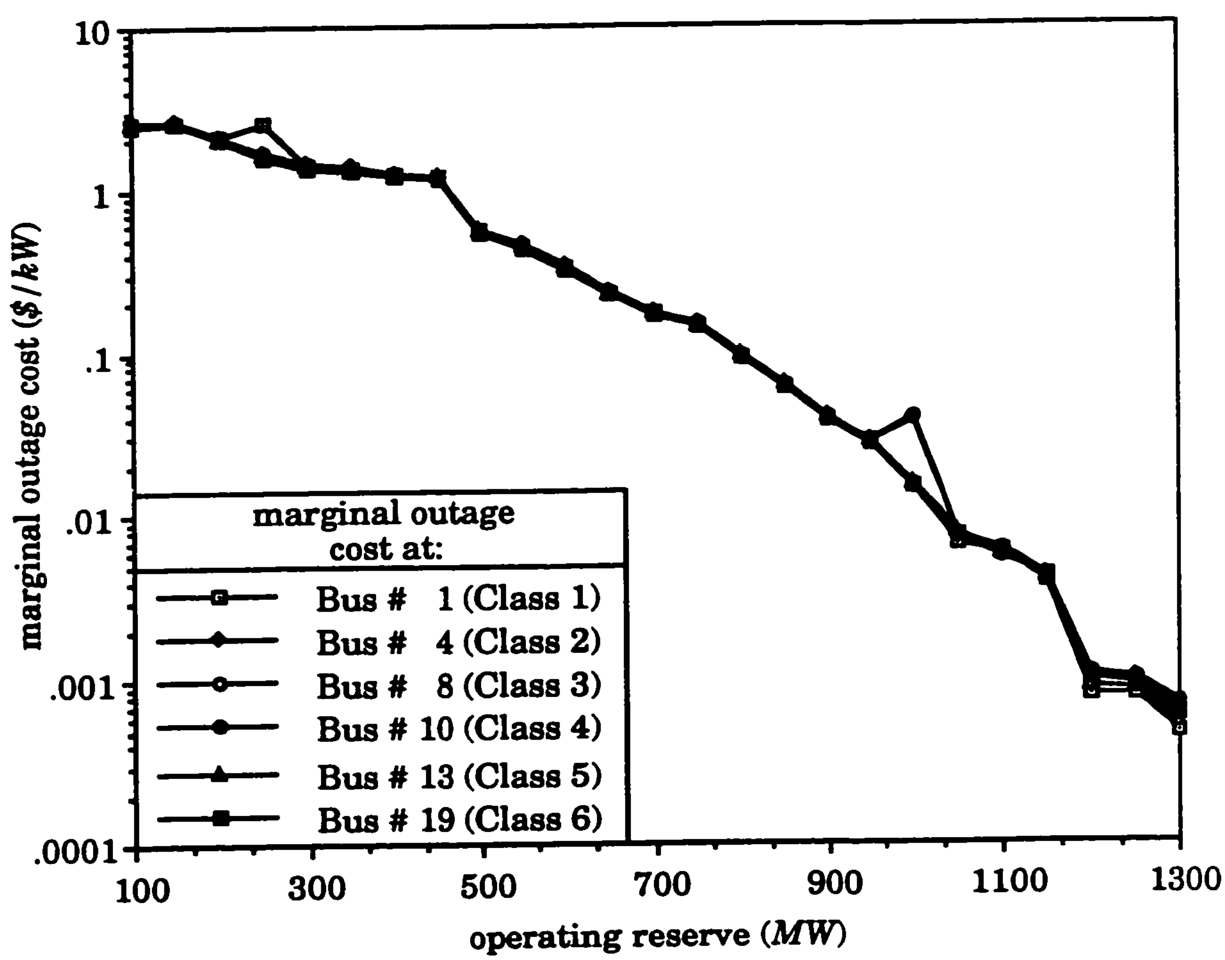

Figure 6.8. Marginal outage cost profiles of selected buses in the *IEEE-RTS*.

Table 6.2. *IEAR* values at each load bus of the *IEEE-RTS*.

load bus	classification	*IEAR* ($\$/kWh$)
Bus 1	Class 1	6.20
Bus 2	Class 1	4.89
Bus 3	Class 3	5.30
Bus 4	Class 2	5.62
Bus 5	Class 2	6.11
Bus 6	Class 2	5.50
Bus 7	Class 1	5.41
Bus 8	Class 3	5.40
Bus 9	Class 4	2.30
Bus 10	Class 4	4.14
Bus 13	Class 5	5.39
Bus 14	Class 6	3.41
Bus 15	Class 5	3.01
Bus 16	Class 5	3.54
Bus 18	Class 5	3.75
Bus 19	Class 6	2.29
Bus 20	Class 6	3.64

In order to determine the contribution of the buses in each class to the overall marginal outage cost, the highest contributions of each class to the marginal outage cost of Bus 4 (Class 2) are compared in Figure 6.9. It can be clearly seen from this figure that buses in Class 5 (230 kV North region) have the highest contribution while those in Class 4 (138 kV South region) have the lowest contribution. This result is very important because buses in class 5 are located far away from those in Class 2 and therefore it was expected that their contribution would be minimal. In addition, the *IEAR* values of the buses in Class 5 are lower than those in Class 2. Therefore, it is concluded that the high unreliability of the buses in Class 5 is responsible for the bulk of the increase in the marginal outage costs at these buses.

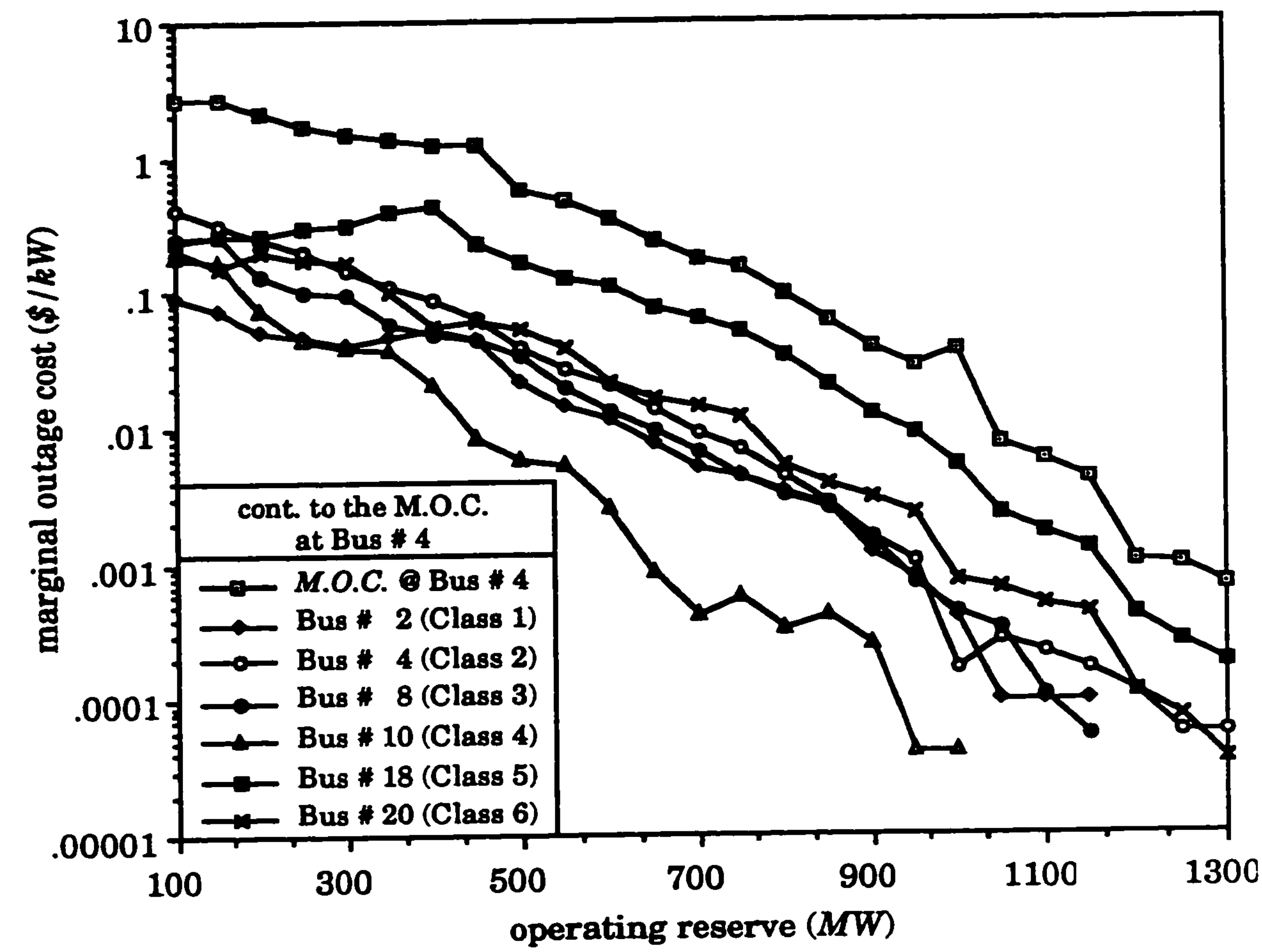

Figure 6.9. Contribution of selected buses in the various classes to the marginal outage cost of Bus 4 in the *IEEE-RTS*.

6.5.1. Comparison between the marginal outage costs of the *IEEE-RTS* calculated at *HLI* and *HLII*

The *IEEE-RTS* is a large power system with many generating units and transmission lines that can affect the value of the marginal outage cost at a particular bus. A comparison between the marginal outage cost profile calculated at *HLI* and that of Bus 4 calculated at *HLII* is made in this section to determine the contributions of the generation and transmission systems. The results from this comparison are shown in Figure 6.10. It can be seen from this figure that the marginal outage cost profiles calculated at *HLI* and *HLII* are in close agreement. The contribution of the transmission system is negligible for most operating reserves except when the system is heavily loaded (i.e. low operating reserve). The discontinuities in this profile indicate that the contribution of the transmission system at these operating reserves is either zero or negligible. The difference between the marginal outage cost profile calculated at *HLI* and the contribution of the generation system at *HLII* is significant in this case as compared to the *RBTS* due to the large size of the *IEEE-RTS*. It is expected, however, that if generating unit contingencies higher than the 4th order are evaluated at *HLII*, the difference between the profile calculated at *HLI* and the contribution of the generation system calculated at *HLII* will decrease.

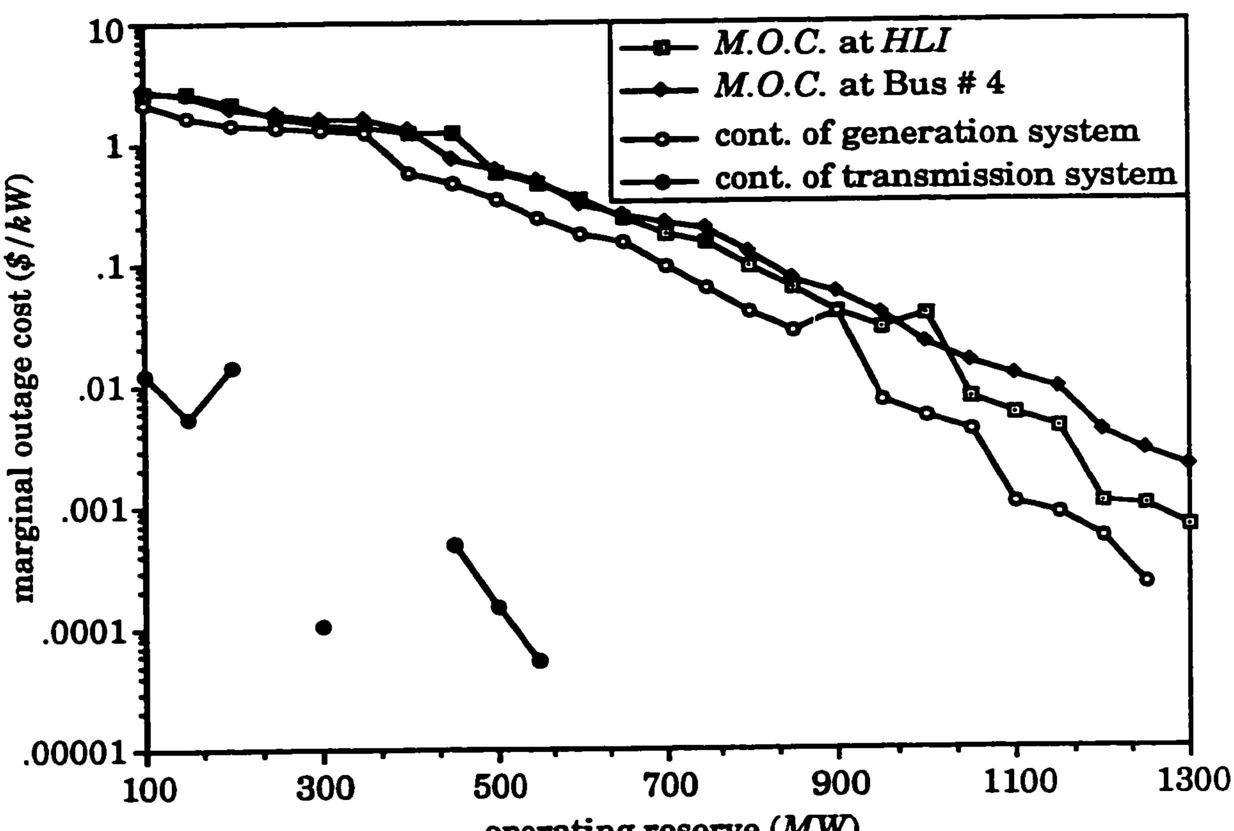

Figure 6.10. Comparison of the marginal outage cost profile calculated at *HLI* and that of Bus 4 calculated at *HLII* with the contributions of the generation and transmission systems of the *IEEE-RTS*.

6.6. Summary

This chapter presents a method for calculating the marginal outage costs at bulk customer load points in a composite generation and transmission system. The proposed method is illustrated by application to the *RBTS* and the *IEEE-RTS*. The application of the proposed method to the *RBTS* shows that the marginal outage cost at any load bus is independent of the location of the bus within the system except when it is radially fed. In the case of the *IEEE-RTS*, it is found that the marginal outage cost profiles at all the load buses are very similar. Comparisons between the marginal outage costs calculated using *HLI* and *HLII* analyses show that the values calculated at *HLI* are very close to those calculated at *HLII*. The contribution of the generation system in *HLII* studies is found to be much more significant than that of the transmission system. The contribution of the transmission system becomes more noticeable however when the system is heavily loaded.

7. SENSITIVITY OF THE MARGINAL OUTAGE COSTS IN COMPOSITE SYSTEMS TO SELECTED PERTINENT FACTORS

7.1. Introduction

The method used in Chapter 6 to calculate the marginal outage costs in composite systems can be considered to be reasonably comprehensive. This technique entails considering every possible contingency and examining it to see if the corresponding system problem will lead to load curtailment. Comprehensive evaluation of composite system reliability is very time consuming when applied to large power systems. In practical system studies, a number of approximations are normally made to the exact method in order to reduce the computing time. These approximations are done due to the lack of computational tools, lack of data or in order to meet the stringent turnaround time constraints of the operating environment. This chapter compares the marginal outage costs calculated using a number of approximations to the exact values of the *RBTS* and the *IEEE-RTS* reported in Chapter 6.

7.2. Sensitivity Studies Using the *RBTS*

Before implementing any approximations to an exact method, a number of sensitivity studies are usually conducted to see their impact on the accuracy of the results. Sensitivity analysis provides the means to examine the impact of perturbing selected pertinent factors and measuring the changes in the results. The high variability of data and the constraints placed on computational tools in the operating environment make such an analysis particularly attractive for marginal outage costing. In addition, sensitivity studies serve to provide further insight into the relationship between the various elements of the system. The following sub-sections illustrate the impacts of selected pertinent factors on the marginal outage costs associated with the composite system of the *RBTS*. The conclusions from these analyses are used in Chapter 8 to make recommendations for practical implementations of the proposed method of calculating the marginal outage costs in composite systems.

7.2.1. Effect of using aggregate system values

The method proposed in Chapter 6 for calculating the marginal outage costs in composite systems involves estimating the values of the *IEAR* and ΔEUE at individual load buses. This section examines the accuracy of evaluating the marginal outage costs using aggregate values for the whole system. The value of the aggregate *IEAR* for the *RBTS* as calculated in Table G.7 is 4.41 $\$/kWh$. The total system ΔEUE resulting from a load change at Bus k can be calculated by adding the values from the individual load buses as follows:

$$\Delta EUE_k(system) = \sum_{i=1}^{nbus} \Delta EUE_{ki}\,. \tag{7.1}$$

The marginal outage cost at Bus k is calculated by multiplying the aggregate system *IEAR* and the incremental expected unserved energy of the whole system resulting from a load increment at that bus. That is,

$$M.O.C._k = IEAR(aggregate) \times \Delta EUE_k(system). \tag{7.2}$$

Chapter 6 shows that there are two distinct marginal outage cost profiles for the *RBTS*. The sensitivity analyses presented in this and the following sub-sections are therefore applied to two different buses in the *RBTS*. The results from the studies conducted in this sub-section are compared to the exact values presented in Chapter 6 in Figure 7.1 for Buses 3 and 6 of the *RBTS*. It can be seen from this figure that there are small differences in the results that can be attributed to the utilization of the aggregate systems values. Further studies in Section 7.3 will examine the accuracy of the approximate method using the *IEEE-RTS*.

7.2.2. Effect of using the composite system *CCDF*

In calculating the *IEAR* values given in Table 6.1, it was necessary to develop a *CCDF* for each load bus in the *RBTS* using the procedure outlined in Appendix G. The development of a load bus *CCDF* requires extensive data to represent the customer outage costs at each load bus in the system. These data may not be available in practical systems and only the composite system *CCDF* may be known. In this case, the resulting *IEAR* values at the various load buses will be much closer to each other due to the utilization of a common cost model.

The purpose of this sub-section is to compare the marginal outage costs in the *RBTS* calculated using a composite system *CCDF* with those calculated using individual *CCDF*'s for each load bus in the system. The study was conducted for Buses 3 and 6 using the *IEAR* values given in Table G.8. All other modelling assumptions and parameters remain unchanged from the base case study reported in Chapter 6. The profiles resulting from the studies conducted in this sub-section are compared with the base case profiles in Figure 7.2.

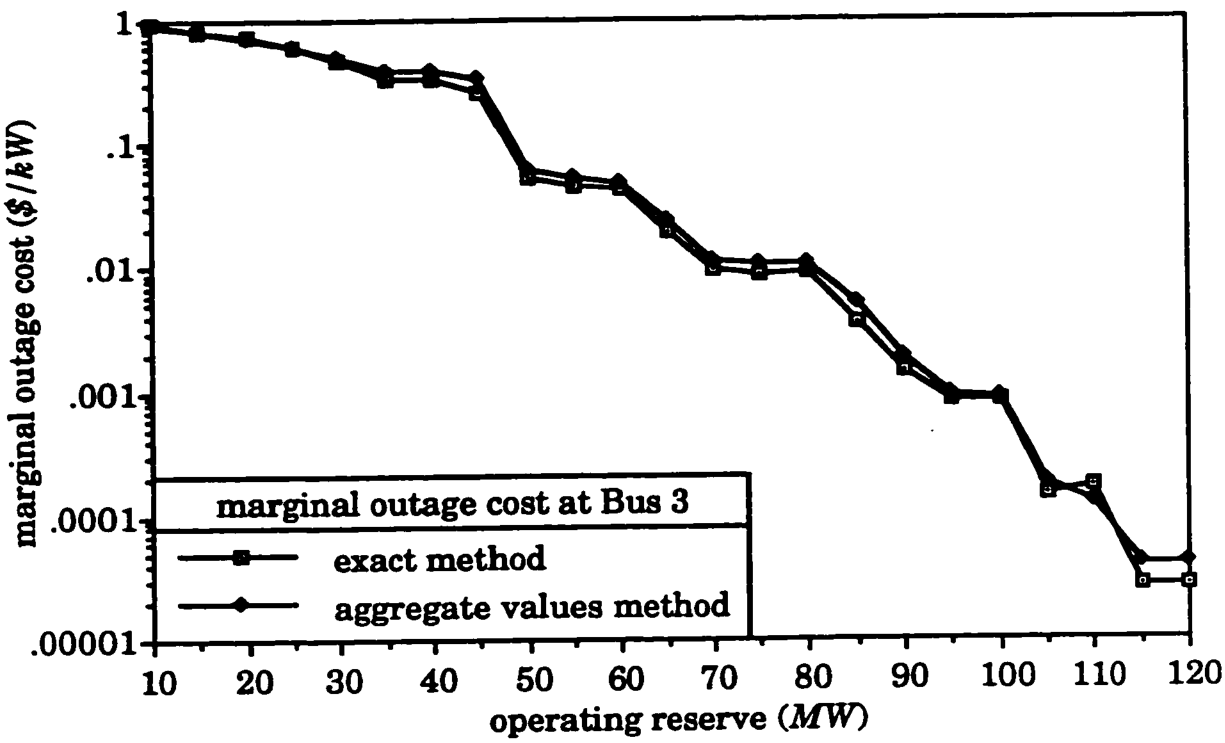

(a)

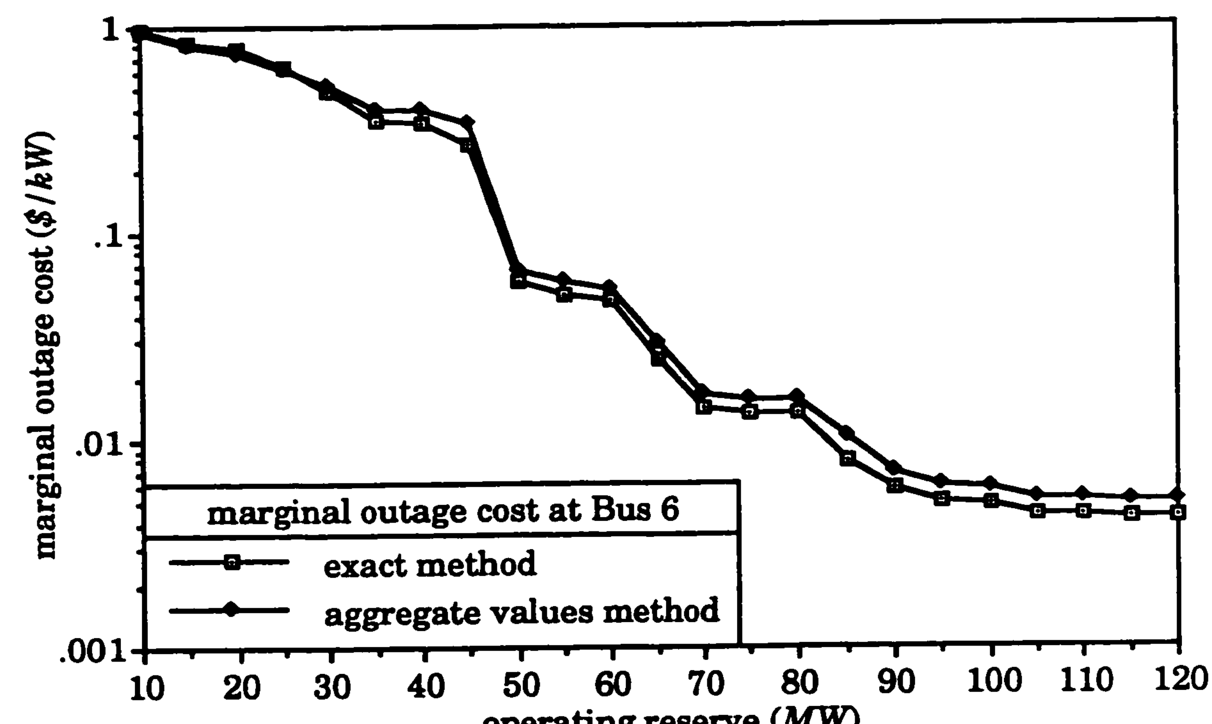

(b)

Figure 7.1. Effect of using the aggregate system values on the marginal outage cost profiles of Bus 3 (a) and Bus 6 (b) of the *RBTS*.

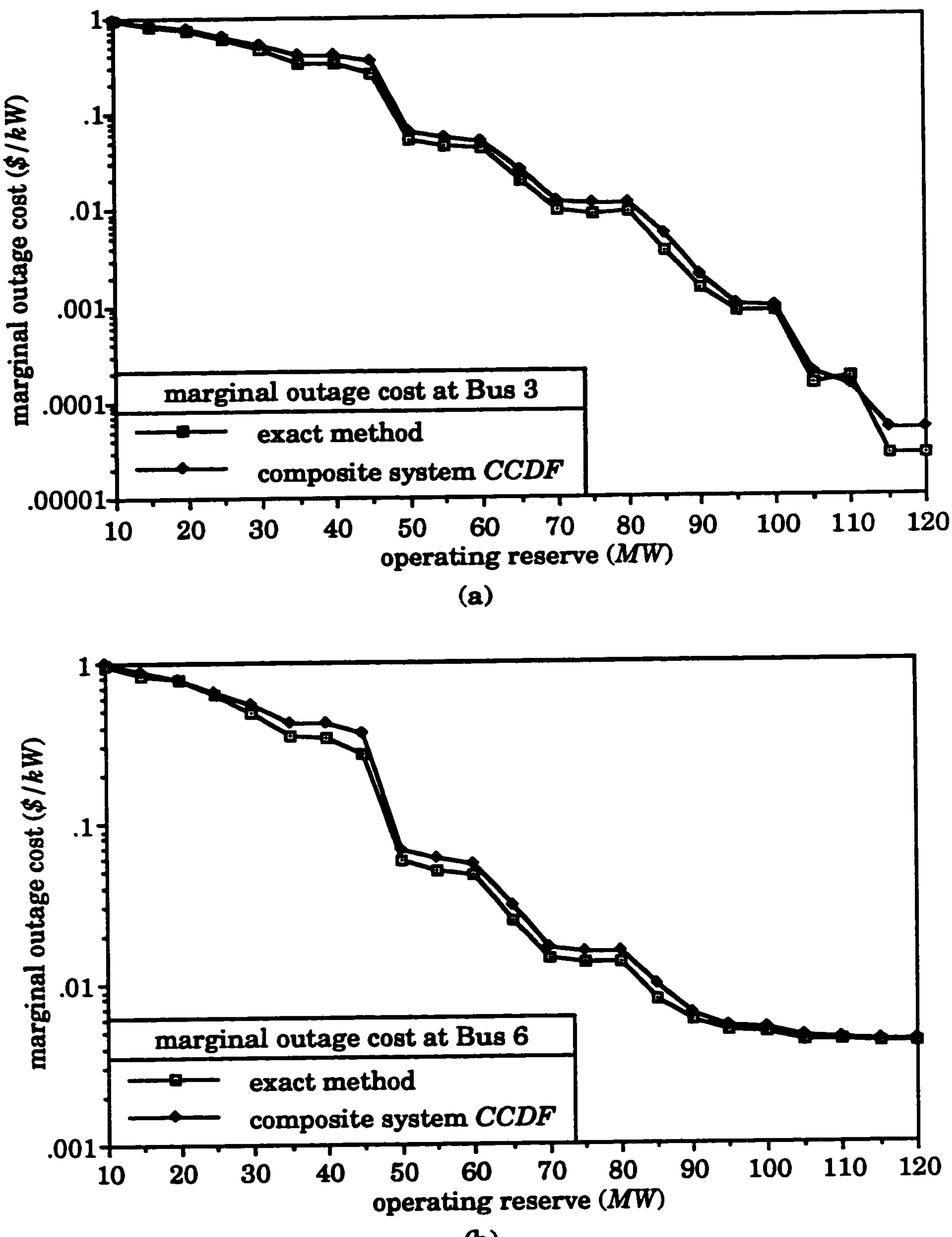

Figure 7.2. Effect of using the composite system *CCDF* on the marginal outage cost profiles of Bus 3 (a) and Bus 6 (b) of the *RBTS*.

It can be seen from Figure 7.2 that the marginal outage cost profiles of Buses 3 and 6 are not affected greatly by using the composite system *CCDF* in the calculation of the load bus interrupted energy assessment rates. Therefore, it can be reasonably concluded that the utilization of the composite system *CCDF* provides adequate estimates of the marginal outage cost at *HLII*.

7.2.3. Effect of *IEAR* variations with the peak load

The marginal outage costs presented in all the studies of Chapter 6 and the previous sub-sections of this chapter were evaluated based on the assumption that the *IEAR* values do not vary with the peak load of the system. In an actual system, the load does not stay at its peak value throughout the year. An evaluation of the marginal outage cost based on constant *IEAR*'s could give quite inaccurate results. The studies conducted in this sub-section examine the variations of the *IEAR* with the peak load and the impact of these variations on the marginal outage costs in the *RBTS*.

Before calculating the marginal outage cost, the variations in the *IEAR* with peak load are examined. The input data for this study are exactly the same as the base case input data except that the system load is varied from 65% to 124% of the given peak load of the *RBTS* (i.e. operating reserve is varied from 10 to 120 *MW*). The resulting variations in the *IEAR* with the peak load are presented graphically in Figure 7.3. It can be seen from this figure that the *IEAR* values of some load buses increase slightly as the peak load increases (operating reserve decreases). The object of the following study is to see if these variations in the *IEAR* values have any impact on the marginal outage costs of Buses 3 and 6 in the *RBTS*.

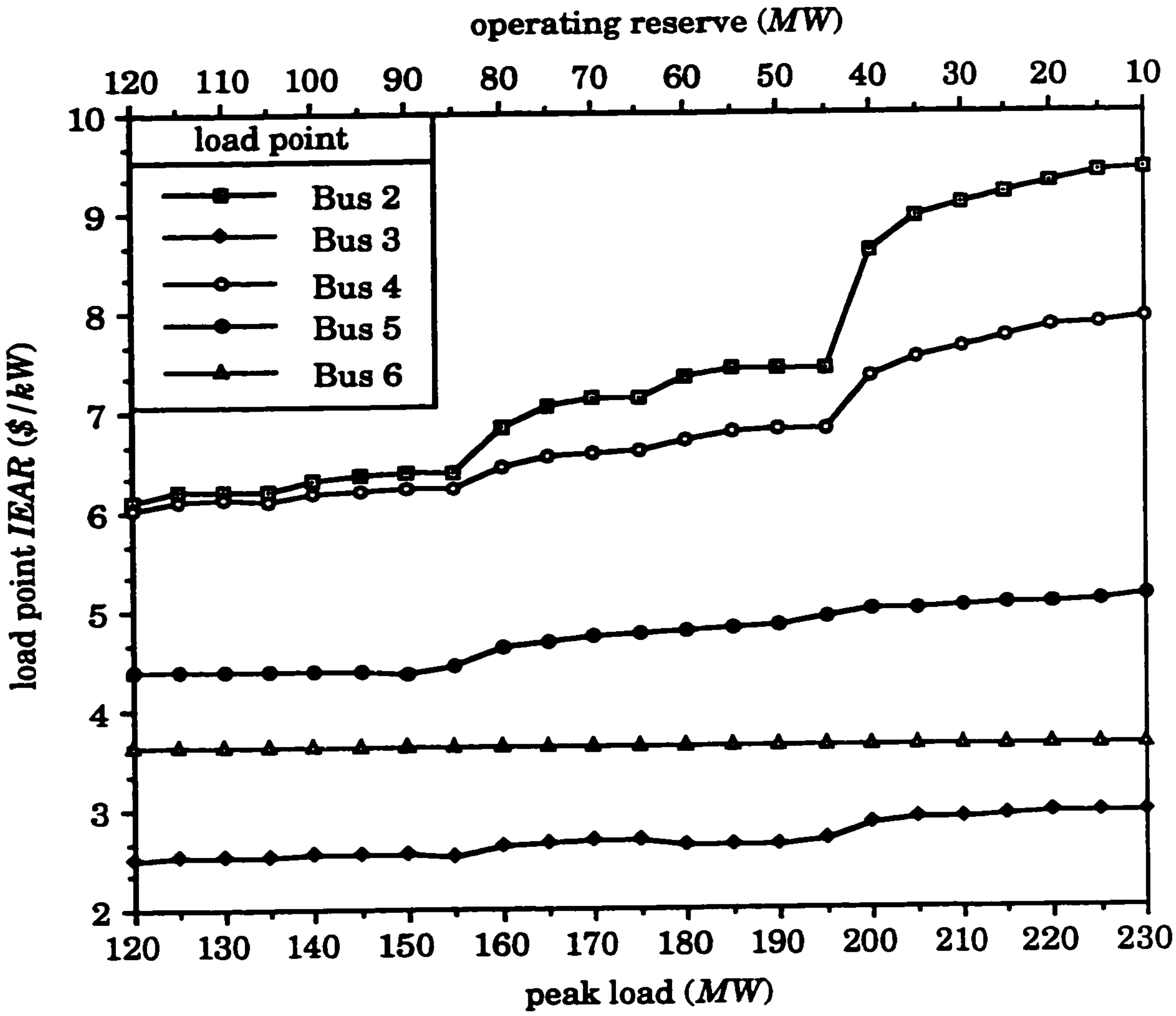

Figure 7.3. Variations of the *IEAR*'s at each load bus in the *RBTS* with the peak load.

The *IEAR* values shown in Figure 7.3 were used with the corresponding *ΔEUE* values at each operating reserve level to calculate the marginal outage costs of Buses 3 and 6 of the *RBTS*. The resulting marginal outage cost profiles are compared to the base case values (constant *IEAR*'s) in Figure 7.4. It can be seen from this figure that the profiles are in close agreement and therefore constant *IEAR* values can be used to calculate the marginal outage costs in small composite power systems.

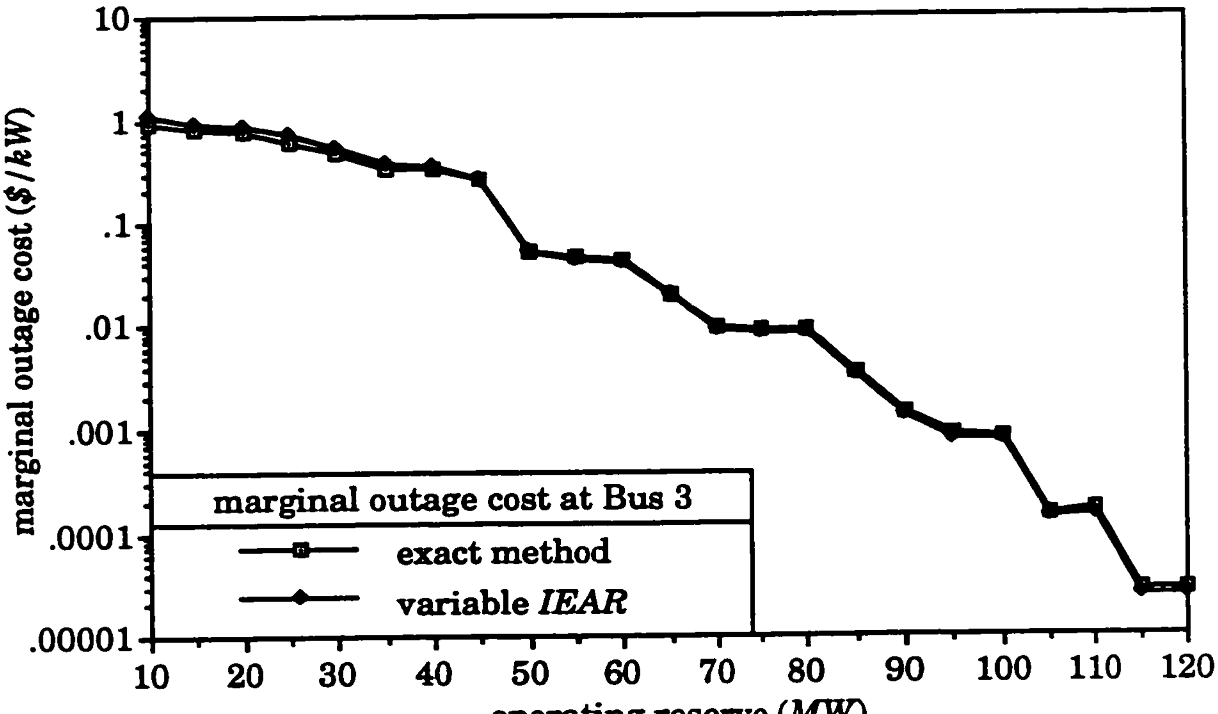

(a)

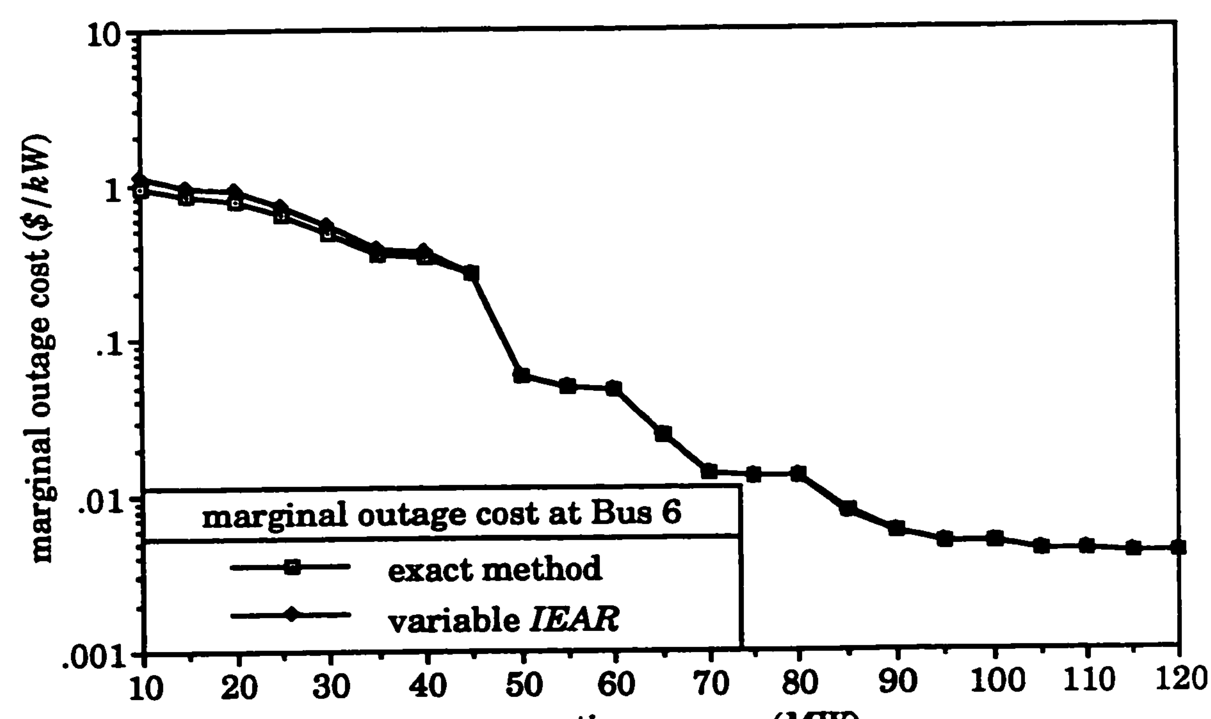

(b)

Figure 7.4. Effect of *IEAR* variations with the peak load on the marginal outage cost profiles of Bus 3 (a) and Bus 6 (b) of the *RBTS*.

7.2.4. Effect of using the average interruption duration to calculate the *IEAR*

The method used to calculate the *IEAR* at *HLII* can be considered to be reasonably comprehensive as this technique involves considering every possible contingency and examining it to see if the corresponding system problem will lead to load curtailment. The expected frequency, duration and load curtailment are used in (6.2) to obtain the *IEAR*. This method requires considerable computing time and storage to examine all the contingencies in a large power system. These requirements can be reduced and acceptable *IEAR* estimates can be calculated from the average interruption duration of power outages [58]. The equation for calculating the *IEAR* at a given Bus i from the average interruption duration is given by [58]:

$$IEAR_i = \frac{C_i(d_{ia})}{d_{ia}} \qquad (\$/kWh), \qquad (7.3)$$

where d_{ia} : average interruption duration for load Bus i (hours) and
$C_i(d_{ia})$: interruption cost to customers at Bus i caused by an outage of duration d_{ia} ($\$/kW$).

The most important benefit of using the above approximate method to calculate the *IEAR* is the fact that the average interruption duration can be calculated using simple programs that are not as detailed as *COMREL*. The *IEAR* values for the various load buses of the *RBTS* were calculated using the above method and the results are given in Table G.8. These values were used together with the corresponding ΔEUE values at the various buses to calculate the marginal outage cost profiles for Buses 3 and 6 of the *RBTS*. These profiles are compared to the corresponding base case profiles in Figure 7.5. It is clear from this figure that the approximate method provides an accurate means of calculating the marginal outage cost at *HLII*.

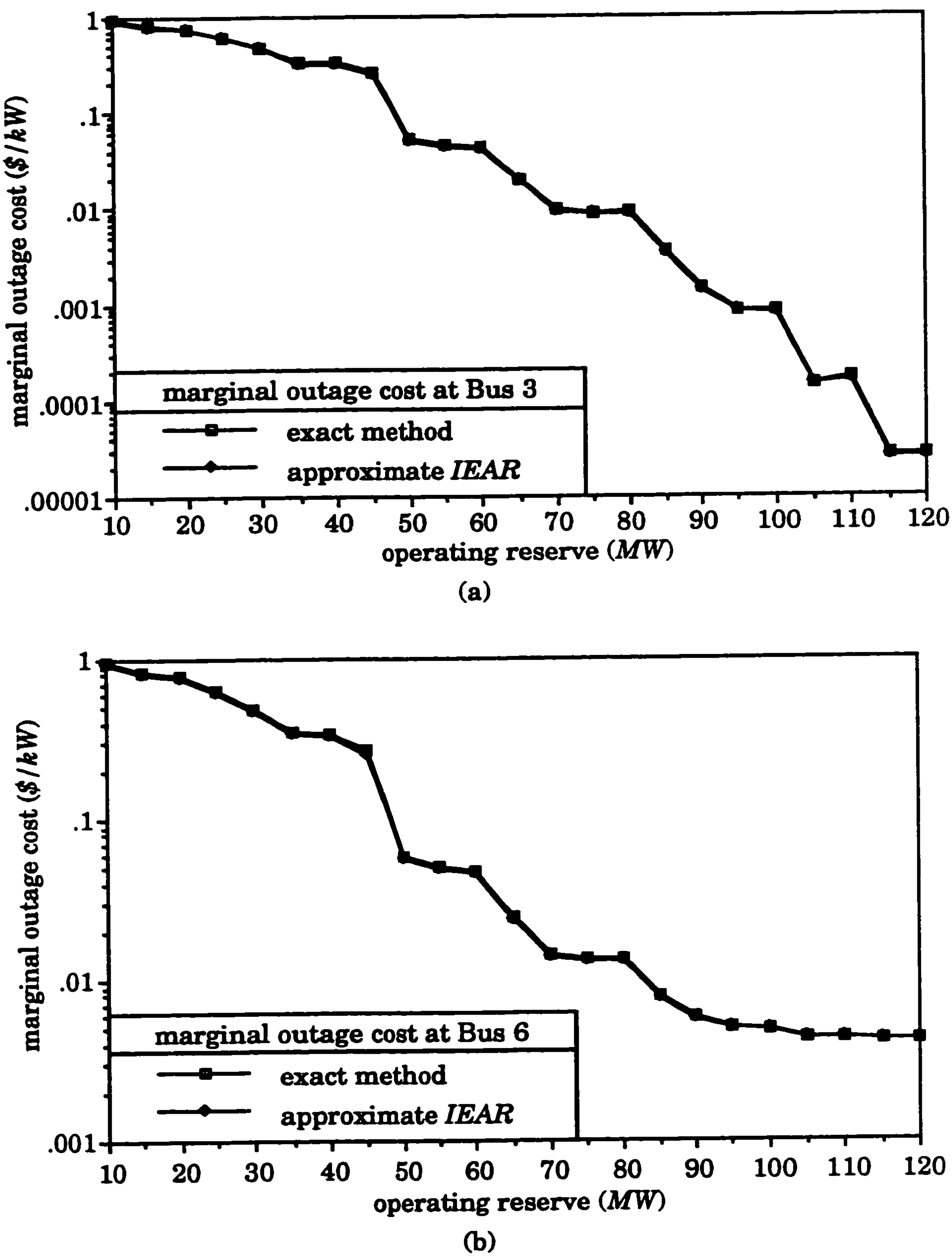

Figure 7.5. Effect of using approximate *IEAR*'s on the marginal outage cost profiles of Bus 3 (a) and Bus 6 (b) of the *RBTS*.

A review of all the studies conducted in the previous sub-sections reveals that the marginal outage cost at *HLII* can be accurately estimated using a constant *IEAR* for the aggregate system. The *IEAR* may be calculated using the same composite system *CCDF* at each load bus and using the approximate method given by (7.3). The sensitivity analyses conducted in the previous sub-sections show that the variation of the *IEAR* with the peak load and bus location have insignificant effects on the marginal outage cost.

7.2.5. Effect of load flow solutions

The adequacy appraisal of a bulk power system entails the solution of a network configuration under selected outage situations. A number of solution techniques, depending on the adequacy criteria employed and the intent behind the studies, are available to analyze the adequacy of a power system, In composite systems reliability evaluation, load flows must be repeated for each examined state in the process and the efficiency of the entire evaluation depends a great deal upon the load flow algorithm employed. The three basic analytical techniques that are usually employed in composite generation and transmission adequacy studies are the network flow method, the *DC* load flow methods and the *AC* load flow methods. In general, line overloads can be estimated from less accurate load flows such as the network flow and the *DC* load flow methods.

The *COMREL* program has the capability of utilizing any one of the three load flow methods in quantitative adequacy assessment of composite systems [76-78]. The purpose of this study is to ascertain the impact of these solutions techniques on the marginal outage cost of the *RBTS*. The *IEAR* values of each load bus in the *RBTS* were calculated using each network solution method and the results are given in Table G.8. These values were then used to calculate the marginal outage cost profiles of Buses 3 and 6 of the *RBTS* as shown in Figure 7.6 . The results from the *AC* and *DC* load flow methods are not profoundly different and for all practical purposes, the results from the network flow method are acceptable when compared with the *AC* load flow method.

7.2.6. Effect of load curtailment philosophy

The curtailment of load at the customer load points in the event of a deficiency in the generation capacity can be decided in a number of ways depending on the relative priority assigned to each of the major load centres. As noted in Sub-section 6.2.5, the load at each load bus is usually designated as curtailable and firm load. The impact of a system disturbance that results in swing bus overload (i.e. an indication of capacity deficiency in the system) can be confined to a small or large region of the system. If the relative importance of the load at a bus is such that the firm load at the customer load point will not be curtailed unless it is inevitable, then it is quite obvious that more buses in the system will experience load curtailment. These provisions have been made in the load curtailment philosophy algorithm utilized in the *COMREL* program by defining three different load curtailment passes. The details of these load curtailment passes are given in [77] and only their salient features are presented in the following paragraph.

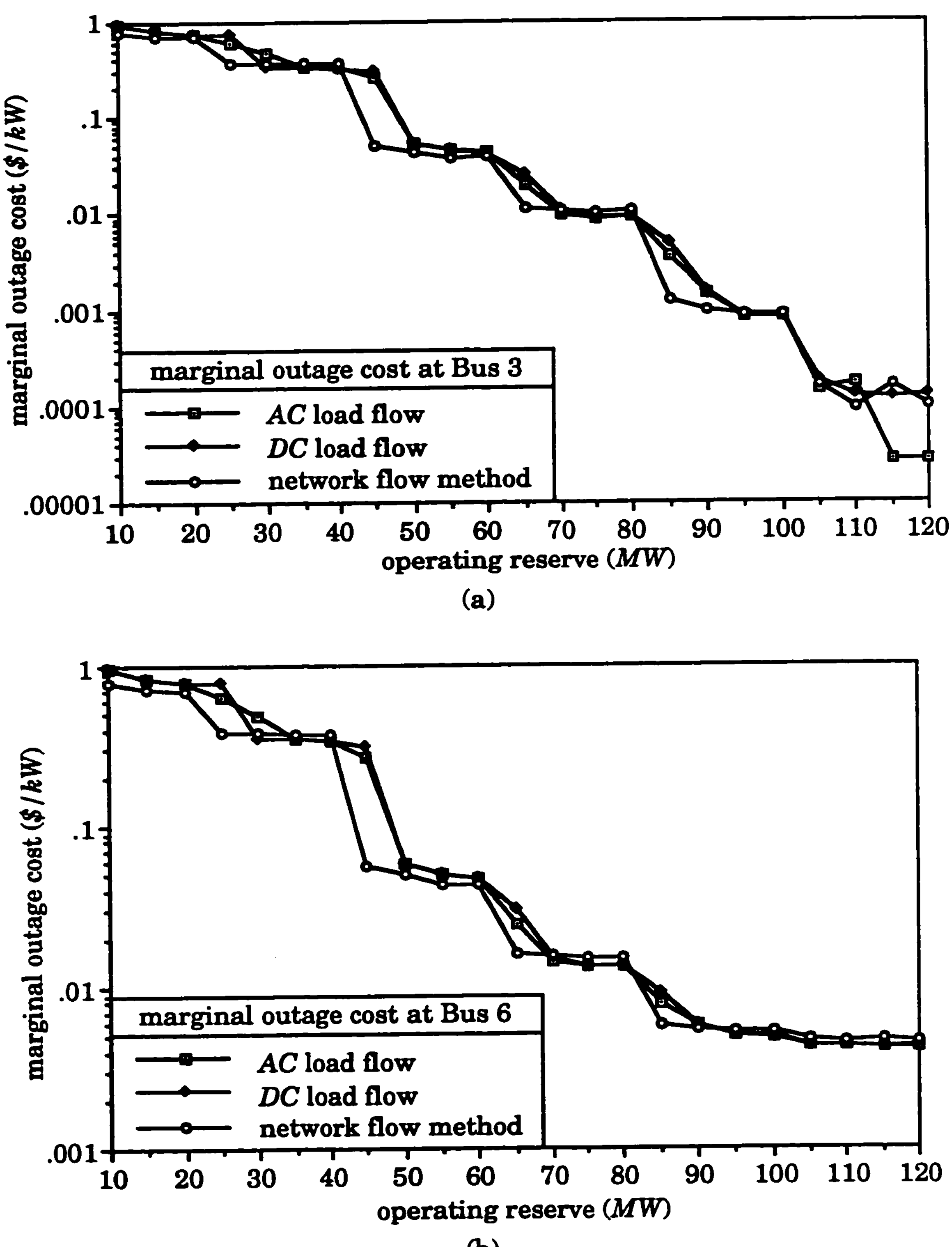

Figure 7.6. Effect of load flow solutions on the marginal outage cost profiles of Bus 3 (a) and Bus 6 (b) of the *RBTS*.

In the case of contingencies involving generating units, load curtailment *Pass 1* covers those buses at which the generating units under outage are physically connected and are one line away and receiving power from these generator buses. In the event of line outages, *Pass 1* encompasses the receiving end bus(es) of the lines under outage and buses that are one line away and taking power from these receiving end buses. In the case of both generator and line outages, *Pass 1* covers those buses at which the generating unit under outage are physically connected, the receiving end bus of the line under outage and those buses which are one line away from the receiving end buses and are taking power for them. The swing bus overload is alleviated by proportional interruption of the curtailable load at the buses that fall under load curtailment *Pass 1*. Load curtailment *Pass 2* covers *Pass 1* and all those buses that are two lines away from the generator outage buses and/or receiving end buses for a line outage and are being fed directly from the buses covered under *Pass 1*. Finally, in load curtailment *Pass 3*, the buses covered are as noted for *Pass 2* and those additional buses which are three lines away from the generator buses and/or receiving end buses for a line outage and are being fed from the buses that are two lines away and covered under *Pass 2*. The previous studies in this chapter were all obtained using *Pass 1*.

The effect of these three passes on the marginal outage costs in the *RBTS* are examined in this study. The *IEAR* values of each load bus in the *RBTS* for *Pass 2* and *Pass 3* are given in Table G.8. The other input data from the base case and the *AC* load flow are used. The outcome of the study for Buses 3 and 6 of the *RBTS* are graphically depicted in Figure 7.7. It can be seen from this figure that the marginal outage cost profiles of Buses 3 and 6 are not affected by the number of load curtailment passes.

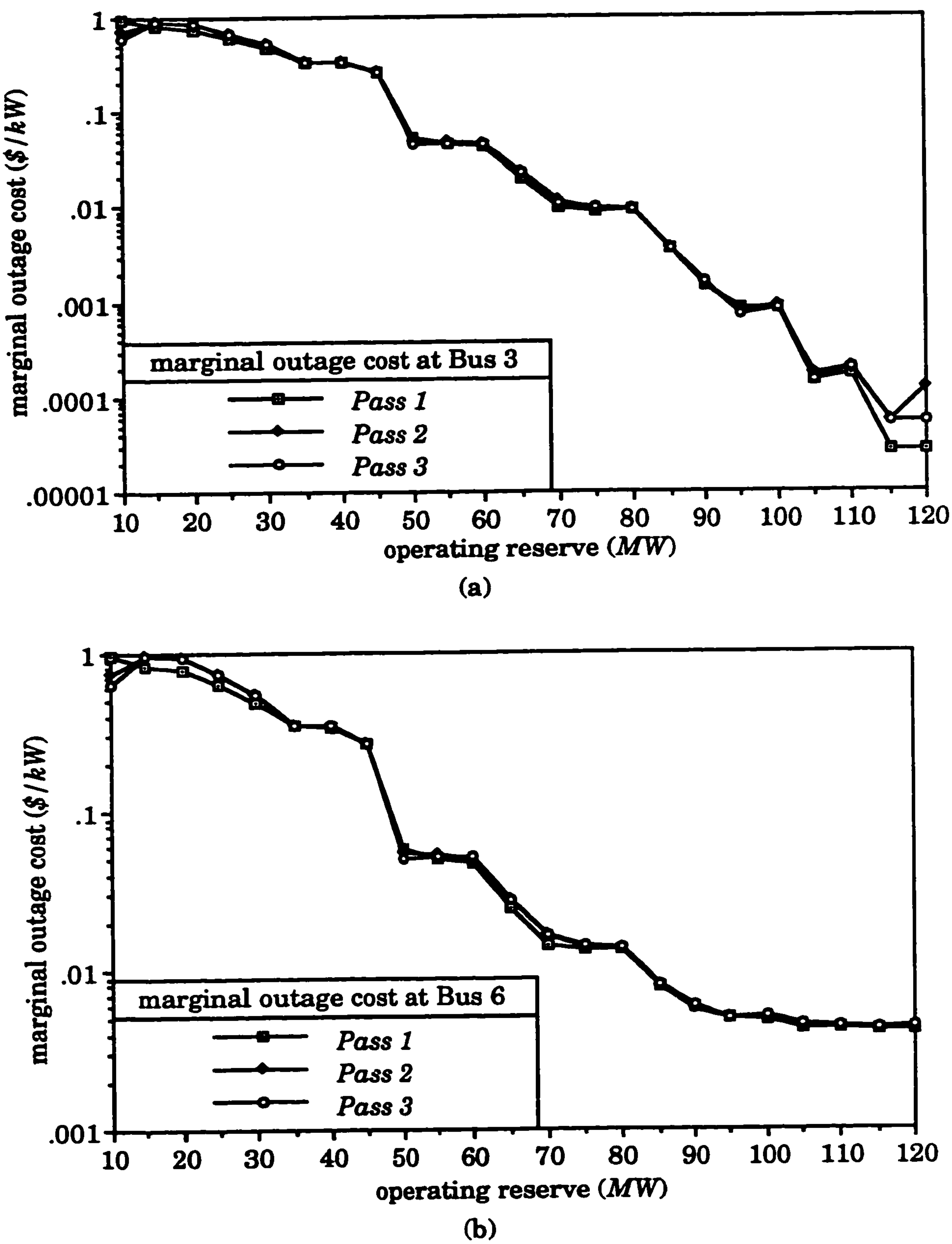

Figure 7.7. Effect of load curtailment philosophy on the marginal outage cost profiles of Bus 3 (a) and Bus 6 (b) of the *RBTS*.

7.2.7. Effect of removing components for maintenance

In practical applications of spot pricing, both the marginal operating cost and the marginal outage cost have to be calculated for every hour in the forecast period given the configuration of the system at that time. This process requires lengthy computations that may prevent the user from utilizing composite system reliability programs due to the stringent turnaround requirements of the operating environment. A number of approximations to the exact method of calculating the marginal outage cost at *HLII* are discussed in the previous sub-sections. The purpose of these approximations is to reduce the computing time without significantly compromising the accuracy of the results. This section examines the effects on the marginal outage cost of removing a few components for maintenance to see if a number of pre-calculated marginal outage cost profiles can be used for selected system topologies.

The first study examines the effects of removing generating units for maintenance on the marginal outage cost profiles of Buses 3 and 6 of the *RBTS*. The results are compared to the base case (i.e. no maintenance) in Figure 7.8. It can be seen from this figure that the effect on the marginal outage cost of removing 10 or 20 *MW* of generating capacity is small. As the capacity on maintenance increases, however, the profiles of both buses decrease. Therefore, it can be concluded that the marginal outage cost at *HLII* is affected by the magnitude of the generating capacity removed for maintenance. The validity of this conclusion will be tested in the following section using the *IEEE-RTS* which is a more practical system.

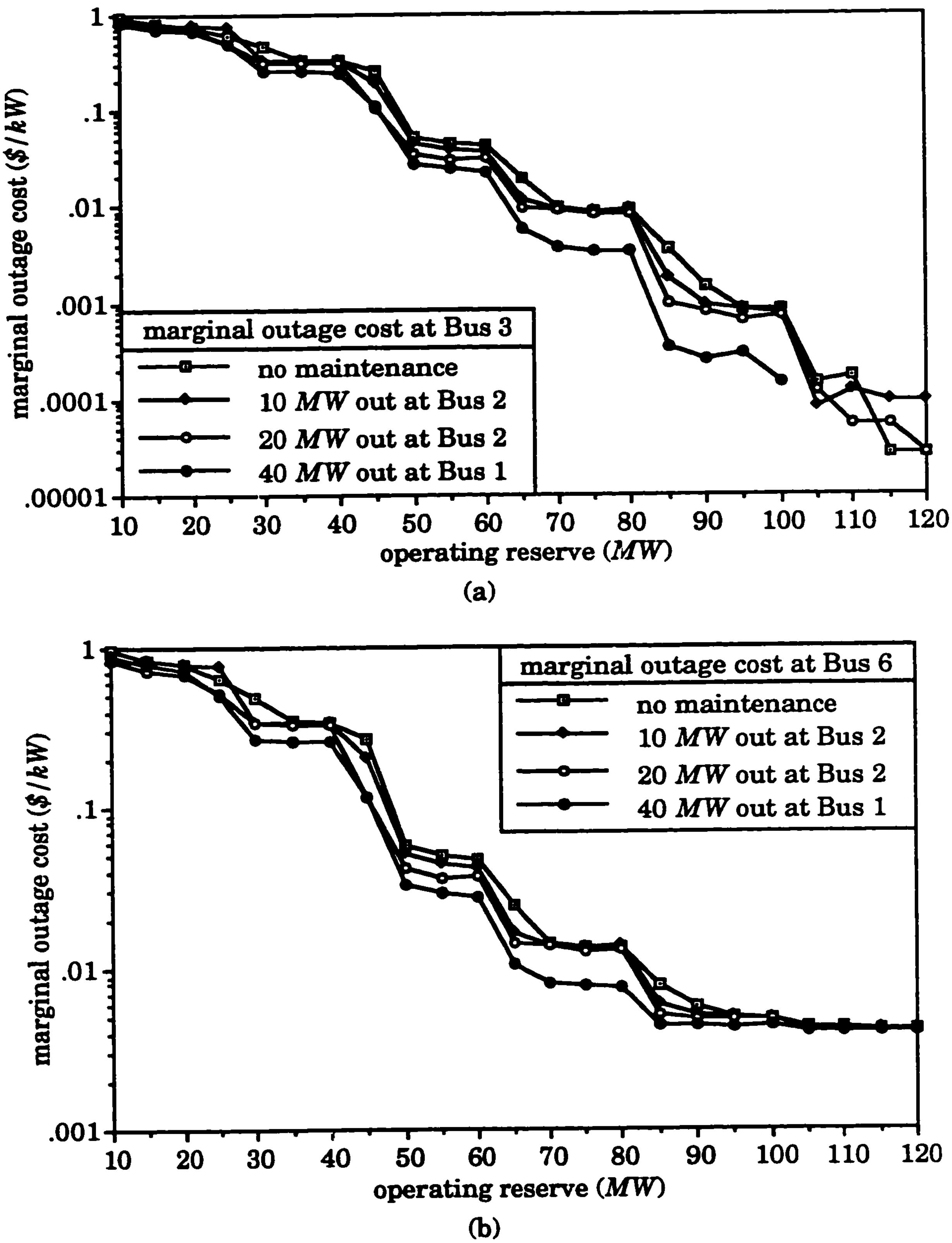

Figure 7.8. Effect of removing a few generating units for maintenance on the marginal outage cost profiles of Bus 3 (a) and Bus 6 (b) of the *RBTS*.

In the second study, all the generating units were assumed to be available and the effects on the marginal outage cost of removing a number of transmission lines for maintenance were examined. The results from this study are compared to the base case (i.e. no maintenance) in Figure 7.9. It can be observed from this figure that the removal of Line *L1* has the largest impact on the marginal outage cost while the effect of removing *L4* or *L5* for maintenance is negligible. Therefore, a number of pre-calculated profiles can be used for selected system topologies instead of performing detailed system studies in each case. The effect of system size on this conclusion will be tested in the following section using the *IEEE-RTS*.

7.3. Sensitivity Studies Using the *IEEE-RTS*

The following sub-sections examine the effects of the approximations discussed in Section 7.2 on the marginal outage costs associated with the composite system of the *IEEE-RTS*. Chapter 6 shows that the marginal outage costs of load buses in all five classes of the *IEEE-RTS* are equivalent and therefore only the results for Bus 4 are presented in the following sub-sections.

7.3.1. Effect of using aggregate system values

In this study, the marginal outage cost of Bus 4 in the *IEEE-RTS* was calculated from the aggregate system values of the *IEAR* and ΔEUE using (7.2). The aggregate *IEAR* value of the *IEEE-RTS* as given in Table H.6 is 4.22 $\$/kWh$. The results from this study are compared to the exact values calculated in Chapter 6 in Figure 7.10. It can be seen from this figure that the profiles compare favourably and therefore the aggregate system values can be used to calculate the marginal outage cost at *HLII* in large power systems.

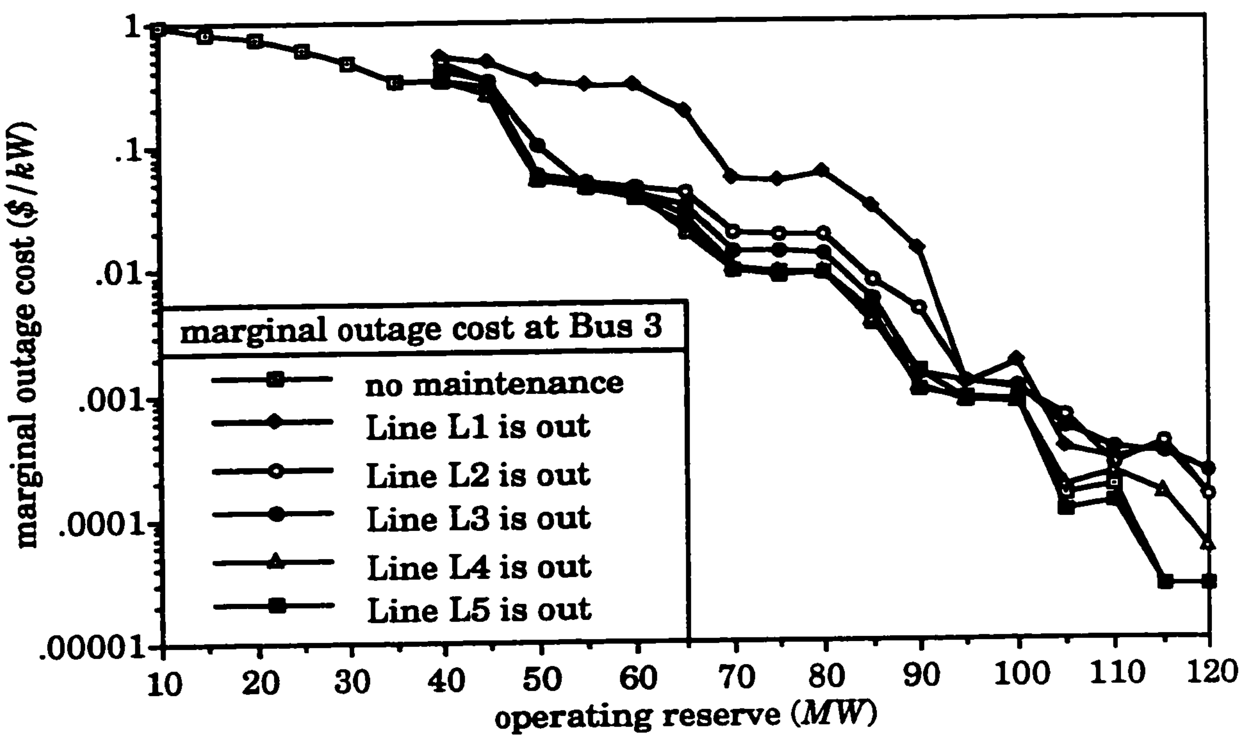

(a)

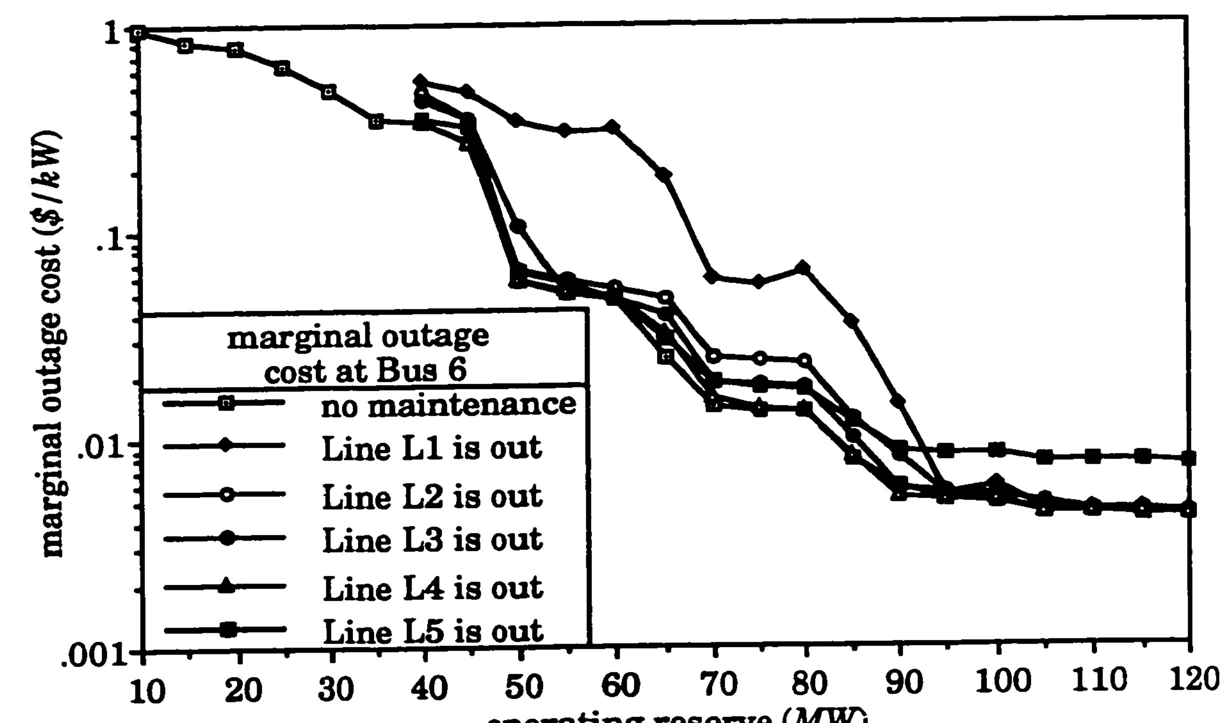

(b)

Figure 7.9. Effect of removing a few transmission lines for maintenance on the marginal outage cost profiles of Bus 3 (a) and Bus 6 (b) of the *RBTS*.

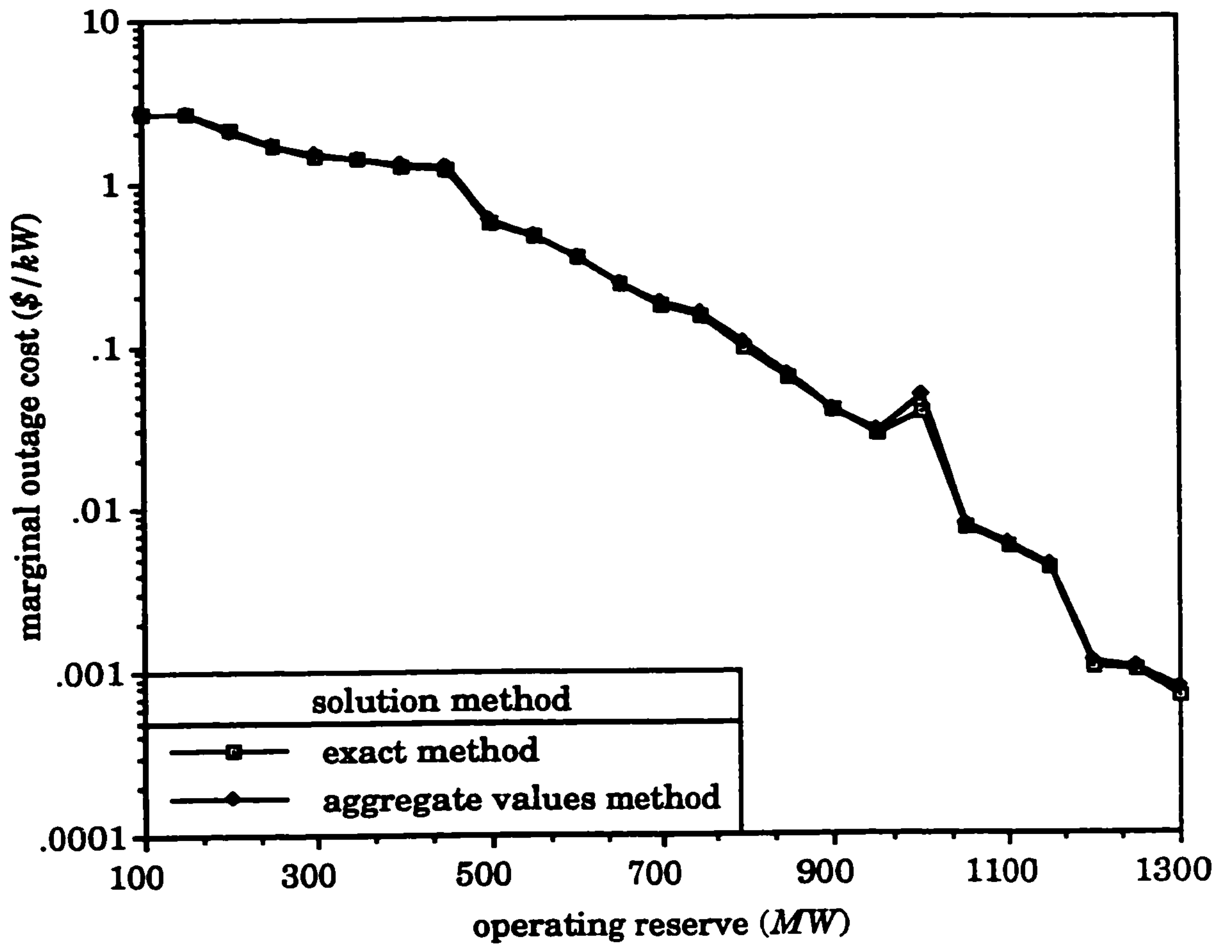

Figure 7.10. Effect of using the aggregate system values on the marginal outage cost profile of Bus 4 of the *IEEE-RTS*.

7.3.2. Effect of using the composite system *CCDF*

The *IEAR* values used in the base case are derived from individual *CCDF*'s for the load buses. This study compares the base case profile of Bus 4 in the *IEEE-RTS* to another one calculated using *IEAR*'s that are derived from the composite system *CCDF*. The *IEAR* values used in this study are given in Table H.7. The two profiles are compared in Figure 7.11 which shows that the difference between them is insignificant.

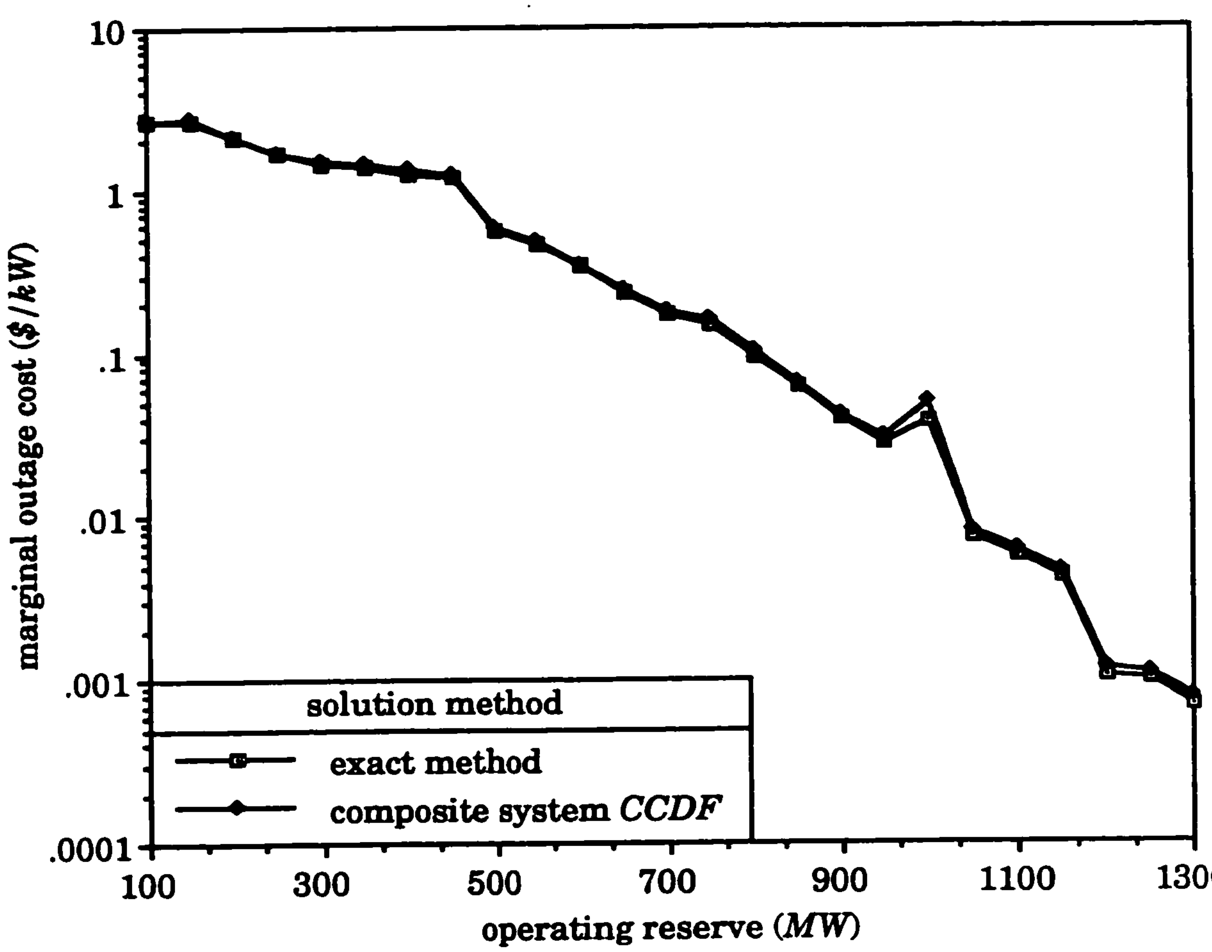

Figure 7.11. Effect of using the composite system *CCDF* on the marginal outage cost profile of Bus 4 of the *IEEE-RTS*.

7.3.3. Effect of *IEAR* variations with the peak load

Variations of the *IEAR* with the peak load and the effects of these variations on the marginal outage cost are discussed in this sub-section. The effect of changing the peak load on the *IEAR*'s of selected buses in each class of the *IEEE-RTS* is illustrated in Figure 7.12. The impact of these variations on the marginal outage cost profile of Bus 4 are shown in Figure 7.13. It is clear from this figure that the variations in the values of the *IEAR*'s have no detectable effect on the marginal outage cost profile of Bus 4.

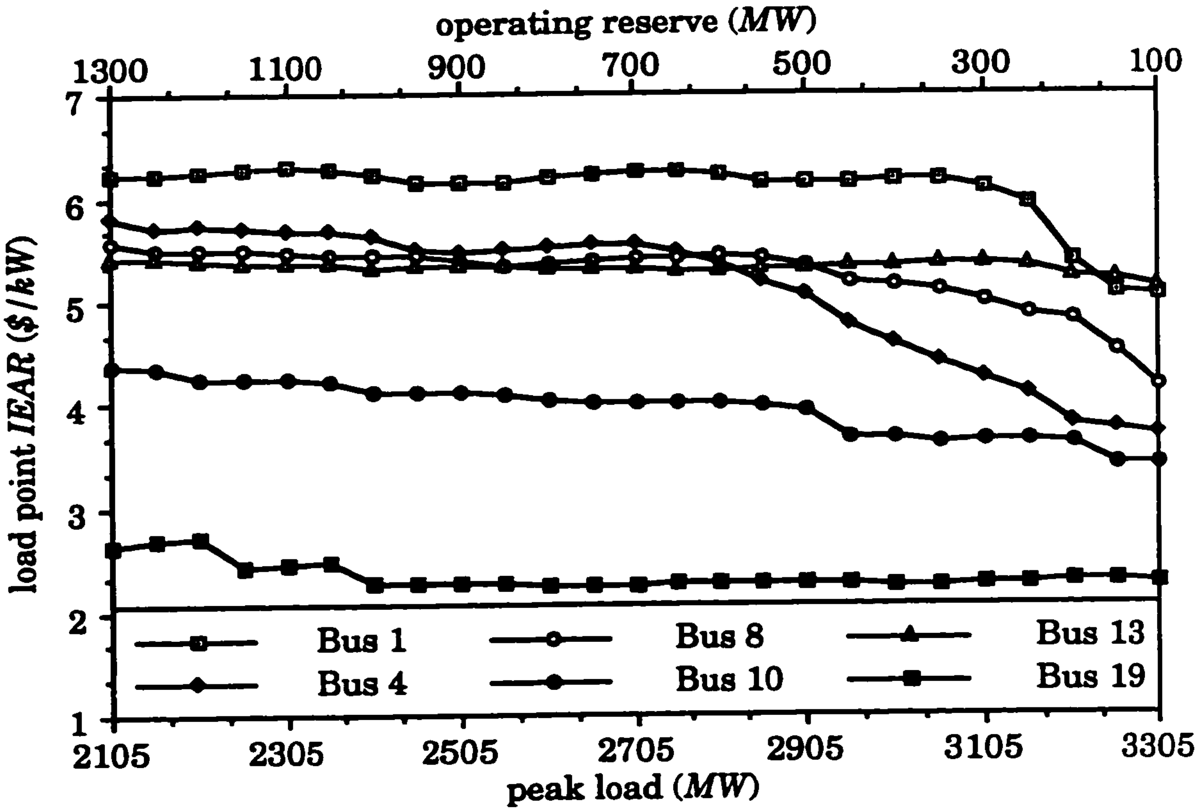

Figure 7.12. Variations of the *IEAR's* at selected buses in each class of the *IEEE-RTS* with the peak load.

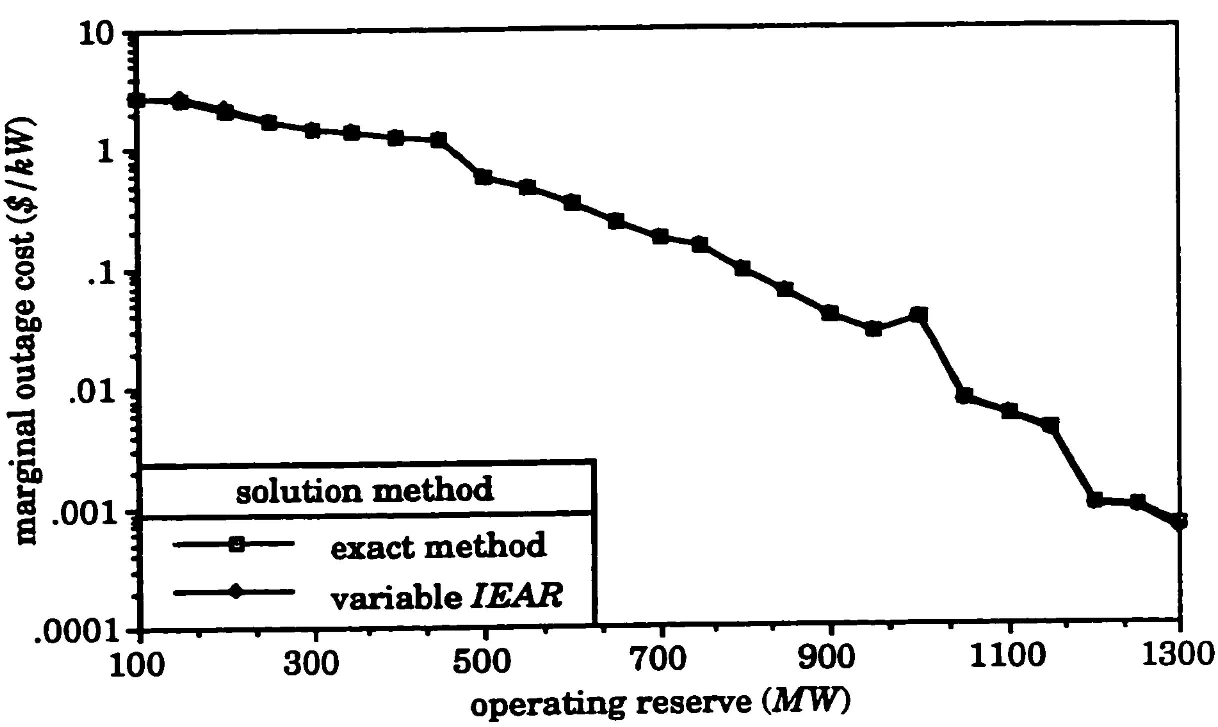

Figure 7.13. Effect of *IEAR* variations with the peak load on the marginal outage cost profile of Bus 4 of the *IEEE-RTS*.

7.3.4. Effect of using the average interruption duration to calculate the *IEAR*

Calculation of the *IEAR* at individual load buses using (6.2) requires the utilization of a composite system reliability program such as *COMREL*. Electric utilities have been reluctant to use such programs in the operating environment due to their excessive computing time requirements. Simpler programs capable of estimating the average values of interruption durations, load curtailed and energy curtailed are used instead. Therefore, it is particularly important to see if the utilization of these average indices has any adverse effect on the marginal outage costs associated with large composite power systems.

In order to do this, the *IEAR* values at each load bus in the *IEEE-RTS* were calculated using the approximate method based on the average interruption duration and given by (7.3). The results are given in Table H.7. The marginal outage cost profile of Bus 4 was calculated from these values and is compared to the base case profile in Figure 7.14. This figure shows that the results from the approximate method are in close agreement with those calculated using the exact method for all operating reserves.

It can be concluded from the studies conducted so far that the marginal outage costs associated with large composite power systems such as the *IEEE-RTS* are not affected by the approximations used to calculate the *IEAR*. A constant *IEAR* value for the aggregate system and derived from the individual *CCDF's* of the load buses or the composite system *CCDF* can be utilized.

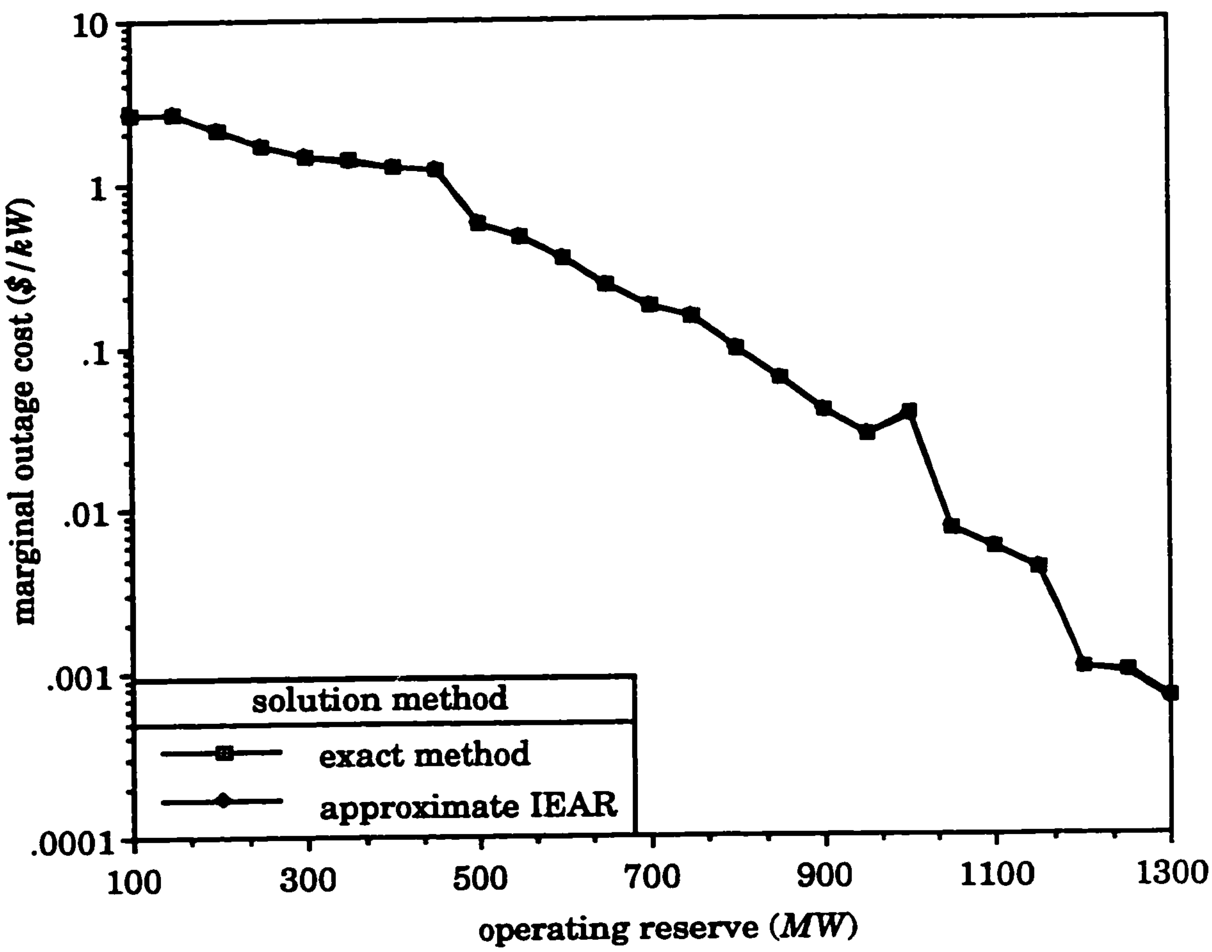

Figure 7.14. Effect of using approximate *IEAR*'s on the marginal outage cost profile of Bus 4 of the *IEEE-RTS*.

7.3.5. Effect of load flow solutions

The evaluation of the marginal outage costs in the *IEEE-RTS* at *HLII* using the *AC* load flow method is very time consuming. This sub-section examines the effect of the other two network solution methods on the marginal outage cost of Bus 4. The *IEAR* values for each solution method used in this study are given in Table H.7. The marginal outage cost profiles of Bus 4 calculated using each one of the network solution methods are compared in Figure 7.15. This figure shows that the results from the *AC* load flow and the *DC* load flow methods are identical. The results of the network flow method are slightly lower but can be used to provide reasonable estimates of the marginal outage cost at *HLII*. Therefore, it can be concluded that any one of the load flow solution methods can be used in marginal outage costing.

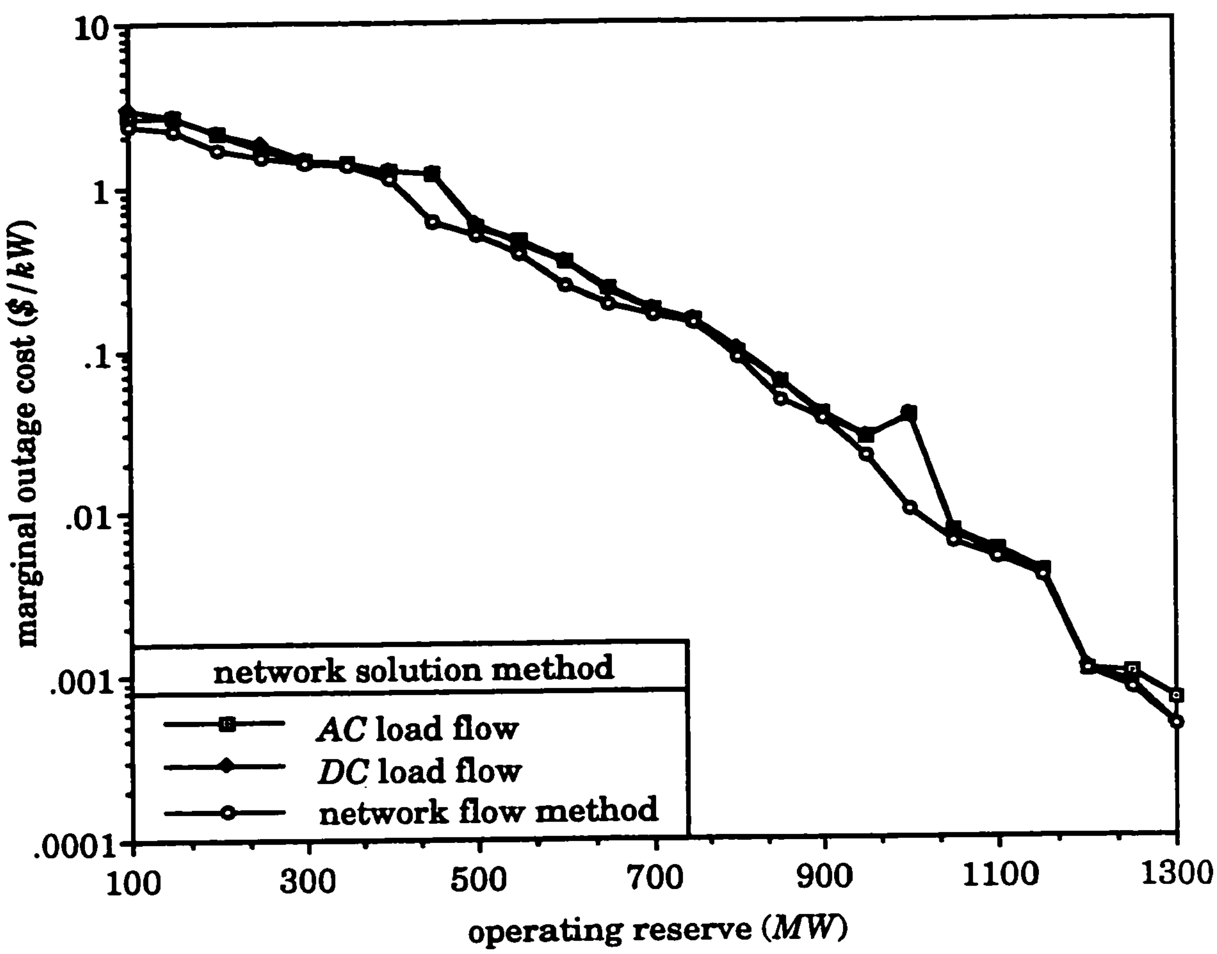

Figure 7.15. Effect of load flow solutions on the marginal outage cost profile of Bus 4 of the *IEEE-RTS*.

7.3.6. Effect of load curtailment philosophy

The effect of the load curtailment philosophy on the marginal outage cost of Bus 4 in the *IEEE-RTS* is examined in this study. The *IEAR* values for each load bus in the *IEEE-RTS* for *Pass 2* and *Pass 3* are given in Table H.7. The other input data from the base case and the *AC* load flow are used.

The results for all three passes are compared in Figure 7.16. It is observed from this figure that the load curtailment philosophy has no significant impact on the marginal outage cost calculated at *HLII*.

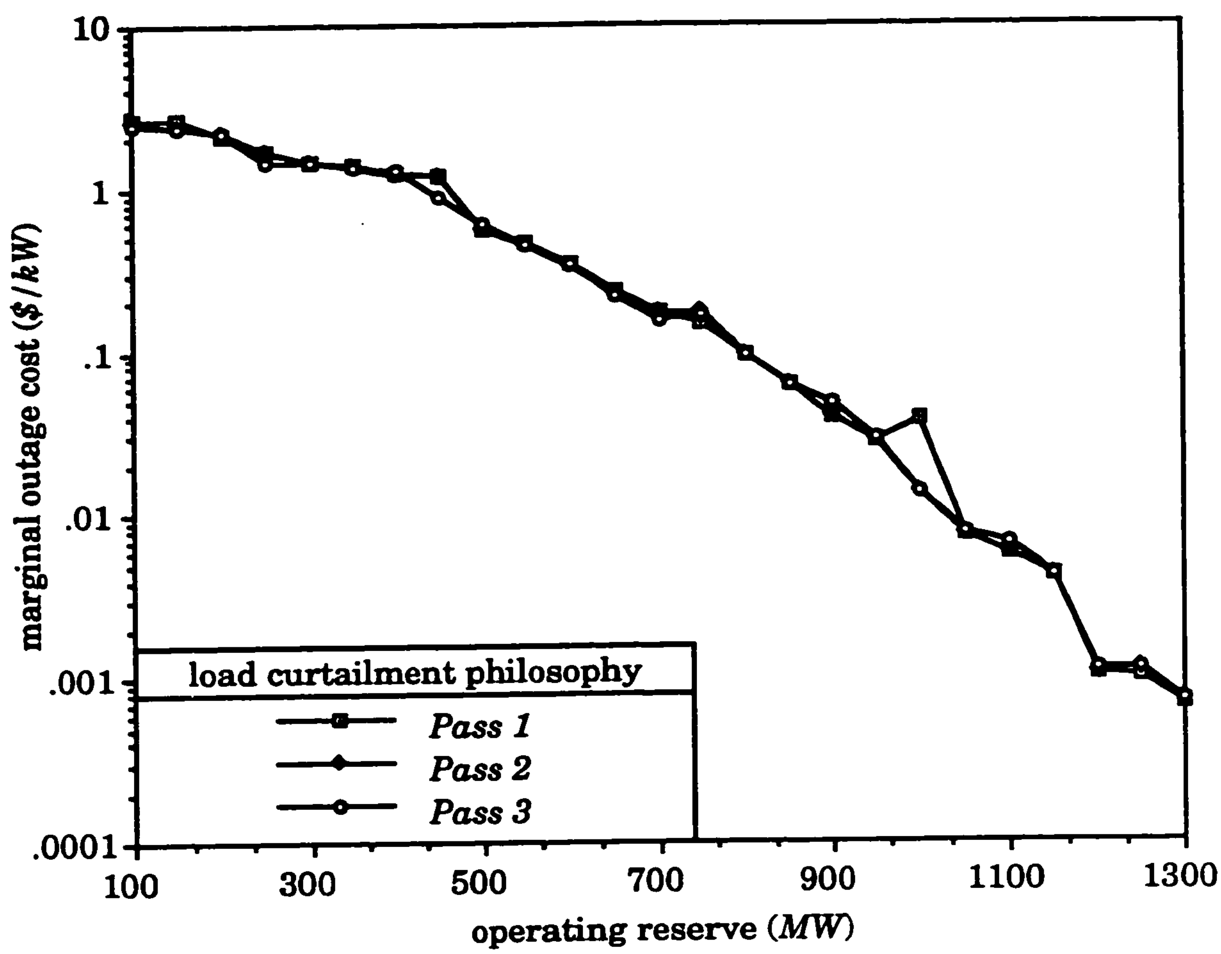

Figure 7.16. Effect of load curtailment philosophy on the marginal outage cost profile of Bus 4 of the *IEEE-RTS*.

7.3.7. Effect of removing components for maintenance

This section illustrates the effects of removing a few components for maintenance on the marginal outage cost profile of Bus 4 in the *IEEE-RTS*. The results of removing a few generating units and transmission lines are compared to the base case (i.e. no components on maintenance) in Figures 7.17 and 7.18 respectively. It can be seen from these figures that the removal of generating units for maintenance has a larger impact on the marginal outage cost of Bus 4 than the removal of transmission lines. This is due in part to the small contribution of the transmission system to the overall marginal outage cost as discussed in Chapter 6. However, it should be noted that if a large number of transmission lines should be removed for maintenance, the remaining lines will become heavily loaded and subsequently their contribution to the marginal outage cost will be more significant.

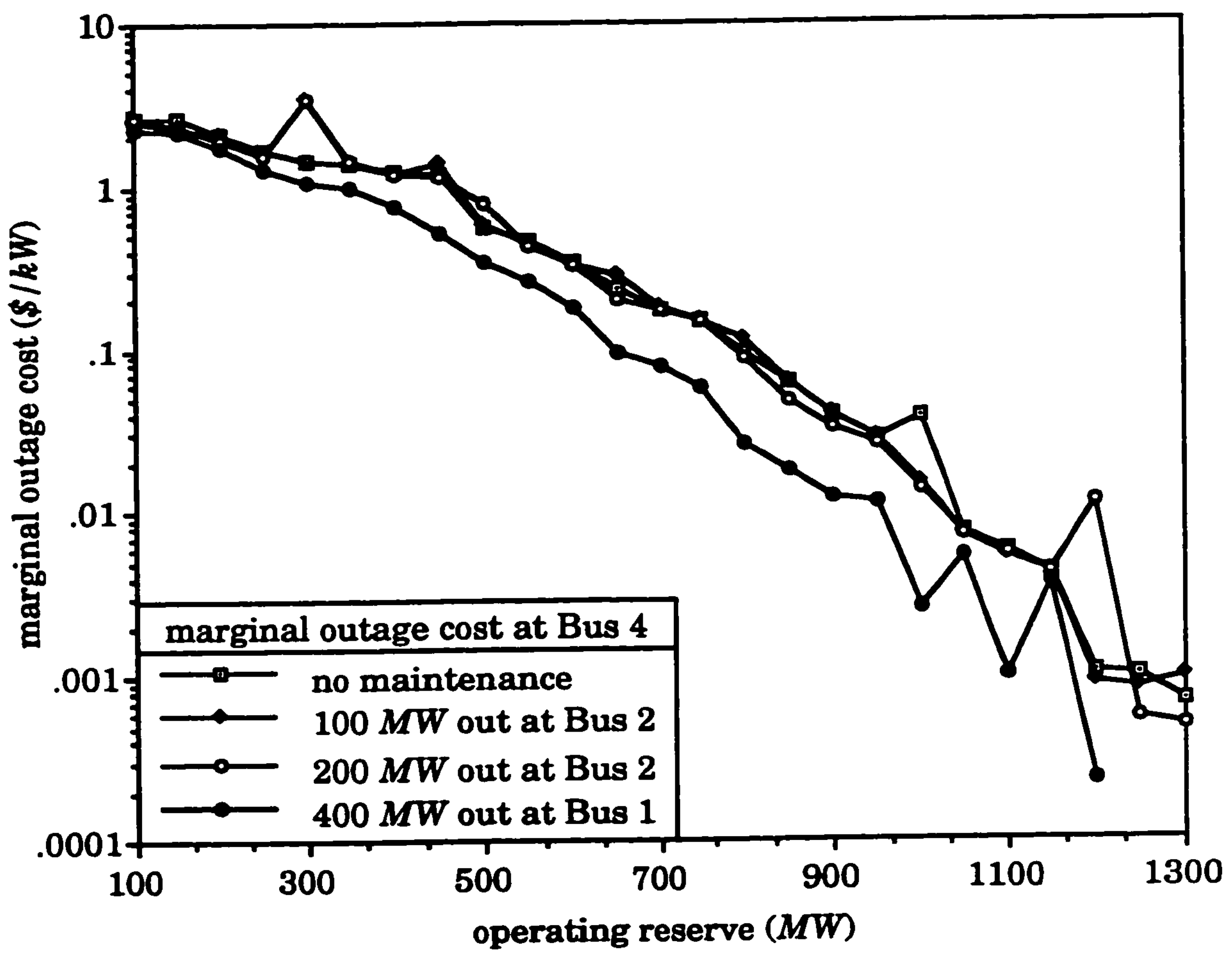

Figure 7.17. Effect of removing a few generating units for maintenance on the marginal outage cost profile of Bus 4 of the *IEEE-RTS*.

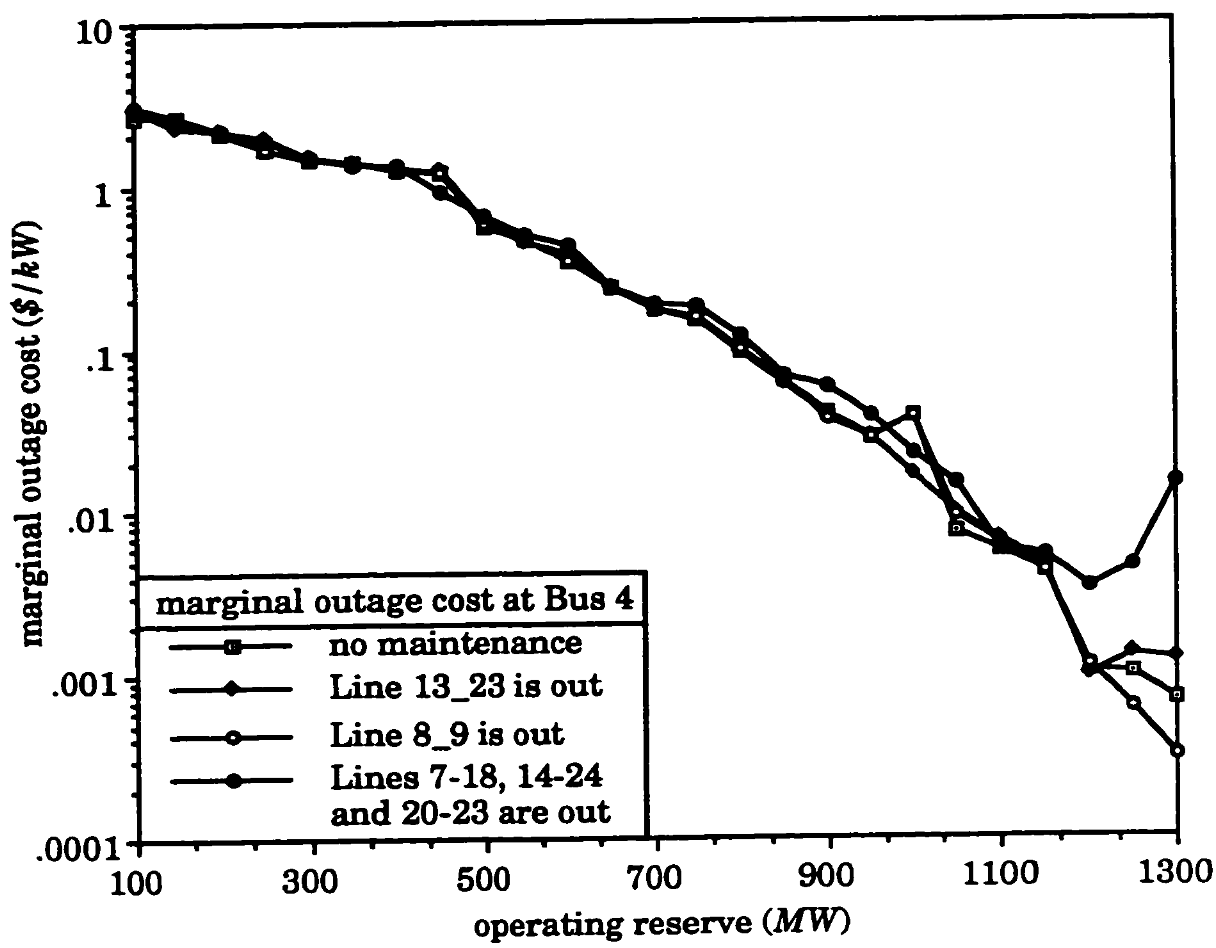

Figure 7.18. Effect of removing a few transmission lines for maintenance on the marginal outage cost profile of Bus 4 of the *IEEE-RTS*.

7.4. Summary

The exact method of calculating the marginal outage cost in composite generating and transmission systems is very time consuming and therefore it may not be suitable for applications in the operating environment. This chapter presents a number of approximations that reflect the impact of changes in selected pertinent factors on the marginal outage cost profiles of the *RBTS* and the *IEEE-RTS*. The results from the sensitivity studies show that the marginal outage cost at a load bus is largely unaffected by approximate values of the *IEAR* and their variations with the peak load.

Therefore, a constant *IEAR* for the aggregate system can be used. Additional studies show that the network flow solution method and the load curtailment philosophy used in the composite system reliability program have quite insignificant impacts on the marginal outage cost. Finally, the removal of large generating capacity for maintenance has a noticeable effect on the marginal outage cost while the effect of removing transmission lines for maintenance in large systems such as the *IEEE-RTS* is very small.

The concepts entailed in calculating the marginal outage costs in generating systems are described in Chapter 2 and illustrated in Chapters 3, 4 and 5 of this thesis using the *RBTS* and the *IEEE-RTS*. Chapters 6 and 7 illustrate the application of composite system reliability methods to calculating the marginal outage costs in composite generation and transmission systems. The following chapter utilizes the findings from all these chapters to provide recommendations for implementing the developed methodologies in practical system studies.

8. PRACTICAL IMPLEMENTATION OF THE PROPOSED METHODS FOR CALCULATING MARGINAL OUTAGE COSTS

8.1. Introduction

A number of methodologies for calculating the marginal outage costs in generating and composite generation and transmission systems are developed in this research work. These methods are illustrated in this thesis using the *RBTS* and the *IEEE-RTS* reliability test systems. The sensitivity studies presented serve to quantify the effects of selected modelling assumptions and pertinent factors on the marginal outage cost. This chapter utilizes the findings from these analyses to provide recommendations for implementing the methods that are developed in practical systems.

Marginal outage costs constitute an important component of electricity spot prices. These costs are defined as the outage costs related to both capacity shortages (generation contribution) and network capacity constraints (transmission contribution) that are incurred in serving an incremental load. The contribution of the generating system to the marginal outage cost is calculated by conducting a quantitative reliability analysis at *HLI* while the contribution of the transmission system is calculated at *HLII* assuming that the generation system is fully reliable.

In practice, the individual contributions may not be important and only the total marginal outage cost is required to calculate the spot prices at bulk customer load points. The studies conducted in Chapter 6 of this thesis show that the contribution of the generation system to the marginal outage cost dominates for the two systems considered. When the transmission network is heavily loaded or transmission lines are removed for maintenance, however, the contribution of the transmission system becomes more significant. Hence, under normal operating conditions, the marginal outage costs associated with the generating system provide reasonable estimates of the total marginal outage cost and the contribution of the transmission system can be ignored.

Evaluation of the marginal outage costs associated with generating systems can be divided into two categories: 1) marginal outage cost evaluation in isolated generating systems and 2) marginal outage cost evaluation in interconnected generating systems. If the contribution of the transmission system is considered to be significant, then an analysis of the composite generation and transmission system is necessary. The following sections in this chapter provide guidelines for implementing the proposed marginal outage cost methodologies in practical systems.

8.2. Marginal Outage Costs in Isolated Generating Systems

A method for calculating the marginal outage costs in generating systems using quantitative power system reliability concepts is proposed in Chapter 2 of this thesis. The utilization of this method is illustrated in Chapters 3 and 4 by application to the *RBTS* and the *IEEE-RTS*. The studies presented in Chapter 3 show that the proposed method can be used to calculate the marginal outage cost for any operating reserve and lead time.

The method is also capable of including a number of modelling features that make it very attractive to practical system applications. For example, the ability to include multi-state modelling of generating units, load forecast uncertainty and the initial generating unit conditions allows the user to accurately model the stochastic nature of the system and to place a certain amount of confidence in the input data.

The basic method illustrated in Chapter 3 is simple to implement and can be used to calculate the marginal outage costs in generating systems of any size at the expense of computing time. Chapter 3 shows that the computing time required to calculate the marginal outage costs in the *IEEE-RTS*, which is a moderately-sized system, is long. The constraints placed on the utilization of marginal outage costing programs by the turnaround time of the operating environment make such computing times unacceptable. Therefore, suitable approximate methods must be utilized in order to reduce the computing time without significantly jeopardizing the accuracy of the results. The following approximate techniques are tested in Chapter 4 to see if they meet these requirements:

1) rounding algorithm,
2) Fast Fourier Transform (*FFT*) algorithm,
3) Gram-Charlier series,
4) high-order Edgeworth expansion and
5) large deviation method.

Comparisons of the results from the approximate methods and the exact recursive technique show that the rounding and the *FFT* algorithms provide the best accuracy in the shortest time. The implementation of the rounding algorithm is found to be simpler however because it is based on the basic and widely used recursive technique. The accuracy of the large deviation method is found to be adequate. However, the application of this method to systems with a large number of generating units having many derated states could result in some challenging problems with the Newton-Raphson algorithm employed.

A *PC*-based computer program capable of calculating the day-ahead marginal outage costs on an hourly basis has been recently developed and implemented using the rounding algorithm [106]. The program is currently being used by a major electric utility in North America as an essential component of its spot pricing scheme. The performance of the program in a practical operating environment proves that the rounding algorithm is sufficiently accurate for practical system studies.

8.3. Marginal Outage Costs in Interconnected Generating Systems

In practice, electric utilities interconnect amongst themselves in order to provide assistance and minimize the overall operating reserve required to achieve a given adequacy level. Since the capacity assistance has an impact on the reliability and the operating reserve requirements of assisted systems, it can also have an impact on the marginal outage cost of these systems. In order to quantify the impact of capacity assistance on the marginal outage cost of interconnected generating systems, a method based on the equivalent assisting unit approach is proposed in Chapter 5. This technique can be applied to interconnected generating systems as well as interconnected areas within the same single system.

Quantitative reliability evaluation of large interconnected generating systems is very time consuming and the application of the equivalent assisting unit approach may not be possible in the operating environment due to either the lack of data describing the interconnected systems in each hour of the forecast period or the computing time requirements or both. A more practical approach consists of performing a series of comparative studies to investigate the accuracy of possible approximations. If successful, the daily analysis can then be conducted using simple models rather than applying more detailed reliability analyses.

In order to quantify the impact of selected approximations, a number of sensitivity studies are conducted in Chapter 5 using 2, 3 and 4 *RBTS* systems interconnected in simple topologies. These studies show that the marginal outage cost of an interconnected system is largely affected by the total assistance available to it from all the assisting systems and restricted by the carrying capabilities of their respective tie-lines. The number of tie-lines and their reliabilities are found to have an insignificant impact on the marginal outage cost. The evaluation of the marginal outage cost in interconnected generating systems therefore can be approximated by a simple model that only considers the total assistance available to the assisted system.

One way of calculating the marginal outage cost profile in interconnected generating systems is to shift the isolated system profile by an amount equal to the total assistance available to it from all the assisting systems. The shifted profile represents a rough approximation of the interconnected system profile. This approximation gives reasonable results that take into consideration the effect of interconnection without having to perform detailed reliability analyses.

The results obtained using the above approximate method provide optimistic estimates of the marginal outage cost in the assisted system. Additional studies can be performed using a 2 or 3 state equivalent model of the capacity assistance. This model provides pessimistic estimates of the marginal outage cost because the actual assistance will consist of many more states each with a capacity and a probability of occurrence. The results from both the optimistic and the pessimistic scenarios can be used by an operator to select reasonable estimates of the marginal outage cost based on judgement and the confidence that can be placed on the assistance available from neighbouring systems.

The ideas discussed in the above paragraphs are focused on the premise that the lack of data in the operating environment makes such approximations very practical. If accurate data are available, however, then the method proposed in Chapter 5 should be used to calculate the exact marginal outage costs in the area of interest. Although, no studies are reported in this thesis using large interconnected generating systems, it can be easily ascertained that such studies will require excessive computing time and therefore the rounding algorithm will have to be used. The selection of a suitable rounding increment depends on the topology of the interconnected systems and the characteristics of the generating units in each system. Therefore, preliminary studies have to be performed using the equivalent assisting unit method in order to determine a suitable rounding increment.

Although, the approximate methods presented in Chapter 4 were not investigated in the interconnected systems studies reported in this thesis, their utilization in reliability evaluation and production costing of interconnected generating systems is well documented [114-118]. Further research in this area is required to determine if some of these methods can provide accurate estimates of the marginal outage cost. The implementation of these methods will then have to be compared to the equivalent assisting unit method with a suitable rounding increment to see if they have any advantage.

8.4. Marginal Outage Costs in Composite Generation and Transmission Systems

As noted earlier in this chapter, the marginal outage cost has two components; generation and transmission systems contributions. The contribution of the generation system dominates during normal operating conditions while the contribution of the transmission system is only significant in heavily loaded systems and therefore it can be ignored in most practical system studies. A composite system reliability evaluation program will be needed to perform the analysis if the transmission system component is required. The utilization of such programs in a utility operating environment is almost non-existent due to the large computing time requirements. One way of reducing these requirements is to use a *DC* load flow or network flow methods instead of a conventional *AC* load flow approach. The small loss in accuracy is insignificant when compared to the reduction in the computing time.

Sensitivity studies presented in Chapter 7 show that the marginal outage cost can be reasonably estimated using the aggregate system values of the Interrupted Energy Assessment Rate (*IEAR*) and the Incremental Expected Unserved Energy (ΔEUE). Furthermore, it is shown in Chapter 7 that the average interruption duration can be used to calculate adequate estimates of the *IEAR*. The variations of the *IEAR* with the peak load have no detectable effect on the marginal outage cost. Therefore, a constant *IEAR* value for the aggregate system can be used to calculate practical estimates of the marginal outage cost. This approximation enables utilities to use commercially available composite system reliability evaluation programs to calculate the marginal outage cost at *HLII*. The accuracy of this approximation increases with the size of the system.

The computing time can also be reduced by calculating the contribution of the generation system using *HLI* analysis and the contribution of the transmission system using *HLII* analysis. This method will give reasonable results because, as shown in Chapter 6, the marginal outage cost calculated at *HLI* and the contribution of the generation system calculated at *HLII* are in close agreement. If this is the case in practical system studies, the number of contingencies that have to be evaluated at *HLII* will be reduced significantly since only the transmission system components will be considered in the analysis. This will lead to considerable savings in the computing time. If the computing time is still large when utilizing the proposed method in the operating environment, then a number of marginal outage cost profiles of the transmission system can be pre-calculated for selected system topologies and used. This approximation may be the best solution because the capacities of the transmission system components do not change frequently from one hour to the next and the topology of the transmission system remains constant for longer periods of time. Maintenance of transmission circuits is normally scheduled months or weeks in advance and hence ample time is available for calculating the contribution of the transmission system to the total marginal outage cost for the forecast topology.

8.5. Summary

The recommendations presented in this chapter are made from observations of the results obtained using the *RBTS* and *IEEE-RTS* and from experience gained during the implementation of the *PC*-based program for calculating the day-ahead marginal outage costs [106]. These recommendations will have to be tested however in each case before actual use in practical systems. Before selecting an approximate method, it should be remembered that the accuracy of the results from any method can only be as good as the accuracy of the input data and models used in the analysis. Therefore, additional precision in the evaluation method will not increase the accuracy of the results if the input data are not accurate in the first place.

9. SUMMARY AND CONCLUSIONS

This thesis extends the scope of application of quantitative power system reliability techniques to marginal outage costing. Marginal outage costs constitute an important component of electricity spot prices. The general strategy adopted in this thesis has been to develop methods for calculating these costs in generating and composite generation and transmission systems. The methods developed are illustrated by application to the *RBTS* and the *IEEE-RTS*.

In Chapter 2, a method based on quantitative power system reliability concepts is proposed for calculating the marginal outage costs in electric power systems. The proposed method calculates the marginal outage cost at a given load level by multiplying the incremental expected unserved energy of the system at that load level by an average cost of unserved energy. Methods were proposed for calculating the incremental expected unserved energy in generating and composite generation and transmission systems using established reliability techniques. The average cost of unserved energy is represented by the interrupted energy assessment rate of the system.

Chapter 3 illustrates the proposed method for calculating the marginal outage costs associated with generating systems by application to the *RBTS* and the *IEEE-RTS*. The application of the proposed method to two reliability test systems of different sizes was performed to show the effect of modelling assumptions and parameters on the marginal outage cost and to draw some general conclusions regarding the applicability of the proposed method to large practical systems. The marginal outage cost profiles of both test systems are calculated as a function of the operating reserve level and the lead time. It was found that the marginal outage cost is equal to the *IEAR* when the system has no operating reserves or when it is reserve deficient. As the reserves become more plentiful, the marginal outage cost decreases. A number of sensitivity analyses are also conducted in Chapter 3 in order to show the effects of selected modelling assumptions such as the initial generating unit conditions, load forecast uncertainty, modelling of derated states, etc. on the marginal outage cost profile.

Chapter 4 illustrates the utilization of a number of approximate techniques in the evaluation of the marginal outage costs associated with generating systems. The approximate techniques investigated in this chapter are the rounding algorithm, the Fast Fourier Transform algorithm, the Gram-Charlier expansion, the high-order Edgeworth expansion and the large deviation method. The results from the approximate techniques are compared to the exact values calculated using the recursive techniques for very high and very low lead time values. It was found from these comparisons that the rounding and the *FFT* algorithms provide the best accuracy for all operating reserves in a reasonable amount of computing time. The implementation of the rounding algorithm is simpler, however, since it is based on the general and widely used recursive technique [26]. The accuracy of the large deviation method falls closely behind the first two techniques. The computing time required by this method, however, was found to be much smaller than that required by the previous techniques, if the proper initial conditions are used in the Newton-Raphson iteration process. The accuracy of the Gram-Charlier and the high-order Edgeworth expansions was found to be a function of the lead time considered. When the lead time is very short, these techniques exhibit peculiar behaviours that produce negative probabilities under certain conditions.

Chapter 5 describes a methodology based on quantitative reliability evaluation techniques for the calculation of the marginal outage costs in interconnected generating systems. The proposed method is illustrated by calculating the marginal outage costs on a regional basis within a system and the impact of assistance from neighbouring systems on these costs. The proposed method is applied to radially interconnected and looped systems. It was found from these studies that, for all interconnection topologies, the marginal outage cost is mostly affected by the total transfer capability of all the tie-lines. The number of tie-lines and their reliabilities have an insignificant impact on the marginal outage cost.

It is also shown in Chapter 5 that the assistance available from one system to another has a significant impact on the shape of the marginal outage cost profile of the assisted system. Therefore, it is not generally recommended to simply shift the marginal outage cost profile of an isolated system by the available assistance in order to calculate its interconnected profile. However, such an approximation provides a quick means of estimating the marginal outage cost of an interconnected generating system without performing any detailed interconnected system reliability studies.

Chapter 6 presents a methodology for calculating the marginal outage costs at bulk customer load points in a composite generation and transmission system. The proposed methodology is illustrated by application to the *RBTS* and the *IEEE-RTS*. The application of the proposed method to the *RBTS* shows that the marginal outage cost at any load bus is independent of the location of the bus within the system except when it is radially fed by one or more lines. In the case of the *IEEE-RTS*, it was found that the marginal outage cost profiles at all the load buses are very similar. Comparisons between the marginal outage costs calculated using *HLI* and *HLII* analyses show that the values calculated at *HLI* are very close to those calculated at *HLII*. The contribution of the generation system calculated at *HLII* studies was found to be much more significant than that of the transmission system. The contribution of the transmission system becomes more noticeable however when the system is heavily loaded.

The exact method of calculating the marginal outage cost in composite generating and transmission systems is very time consuming and therefore it may not be suitable for applications in the utility operating environment. Chapter 7 presents a number of sensitivity studies that reflect the impact of changes in selected pertinent factors on the marginal outage cost profiles of the *RBTS* and the *IEEE-RTS*. The results from the sensitivity studies show that the marginal outage cost at a load bus is largely unaffected by approximate values of the *IEAR* and their variations with the peak load. Therefore, a constant *IEAR* for the aggregate system can be used. Additional studies show that the network flow solution method and the load curtailment philosophy used in the composite system reliability program have no noticeable effects on the marginal outage cost. Finally, it was found that the removal of large generating capacity for maintenance has a significant effect on the marginal outage cost, while the effect of removing transmission lines for maintenance in large systems such as the *IEEE-RTS* is very small.

The results of the sensitivity analyses conducted in Chapters 3, 4, 5, 6 and 7 are used in Chapter 8 to provide recommendations for implementing the methodologies that are developed in practical system studies. The recommendations presented in this chapter are also derived from the experience gained during the implementation of a *PC*-based computer program for calculating the day-ahead marginal outage costs on an hourly basis in an actual utility operating environment.

REFERENCES

1. Turvey, R., *Optimal Pricing and Investment in Electricity Supply*, The MIT Press, Massachusetts Institute of Technology, Cambridge, Massachusetts, 1968.

2. Khan, A., *The Economics of Regulation: Principles and Institutions*, New York, N.Y., John Wiley & Sons, Inc., 1971.

3. Munasinghe, M., "Principles of Modern Electricity Pricing", *Proceedings of the IEEE*, Vol. 69, No. 3, March 1981.

4. Morgan, G. and Talukdar, S., "Electric Power Load Management: Some Technical, Economic, Regulatory and Social Issues", *Proceedings of the IEEE*, Vol. 67, No. 2, February 1979.

5. *EPRI* Report, *Electric Utility Rate Design Study*, Electric Power Research Institute, Palo Alto, California, 1979.

6. *EPRI* Report, *Innovative Rate Design Study*, Electric Power Research Institute, Report EA-3820, Palo Alto, California, January 1985.

7. Berg, S.V., *Innovative Electric Rates: Issues in Cost-Benefit Analysis*, LexingtonBooks, D.C. Heath and Company, Lexington, Massachusetts, 1983.

8. Lescoeur, B. and Galland, J.B., "Tariffs and Load Management: The French Experience", *IEEE Trans. on PWRS*, Vol. 2, No. 2, pp. 458-464, May 1987.

9. Ahlstrand, P., "Real Time Pricing: A *DSM* Alternative", *Electrical World*, pp. 61, December 1986

10. Sanghvi, A.P., "Flexible Strategies for Load/Demand Management Using Dynamic Pricing", *IEEE Trans. on PWRS*, Vol. 4, No. 1, pp. 83-93, February 1989.

11. Garcia, E.V. and Runnels, J.E., "The Utility Perspective of Spot Pricing", *IEEE Trans. on PAS*, Vol. PAS-104, No. 6, pp. 1391-1393, June 1985.

12. Schweppe, F.C., Caramanis, M.C., Tabors, R.D. and Bohn, R.E., *Spot Pricing of Electricity*, Kluwer Academic Publishers, Boston, Massachusetts, 1988.

13. Sioshansi, F.P., "The Pros and Cons of Spot Pricing - Electric Utility Perspective", *Energy Policy*, pp. 353-358, August 1988.

14. Vikery, W., "Responsive Pricing and Public Utilities", *Bell Journal of Economics and Management Sciences*, Vol. 2, No. 1, 1971.

15. Schweppe, F.C., Tabors, R.D., Kirtley, J, Outhred, H., Pickel, F. and Cox, A, "Homeostatic Utility Control", *IEEE Trans. on PAS*, Vol. PAS-99, No. 3, pp. 1151-1163 , May/June 1980.

16. Schweppe, F.C., "Power Systems '2000': Hierarchical Control Strategies", *IEEE Spectrum*, pp. 42-47, July 1978.

17. Caramanis, M.C., Bohn, R.E. and Schweppe, F.C., "Optimal Spot Pricing: Practice and Theory", *IEEE Trans. on PAS*, Vol. PAS-101, No. 9, pp. 3234-3245, September 1982.

18. Schweppe, F.C., Caramanis, M.C. and Tabors, R.D., "Evaluation of Spot Price Based Electricity Rates", *IEEE Trans. on PAS*, Vol. PAS-104, No. 7, pp. 1644-1655, July 1985.

19. Kaye, R.J. and Outhred, H.R., "A Theory of Electricity Tariff Design for Optimal Operation and Investment", *IEEE Trans. on PWRS*, Vol. 4, No. 2, pp. 606-613, May 1989.

20. Caramanis, M.C., "Investment Decisions and Long-Term Planning Under Electricity Spot Pricing", *IEEE Trans. on PAS*, Vol. PAS-101, No. 12, pp. 4640-4648, December 1982.

21. Barrie, T.W., "Power System Planning Under Spot Pricing", *IEEE Trans. on PWRS*, Vol. 2, pp. 744-750, August 1987.

22. Kirsch, L.D., Sullivan, R.L., Flaim, T.A., Hipius, J.J. and Krantz, M.G., "Developing Marginal Costs for Real-Time Pricing", *IEEE Trans. on PWRS*, Vol. 3, No. 3, pp. 1133-1138, August 1988.

23. Wood, A.J. and Wollenberg, B.F., *Power Generation, Operation and Control*, John Wiley & Sons, Inc., New York, 1984.

24. Billinton, R. and Allan, R.N., "Power System Reliability in Perspective", *IEE Electronics & Power*, pp. 231-236, March 1984.

25. Billinton, R. and Allan, R.N., *Reliability Assessment of Large Electric Power Systems*, Kluwer Academic Publishers, 1988

26. Billinton, R. and Allan, R.N., *Reliability Evaluation of Power Systems*, Plenum Press, New York, 1984.

27. Billinton, R., "Bibliography on the Application of Probability Methods in Power System Reliability Evaluation", *IEEE Trans. on PAS*, Vol. PAS-91, pp. 649-660, March/April 1972.

28. *IEEE* Committee Report, "Bibliography on the Application of Probability Methods in Power System Reliability Evaluation: 1971-1977", *IEEE Trans. on PAS*, Vol. PAS-97, No. 6, pp. 2235-2245, November/December 1978.

29. Allan, R.N., Billinton, R. and Lee, S.H., "Bibliography on the Application of Probability Methods in Power System Reliability Evaluation: 1977-1982", *IEEE Trans. on PAS*, Vol. PAS-103, No. 2, pp. 275-282, February 1984.

30. Allan, R.N., Billinton, R., Shahidehpour, S.M. and Singh, C., "Bibliography on the Application of Probability Methods in Power System Reliability Evaluation: 1982-1987", *IEEE Trans. on PWRS*, Vol. 3, No. 4, pp. 1555-1564, November 1988.

31. Allan, R.N., Billinton, R., Breipohl, A.M. and Grigg, C.H., "Bibliography on the Application of Probability Methods in Power System Reliability Evaluation: 1987-1991", *Paper No. 93 WM 166-9 PWRS accepted and presented at the 1993 IEEE Winter Meeting*, Columbus, Ohio, January 31-February 5, 1993.

32. Schilling, M.Th., Billinton, R., Leite da Silva, A.M. and El-Kady, M.A., "Bibliography on Composite System Reliability: 1964-1988", *IEEE Trans. on PWRS*, Vol. 4, No. 3, pp. 1122-1132, August 1989.

33. Billinton, R., Allan, R.N. and Salvaderi, L., *Applied Reliability Assessment in Electric Power Systems*, IEEE Press, New York, 1991.

34. Oteng-Adjei, J., *Cost/Benefit Assessment in Electric Power Systems*, Ph.D. Thesis submitted to the College of Graduate Studies and Research, University of Saskatchewan, Saskatoon, Saskatchewan, January 1990.

35. Billinton, R., et. al., "A reliability Test System for Educational Purposes - Basic Data", *IEEE Trans. on PWRS*, Vol. 4, No. 3, pp. 1238-1244, August 1989.

36. A Report Prepared by the Reliability Test System Task Force of the Application of Probability Methods Subcommittee, "*IEEE* Reliability Test System", *IEEE Trans. on PAS*, Vol. PAS-98, No. 6, pp. 2047-2054, November/December 1979.

37. Nelson, J.R., *Marginal Cost Pricing in Practice*, Prentice-Hall, Inc., Englewood Cliffs, N.J., 1964.

38. Joskow, P., "Contributions to the Theory of Marginal Cost Pricing", *The Bell Journal of Economics*, Vol. 7, No. 1, Spring 1976.

39. *EPRI* Report, *An Evaluation of Four Marginal Costing Methodologies*, Electric Power Research Institute, Report EURDS-67, Palo Alto, California, June 12, 1980.

40. Munasinghe, M., *Electric Power Economics*, Butterworths & Co (Publishers) Ltd., 1990.

41. Scherer, C.R., *Estimating Electric Power System Marginal Costs*, North-Holland Publishing Company, New York, 1977.

42. Andersson, R. and Bohman, M., "Short- and Long-Run Marginal Cost Pricing: On their alleged Equivalence", *Energy Economics*, Vol. 7, pp. 279-288, October 1985.

43. Schramm, G., "Marginal Cost Pricing Revisited", *Energy Economics*, pp. 245-249, October 1991.

44. Shipley, R.B., Patton, A.D. and Denison, J.S., "Power Reliability Versus Worth", *IEEE Trans. on PAS*, Vol. PAS-91, pp. 2204-2212, July-December 1972.

45. Sanghvi, A.P., "Economic Costs of Electricity Supply Interruptions: US and Foreign Experience", *Energy Economics*, Vol. 4, No. 3, pp. 180-198, July 1982

46. Wacker, G., Wojczynski, E. and Billinton, R., *Customer Damage Resulting from Electric Service Interruptions*, Canadian Electrical Association, R&D Project 907, U131 Report, Suite 500, One Westmount Square, Montreal, Quebec, Canada, 1982.

47. Skof, L.V., *Ontario Hydro Surveys on Power System Reliability: Summary of Customer Viewpoints*, Ontario Hydro Report R&MR 80-12, 700 University Avenue, Toronto, Canada, 1980.

48. *EPRI* Report, *Value of Service Reliability to Consumers*, Electric Power Research Institute, Report EA-4495, Criterion Inc., Palo Alto, California, May 1986.

49. Andersson, R. and Taylor, L., "The Social Cost of Unserved Electricity", *The Journal of Energy Economics*, Vol. 8, No. 3, pp. 139-146, July 1986.

50 Billinton, R., Wacker, G. and Brewer, R., *Farm Losses Resulting from Electric Service Interruptions*, Canadian Electrical Association, R&D Project 309, U403 Report, Suite 500, One Westmount Square, Montreal, Quebec, Canada, May 1987.

51. Munasinghe, M. and Sanghvi, A., "Reliability of Electricity Supply, Outage Costs and Value of Service: An Overview", *The Energy Journal*, Volume 9, Special Issue on Electricity Reliability, pp. 1-18, 1988.

52. Tollefson, G., Billinton, R., Wacker, G., Chan, E. and Aweya, J., "A Canadian Customer Survey to Assess Power System Reliability Worth", *Paper 93 WM 175-0 PWRS Accepted and Presented at the 1993 IEEE Winter Meeting*, Columbus, Ohio, January 31 - February 5, 1993.

53. Billinton, R., Wacker, G. and Wojczynski, E., "Comprehensive Bibliography on Electrical Service Interruption Costs", *IEEE Trans. on PAS*, Vol. PAS-102, pp. 1831-1837, 1983.

54. Tollefson, G., Billinton, R. and Wacker, G., "Comprehensive Bibliography on Reliability Worth and Electrical Service Consumer Interruption Costs: 1980 - 1990", *IEEE Trans. on PWRS*, Vol. 6, No. 4, pp. 1508-1514, November 1991.

55. Bental, B. and Ravid, S., "A Simple Method for Evaluating the Marginal Cost of Unserved Electricity", *The Bell Journal of Economics*, Vol. 13, Issue 1, pp. 249-253, 1982.

56. Billinton, R., Tollefson, G. and Wacker, G., "Assessment of Electric Service Reliability Worth", *Proceedings of the Third International Conference on Probabilistic Methods Applied to Electric Power Systems*, IEE Conference Publication No. 338, London, U.K., pp. 9-14, July 1991.

57. Billinton, R., Oteng-Adjei, J. and Ghajar, R., "Comparison of Two Alternate Methods to Establish an Interrupted Energy Assessment Rate", *IEEE Trans. on PWRS*, Vol. 2, No. 3, pp. 751-757, August 1987.

58. Oteng-Adjei, J. and Billinton, R., "Evaluation of Interrupted Energy Assessment Rates in Composite Systems", *IEEE Trans. on PWRS*, Vol. 5, No. 4, pp. 1317-1323, November 1990.

59. Noferi, P.L. and Paris, L., "Quantitative Evaluation of Power System Reliability in Planning Studies", *IEEE Trans. on PAS*, Vol. PAS-91, pp. 611-618, March/April 1971.

60. Ghajar, R. and Billinton, R., "A Monte Carlo Simulation Model for the Adequacy Evaluation of Generating Systems", *Reliability Engineering and System Safety*, pp. 173-186, 1988

61. Billinton, R. and Ghajar, R., "Evaluation of the Marginal Outage Costs of Generating Systems for the Purposes of Spot Pricing", *Paper No. 93 WM 147-9 PWRS accepted and presented at the 1993 IEEE Winter Meeting*, Columbus, Ohio, January 31-February 5, 1993.

62. Billinton, R., "Composite System Reliability Evaluation", *IEEE Trans. on PAS*, Vol. PAS-88, No. 4, pp. 276-280, April 1969.

63. Billinton, R. and Bhavaraju, M.P., "Transmission Planning Using a Reliability Criterion: Part I - A Reliability Criterion", *IEEE Trans. on PAS*, Vol. PAS-89, No. 1, pp. 28-34, January 1970.

64. Bhavaraju, M.P. and Billinton, R., "Transmission Planning Using a Reliability Criterion: Part II - Transmission Planning", *IEEE Trans. on PAS*, Vol. PAS-90, No. 1, pp. 70-78, January 1971.

65. Endrenyi, J., Albrecht, P.F., Billinton, R., Marks, G.E., Reppen, N.D. and Salvaderi, L., "Bulk Power System Reliability Assessment - Why and How? Part I: Why?", *IEEE Trans. on PAS*, Vol. PAS-101, NO. 9, pp. 3439-3445, September 1982.

66. Endrenyi, J., Albrecht, P.F., Billinton, R., Marks, G.E., Reppen, N.D. and Salvaderi, L., "Bulk Power System Reliability Assessment - Why and How? Part II: How?", *IEEE Trans. on PAS*, Vol. PAS-101, NO. 9, pp. 3446-3456, September 1982.

67. Noferi, P.L., Paris, L. and Salvaderi, L., "Monte Carlo Method for Power System Reliability Evaluation in Transmission and Generation Planning", *Proceedings of the Annual Reliability and Maintainability Symposium*, Washington, pp. 449-459, January 1975.

68. Allan, R.N. and Billinton, R., "Power System Reliability and its Assessment, Part 2 - Composite Generation and Transmission Systems", *Power Engineering Journal*, pp. 291-297, November 1992.

69. Ford, L.R. and Fulkerson, D.R., *Flows in Networks*, Princeton University Press, Princeton, N.J., 1962.

70. *EPRI* Report, *Transmission System Reliability Methods - Mathematical Methods, Computing Methods and Results*, Electric Power Research Institute, Technical Report EL-2126, Power Technologies Inc., New York, July 1982.

71. Stagg, B. and El-Abiad, A.H., *Computer Methods in Power System Analysis*, McGraw-Hill Book Company, New York, 1968.

72. Scott, B. and Alsac, O., "Fast Decoupled Load Flow", *IEEE Trans. on PAS*, Vol. PAS-93, pp. 859-869, May/June 1974.

73. Salvaderi, L. and Billinton R., "A Comparison Between Two Fundamentally Different Approaches to Composite System Reliability Evaluation", *IEEE Trans. on PAS*, Vol. PAS-104, No. 2, pp. 3486-3493, December 1985.

74. Billinton, R. and Khan, E., "Utilization of Contingency Selection Techniques in the Adequacy Evaluation of a Composite Generation and Transmission System", *Canadian Electrical Association Paper No. 89-SP-156*, Vol. 28, Part 4, 1989.

75. Rubinstein, R.Y., *Simulation and the Monte Carlo Method*, John Wiley & Sons, New York, 1981.

76. Medicherla, T.K.P. and Billinton, R., "Overall Approach to the Reliability Evaluation of Composite Generation and Transmission Systems", *IEE Proceedings*, Part C, Vol. 127, No. 2, pp. 72-81, March 1980.

77. Sachdev, M.S., Medicherla, T.K.P. and Billinton, R., "Generation Rescheduling and Load Schedding to Alleviate Line Overloads - Analysis", *IEEE Trans. on PAS*, Vol. PAS-98, pp. 1876-1884, 1979.

78. Billinton, R. and Kumar, S., "Pertinent Factors in the Adequacy Assessment of Composite Generation and Transmission Systems", *Canadian Electrical Association Paper No. 86-SP-141*, Vol. 25, Part 3, March 1986.

79. Billinton, R. and Li, W., "Hybrid Approach for Reliability Evaluation of Composite Generation and Transmission Systems Using Monte Carlo and Enumeration Technique", *IEE Proceedings*, Part C, Vol. 138, No. 3, pp. 233-241, May 1981.

80. Billinton, R. and Li, W., "Consideration of Multi-state Generating Unit Models in Composite System Adequacy Assessment Using Monte Carlo Simulation", *Canadian Journal for Electrical & Computer Engineering*, Vol. 17, No. 1, pp. 24-28, 1992.

81. Billinton, R. and Allan, R.N., *Reliability Evaluation of Engineering Systems: Concepts and Techniques*, Plenum Press, New York, 1983.

82. Ghajar, R. and Billinton, R., "Comparison of Alternative Techniques for Evaluating the Marginal Outage Costs of Generating Systems", *Paper No. 93 WM 146-1 PWRS accepted and presented at the 1993 IEEE Winter Meeting*, Columbus, Ohio, January 31-February 5, 1993.

83. Billinton, R., et. al., "A Reliability Test System for Educational Purposes - Basic Results", *IEEE Trans. on PWRS*, Vol. 5, No. 1, pp. 319-325, February 1990.

84. Allan, R.N., Billinton, R. and Abdel-Gawad, N.M.K., "The IEEE Reliability Test System: Extensions to and Evaluation of Generating System", *IEEE Trans. on PWRS*, Vol. 1, No. 4, pp. 1-7, November 1986.

85. Kos, P., *Cost of Electricity Supply Interruptions to Agricultural Sector Customers*, M.Sc. Thesis, College of Graduate Studies of Research, University of Saskatchewan, Saskatoon, Saskatchewan, October 1989.

86. Bhavaraju, M.M., "An Analysis of Generating Capacity Reserve Requirements", *Paper No. C-74-135-0*, Abstract in *IEEE* Trans. on PAS, Vol. PAS-93, July 1974.

87. Allan, R.N. and Takieddine, F.N., "Generation Modelling in Power System Reliability Evaluation", *International Conference on Reliability of Power Supply Systems*, IEE Conference Publication Number 148, pp. 47-50, February 1977.

88. Allan, R.N., Leite da Silva, A.M., Abu-Nasser, A.A. and Burchett, R.C., "Discrete Convolution in Power System Reliability", *IEEE Trans. on Reliability*, Vol. R-30, No. 5, pp. 452-456, December 1981.

89. Brigham, E.O., *The Fast Fourier Transform*, Prentice-Hall, Inc., Englewood Cliffs, N.J., 1974.

90. Feller, W., *An Introduction to Probability Theory and Its Applications*, Volume II, John Wiley & Sons, Inc., New York, 1971.

91. Rau, N.S. and Schenk, K.F., "Application of Fourier Methods for the Evaluation of Capacity Outage Probabilities", *Paper No. A-79-103-3*, IEEE PES Winter Meeting, New York, February 1979.

92. Kendall, M.G. and Stuart, A., *The Advanced Theory of Statistics*, Volume I, Distribution Theory, Hafner Publishing Company, New York, 1962.

93. Levy, D.J. and Khan, E.P., "Accuracy of the Edgeworth Approximation for *LOLP* Calculations in Small Power Systems", *IEEE Trans. on PAS*, Vol. PAS-101, No. 4, pp. 986-996, April 1982.

94. Stremel, J.P. and Rau, N.S., "The cumulant Method of Calculating *LOLP*", *Paper No. A-79-506-7*, IEEE PES Summer Meeting, 1979.

95. Stremel, J.P., "Sensitivity Study of the Cumulant Method of Calculating Generation System Reliability", *IEEE Trans. on PAS*, Vol. PAS-100, No. 2, pp. 771-778, February 1981.

96. Hamoud, G. and Billinton, R., "An Approximate and Practical Approach to Including Uncertainty Concepts in Generating Capacity Reliability Evaluation", *IEEE Trans. on PAS*, Vol. PAS-100, NO. 3, pp. 1259-1265, March 1981.

97. Billinton, R. and Hamoud, G., "Considerations in Including Uncertainty in *LOLE* Calculations for Practical Systems", *Paper No. A-79-075-3*, IEEE PES Winter Meeting, New York, N.Y., February 1979.

98. Stremel, J.P., Jenkins, R.T., Babb, R.A. and Bayless, W.D., "Production Costing Using the Cumulant Method of Representing the Equivalent Load Curve", *IEEE Trans. on PAS*, Vol. PAS-99, No. 5, pp. 1947-1956, September/October 1980.

99. Rau, N.S., Toy, P. and Schenk, K.F., "Expected Energy Production Costs by the Method of Moments", *IEEE Trans. on PAS*, Vol. PAS-99, No. 5, pp. 1908-1917, September/October 1980.

100. El-Sheikhi, F.A. and R. Billinton, R., "Generating Unit Maintenance Scheduling for Single and Interconnected Systems", *IEEE Trans. on PAS*, Vol. PAS-103, No. 5, pp. 1038-1044, May 1984.

101. Mazumdar, M. and Gaver, D.P., "A Comparison of Algorithms for Computing Power Generating System Reliability Indices", *IEEE Trans. on PAS*, Vol. PAS-103, No. 1, pp. 92-99, January 1984.

102. Mazumdar, M. and Gaver, D.P., "On the Computation of Power-Generating System Reliability Indexes", *Technometrics*, Vol. 26, No. 2, pp. 173-185, May 1984.

103. Mazumdar, M. and Wang, Y.P., "On the Application of Esscher's Approximation to Computation of Generating System Reliability and Production Costing Indexes", *IEEE Trans. on PAS*, Vol. PAS-104, No. 11, pp. 3029-3036, November 1985.

104. Beard, R.E., Pentikainen, T. and Pesonen, E., *Risk Theory: The Stochastic Basis of Insurance*, Third Edition, Chapman and Hall, London, 1984.

105. Grove, W.E., *Brief Numerical Methods*, Prentice-Hall, Inc., Englewood Cliffs, N.J., 1966.

106. Ghajar, R. and Billinton, R., *MAROCUS: Marginal Outage Cost Evaluation Program*, Users' Manual of a PC-based computer program, University of Saskstchewan, Saskatoon, Saskatchewan, December 1992.

107. Cook, V.M., Galloway, C.D., Steinberg, M.J. and Wood, A.J., "Determination of Reserve Requirements of Two Interconnected Systems", *AIEE Transactions*, Vol. PAS-82, Part III, pp. 18-33, April 1963

108. Billinton, R. and Jain, A.V., "Interconnected System Spinning Reserve Requirements", *IEEE Trans. on PAS*, Vol. PAS-91, No. 2, pp. 517-525, March/April 1972.

109. Pang, C.K. and Wood A.J., "Multi-Area Generation System Reliability Calculations", *IEEE Trans. on PAS*, Vol. PAS-94, No. 2, pp. 508-517, March/April 1975.

110. Billinton, R. and Singh C., "Generating Capacity Reliability Evaluation in Interconnected Systems Using a Frequency and Duration Approach: Part I - Mathematical Analysis", *IEEE Trans. on PAS*, Vol. PAS-90, pp. 1654-1664, 1971.

111. Billinton, R. and Wee C.L., "A Frequency and Duration Method for Interconnected System Reliability Evaluation", *IEEE Trans. on PAS*, Vol. PAS-101, pp. 1030-1039, May 1982.

112. Billinton, R. and Jain, A.V., "Power System Spinning Reserve Determination in a Multi System Configuration", *IEEE Trans. on PAS*, Vol. PAS-92, No. 2, pp. 433-441, March/April 1973.

113. Billinton, R. and Gan, L., "A Monte Carlo Simulation Model for Adequacy Assessment of Multi-Area Generating Systems", Third International Conference on Probabilistic Methods Applied to Electric Power Systems", PMAPS 91, *IEE Conference Proceedings No. 338*, pp. 317-322, July 3-5 1991.

114. Rau. N.S., Necsulescu, C., Schenk, K.F. and Misra, R.B., "Reliability of Interconnected Power Systems With Correlated Demands", *IEEE Trans. on PAS*, Vol. PAS-101, No. 9, pp. 3421-3430, September 1982.

115. Noyes, L.R., "Two-Area Probabilistic Production Costing by the Method of Bi-variant Cumulants", *IEEE Trans. on PAS*, Vol. PAS-102, No. 2, pp. 433-443, February 1983.

116. Ahsan, Q., Schenk, K.F. and Misra, R.B., "Expected Energy Production Cost of Two Interconnected Systems With Correlated Demands", *IEEE Trans. on PAS*, Vol. PAS-102, No. 7, pp. 2155-2164, July 1983.

117. Ahsan, Q. and Schenk, K.F., "Sensitivity Study of the Cumulant Method for Evaluating Reliability Measures of Two Interconnected Systems", *IEEE Trans. on Reliability*, Vol. R-36, pp. 429-432, 1987.

118. Yin, C.K. and Mazumdar, M., "Reliability Computations for Interconnected Generating Systems Via Large Deviation Approximation", *IEEE Trans. on PWRS*, Vol. 4, No. 1, pp. 1-8, February 1989.

119. *CEA* Report, *Forced Outage performance of Transmission Equipment*, Equipment Reliability Information System, Canadian Electrical Association, Suite 500, One Westmount Square, Montreal, Quebec, H3Z 2P9, Canada.

120. Caramanis, M.C., Bohn, R.E. and Schweppe, F.C., "The Cost of Wheeling and Optimal Wheeling Rates", *IEEE Trans. on PWRS*, Vol. 1, No. 1, pp. 63-73, February 1986.

121. Schweppe, F.C. and Merrill, H.M., "Weeling - A Primer for Engineers", *Transmission & Distribution*, pp. 68-70, October 1987.

122. Caramanis, M.C., Roukos, N. and Schweppe, F.C., "*WRATES*: A Tool for Evaluating the Marginal Cost of Wheeling", *IEEE Trans. on PWRS*, Vol. 4, No. 2, pp. 594-605, May 1989.

123. Merrill, H.M. and Erickson, B.W., "Wheeling Rates Based on Marginal-Cost Theory", *IEEE Trans. on PWRS*, Vol. 4, No. 4, pp. 1445-1451, October 1989.

A. DESCRIPTION OF THE ROY BILLINTON TEST SYSTEM

The single line diagram of the 6-bus Roy Billinton Test System (*RBTS*) is shown in Figure A.1 [35]. The system has 2 generator (*PV*) buses, 4 load (*PQ*) buses, 9 transmission lines and 11 generating units. The total installed generating capacity for this system is 240 *MW* with a system peak load demand of 185 *MW*.

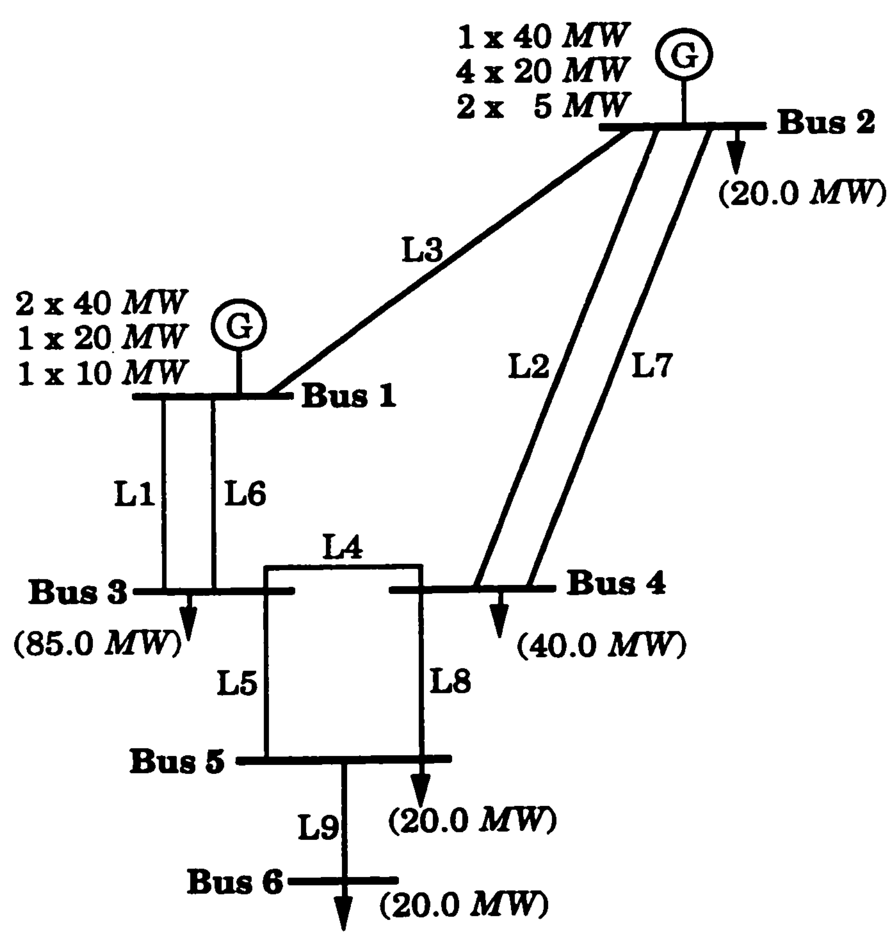

Figure A.1. Single line diagram of the *RBTS*.

The generating unit ratings and reliability data for the *RBTS* are given in Table A.1. The minimum and maximum ratings of the generating units are 5 *MW* and 40 *MW* respectively.

Table A.1. Generating unit reliability data for the *RBTS*.

unit No.	bus No.	rating (*MW*)	type	*FOR*	λ (f/yr)	μ (r/yr)
1	1	10	thermal	0.020	4.0	196.0
2	1	20	thermal	0.025	5.0	195.0
3	1	40	thermal	0.030	6.0	194.0
4	1	40	thermal	0.030	6.0	194.0
5	2	5	hydro	0.010	2.0	198.0
6	2	5	hydro	0.010	2.0	198.0
7	2	20	hydro	0.015	2.4	157.6
8	2	20	hydro	0.015	2.4	157.6
9	2	20	hydro	0.015	2.4	157.6
10	2	20	hydro	0.015	2.4	157.6
11	2	40	hydro	0.020	3.0	147.0

In order to recognize that large thermal units can operate in one or more derated states, the two 40 *MW* thermal units have been given an optional three-state representation [35,83]. The capacity of each state and the associated transition rates are given in Table A.2.

Table A.2. Three-state model for the two 40 *MW* thermal units in the *RBTS*.

state	capacity available (*MW*)	transition rate to state		
		1	2	3
1	40	0.0	2.0	4.0
2	20	96.0	0.0	0.0
3	0	192.0	0.0	0.0

The *RBTS* has a single transmission voltage level at 230 *kV*. The minimum and maximum voltage limits for the system buses are assumed to be 0.97 p.u. and 1.05 p.u. respectively. The transmission line ratings and reliability data are given in Table A.3. The bus data are given in Table A.4. The base unit is 100 *MVA*.

Table A.3. Transmission line data for the *RBTS*.

line No.	buses from	buses to	current rating (*p.u.*)	R	X	B/2	λ (*f/yr*)	μ (*r/yr*)
1	1	3	0.85	0.0342	0.180	0.01060	1.50	0.00114
2	2	4	0.71	0.1140	0.600	0.03520	5.00	0.00114
3	1	2	0.71	0.0912	0.480	0.02820	4.00	0.00114
4	3	4	0.71	0.0228	0.120	0.00705	1.00	0.00114
5	3	5	0.71	0.0228	0.120	0.00705	1.00	0.00114
6	1	3	0.85	0.0342	0.180	0.01060	1.50	0.00114
7	2	4	0.71	0.1140	0.600	0.03520	5.00	0.00114
8	4	5	0.71	0.0228	0.120	0.00705	1.00	0.00114
9	5	6	0.71	0.0228	0.120	0.00705	1.00	0.00114

Table A.4. Bus data for the *RBTS*.

bus No.	load (p.u.) P	load (p.u.) Q	P_g (*p.u.*)	Q_{max} (*p.u.*)	Q_{min} (*p.u.*)	V_0 (*p.u.*)	V_{max} (*p.u.*)	V_{min} (*p.u.*)
1	0.00	0.000	1.000	0.50	-0.40	1.05	1.05	0.97
2	0.20	0.000	1.200	0.75	-0.40	1.05	1.05	0.97
3	0.85	0.000	0.000	0.00	0.00	1.00	1.05	0.97
4	0.40	0.000	0.000	0.00	0.00	1.00	1.05	0.97
5	0.20	0.000	0.000	0.00	0.00	1.00	1.05	0.97
6	0.20	0.000	0.000	0.00	0.00	1.00	1.05	0.97

B. DESCRIPTION OF THE *IEEE*-RELIABILITY TEST SYSTEM

The *IEEE*-Reliability Test System (*IEEE-RTS*) has been and is still being used as a reference network to test and develop different methods for power system reliability assessment. The single line diagram of the 24-bus *IEEE-RTS* is shown in Figure B.1 [36]. The system has 10 generator (*PV*) buses, 10 load (*PQ*) buses, 33 transmission lines, 5 transformers and 32 generating units. The total installed generating capacity for this system is 3405 *MW* with a system peak load demand of 2850 *MW*. The minimum and maximum ratings of the generating units are 12 *MW* and 400 *MW* respectively. The generating unit ratings and reliability data for the *IEEE-RTS* are given in Table B.1.

Table B.1. Generating unit reliability data for the *IEEE-RTS*.

number of units	rating (*MW*)	*FOR*	λ (*f/yr*)	repair time (*hours*)
5	12	0.02	2.98	60
4	20	0.01	19.47	50
6	50	0.01	4.42	20
4	76	0.02	4.47	40
3	100	0.04	7.30	50
4	155	0.04	9.13	40
3	197	0.05	9.22	50
1	350	0.08	7.62	100
2	400	0.12	7.96	150

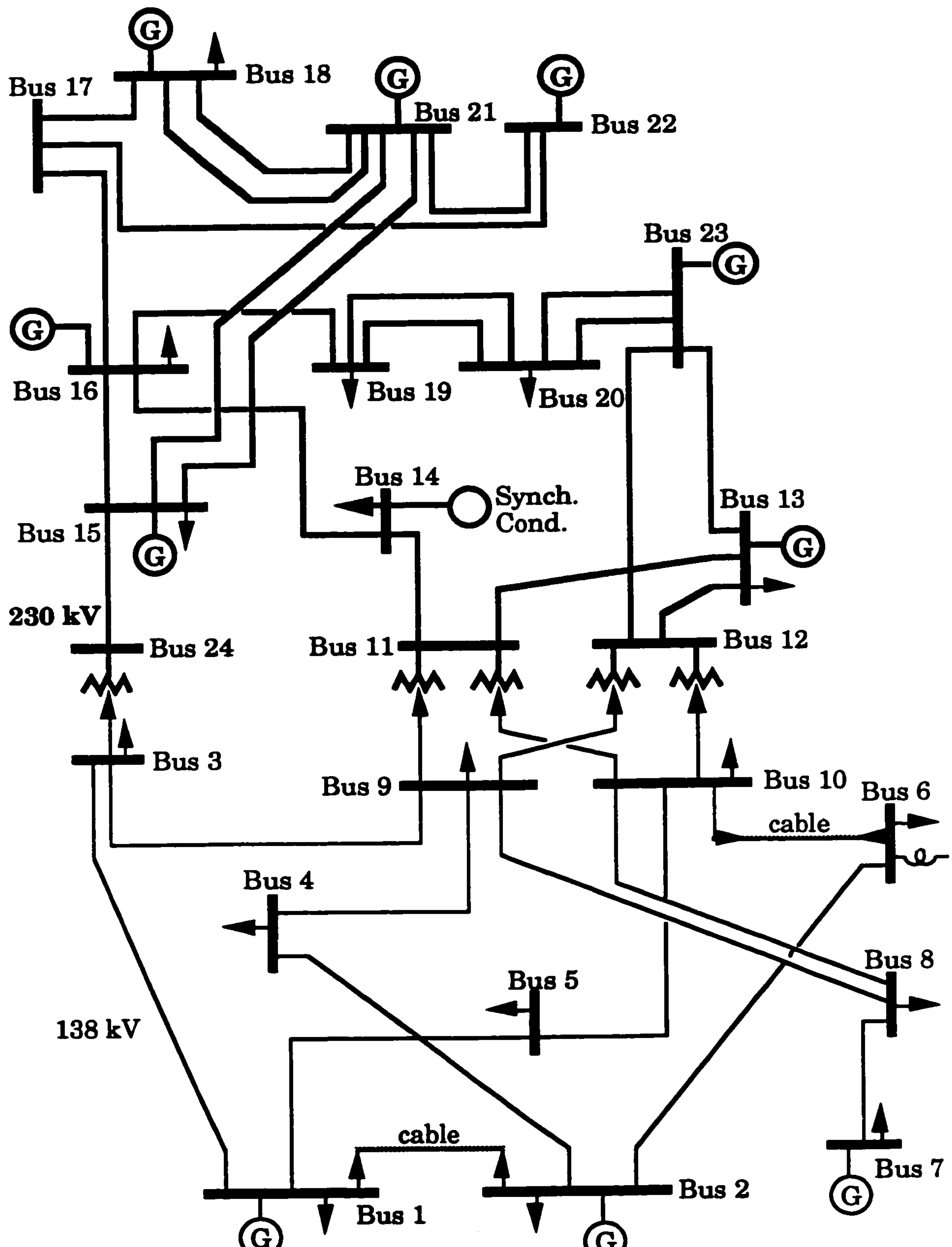

Figure B.1. Single line diagram of the *IEEE-RTS*.

The locations of generating units relative to the buses of the *IEEE-RTS* are given in Table B.2.

Table B.2. Generating unit locations for the *IEEE-RTS*.

bus No.	unit 1 (*MW*)	unit 2 (*MW*)	unit 3 (*MW*)	unit 4 (*MW*)	unit 5 (*MW*)	unit 6 (*MW*)
1	20	20	76	76		
2	20	20	76	76		
7	100	100	100			
13	197	197	197			
15	12	12	12	12	12	155
16	155					
18	400					
21	400					
22	50	50	50	50	50	50
23	155	155	350			

In order to recognize that large thermal units can operate in one or more derated states, the 350 *MW* and the 400 *MW* units of the *IEEE-RTS* have been given a 50% derated state [84]. The capacity of each state and its associated transition rates are given in Table B.3.

Table B.3. Three-state model of the 350 and 400 *MW* units in the *IEEE-RTS*.

state	capacity available (*MW*)	transition rate to state		
		1	2	3
1	350	0.00	7.62	7.62
2	175	146.00	0.00	0.00
3	0	125.14	0.00	0.00
1	400	0.00	7.96	7.96
2	200	87.60	0.00	0.00
3	0	87.60	0.00	0.00

There are two transmission voltage levels in the *IEEE-RTS*, 230 kV in the North region and 138 kV in the South region. The transmission line ratings and reliability data are given in Table B.4.

Table B.4. Transmission line data for the *IEEE-RTS*.

line No.	buses from	buses to	I (*p.u.*)	R	X	B/2	tap	λ (f/yr)	μ (r/yr)
1	1	2	1.93	0.0026	0.0139	0.2306	1.0	0.24	0.00183
2	1	3	2.08	0.0546	0.2112	0.0286	1.0	0.51	0.00114
3	1	5	2.08	0.0218	0.0845	0.0115	1.0	0.33	0.00114
4	2	4	2.08	0.0328	0.1267	0.0172	1.0	0.39	0.00114
5	2	6	2.08	0.0497	0.1920	0.0260	1.0	0.48	0.00114
6	3	9	2.08	0.0308	0.1190	0.0161	1.0	0.38	0.00114
7	3	24	5.10	0.0023	0.0839	0.0000	1.0	0.02	0.08767
8	4	9	2.08	0.0268	0.1037	0.0141	1.0	0.36	0.00114
9	5	10	2.08	0.0228	0.0883	0.0120	1.0	0.34	0.00114
10	6	10	1.93	0.0139	0.0605	1.2295	1.0	0.33	0.00400
11	7	8	2.08	0.0159	0.0614	0.0166	1.0	0.30	0.00114
12	8	9	2.08	0.0427	0.1651	0.0224	1.0	0.44	0.00114
13	8	10	2.08	0.0427	0.1651	0.0224	1.0	0.44	0.00114
14	9	11	6.00	0.0023	0.0839	0.0000	1.0	0.02	0.08767
15	9	12	6.00	0.0023	0.0839	0.0000	1.0	0.02	0.08767
16	10	11	6.00	0.0023	0.0839	0.0000	1.0	0.02	0.08767
17	10	12	6.00	0.0023	0.0839	0.0000	1.0	0.02	0.08767
18	11	13	6.00	0.0061	0.0476	0.0500	1.0	0.40	0.00126
19	11	14	6.00	0.0054	0.0418	0.0440	1.0	0.39	0.00126
20	12	13	6.00	0.0061	0.0476	0.0500	1.0	0.40	0.00126
21	12	23	6.00	0.0124	0.0966	0.1015	1.0	0.52	0.00126
22	13	23	6.00	0.0111	0.0865	0.0909	1.0	0.49	0.00126
23	14	16	6.00	0.0050	0.0389	0.0409	1.0	0.38	0.00126
24	15	16	6.00	0.0022	0.0173	0.0364	1.0	0.33	0.00126
25	15	21	6.00	0.0063	0.0490	0.0515	1.0	0.41	0.00126
26	15	21	6.00	0.0063	0.0490	0.0515	1.0	0.41	0.00126
27	15	24	6.00	0.0067	0.0519	0.0546	1.0	0.41	0.00126
28	16	17	6.00	0.0033	0.0259	0.0273	1.0	0.35	0.00126
29	16	19	6.00	0.0030	0.0231	0.0243	1.0	0.34	0.00126
30	17	18	6.00	0.0018	0.0144	0.0152	1.0	0.32	0.00126
31	17	22	6.00	0.0135	0.1053	0.1106	1.0	0.54	0.00126
32	18	21	6.00	0.0033	0.0259	0.0273	1.0	0.35	0.00126
33	18	21	6.00	0.0033	0.0259	0.0273	1.0	0.35	0.00126
34	19	20	6.00	0.0051	0.0396	0.0417	1.0	0.38	0.00126
35	19	20	6.00	0.0051	0.0396	0.0417	1.0	0.38	0.00126
36	20	23	6.00	0.0028	0.0216	0.0228	1.0	0.34	0.00126
37	20	23	6.00	0.0028	0.0216	0.0228	1.0	0.34	0.00126
38	21	22	6.00	0.0087	0.0678	0.0712	1.0	0.45	0.00126

The minimum and maximum voltage limits for the system buses are assumed to be 0.95 p.u. and 1.05 p.u. respectively. Approximately 80% of the installed generating capacity and 53% of the system load are located in the North region. The surplus capacity in this region is used to supply the load in the generating capacity deficient South region. The bus data of the *IEEE-RTS* are given in Table B.5. The base unit is 100 *MVA*.

Table B.5. Bus data for the *IEEE-RTS*.

bus No.	load (p.u.)		P_g (*p.u.*)	Q_{max} (*p.u.*)	Q_{min} (*p.u.*)	V_0 (*p.u.*)	V_{max} (*p.u.*)	V_{min} (*p.u.*)
	P	Q						
1	1.08	0.22	1.720	1.20	-0.75	1.02	1.05	0.95
2	0.97	0.20	1.720	1.20	-0.75	1.02	1.05	0.95
3	1.80	0.37	0.000	0.00	0.00	1.00	1.05	0.95
4	0.74	0.15	0.000	0.00	0.00	1.00	1.05	0.95
5	0.71	0.14	0.000	0.00	0.00	1.00	1.05	0.95
6	1.36	0.28	0.000	0.00	0.00	1.00	1.05	0.95
7	1.25	0.25	3.000	2.70	0.00	1.02	1.05	0.95
8	1.71	0.35	0.000	0.00	0.00	1.00	1.05	0.95
9	1.75	0.36	0.000	0.00	0.00	1.00	1.05	0.95
10	1.95	0.40	0.000	0.00	0.00	1.00	1.05	0.95
11	0.00	0.00	0.000	0.00	0.00	1.00	1.05	0.95
12	0.00	0.00	0.000	0.00	0.00	1.00	1.05	0.95
13	2.65	0.54	5.500	3.60	0.00	1.02	1.05	0.95
14	1.94	0.39	0.000	3.00	-0.75	1.00	1.05	0.95
15	3.17	0.64	2.100	1.65	-0.75	1.02	1.05	0.95
16	1.00	0.20	1.450	1.20	-0.75	1.02	1.05	0.95
17	0.00	0.00	0.000	0.00	0.00	1.00	1.05	0.95
18	3.33	0.68	4.000	3.00	-0.75	1.02	1.05	0.95
19	1.81	0.37	0.000	0.00	0.00	1.00	1.05	0.95
20	1.28	0.26	0.000	0.00	0.00	1.00	1.05	0.95
21	0.00	0.00	3.500	3.00	-0.75	1.02	1.05	0.95
22	0.00	0.00	2.500	1.45	-0.90	1.02	1.05	0.95
23	0.00	0.00	6.600	4.50	-1.75	1.02	1.05	0.95
24	0.00	0.00	0.000	0.00	0.00	1.00	1.05	0.95

C. POWER INTERRUPTIONS COST DATA

A variety of approaches have been used to investigate the cost of power interruptions [53,54]. One of the most commonly used methods to gather these data is to survey electrical customers, sector by sector, to determine the costs or losses resulting from power interruptions. The Power Systems Research Group of the University of Saskatchewan has been involved with postal surveys of electric customers for the last decade. Three major surveys have been conducted, the third of which is currently underway. The first two surveys were sponsored by the Canadian Electrical Association (*CEA*) and the latest is being funded by the Natural Sciences and Engineering Research Council (*NSERC*) of Canada. The first survey was conducted in 1980 in the large users, residential, commercial and industrial sectors. The second survey was conducted in 1985 and covered the agricultural sector. The detailed results from these two surveys are contained in [46,50] and only the final results are summarized in this section. The latest survey is being undertaken to renew the data from the initial surveys and to develop and test new surveying techniques and specific utility planning applications [52]. Since the complete data from the latest survey are not yet available, the cost of interruption data used in this thesis are obtained from the original two surveys.

The cost of interruption data from the first two surveys were escalated to 1987 dollars using appropriate escalation factors [85]. This was typically done at the individual *SIC* (Standard Industrial Classification) class level in order to take into consideration the variation of inflation in the constituent industries. The escalated cost data were then used to obtain a function of the interruption cost versus interruption duration for each sector. This function is referred to as a Customer Damage Function (*CDF*). The *CDF's* can be calculated in terms of cost per respondent, cost normalized by the user's annual consumption ($\$/kWh$) or cost normalized by the user's annual peak demand ($\$/kW$). Weighting is used to combine individual or group costs for each duration and generate a "representative" group or sector cost function. The sector *CDF's* for a given service area, expressed in 1987 dollars, are given in Table C.1.

Table C.1. Sector interruption cost estimates (*CDF's*) expressed as cost per kW of annual peak demand ($\$/kW$).

user sector	interruption duration 1 min	20 min	1 hr	4 hrs	8 hrs
large users	1.005	1.508	2.225	3.968	8.240
industrial	1.625	3.868	9.085	25.163	55.808
commercial	0.381	2.969	8.552	31.317	83.008
agricultural	0.060	0.343	0.649	2.064	4.120
residential	0.001	0.093	0.482	4.914	15.690
govt. & inst.	0.044	0.369	1.492	6.558	26.040
office & bldg.	4.778	9.878	21.065	68.830	119.160

The cost of interruption at a single customer load point is dependent entirely on the cost characteristics of that customer. As the supply point in question moves away from the actual customer load point, the consequences of an outage of the supply point involves an increasing number of customers. As the supply point becomes the generating system, potentially all system customers are involved. The customer cost associated with a particular outage at a specific point in the system involves an amalgamation of the costs associated with the customers affected by the interruptions at that point in the system. This amalgamation or consolidation of costs is known as a Composite Customer Damage Function (*CCDF*).

C.1. Creating a Composite Customer Damage Function

Conceptually, the *CCDF* for a particular service area is an estimate of the cost associated with power supply interruptions as a function of the interruption duration for the customer mix in the service area. Each customer or type of customer has a different cost for a particular outage duration and the method for combining the individual costs is to perform a weighted average according to the annual peak demand or energy consumption of the individual customers or customer group. Weighting by annual peak demand is used for short duration interruptions and weighting by the energy consumption is used for interruptions longer than one-half hour [46]. The load composition of the service area used in all the studies reported in this thesis is given in Table C.2.

Table C.2. Load composition of the service area, based on annual peak demand and annual energy consumption.

user sector	sector peak (%)	sector energy (%)
large users	30.0	31.0
industrial	14.0	19.0
commercial	10.0	9.0
agricultural	4.0	2.5
residential	34.0	31.0
govt. & inst.	6.0	5.5
office & bldg.	2.0	2.0
Total	*100.0*	*100.0*

In order to calculate the *CCDF*, the user sector costs given in Table C.1 are weighted in accordance with the load composition of the service area given in Table C.2. The weighted costs are then summed for each duration and the results are presented in Table C.3 and shown graphically in Figure C.1. Despite the uncertainties affecting the development of a *CCDF*, it is the most suitable function available for determining monetary estimates of reliability worth. The *CCDF* can be tailored to reflect the individual nature of the system, a region within it and in the limit, any particular customer.

Table C.3. Composite customer damage function for the service area.

service area of system	interruption duration				
	1 min	20 min	1 hr	4 hrs	8 hrs
interruption cost (1987 *$/kW*)	0.67	1.56	3.85	12.14	29.41

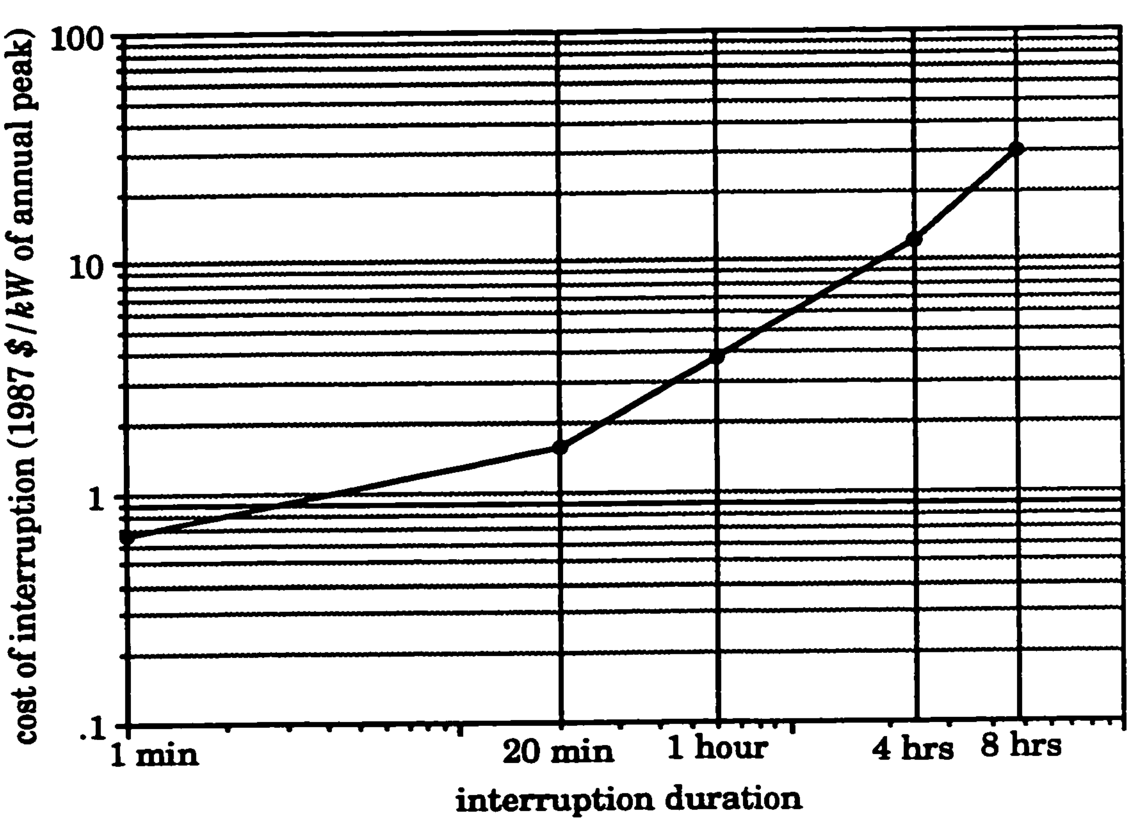

Figure C.1. Composite customer damage function for the service area.

D. REPRESENTATION OF CAPACITY OUTAGES IN GENERATING SYSTEMS USING NORMAL AND FOLDED NORMAL DISTRIBUTIONS

The two parameters which characterize a normal distribution are the mean value μ and the standard deviation σ. If each generating unit has a binary representation, the capacity on forced outage for each Unit i in the system can be represented by two pulses, one at zero outage with probability $1 - q_i$ and the other at the full outage C_i with probability q_i where q_i is the forced outage rate or the outage replacement rate of the unit. The probability density function of a two-state generating unit model is shown in Figure D.1.

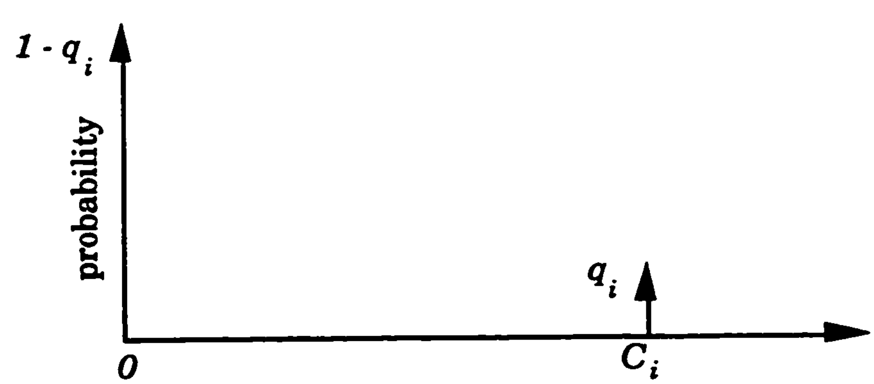

Figure D.1. Probability density function of capacity outages of a generating unit.

The mean and the variance of the discrete random variable representing the capacity on outage of the generating unit can be found from Figure D.1 as follows:

$$\mu_i = 0(1-q_i) + C_i q_i \text{ and} \tag{D.1}$$

$$\sigma_i^2 = 0^2(1-q_i) + C_i^2 q_i - C_i^2 q_i^2 = C_i^2 q_i (1-q_i). \tag{D.2}$$

According to the central limit theorem, the summation of a large number of independent random variables can be approximated to a normal distribution. Thus, a normal approximation to the discrete system capacity model is possible. The mean and the variance of the distribution of capacity outages in the generating system are therefore given by:

$$\mu = \sum_{i=1}^{m} \mu_i = \sum_{i=1}^{m} C_i q_i \text{ and} \tag{D.3}$$

$$\sigma^2 = \sum_{i=1}^{m} \sigma_i^2 = \sum_{i=1}^{m} C_i^2 q_i (1-q_i), \tag{D.4}$$

where m denotes the number of generating units in the system. If the system has generating units with derated states, Equations (D.3) and (D.4) can be modified to include the effect of unit deratings [91]. The first step in this process involves calculating the first and second order moments for each unit as shown in (D.5) and (D.6) respectively.

$$m_1(i) = \sum_{j=1}^{n_i} C_{ij} q_{ij} \text{ and} \tag{D.5}$$

$$m_2(i) = \sum_{j=1}^{n_i} C_{ij}^2 q_{ij}, \tag{D.6}$$

where $m_1(i)$: first order moment of Unit i,
$m_2(i)$: second order moment of Unit i,
C_{ij} : capacity outage of State j for Unit i,
q_{ij} : probability that Unit i is residing in State j and
n_i : number of states for Unit i.

The mean and the variance of the distribution of capacity outages in the generating system can be calculated from $m_1(i)$ and $m_2(i)$ using (D.7) and (D.8) respectively. That is,

$$\mu = \sum_{i=1}^{m} m_1(i) \text{ and} \tag{D.7}$$

$$\sigma^2 = \sum_{i=1}^{m} m_2(i) - m_1^2(i). \tag{D.8}$$

Having determined the mean and the variance of the normal distribution, the generating system capacity outage model can be expressed by the following probability density function [92]:

$$f(x) = \frac{1}{\sigma\sqrt{2\pi}} e^{-\frac{1}{2}\left(\frac{x-\mu}{\sigma}\right)^2} \qquad \text{for } -\infty \le x \le \infty, \tag{D.9}$$

where the continuous random variable ($r.v.$) X represents the capacity on outage. If the mean value μ is set to zero by defining a new random variable and all the deviations are measured from the mean in terms of the standard deviation σ, the equation for $f(x)$ becomes:

$$N(z) = \frac{1}{\sqrt{2\pi}} e^{-\frac{1}{2}z^2} \qquad \text{where } Z = \frac{X-\mu}{\sigma}. \tag{D.10}$$

The generating system capacity outage model can now be built up using any suitable step size which will determine the outages X. The probability of encountering a capacity on outage equal to or greater than x_i is given by:

$$prob\{capacity outage \ge x_i\} = \int_{z_i}^{\infty} N(z)dz \qquad \text{where } z_i = \frac{x_i-\mu}{\sigma}. \tag{D.11}$$

This probability can be evaluated using look-up tables [92] or by approximate methods that can be implemented on a digital computer [81].

D.1. Calculation of the Probability of a Capacity Outage Using the Folded Normal Distribution

The probability density function of the folded normal distribution is given by:

$$f(x) = \frac{1}{\sigma\sqrt{2\pi}} \left\{ e^{-\frac{1}{2}\left(\frac{x-\mu}{\sigma}\right)^2} + e^{-\frac{1}{2}\left(\frac{x+\mu}{\sigma}\right)^2} \right\} \qquad \text{for } x \geq 0 \qquad \text{(D.12)}$$

with parameters μ and σ as defined by (D.7) and (D.8) respectively. The probability of encountering a capacity on outage equal to or greater than x can be obtained using the following equation:

$$Prob\{capacity\,outage \geq x\} = \int_{z_1}^{\infty} N(z)\,dz + \int_{z_2}^{\infty} N(z)\,dz, \qquad \text{(D.13)}$$

where $N(z)$ is the standard normal distribution (i.e. zero mean and unit variance) and z_1 and z_2 are defined by:

$$z_1 = \frac{x-\mu}{\sigma} \text{ and } z_2 = \frac{x+\mu}{\sigma}. \qquad \text{(D.14)}$$

E. REPRESENTATION OF CAPACITY OUTAGES IN GENERATING SYSTEMS USING GRAM-CHARLIER SERIES

It has been observed in [91] that the folded normal model of capacity outages is relatively inaccurate when compared to the recursive technique, particularly for large capacity outages. An improvement in the accuracy of the model can be achieved using the Gram-Charlier series [90,91]. To do this, the probability density function of the folded normal distribution given by (D.12) can be modified and written in terms of the standard normal distribution $N(z)$ as follows [92]:

$$f(z) = \sum_{j=0}^{\infty} \alpha_j H_j(z) N(z), \tag{E.1}$$

where $H_j(z)$ denotes a Tchebychev-Hermite polynomial of degree j and α_j's are the coefficients of the series. The general form of the polynomial, $H_j(z)$, is given by:

$$H_j(z) = (-1)^j e^{\frac{z^2}{2}} \frac{d^j}{dz^j} e^{\frac{-z^2}{2}}. \tag{E.2}$$

The detailed expressions of these polynomials up to the eight order are given by (E.3),

$$
\begin{aligned}
H_0 &= 1, \\
H_1 &= z, \\
H_2 &= z^2 - 1, \\
H_3 &= z^3 - 3z, \\
H_4 &= z^4 - 6z^2 + 3, \\
H_5 &= z^5 - 10z^3 + 15z, \\
H_6 &= z^6 - 15z^4 + 45z^2 - 15, \\
H_7 &= z^7 - 21z^5 + 105z^3 - 105z \text{ and} \\
H_8 &= z^8 - 28z^6 + 210z^4 - 420z^2 + 105.
\end{aligned} \tag{E.3}
$$

The coefficients α_j are obtained using the orthogonality property of the Hermite polynomials and are given by:

$$
\begin{aligned}
\alpha_j &= \frac{1}{j!} \int_{-\infty}^{+\infty} f(z) H_j(z) dz, \\
&= \frac{1}{j!} \left[m'_j - \frac{j^2}{2 \times 1!} m'_{j-2} + \frac{j^4}{2^2 \times 2!} m'_{j-4} - \dots \right],
\end{aligned} \tag{E.4}
$$

where m'_j denotes the j^{th} moment of $f(z)$ about the origin. In particular, for the moments m_j about the mean, the coefficients α_j can be expressed as follows:

$$
\begin{aligned}
\alpha_0 &= 1, \\
\alpha_1 &= 0, \\
\alpha_2 &= \frac{1}{2!}(m_2 - 1), \\
\alpha_3 &= \frac{1}{3!} m_3, \\
\alpha_4 &= \frac{1}{4!}(m_4 - 6m_2 + 3), \\
\alpha_5 &= \frac{1}{5!}(m_5 - 10m_3), \\
\alpha_6 &= \frac{1}{6!}(m_6 - 15m_4 + 45m_2 - 15), \\
\alpha_7 &= \frac{1}{7!}(m_7 - 21m_5 + 105m_3) \text{ and} \\
\alpha_8 &= \frac{1}{8!}(m_8 - 28m_6 + 210m_4 - 420m_2 + 105).
\end{aligned} \tag{E.5}
$$

If the coefficients α_j of (E.1) are expressed as a function of the central moments (i.e. moments about the mean), the series can be expanded by substituting the values of α_j given by (E.5) and the values of $H_j(z)$ given by (E.3) into (E.1). If, however, the coefficients α_j are expressed in terms of the cumulants of $f(z)$, they will have to be calculated differently as shown in (E.6).

$$
\begin{aligned}
\alpha_0 &= 1, \\
\alpha_1 &= 0, \\
\alpha_2 &= 0, \\
\alpha_3 &= \frac{1}{3!}K_3, \\
\alpha_4 &= \frac{1}{4!}K_4, \\
\alpha_5 &= \frac{1}{5!}K_5, \\
\alpha_6 &= \frac{1}{6!}\left(K_6 - 16K_3^2\right), \\
\alpha_7 &= \frac{1}{7!}\left(K_7 - 35K_4K_3\right) \text{ and} \\
\alpha_8 &= \frac{1}{8!}\left(K_8 - 56K_5K_3 + 35K_4^2\right).
\end{aligned}
\tag{E.6}
$$

where K_j represents the cumulant of order j of $f(z)$. These cumulants can be expressed in terms of either the moments about the origin or the moments about the mean of the function $f(z)$. The first eight cumulants expressed in terms of the moments about the origin are given by the following equations [92]:

$$
\begin{aligned}
K_1 &= m_1', \\
K_2 &= m_2' - m_1'^2, \\
K_3 &= m_3' - 3m_2'm_1' + 2m_1'^3, \\
K_4 &= m_4' - 4m_3'm_1' - 3m_2'^2 + 12m_2'm_1'^2 - 6m_1'^4,
\end{aligned}
$$

$$K_5 = m_5' - 5m_4'm_1' - 10m_3'm_2' + 20m_3'm_1'^2 + 30m_2'^2m_1' - 60m_2'm_1'^3 + 24m_1'^5,$$

$$K_6 = m_6' - 6m_5'm_1' - 15m_4'm_2' + 30m_4'm_1'^2 - 10m_3'^2 + 120m_3'm_2'm_1' - 120m_3'm_1'^3 + 30m_2'^3 - 270m_2'^2m_1'^2 + 360m_2'm_1'^4 - 120m_1'^6,$$

$$K_7 = m_7' - 7m_6'm_1' - 21m_5'm_2' + 42m_5'm_1'^2 - 35m_4'm_3' + 210m_4'm_2'm_1' - 210m_4'm_1'^3 + 140m_3'^2m_1' + 210m_3'm_2'^2 - 1260m_3'm_2'm_1'^2 + 840m_3'm_1'^4 - 630m_2'^3m_1' + 2520m_2'^2m_1'^3 - 2520m_2'm_1'^5 - 720m_1'^7 \text{ and}$$

$$K_8 = m_8' - 8m_7'm_1' - 28m_6'm_2' + 56m_6'm_1'^2 - 56m_5'm_3' + 336m_5'm_2'm_1' - 336m_5'm_1'^3 - 35m_4'^2 + 560m_4'm_3'm_1' + 420m_4'm_2'^2 - 2520m_4'm_2'm_1'^2 + 1680m_4'm_1'^4 + 560m_3'^2m_2' - 1680m_3'^2m_1'^2 - 5040m_3'm_2'^2m_1' + 13440m_3'm_2'm_1'^3 - 6720m_3'm_1'^5 - 630m_2'^4 + 10080m_2'^3m_1'^2 - 25200m_2'^2m_1'^4 + 20160m_2'm_1'^6 - 5040m_1'^8. \qquad \text{(E.7)}$$

In the case under consideration, the function $f(z)$ is not known and the cumulants of $f(z)$ can be expressed in terms of the cumulants of each generating unit's *pdf*. The system cumulants are therefore equal to:

$$K_j = \sum_{i=1}^{m} K_j(i) \qquad \text{for } j=1,2,\dots,8, \qquad \text{(E.8)}$$

where m represents the number of generating units in the system and $K_j(i)$ is the j^{th} order cumulant of unit i as defined by (E.7).

The expansion coefficients, α_j, given by (E.6) have been obtained under the assumption that the function $f(z)$ is in the standard format and therefore the cumulants of the function are calculated in terms of the original function $f(x)$. The relationship between the standard *r.v.* Z and the *r.v.* X is given by:

$$Z = \frac{X-\mu}{\sigma}, \qquad \text{(E.9)}$$

where μ and σ are the mean and standard deviation of the function $f(x)$. If the cumulants of the *r.v.* X are known, then the cumulants of the *r.v.* Z

(standard variable) are obtained by dividing the cumulant of X by the standard deviation raised to the power of the order of that cumulant. That is, the j^{th} cumulant of Z, $K_j(z)$, can be calculated from the j^{th} cumulant of the generating system's *pdf*, $K_j(x)$, as follows:

$$K_j(z) = \frac{K_j(x)}{\sigma^j}. \tag{E.10}$$

Using the coefficients derived in (E.6) and the cumulants of the distribution, an expression for the probability distribution of capacity outages can be written as:

$$\begin{aligned} f(z) = N(z) &- \frac{K_3}{3!}N^{(3)}(z) + \frac{K_4}{4!}N^{(4)}(z) - \frac{K_5}{5!}N^{(5)}(z) + \frac{1}{6!}\left(K_6 + 10K_3^2\right)N^{(6)}(z) \\ &- \frac{1}{7!}\left(K_7 + 35K_4K_3\right)N^{(7)}(z) + \frac{1}{8!}\left(K_8 + 56K_3K_5 + 35K_4^2\right)N^{(8)}(z) - \ldots \end{aligned} \tag{E.11}$$

which is the general form of the Edgeworth expansion of a distribution. The Gram-Charlier expansion can be derived from this general expansion by considering all the terms up to the fourth order as given by (E.12),

$$f(z) = N(z) - \frac{K_3}{3!}N^{(3)}(z) + \frac{K_4}{4!}N^{(4)}(z) + \frac{10K_3^2}{6!}N^{(6)}(z). \tag{E.12}$$

Based on the expansions given by (E.11) and (E.12), any random variable X with a *pdf* $f(x)$ and finite moments can be expressed in terms of the standard *pdf*, $N(z)$, and its corresponding derivatives and cumulants. The procedure used to calculate the probability of encountering a capacity outage equal to or greater than x is discussed in the following section.

E.1. Calculation of the Probability of a Capacity Outage Using the Gram-Charlier Expansion of a distribution

The cumulative probability of a capacity outage equal to or greater than x is given by:

$$
\begin{aligned}
prob\{capacity\, outage \geq x\} &= \int_{z_1}^{\infty} f(z)dz + \int_{z_2}^{\infty} f(z)dz, \\
&= \int_{z_1}^{\infty} N(z)dz + \int_{z_2}^{\infty} f(z)dz + Correc1 + Correc2, \quad \text{(E.13)} \\
&= Area1 + Area2 + Correc1 + Correc2,
\end{aligned}
$$

where: $z_1 = \dfrac{x-\mu}{\sigma}$,

$z_2 = \dfrac{x+\mu}{\sigma}$,

$Correc1 = \dfrac{K_3}{3!}N^{(2)}(z_1) - \dfrac{K_4}{4!}N^{(3)}(z_1) + \dfrac{K_5}{5!}N^{(4)}(z_1) - \ldots$ and

$Correc2 = \dfrac{K_3}{3!}N^{(2)}(z_2) - \dfrac{K_4}{4!}N^{(3)}(z_2) + \dfrac{K_5}{5!}N^{(4)}(z_2) - \ldots.$

Area1 and *Area2* are defined in Figure E.1 and can be calculated from look-up tables [72] or using an approximate method that can be implemented on a digital computer [81].

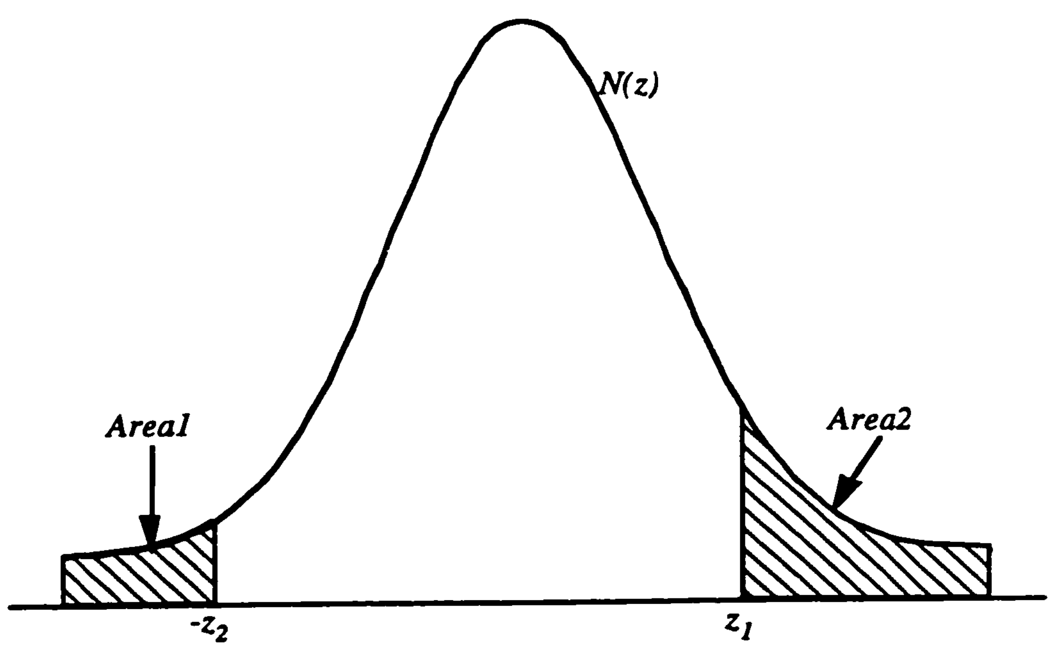

Figure E.1. Representation of *Area1* and *Area2* on the *pdf* of a standardized normal distribution.

In calculating the probability given by (E.13), it is found that the following approximations are necessary in order to save computing time without compromising the accuracy of the results [91].

$$\begin{array}{lll} Case\,1: & if\; z_2 \le 2 & neglect\; Correc1\; and\; Correc2, \\ Case\,2: & if\; 2 < z_2 \le 5 & include\; all\; 4\; terms\; of\; (E.1)\; \text{and} \\ Case\,3: & if\; z_2 > 5 & neglect\; Area1\; and\; Area2. \end{array} \qquad (E.14)$$

F. CALCULATION OF THE PROBABILITY OF A CAPACITY OUTAGE USING THE LARGE DEVIATION METHOD

The large deviation method can be best explained by reference to the tail probability determination of the sum of m *i.i.d.* (independent and identically distributed) positive random variables $(X_1+X_2+\ldots+X_m)$ with a common probability density function $f(x)$. This formulation can be used to derive an expression for ΔEUE as follows:

$$\Delta EUE = prob\{X_1+X_2+\ldots+X_m \geq y\}, \tag{F.1}$$

where X_i : random variable that describes the *pdf* of Unit i,

y : a constant equal to installed capacity minus load level and

m : number of generating units in the system.

The value of y can lie on the left tail, the right tail or the centre of the distribution depending on the installed capacity of the system and the load level for which ΔEUE is desired. In order to simplify the following derivation, however, it is assumed that the value of y lies in the right tail of the distribution. An adjustment to the final result will be required if y lies on the left tail of the distribution. This adjustment will be discussed in Section F.3.

Using the above assumption, define the following expressions for some $S>0$ [101,102]:

$$\nu(x) = \frac{e^{Sx} f(x)}{\hat{F}(S)} \text{ where} \tag{F.2}$$

$$\hat{F}(S) = \int_0^{\infty} e^{Sx} f(x)\, dx. \tag{F.3}$$

Since all the random variables, X_i, are bounded for the case under consideration (i.e. capacity on outage can vary between zero and the rated capacity of the generating unit), then $\hat{F}(S)$ is finite for $S>0$. In probability theory, $\hat{F}(S)$ is referred to as the moment generating function (*m.g.f.*) and $\upsilon(x)$ as the associated density function. Thus, $\upsilon(x)$ is a valid *pdf* which has its mass shifted to the right of that of $f(x)$.

Denote the m-fold convolutions of the densities $f(x)$ and $\upsilon(x)$ by $f_m^*(x)$ and $\nu_m^*(x)$ respectively. The *pdf* of the sum of m $i.i.d.$ $(X_1+X_2+\ldots+X_m)$ variables can be expressed in terms of the *m.g.f.* and the associated density function as follows [101,102]:

$$f_m^*(x) = \left[\hat{F}(S)\right]^m e^{-Sx} \nu_m^*(x). \tag{F.4}$$

This *pdf* can be used to calculate the probability expression given by (F.1) as follows:

$$\begin{aligned} \Delta EUE &= \int_y^{\infty} f_m^*(x)dx\,, \\ &= \left[\hat{F}(S)\right]^m \int_y^{\infty} e^{-Sx} \nu_m^*(x)\, dx. \end{aligned} \tag{F.5}$$

The value of S must be chosen such that y equals the mean of $\nu_m^*(x)$. With this choice, the integration will be done in a region where $\nu_m^*(x)$ can be more accurately approximated by a normal distribution or an asymptotic expansion of this distribution using the Edgeworth series. The effect of the multiplier e^{-Sx} is to de-emphasize the contribution of $v_m^*(x)$ for values of x in the tail. This is precisely the region where the normal approximation is likely to be inaccurate.

The large deviation method derived in this section assumes that all the generating units are represented by two-state models [101,102]. The implementation of multi-state models is discussed in Section F.1. For a given value of S, the *m.g.f.* of X_i and that of $X=X_1+X_2+\ldots+X_m$ are given by:

$$\hat{F}_i(S) = e^{SC_i}\, q_i + (1-q_i) \text{ and} \tag{F.6}$$

$$\left[\hat{F}(S)\right]^m = \prod_{i=1}^{m} \hat{F}_i(S), \tag{F.7}$$

where C_i and q_i are defined in Figure D.1. It has been shown in [101,102] that the mean, $\psi'(S)$, and the variance, $\psi''(S)$, of $v_m^*(x)$ can be calculated using the following equations:

$$\psi'(S) = \sum_{i=1}^{m} \frac{q_i\, C_i}{q_i + (1-q_i)\, e^{-SC_i}} \text{ and} \tag{F.8}$$

$$\psi''(S) = \sum_{i=1}^{m} \frac{q_i\, C_i^2 (1-q_i)\, e^{-SC_i}}{\left[q_i + (1-q_i)\, e^{-SC_i}\right]^2}. \tag{F.9}$$

In order to calculate the value of S which represents the amount by which $v_m^*(x)$ must be shifted to center at y, the following equation must be solved:

$$\psi'(S) = y. \tag{F.10}$$

Finding a solution to (F.10) takes considerable computational efforts but the solution can be found using the Newton-Raphson or Secant method [105]. If the solution found is designated as S_0 and the pdf of $v_m^*(x)$ is replaced by a normal probability density function with mean $\psi'(S_0)$ and variance $\psi''(S_0)$, the expression for ΔEUE becomes:

$$\begin{aligned} \Delta EUE &\approx \Delta EUE_1, \\ &= \prod_{i=1}^{m} \hat{F}_i(S_0)\, e^{-S_0\,\psi'(S_0) + \frac{S_0^2\,\psi''(S_0)}{2}} \left[1 - \Phi\left(S_0\sqrt{\psi''(S_0)}\right)\right], \end{aligned} \tag{F.11}$$

where $\Phi(x) = \frac{1}{\sqrt{2\pi}} \int_{-\infty}^{x} e^{-\frac{z^2}{2}}\, dz$ is the area under the standard normal curve to the left of x.

F.1. Modelling of Multi-State Generating Units

Assume that Unit i has n capacity states $(n \geq 2)$ and X_i, the $r.v.$ representing the capacity on outage for Unit i, has the following probability distribution:

$$X_i = C_{ij} \text{ with probability } q_{ij}, \tag{F.12}$$

where C_{ij} is the capacity on outage of Unit i in State j and q_{ij} is the probability that this event occurs. The procedure for applying the large deviation method remains unchanged, but the expressions for the mean and the variance of $v_m^*(x)$ are different. In order to calculate these variables, the r^{th} order cumulants of $v_m^*(x)$ must be calculated as follows [103]:

$$\psi^{(r)}(S) = \sum_{i=1}^{m} \psi_i^{(r)}(S) \qquad r = 1, 2, \ldots, \tag{F.13}$$

where the r^{th} cumulant of Unit i is given by:

$$\psi_i^{(r)}(S) = \frac{d^r}{dS^r}\left[ln \sum_{j=1}^{n} e^{SC_{ij}}\ q_{ij} \right]. \tag{F.14}$$

In order to obtain explicit expressions for (F.14), it is convenient to define the following function:

$$f_k(S) = \sum_{j=1}^{n} C_{ij}^k q_{ij} e^{SC_{ij}}. \tag{F.15}$$

It can be observed from this function that

$$f_k^{(r)}(S) = \frac{d^r}{dS^r} f_k(S) = f_{r+k}(S) \qquad r = 1, 2, ... \tag{F.16}$$

Now, define the following parameter:

$$R_k(S) = \frac{f_k(S)}{f_0(S)} \qquad k = 1, 2, ... \tag{F.17}$$

The successive order derivatives of $\psi_i(S)$ can now be derived from (F.16) and (F.17) as follows:

$$\psi'(S) = R_1(S) = \frac{f_1(S)}{f_0(S)}, \tag{F.18}$$

$$\psi''(S) = R_2(S) - R_1^2(S), \tag{F.19}$$

$$\psi'''(S) = R_3(S) - 3R_1(S)R_2(S) + 2R_1^3(S) \text{ and} \tag{F.20}$$

$$\psi^{(4)}(S) = R_4(S) - 4R_1(S)R_3(S) - 3R_2^2(S) + 12R_1^2(S)R_2(S) - 6R_1^4(S). \tag{F.21}$$

The above formulas can be checked by substituting the value of $n=2$ in (F.14) and (F.15) and comparing the resulting expressions of the first and second order cumulants to those shown in (F.8) and (F.9) respectively.

F.2. Formulation With Edgeworth Expansion for $v_m^*(x)$

The motivation to replace the distribution of the system capacity outage by an appropriate Edgeworth expansion was justified in Appendix E. Therefore, it seems reasonable to use the same type of expansion to replace $v_m^*(x)$. Mazumdar et. al. [101-103] have studied this possibility and concluded that the Edgeworth expansion involving the second order terms (i.e. those involving terms up to the first four order cumulants) is generally more accurate than the corresponding normal or first order Edgeworth expansion. The expressions for the first and second order expansions are derived in this section.

The Edgeworth expansion of a density function $f(x)$ whose first four cumulants are K_1, K_2, K_3 and K_4 was developed in Appendix E and can be written as:

$$f(z) = N(z) - \frac{K_3}{3!} N^{(3)}(z) + \frac{K_4}{4!} N^{(4)}(z) + \frac{10K_3^2}{6!} N^{(6)}(z), \qquad \text{(F.22)}$$

where $z = \dfrac{x - K_1}{\sqrt{K_2}}$, $\qquad N(z) = \dfrac{1}{\sqrt{2\pi}} e^{-\frac{z^2}{2}}$,

$N^{(r)}(z) = \dfrac{d^r}{dz^r} N(z)$ and $\qquad K_j = \dfrac{K_j(x)}{\sqrt[j/2]{K_2(x)}}$

$K_j(x)$ is the j^{th} cumulant of $f(x)$ as defined by (E.7). For the case under consideration, the first four cumulants of $v_m^*(x)$ are given by (F.18) thru (F.21). Let S_0 be the solution of the equation $\psi'(S) = y$ and define the following parameters:

$$u = S_0\sqrt{\psi''(S_0)}, \qquad E_0(u) = e^{\frac{u^2}{2}}\left[1-\Phi(u)\right],$$

$$K_3 = \frac{\psi'''(S_0)}{\sqrt{\left[\psi''(S_0)\right]^3}}, \qquad K_4 = \frac{\psi^{(4)}(S_0)}{\left[\psi''(S_0)\right]^2},$$

$$w = \sqrt{2\pi}\,E_0(u), \qquad v = u^3 - \frac{u^2-1}{w} \text{ and} \tag{F.23}$$

$$\hat{F}(S_0) = \prod_{i=1}^{m}\hat{F}_i(S_0) = e^{\psi(S_0)}.$$

The expression for ΔEUE shown in (F.5) can be evaluated by substituting $v_m^*(x)$ with the appropriate normal and Edgeworth expansions using the first and second order terms only. The resulting expressions are given by:

$$\Delta EUE = prob\left\{X_1 + X_2 + \ldots + X_m \geq y\right\},$$

$$\approx \Delta EUE_1 = e^{\psi(S_0)-S_0 y}\,E_0(u) \qquad \text{(normal)}, \tag{F.24}$$

$$\approx \Delta EUE_2 = \Delta EUE_1\left\{1 - \frac{K_3}{3!}v\right\} \qquad (1^{st} \text{ order Edgeworth) and} \tag{F.25}$$

$$\approx \Delta EUE_3 = \Delta EUE_2 + \Delta EUE_1\left\{\frac{K_4}{4!}uv + \frac{10K_3^2}{6!}\left[u^3 v - \frac{3u}{v}\right]\right\} \qquad (2^{nd} \text{ order Edgeworth}). \tag{F.26}$$

F.3. Modelling Adjustments for Negative Values of S_0

The preceding derivations have been done assuming that the value of S_0 is positive (i.e. y lies on the right tail of the distribution). If this assumption is not valid, the large deviation can still be used to calculate ΔEUE; but the equations will have to be adjusted to account for the negative values of S_0. This condition occurs when the following inequality is valid,

$\psi'(0) = E\{X_1 + X_2 + \ldots + X_m\} < y$. The value of ΔEUE can still be calculated under this condition by defining the following equation and using the large deviation method to estimate its right side,

$$\begin{aligned} \Delta EUE &= prob\{X_1 + X_2 + \ldots + X_m \geq y\}, \\ &= 1 - prob\{X_1 + X_2 + \ldots + X_m < y\} = 1 - \overline{\Delta EUE}. \end{aligned} \quad \text{(F.27)}$$

The detailed derivation of $\overline{\Delta EUE}$ is outlined in [103] and the results are summarized below.

$$\overline{\Delta EUE} = prob\{X_1 + X_2 + \ldots + X_m < y\},$$

$$\approx \overline{\Delta EUE_1} = e^{\psi(s_0) - s_0 y}\, \overline{E}_0(u), \qquad \text{(normal)}, \qquad \text{(F.28)}$$

$$\approx \overline{\Delta EUE_2} = \overline{\Delta EUE_1}\left\{1 - \frac{K_3}{3!}v'\right\} \qquad (1^{st} \text{ order Edgeworth) and} \qquad \text{(F.29)}$$

$$\approx \overline{\Delta EUE_3} = \overline{\Delta EUE_2} + \overline{\Delta EUE_1}\left\{\frac{K_4}{4!}uv' + \frac{10K_3^2}{6!}\left[u^3v' - \frac{3u}{w'}\right]\right\} \quad (2^{nd} \text{ order Edgeworth}), \qquad \text{(F.30)}$$

where u, K_3 and K_4 are defined by (F.23) and

$$\begin{aligned} \overline{E_0}(u) &= e^{\frac{u^2}{2}}\,\Phi(u), \\ w' &= -\sqrt{2\pi}\,\overline{E_0}(u) \text{ and} \\ v' &= u^3 - \frac{u^2 - 1}{w'}. \end{aligned} \qquad \text{(F.31)}$$

G. GENERATING A COMPOSITE CUSTOMER DAMAGE FUNCTION AND AN *IEAR* FOR EACH LOAD BUS IN THE *RBTS*

One of the most basic requirements for evaluating the *IEAR* at *HLII* are the Composite Customer Damage Functions (*CCDF*'s) at each load bus in the system. These functions can be calculated by assigning different sectors to specific load buses in the system. The sector allocation must be chosen in such a way that meets the following two requirements:

$$\sum_{\substack{all \\ sectors}} sector\ peak\ at\ Bus\ i = peak\ load\ at\ Bus\ i \text{ and} \tag{G.1}$$

$$\sum_{\substack{all \\ buses}} sector\ peak\ at\ Bus\ i = sector\ peak\ of\ the\ system. \tag{G.2}$$

The sector load allocation at each load bus of the *RBTS* is given in Table G.1. It can be seen from this table that there are some residential and commercial sector customers at every load bus of the *RBTS*. As an example, Bus 2 has industrial, commercial, residential and government and institutional users allotted to it. The *CCDF* for the load buses will be different due to the sector allocations and therefore the corresponding *IEAR* values will also be different as will be shown later in Section G.1.

Table G.1. Sector allocation at each load bus of the *RBTS*.

user sector	peak load allocation (*MW*)					
	Bus 2	Bus 3	Bus 4	Bus 5	Bus 6	system
large users		55.50				*55.50*
industrial	3.50	3.05	16.30		3.05	*25.90*
commercial	3.70	4.70	4.70	3.70	1.70	*18.50*
agricultural					7.40	*7.40*
residential	7.25	19.90	19.00	8.90	7.85	*62.90*
govt. & inst.	5.55			5.55		*11.10*
office & bldg.		1.85		1.85		*3.70*
total	*20.00*	*85.00*	*40.00*	*20.00*	*20.00*	*185.00*

In addition to the sector allocation at the system load buses, the annual peak load and energy consumption distributions are required to calculate the *CCDF* at the various load buses. The annual peak load distribution of a given sector at Bus i can be calculated using (G.3). This distribution is given for every load bus in the *RBTS* and for the whole system in Table G.2.

$$\textit{sector peak distribution at Bus } i = \frac{\textit{sector allocation at Bus } i}{\textit{peak load at Bus } i} \times 100. \qquad \text{(G.3)}$$

Table G.2. Sector peak load distribution at each load bus of the *RBTS*.

user sector	sector peak distribution (%)					
	Bus 2	Bus 3	Bus 4	Bus 5	Bus 6	system
large users		65.29				*30.0*
industrial	17.50	3.59	40.75		15.25	*14.0*
commercial	18.50	5.53	11.75	18.50	8.50	*10.0*
agricultural					37.00	*4.0*
residential	36.25	23.41	47.50	44.50	39.25	*34.0*
govt. & inst.	27.75			27.75		*6.0*
office & bldg.		2.18		9.25		*2.0*
total	*100.00*	*100.00*	*100.00*	*100.00*	*100.00*	*100.0*

There are many ways of allocating the energy consumption of each user sector to the various buses of a power system. One of the easiest ways, however, consists of using the same sector Load Factor *(L.F.)* for each load bus in the system. This method ensures that the energy consumption of each sector is consistent at *HLI* and *HLII*. In a practical system, it is expected that the energy consumption of a given sector will not vary greatly from one bus to another due to the aggregate effect of the various *SIC* groups within the sector.

The load factor of a given sector can be calculated from the system load factor, the sector energy distribution and the sector peak load distribution as follows:

$$sector\ L.F. = \frac{sector\ energy\ distribution\,(\%)}{sector\ peak\ distribution\,(\%)} \times system\ L.F. \tag{G.4}$$

The load factor of a given system depends on the load model used. In the case of the *RBTS*, it is reported in [35] that this system has the same load model as the *IEEE-RTS* [36]. The load model of the *IEEE-RTS* is known to have a load factor of <u>61.40%</u> [36]. This value can be used together with the sector peak and energy distributions given in Table C.2 to calculate the load factor of each sector using (G.4). The results from these calculations are given in Table G.3.

Table G.3. Load factors of each user sector in the *RBTS*.

user sector	sector peak (%)	sector energy (%)	sector *L.F.* (%)
large users	30.0	31.0	63.45
industrial	14.0	19.0	83.33
commercial	10.0	9.0	55.26
agricultural	4.0	2.5	38.38
residential	34.0	31.0	55.98
govt. & inst.	6.0	5.5	56.28
office & bldg.	2.0	2.0	61.40
total	*100.0*	*100.0*	61.40

The sector load factors given in Table G.3 can be used together with the sector peak load allocation given in Table G.1 to calculate the average sector load at each bus using (G.5). The average loads of each sector at every load bus in the *RBTS* and for the whole system are given in Table G.4.

$$sector\,average\,load\,at\,Bus\,i = sector\,L.F.\times sector\,peak\,load\,at\,Bus\,i. \qquad (G.5)$$

Table G.4. Sector average load at each load bus of the *RBTS*.

user sector	average loads (*MW*)					
	Bus 2	Bus 3	Bus 4	Bus 5	Bus 6	system
large users		35.21				*35.21*
industrial	2.92	2.54	13.58		2.54	*21.58*
commercial	2.04	2.60	2.60	2.04	0.94	*10.22*
agricultural					2.84	*2.84*
residential	4.06	11.14	10.64	4.98	4.39	*35.21*
govt. & inst.	3.12			3.12		*6.25*
office & bldg.		1.14		1.14		*2.27*
total	*12.14*	*52.63*	*26.82*	*11.29*	*10.72*	*113.59*

The energy consumption distribution of each sector and each bus of the *RBTS* is calculated in Table G.5 from the data in Table G.4 using (G.6).

$$sector\,energy\,distribution\,at\,Bus\,i = \frac{average\,load\,of\,sector\,at\,Bus\,i}{average\,load\,at\,Bus\,i}\times 100. \qquad (G.6)$$

Table G.5. Sector energy distribution at each load bus of the *RBTS*.

user sector	sector energy distribution (%)					
	Bus 2	Bus 3	Bus 4	Bus 5	Bus 6	system
large users		66.91				*31.0*
industrial	24.02	4.83	50.65		23.72	*19.0*
commercial	16.84	4.94	9.69	18.12	8.77	*9.0*
agricultural					26.50	*2.5*
residential	33.42	21.17	39.66	44.14	41.01	*31.0*
govt. & inst.	25.72			27.68		*5.5*
office & bldg.		2.16		10.06		*2.0*
total	*100.00*	*100.00*	*100.00*	*100.00*	*100.00*	*100.0*

The *CCDF* for each load bus in the *RBTS* are calculated by weighting the user sector costs given in Table C.1 for each interruption duration. The sector peak load distribution (Table G.2) is used for weighting the sector user costs for short durations and the sector energy distribution (Table G.5) is used to weight the sector user costs for interruption durations longer than one half hour. The results are given Table G.6.

Table G.6. *CCDF* for each bus of the *RBTS* (1987 $\$/kW$).

system bus	interruption duration				
	1 min	20 min	1 hr	4 hrs	8 hrs
Bus 2	0.367	1.362	4.167	14.646	39.322
Bus 3	0.840	1.524	2.906	7.941	18.198
Bus 4	0.707	1.969	5.621	17.727	42.530
Bus 5	0.525	1.607	4.295	16.585	41.163
Bus 6	0.303	1.006	3.274	11.276	28.041

The utilization of these functions together with the basic reliability data of the *RBTS* to calculate the *IEAR* at each load bus and the aggregate system *IEAR* is presented in the following section.

G.1. Development of the *IEAR* at Each Load Bus of the *RBTS*

The *IEAR* calculated at *HLI* is an expected value of the cost of unserved energy resulting from the inadequacy of the generating system. This idea of utilizing expected values has also been used to evaluate practical *IEAR* estimates for the individual load buses and the overall system in a composite generation and transmission system adequacy assessment [58]. This work was done using the *COMREL* program.

The *IEAR* at a given load bus i is calculated by examining all the contingencies that lead to load curtailment at that bus. For each contingency j, the variables generated by *COMREL* are the magnitude L_{ij}

(MW) of load curtailment, the frequency f_j (occ/yr) and the duration d_j ($hours$) of the contingency j.

The EUE at Bus i (EUE_i) due to all the contingencies that lead to load curtailment is given by (G.7). The cost $C_{ij}(d_j)$ of an outage of duration d_j can be obtained from the $CCDF$ of Bus i. The expected total cost of power interruptions to customers at Bus i ($ECOST_i$) for all contingencies is given by (G.8). The $IEAR$ at Bus i is evaluated using (G.9) and the aggregate system $IEAR$ is calculated using (G.10).

$$EUE_i = \sum_{j=1}^{NC} L_{ij} f_j d_j \qquad (MWh/yr), \qquad (G.7)$$

$$ECOST_i = \sum_{j=1}^{NC} L_{ij} f_j c_{ij}(d_j) \qquad (MW \times occ/yr \times \$/kW), \qquad (G.8)$$

$$IEAR_i = \frac{\sum_{j=1}^{NC} L_{ij} f_j c_{ij}(d_j)}{\sum_{j=1}^{NC} L_{ij} f_j d_j} \qquad (\$/kWh) \text{ and} \qquad (G.9)$$

$$IEAR(aggregate) = \sum_{i=1}^{nbus} IEAR_i \times q_i \qquad (\$/kWh). \qquad (G.10)$$

where NC : number of contingencies that lead to power interruption at Bus i,

$nbus$: number of load buses in the system and

q_i : fraction of the system load utilized by the customers at Bus i.

Evaluation of the $IEAR$ at each load bus of the $RBTS$ was performed using the generation, transmission and load data given in Appendix A and the following assumptions for the $COMREL$ program. A summary of the results is given in Table G.7. The table also shows how the aggregate system $IEAR$ is obtained from the individual bus values.

1) The peak load of the *RBTS* was set at 185 *MW*.
2) A single step load model was used in the analysis. The effect of multi-step load model can be included in composite system reliability studies in order to produce more representative annual *IEAR* values at the expense of computational time.
3) All load buses were assumed to have 20% curtailable load.
4) *Pass 1* load curtailment philosophy was used.
5) The *AC* load flow technique was used.
6) Contingency enumeration of up to the following contingencies was used:
   i) four or less generating units were examined,
   ii) three or less transmission lines were examined and
   iii) up to two generating units and one line and one generating unit and two lines were considered.
7) The effects of station originated outages were not considered and
8) The effects of common-mode outages were not considered.

Table G.7. *IEAR* values for each load bus in the *RBTS*.

system bus	*ECOST* ($K\$/yr$)	*EUE* (MWh/yr)	*IEAR* ($\$/kWh$)	weight	weighted *IEAR*
Bus 2	903.1160	121.9129	7.41	0.1081	0.80
Bus 3	2217.1741	824.5026	2.69	0.4595	1.24
Bus 4	1793.4840	264.6350	6.78	0.2162	1.47
Bus 5	13.1077	2.7216	4.82	0.1081	0.52
Bus 6	724.8094	199.7049	3.63	0.1081	0.39
			IEAR (aggregate)		4.41

In addition to the basic results given in Table G.7, a number of sensitivity studies were conducted to show the effect of selected pertinent factors on the value of the *IEAR* [34]. The effect of the following pertinent factors were examined and the results are given in Table G.8.

Case 1: effect of using the composite system *CCDF* (Table C.3),
Case 2: effect of using the average interruption duration,

Case 3: effect of using the *DC* load flow method,

Case 4: effect of using the network flow method,

Case 5: effect of using *Pass 2* in the load curtailment philosophy and

Case 6: effect of using *Pass 3* in the load curtailment philosophy.

Table G.8. Effects of selected pertinent factors on the value of the *IEAR* in the *RBTS*.

load point	*IEAR* ($/kWh)					
	Case 1	Case 2	Case 3	Case 4	Case 5	Case 6
Bus 2	4.80	7.29	7.41	7.23	7.41	7.41
Bus 3	4.66	2.57	2.69	2.71	2.69	2.69
Bus 4	4.75	6.67	6.78	6.73	6.78	6.78
Bus 5	3.47	4.79	4.82	6.80	6.57	6.57
Bus 6	3.79	3.62	3.63	3.95	3.63	3.78
aggregate	4.47	4.32	4.42	4.64	4.60	4.62

H. GENERATING A COMPOSITE CUSTOMER DAMAGE FUNCTION AND AN *IEAR* FOR EACH LOAD BUS IN THE *IEEE-RTS*

The *CCDF* at each load bus of the *IEEE-RTS* can be calculated using the same concepts outlined in Appendix G. The sector load allocation at each load bus of the *IEEE-RTS* is given in Table H.1 where:

L	represents the large users sector,
I	represents the industrial sector,
C	represents the commercial sector,
A	represents the agricultural sector,
R	represents the residential sector,
G&I	represents the government and institutions sector and
O&B	represents the office and buildings sector.

The annual peak load distribution for every load bus in the *IEEE-RTS* is given in Table H.2. The values in this table were calculated using (G.3).

The average loads of each sector at every load bus in the *IEEE-RTS* and for the whole system are given in Table H.3. These values are calculated using the sector load factors given in Table G.3. The energy consumption distribution of each sector and each bus in the *IEEE-RTS* are calculated using (G.6) and the results are given in Table H.4.

Table H.1. Sector allocation at each load bus of the *IEEE-RTS*.

load point	peak load allocation (*MW*)							
	L	I	C	A	R	G&I	O&B	system
Bus 1		39.90	14.25		36.85	17.00		*108.00*
Bus 2			14.25		48.45	34.30		*97.00*
Bus 3		59.80	14.25	11.45	94.50			*180.00*
Bus 4			14.25		25.55	34.20		*74.00*
Bus 5		19.90	14.25		36.85			*71.00*
Bus 6		39.95	14.25	11.45	67.50		2.85	*136.00*
Bus 7		39.95	14.25	22.70	48.10			*125.00*
Bus 8		19.90	28.55		94.05	25.65	2.85	*171.00*
Bus 9	85.50		8.50	33.80	41.50		5.70	*175.00*
Bus 10	42.75	39.95	14.25	17.90	80.15			*195.00*
Bus 13	42.75	59.80	28.55	16.70	80.15	25.65	11.40	*265.00*
Bus 14	85.47	39.95	5.60		62.98			*194.00*
Bus 15	213.75		34.50		54.50		14.25	*317.00*
Bus 16	42.75		14.25		25.90	17.10		*100.00*
Bus 18	188.20	39.90	22.55		62.40		19.95	*333.00*
Bus 19	110.97		14.25		55.78			*181.00*
Bus 20	42.86		14.25		53.79	17.10		*128.00*
total	*855.00*	*399.00*	*285.00*	*114.00*	*969.00*	*171.00*	*57.00*	*2850.00*

Table H.2. Sector peak load distribution at each load bus of the *IEEE-RTS*.

load point	sector peak load distribution (%)							
	L	I	C	A	R	G&I	O&B	system
Bus 1		36.94	13.19		34.12	15.74		*100.00*
Bus 2			14.69		49.95	35.36		*100.00*
Bus 3		33.22	7.92	6.36	52.50			*100.00*
Bus 4			19.26		34.53	46.22		*100.00*
Bus 5		28.03	20.07		51.90			*100.00*
Bus 6		29.38	10.48	8.42	49.63		2.10	*100.00*
Bus 7		31.96	11.40	18.16	38.48			*100.00*
Bus 8		11.64	16.70		55.00	15.00	1.67	*100.00*
Bus 9	48.86		4.86	19.31	23.71		3.26	*100.00*
Bus 10	21.92	20.49	7.31	9.18	41.10			*100.00*
Bus 13	16.13	22.57	10.77	6.30	30.25	9.68	4.30	*100.00*
Bus 14	44.06	20.59	2.89		32.46			*100.00*
Bus 15	67.43		10.88		17.19		4.50	*100.00*
Bus 16	42.75		14.25		25.90	17.10		*100.00*
Bus 18	56.52	11.98	6.77		18.74		5.99	*100.00*
Bus 19	61.31		7.87		30.82			*100.00*
Bus 20	33.48		11.13		42.02	13.36		*100.00*

Table H.3. Sector average load at each load bus of the *IEEE-RTS*.

load point	average loads (*MW*)							
	L	I	C	A	R	G&I	O&B	system
Bus 1		33.25	7.87		20.63	9.57		*71.32*
Bus 2			7.87		27.12	19.31		*54.30*
Bus 3		49.83	7.87	4.39	52.90			*115.00*
Bus 4			7.87		14.30	19.25		*41.43*
Bus 5		16.58	7.87		20.63			*45.09*
Bus 6		33.29	7.87	4.39	37.79		1.75	*85.10*
Bus 7		33.29	7.87	8.71	26.93			*76.80*
Bus 8		16.58	15.78		52.65	14.44	1.75	*101.20*
Bus 9	54.25		4.70	12.97	23.23		3.50	*98.65*
Bus 10	27.12	33.29	7.87	6.87	44.87			*120.03*
Bus 13	27.12	49.83	15.78	6.41	44.87	14.44	7.00	*165.45*
Bus 14	54.23	33.29	3.09		35.26			*125.87*
Bus 15	135.62		19.06		30.51		8.75	*193.94*
Bus 16	27.12		7.87		14.50	9.62		*59.12*
Bus 18	119.41	33.25	12.46		34.93		12.25	*212.30*
Bus 19	70.41		7.87		31.23			*109.51*
Bus 20	27.19		7.87		30.11	9.62		*74.81*
total	*542.47*	*332.48*	*157.49*	*43.75*	*542.47*	*96.24*	*35.00*	*1749.90*

Table H.4. Sector energy distribution at each load bus of the *IEEE-RTS*.

load point	sector energy distribution (%)							
	L	I	C	A	R	G&I	O&B	system
Bus 1		46.62	11.04		28.93	13.42		*100.00*
Bus 2			14.50		49.95	35.55		*100.00*
Bus 3		43.33	6.85	3.82	46.00			*100.00*
Bus 4			19.01		34.53	46.46		*100.00*
Bus 5		36.78	17.47		45.76			*100.00*
Bus 6		39.12	9.25	5.16	44.41		2.06	*100.00*
Bus 7		43.34	10.25	11.34	35.06			*100.00*
Bus 8		16.39	15.59		52.03	14.27	1.73	*100.00*
Bus 9	54.99		4.76	13.15	23.55		3.55	*100.00*
Bus 10	22.60	27.74	6.56	5.72	37.38			*100.00*
Bus 13	16.39	30.12	9.54	3.87	27.12	8.73	4.23	*100.00*
Bus 14	43.08	26.45	2.46		28.01			*100.00*
Bus 15	69.93		9.83		15.73		4.51	*100.00*
Bus 16	45.88		13.32		24.52	16.28		*100.00*
Bus 18	56.24	15.66	5.87		16.45		5.77	*100.00*
Bus 19	64.29		7.19		28.52			*100.00*
Bus 20	36.35		10.53		40.26	12.87		*100.00*

The *CCDF* for each load bus in the *IEEE-RTS* is calculated by weighting the user sector costs given in Table C.1 for each interruption duration. The sector peak load distribution (Table H.2) is used for weighting the sector user costs for short durations and the sector energy distribution (Table H.4) is used to weight the sector user costs for interruption durations longer than one half hour. The results are given Table H.5.

Table H.5. *CCDF* for each bus of the *IEEE-RTS* (1987 *$/kW*).

system bus	interruption duration				
	1 min	20 min	1 hr	4 hrs	8 hrs
Bus 1	0.658	1.911	5.519	17.489	43.213
Bus 2	0.072	0.613	2.011	9.327	29.131
Bus 3	0.574	1.591	4.769	15.387	37.241
Bus 4	0.094	0.774	2.485	10.697	33.295
Bus 5	0.532	1.728	5.056	16.973	42.202
Bus 6	0.623	1.729	5.026	16.446	39.144
Bus 7	0.574	1.673	5.057	16.075	38.669
Bus 8	0.340	1.217	3.650	13.688	36.024
Bus 9	0.677	1.291	2.577	7.544	16.948
Bus 10	0.587	1.410	3.801	11.885	28.888
Bus 13	0.784	1.946	5.094	16.113	37.804
Bus 14	0.789	1.577	3.707	10.511	24.746
Bus 15	0.934	1.800	3.423	9.731	21.766
Bus 16	0.492	1.155	2.521	8.264	22.923
Bus 18	1.075	2.126	4.471	12.791	27.704
Bus 19	0.646	1.187	2.183	6.204	15.741
Bus 20	0.385	0.924	2.095	7.561	21.400

The utilization of these functions together with the basic reliability data of the *IEEE-RTS* to calculate the *IEAR* at each load bus and the aggregate system *IEAR* is presented in the following section.

H.1. Development of the *IEAR* at Each Load Bus of the *IEEE-RTS*

Evaluation of the *IEAR* at each load bus of the *IEEE-RTS* was performed using the generation, transmission and load data given in

Appendix B and the procedure outlined in Appendix G. The assumptions used in the *COMREL* program are the same as those used in the case of the *RBTS* except the peak load which is set at 2850 *MW*. A summary of the results is given in Table H.7. The table also shows how the aggregate system *IEAR* is obtained from the individual bus values.

Table H.6. *IEAR* values for each load bus in the *IEEE-RTS*.

system bus	*ECOST* (*K$/yr*)	*EUE* (*MWh/yr*)	*IEAR* (*$/kWh*)	weight	weighted *IEAR*
Bus 1	12387.6816	1998.2441	6.20	0.03789	0.23
Bus 2	17930.6289	3670.0325	4.89	0.03404	0.17
Bus 3	24062.8809	4543.2339	5.30	0.06316	0.33
Bus 4	11718.9941	2086.6218	5.62	0.02596	0.15
Bus 5	10638.8984	1741.7764	6.11	0.02491	0.15
Bus 6	21250.6133	3863.0203	5.50	0.04772	0.26
Bus 7	9843.5723	1818.3523	5.41	0.04386	0.24
Bus 8	20802.7793	3855.5020	5.40	0.06000	0.32
Bus 9	1425.8457	619.8625	2.30	0.06140	0.14
Bus 10	2644.1968	639.0935	4.14	0.06842	0.28
Bus 13	125268.9219	23258.3652	5.39	0.09298	0.50
Bus 14	6292.6504	1843.3873	3.41	0.06807	0.23
Bus 15	84045.2422	27895.0078	3.01	0.11123	0.34
Bus 16	8675.5459	2452.2488	3.54	0.03509	0.12
Bus 18	190810.6094	50921.0938	3.75	0.11684	0.44
Bus 19	4751.9922	2077.2766	2.29	0.06351	0.15
Bus 20	42503.0273	11681.1514	3.64	0.04491	0.16
			IEAR (aggregate)		4.22

In addition to the basic results given in Table H.6, a number of sensitivity studies were conducted to show the effect of selected pertinent factors on the value of the *IEAR* [34]. The effect of the following pertinent factors were examined and the results are given in Table H.7.

Case 1: effect of using the composite system *CCDF* (Table C.3),
Case 2: effect of using the average interruption duration,
Case 3: effect of using the *DC* load flow method,
Case 4: effect of using the network flow method,

Case 5: effect of using *Pass 2* in the load curtailment philosophy and
Case 6: effect of using *Pass 3* in the load curtailment philosophy.

Table H.7. Effects of selected pertinent factors on the value of the *IEAR* in the *IEEE-RTS*.

load point	*IEAR* ($/kWh)					
	Case 1	Case 2	Case 3	Case 4	Case 5	Case 6
Bus 1	4.16	6.16	6.20	6.52	6.20	6.20
Bus 2	4.16	4.79	4.89	5.47	4.89	4.89
Bus 3	4.19	5.26	5.29	5.52	5.32	5.50
Bus 4	4.18	5.50	5.63	6.23	5.68	5.76
Bus 5	4.18	6.06	6.11	6.41	6.14	6.18
Bus 6	4.18	5.47	5.50	5.71	5.52	5.55
Bus 7	4.14	5.39	5.41	5.70	5.41	5.41
Bus 8	4.17	5.34	5.40	5.76	5.39	5.49
Bus 9	4.22	2.27	2.30	2.35	2.34	2.34
Bus 10	4.20	4.08	4.15	4.30	4.27	4.27
Bus 13	4.30	5.33	5.39	5.44	5.40	5.41
Bus 14	4.13	3.39	3.41	3.57	3.42	3.41
Bus 15	4.38	2.99	3.01	3.00	3.02	3.02
Bus 16	4.16	3.49	3.54	3.85	3.54	3.54
Bus 18	4.45	3.73	3.75	3.71	3.75	3.74
Bus 19	4.15	2.26	2.29	2.43	2.39	2.48
Bus 20	4.35	3.53	3.64	3.66	3.61	3.62
aggregate	4.25	4.18	4.22	4.38	4.24	4.27